NASA CONTRACTOR REPORT

NASA CR-244

NASA CR-244

N65-28691
(ACCESSION NUMBER)
210
(PAGES)
(NASA CR OR TMX OR AD NUMBER)
(THRU)
1
(CODE)
12
(CATEGORY)
FACILITY FORM 602

GPO PRICE $ _____
OTS PRICE(S) $ _____
Hard copy (HC) _____
Microfiche (MF) _____

ANALYTICAL INVESTIGATION OF FLUID AMPLIFIER DYNAMIC CHARACTERISTICS

VOLUME I

Prepared under Contract No. NAS 8-11236 *by*
SPERRY UTAH COMPANY
Salt Lake City, Utah
for

NATIONAL AERONAUTICS AND SPACE ADMINISTRATION • WASHINGTON, D. C. • JULY 1965

NASA CR-244

ANALYTICAL INVESTIGATION OF FLUID AMPLIFIER DYNAMIC CHARACTERISTICS

VOLUME I

Distribution of this report is provided in the interest of information exchange. Responsibility for the contents resides in the author or organization that prepared it.

Prepared under Contract No. NAS 8-11236 by
SPERRY UTAH COMPANY
Salt Lake City, Utah

for

NATIONAL AERONAUTICS AND SPACE ADMINISTRATION

For sale by the Clearinghouse for Federal Scientific and Technical Information
Springfield, Virginia 22151 – Price $6.00

FOREWORD AND ACKNOWLEDGEMENTS

This research study was made for the Astrionics Laboratory of the George C. Marshall Space Flight Center, National Aeronautics and Space Administration by the Sperry Utah Company of the Sperry Rand Corporation, under Contract NAS 8-11236.

Volume I of this Final Report presents analytical fluid dynamics investigations and some experimental work which have been carried out under this contract.

Volume II presents analytical circuit investigations, tutorial material and an organized compilation of fluid dynamics and circuit data, to form the basis of a Fluid Control Handbook for the fluid control system designer. In some instances, the results of Volume I are summarized and generalized in Volume II.

The following authors have contributed to this report:

Volume I

F. R. Goldschmied: All of Volume I, except as noted

D. L. Letham : Section 3.6

C. E. Pearson and R. E. Esch: Section 1.1.3
(Sperry Rand Research Center)

T. J. Lechner and P. H. Sorenson: Section 3.5.4
(Johnson Service Company)

Volume II

D. L. Letham: All of Volume II, except as noted

F. R. Goldschmied: Section 1.

H. L. Fox: Section 3 and parts of Section 4.

ABSTRACT OF VOLUME I

This report covers four separate investigations bearing on the subject of analytical and experimental investigation of fluid amplifier dynamic characteristics.

The first investigation is a theoretical effort aimed at the numerical solution of the time-dependent incompressible two-dimensional Navier-Stokes equations for the case of a viscous jet in an arbitrary flow field. A FORTRAN program has been prepared and an initial computer run made for an initial simplified flow field; it is seen that streamline patterns can be obtained and interpreted physically for a sequence of time points.

The second investigation is an experimental effort aimed at establishing realistic dynamic test standards for NOR and NAND fluid digital amplifiers. The proposed test circuit comprises two active logic levels both upstream and downstream of the test component; preliminary experimental results demonstrate that the proposed test standards are both practical and useful.

The third investigation is a theoretical analysis of a passive circuit consisting of a volume-terminated transmission tube, for a viscous compressible fluid. The analysis extends from steady-state to a frequency corresponding to the onset of transverse acoustic waves in the tube.

It is shown that all the dynamic processes can be described in terms of three dimensionless parameters, the classical Reynolds Number, the Acoustic Reynolds Number and the classical Stokes Number, plus the aspect ratio of the tube and the volume ratio. Similarity laws are derived and presented for the case of constant fluid absolute viscosity and for the case of constant tube diameter.

Finally the electrical analogy is examined, comparing the simple electrical analog circuit first to an elementary fluid theory and then to a corrected fluid theory. Criteria for the validity of the analogy are given; also it is seen that there are three possible fluid analogies, depending on whether volume flow, mass flow or weight flow is chosen as the current.

The fourth investigation is an experimental study of the feasibility of a Fluid Control Subsystem for a hybrid Thrust-vector-control Servosystem. The hybrid system comprises a conventional servovalve and actuator for the Power Subsystem, while the Fluid Control Subsystem has an electric/fluid command transducer, a fluid position-feedback transducer and a fluid operational amplifier. The interface between the two subsystems is given by push-pull bellows which accept the fluid pressure output from the operational amplifier and provide the force input to the servovalve. Satisfactory steady-state linearity is demonstrated experimentally for the transducers, the amplifier and for the complete Fluid Control Subsystem.

VOLUME I

TABLE OF CONTENTS.

1.0 THEORETICAL AND EXPERIMENTAL STUDY OF DIGITAL FLUID AMPLIFIER DYNAMICS

The initial phase of the program is concerned with a theoretical and experimental study of digital fluid amplifier dynamics, to extend the company-funded work which has led to improved numerical techniques for the solution of the time-dependent two-dimensional Navier-Stokes equations and to the conception and successful development of the axisymmetric focussed-jet NOR amplifier.

This phase covered a period of five working weeks, from June 20 to August 6, 1964. Following this, the work was redirected toward proportional fluid amplifiers to better fulfill the requirements of NASA servosystems, particularly for thrust-vector-control.

1.1 Theoretical Study of Time-Dependent Viscous Jets by Numerical Solution of the Navier-Stokes Equations of Motion

1.1.1 Introduction

The Navier-Stokes equations of motion for a time-dependent two-dimensional incompressible viscous fluid are strongly non-linear and admit few exact solutions, even for steady-state flow. A rather complete discussion of viscous fluid fundamentals is given by Schlichting in his well known book,(Ref.1) "Boundary Layer Theory," Chapters I to V. In recent years, numerical techniques have made considerable advances and computers have increased in size and speed to the point where theoretical fluid research can be conceived to be carried out by numerical solutions rather than by mathematical solutions, exact or approximate.

In the study of fluid amplifier dynamic characteristics, the fundamental problem is that of the dynamic behavior of the jet during the transient switching phase as it detaches from the wall. Furthermore, since the smallest size and power consumption (i.e., small Reynolds Numbers) is sought for digital fluid amplifiers, a study of the Navier-Stokes equations would yield the desired information, because these equations apply exactly to the case of the viscous jet at small Reynolds Numbers.

1.1.2 Numerical Solution of Time-Dependent Viscous Fluid Problems

1.1.2.1 Prior Work in this Field. The most extensive attempt to solve numerically a problem of time-dependent two-space-dimensional incompressible viscous flow is probably that reported in 1963 by Fromm and Harlow at Los Alamos (Ref. 2, 3). A large number of vortex street patterns about obstacles are presented in the Los Alamos reports, such as those reproduced here as Figures 1.1-1, 2 and 3, which show the development of a vortex street behind an obstacle. Qualitative agreement with experiment appears very good, and this work must be considered to be a substantial contribution to numerical computation of viscous flow problems. The growth, detachment and dissipation of the Karman vortices can be clearly followed in time from figure to figure.

Streamline Flow Patterns.

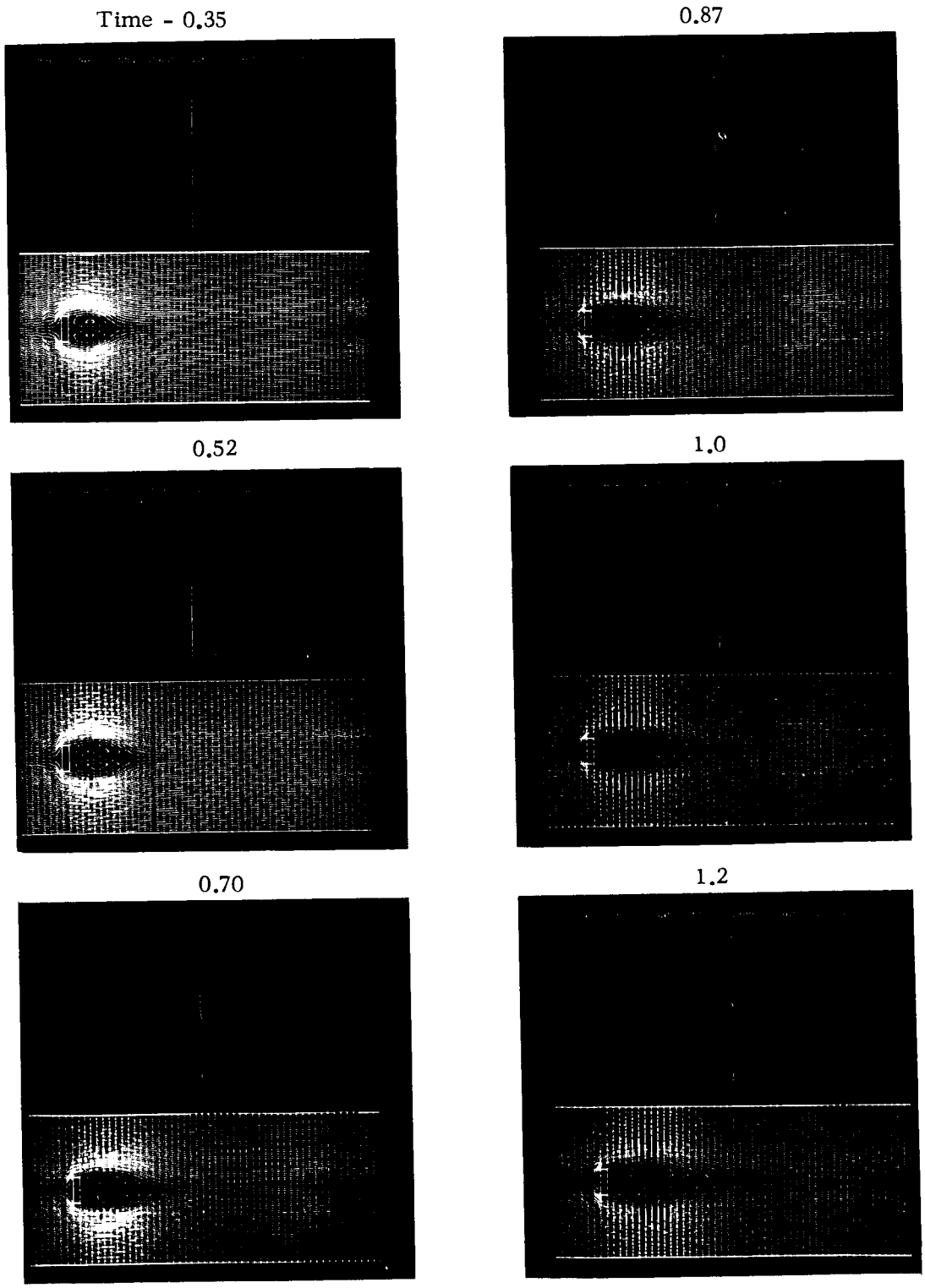

FIGURE 1.1-1

Numerical Solution of the Karman Vortex Street (Fromm[3])

Streamline Flow Patterns.

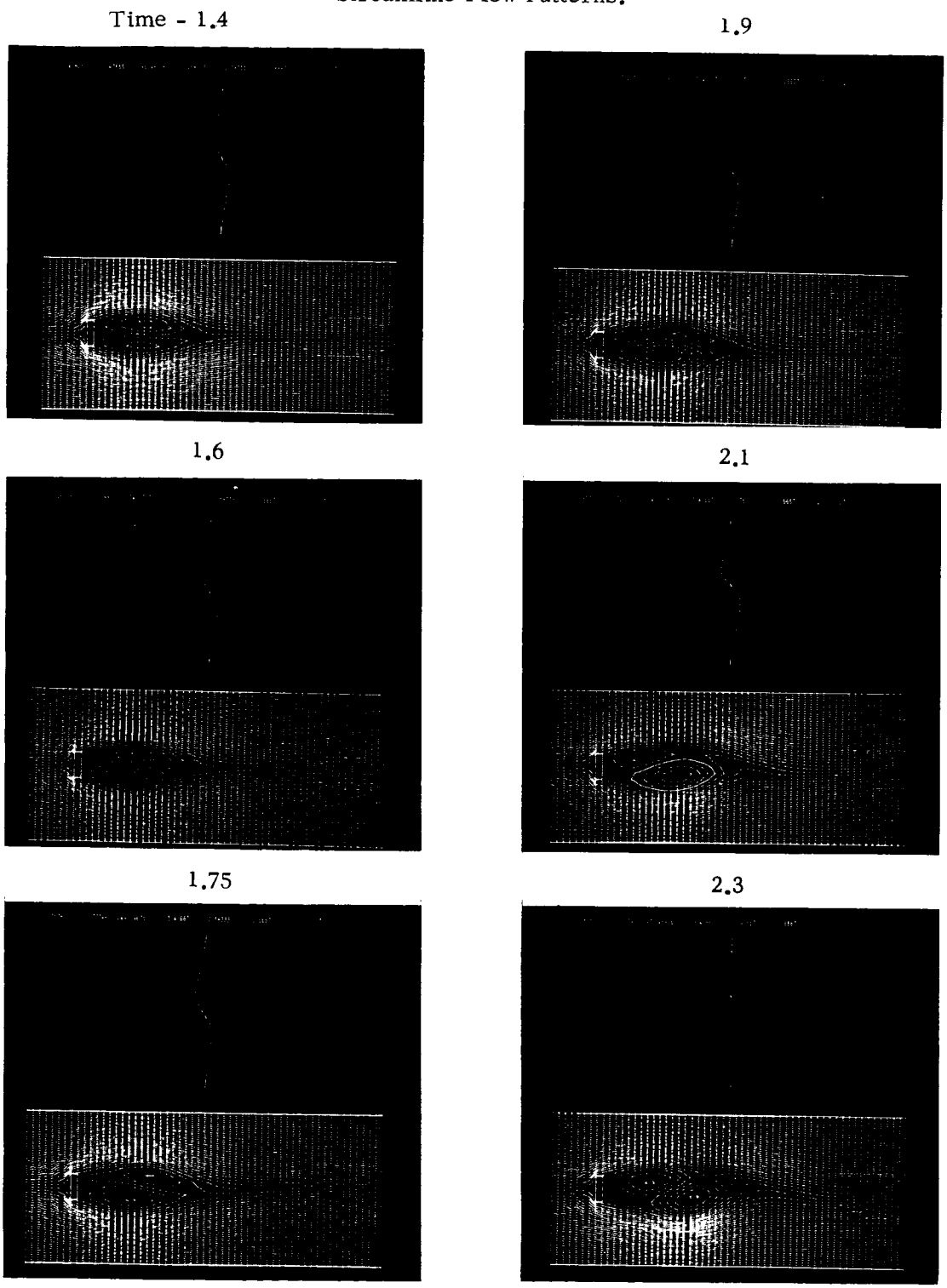

FIGURE 1.1-2

Numerical Solution of the Karman Vortex Street (Fromm[3])

Streamline Flow Patterns.

Time - 2.45

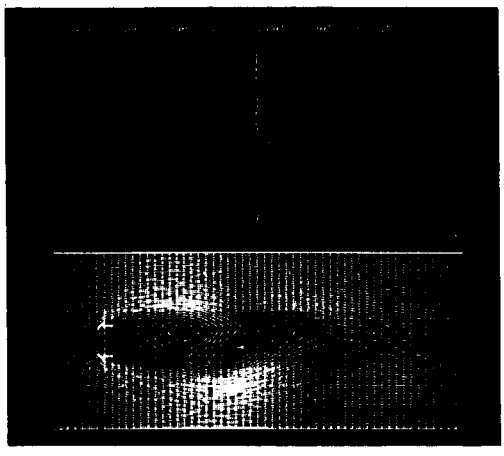

3.0

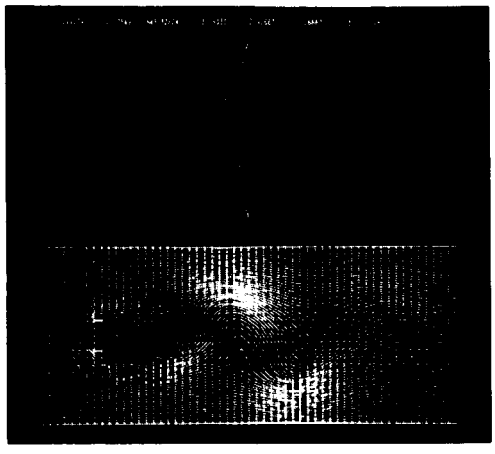

2.65

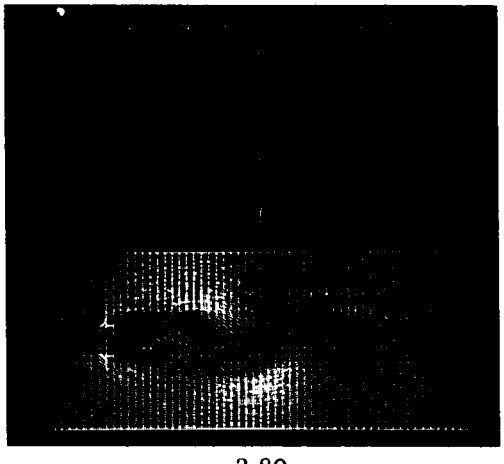

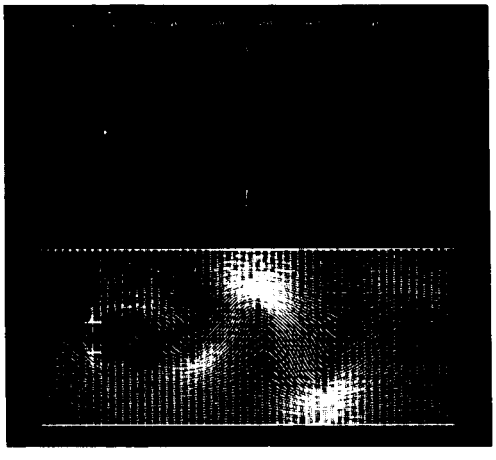

2.80

Streak Flow Pattern - Time 2.8

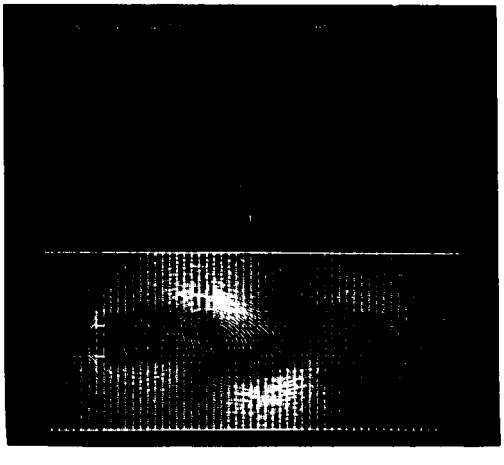

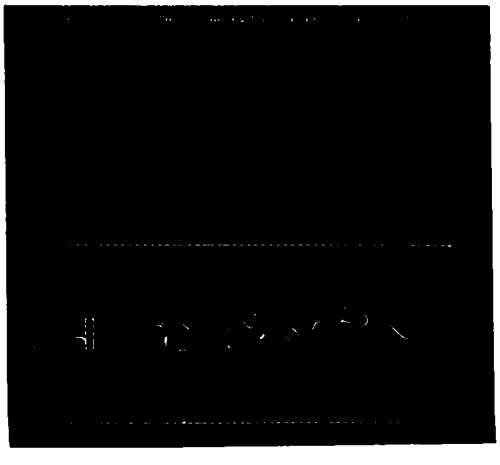

FIGURE 1.1-3

Numerical Solution of the Karman Vortex Street (Fromm[3])

However, there are several reasons for dissatisfaction with the numerical procedure. The wall boundary condition used, which has the greatest advantage of decoupling the vorticity and stream function parts of the problem and thereby yielding a major computational simplification, does not correspond to the correct boundary condition except in the early stages of the flow; consequently the flow about the obstacle can be correct only until the vorticity generated at the obstacle begins to be felt (appreciably) at the walls. This is perhaps also one reason why the pressure calculations on the obstacle, required for lift and drag determination, are admittedly incorrect. The use of the DuFort-Frankel process (see Appendix I) has the advantage of permitting a longer time step than the conventional explicit process; however, it is shown by Pearson (Ref. 4) that for comparable accuracy the time step in the former process can be no longer than that in the latter. In fact, the authors do choose the very small time step that stability considerations would require for the explicit process, and so receive no compensation for the added complexity of the DuFort-Frankel process. The non-use of an over-relaxation process is surprising; this alone probably doubles or triples the requisite computation time. Finally, the problem itself is somewhat artificial, because of the periodicity, the use of moving walls to drive the flow, and the rather special mesh-obstacle geometry.

We will now discuss some other computational results that have been recently reported. At M.I.T., Dix (Ref. 5) has solved numerically the two-dimensional problem of the steady-state flow of a viscous incompressible fluid past a flat plate; although he included the effects of a magnetic field, this probably introduces no important complication in the numerical calculation. Although time-dependent effects were not included, his methods and results are nevertheless of interest, because of his discovery of a means of controlling the instability associated with the boundary conditions, a pernicious effect that has frustrated previous attempts at numerical solution of such problems. Unfortunately, Dix's device does not correspond to following the time-history of an actual flow correctly, but it does provide valuable clues as to the nature of the trouble and its remedy.

The time-dependent flow in a jet has been calculated by Payne (Ref. 6) at Manchester; an explicit equation is used for the time step process in the vorticity diffusion equation, and velocities are obtained by a Green's function-type formula involving an area integration of the vorticity. An image method is used which satisfies boundary conditions only approximately.

A group at the University of Michigan, (Ref. 7 and 8) have computed the two-dimensional flow and temperature fields for some idealized natural convection problems involving a viscous fluid. The effects of pressure are neglected so that substantial simplifications can be made in the governing equations. Of particular interest is the discussion of the effect of added terms in the diffusion equation.

The most recent work by Wilkes (Ref. 9) of the Michigan group is particularly interesting. The equations differ slightly in that temperature effects are now included; however, this has little effect on the finite difference equation procedure - the basic difficulties still arise from the Navier-Stokes equations.

1.1.2.2 Recent Work at the Sperry Rand Research Center. A company-funded research project at the Sperry Rand Research Center during the past year has yielded computational methods, and computer programs, for the analysis of time-dependent two-dimensional viscous flow problems (Ref. 4).

Mathematically, the problem is that of solving numerically a fourth-order partial differential equation, in three independent variables, containing non-linear terms. It is known that even without the added complications of time variation or non-linearity, numerical techniques for fourth-order equations of biharmonic character tend to require large amounts of computer time; also, the presence of the non-linear terms tends to induce computational instabilities. Moreover, the most natural boundary conditions to impose - those in which velocities are prescribed at the boundary - are also among those which are the most difficult to handle computationally. These various difficulties are illustrated in the recent work carried out for a special case of the general problem by a group at Los Alamos (discussed above); it was there found necessary to approximate the boundary conditions in a way which seriously affected accuracy, and also to take such small time steps (for reasons of stability and accuracy) that the computer time became excessive.

The Sperry program appears to be a major step forward in all of computer speed, stability and accuracy; of course, the process of modification and improvement is by no means at an end. The program permits arbitrary prescription of velocities at the boundaries of the region. So far, emphasis has been placed on devising a suitable general method; extensions to permit curved boundaries, variable mesh spacings in both space and time, or satisfaction of circuital conditions for multiply-connected regions, have yet to be made.

Most experimentation with the program has been in connection with a test problem, whose exact solution is known. Accuracies of a fraction of a percent are obtained, even with time-steps up to 50 times as great as those permitted by conventional stability limitations. The general method has also been applied to two problems whose solutions are not known. One of them concerns the injection of fluid into a rectangular region; the final result was verified by rerunning with different time meshes. Computations have been successfully carried out at Reynolds numbers of 60 to 600 (the Reynolds number being based on a rectangle side and the injection velocity). The other problem is a time-dependent version of the well-known Karman disk problem; although this later problem is one-dimensional in nature and so of a fundamentally simpler nature, there is enough difference in the formal equation structure to provide a good added test for the method. Results for the injection problem are given in reference 4 by Pearson; the disk problem results are described in reference 10 by Pearson. An alternative approach to the handling of boundary conditions in viscous time-dependent flow problems is given by Esch (Ref. 11).

A brief summary of the analytical work carried out at the Sperry Rand Research Center and at Sperry Utah prior to this contract is given in Appendix I.

1.1.3 Numerical Program and Preliminary Results

This portion of the work was performed at the Sperry Rand Research Center, Applied Mechanics Department.

The objective was to prepare a program for the numerical solution of the time-dependent two-dimensional incompressible Navier-Stokes equations for the configuration shown in Figure 1.1.4. The power jet width b and the control jet width c should comprise at least 3 computing cells.

The development and use of this program was to be aimed at studies of the effects of various parameters, including most importantly Re = Ub/ν, θ and u/U. To a lesser extent the effects of N/b, d, c, exit condition, and control pulse shape were to be explored. Among the results were to be full time histories of flows, extending from a time before control input (to show steady state flow behavior) to a time when switching is essentially complete. Another form of result will be plots of switching time, defined in some physically meaningful way and expressed in appropriate Strouhal Number dimensionless form, against Re, under various conditions. Evidence was also to be obtained regarding flow instabilities and fluctuations.

A sufficient number of computer runs were to be carried out to allow study of the effects of Re, u/U, and (to a lesser extent) N/b variation. The values u/U = 0.1, 0.2, ..., 1.0; and N/b = 20, 30, 40 and 50, were to be considered. The range of R of physical interest is 100 to 1000, and attempts were to be made to cover as much of this range as possible.

The fluid will be allowed to exit at either OP or AB; the region AB is preferred for close simulation of physical devices, but in some cases it may be desirable to use region OP in order to ensure jet adherence to the upper wall in the absence of a control pulse.

It was decided to begin with a slightly modified geometry, in which the inlet jet is horizontal, in order to treat first a case very similar to problems in which the Sperry Rand Research Center has had computational experience. The computational flow field is shown below:

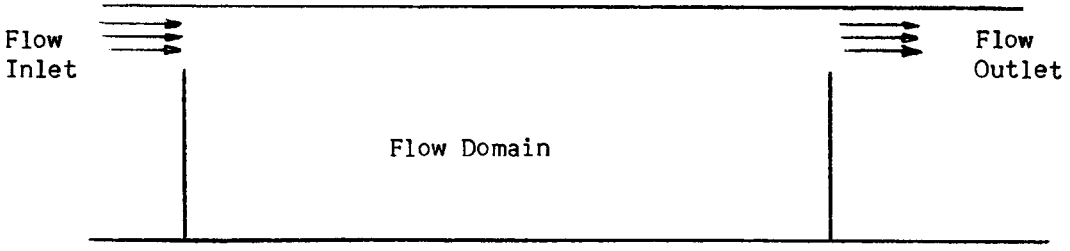

Physically, this work was intended to provide exact time-dependent information on the attachment of a viscous fluid jet to a plane wall and on its subsequent switching-off because of a transverse flow step of varying magnitude. The numerical solutions for each time point can be plotted and laid out in time sequence like frames of a motion picture, yielding detailed flow patterns which are impossible to obtain experimentally.

A Fortran program was prepared and checked out for the solution of time-dependent two-dimensional incompressible viscous flow problems in a rectangular region comprising 21 horizontal cells and 11 vertical cells. The program was designed to be efficient and flexible, to facilitate the solution for various

input configurations. It is only necessary, generally, to modify and recompile the subroutine "DATA" for each new configuration or for a change in program parameter such as cell mesh size, tolerances, etc. The output format makes rapid analysis possible and allows direct sketching of the streamlines on the computer output sheets. A chart indicating the general structure of the program is given in Figure 1.1-5. The program itself is given in Table 1.1-1. An initial computer run has been made for the boundary conditions sketched below:

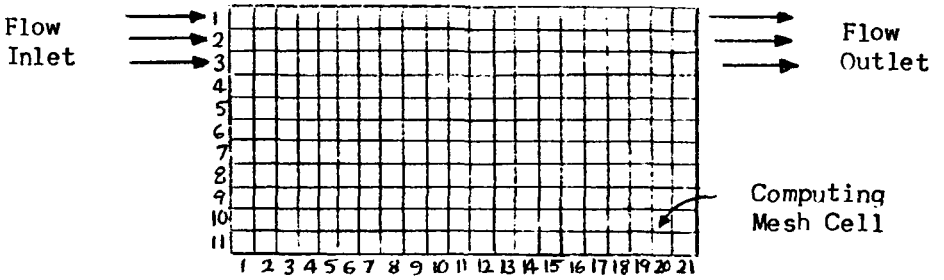

This is the case of the simple attached jet which is started from rest and forced by arbitrary injection and extraction of flow at the boundaries, as shown above. The time dependence of the jet had the form $1- e^{-at}$. In this initial computer run, $a = 20$ and the time $t = 0.9$ was reached, so input and output flow had built up to nearly their final values from rest. The Reynolds Number (based on the side of the rectangular flow field) was 100, which is certainly in the physical viscous flow regime. The actual output sheets of this initial run are inclosed in Appendix II. These results apply directly to the case of the transient flow into a tank, which has an important bearing on the physical understanding of fluid "capacitance." Numerical solutions at four time-points are shown in Figure 1.1-6 for $t = 0.1$, $t = 0.4$, $t = 0.7$ and $t = 0.9$, displaying the streamline pattern in the rectangular flow field. It is seen that reverse circulation (countervortex) is building up in the lower left-hand corner of the flow field at $t = 0.09$.

1.1.4 Recommendations

In view of the success achieved in this difficult and sophisticated field, it is recommended that further support be made available to this fundamental research effort, in order to reach a time understanding of the transient switching processes of the viscous jet. True "step" control inputs may be introduced numerically without difficulty and therefore "optimum" switching speeds and also jet stability criteria may be obtained. It is entirely probable that a particular Reynolds Number will emerge as the optimum for the switching process, therefore determining the fluid dynamic "scale" of digital fluid amplifiers. This will also answer the question of the smallest size for fluid amplifiers; once the Reynolds Number is given, the size will be determined for any given fluid and jet velocity.

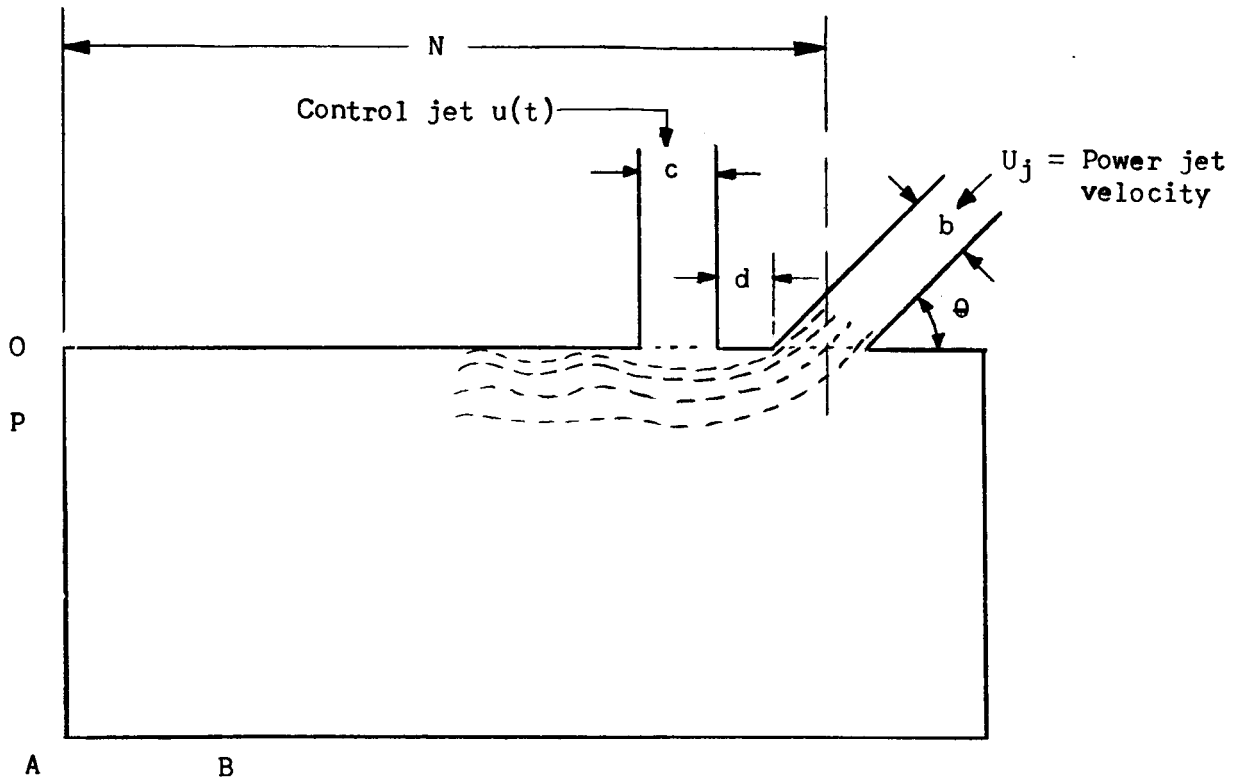

Figure 1.1-4

COMPUTATIONAL FLOW FIELD FOR

TIME-DEPENDENT VISCOUS JET WITH CONTROL

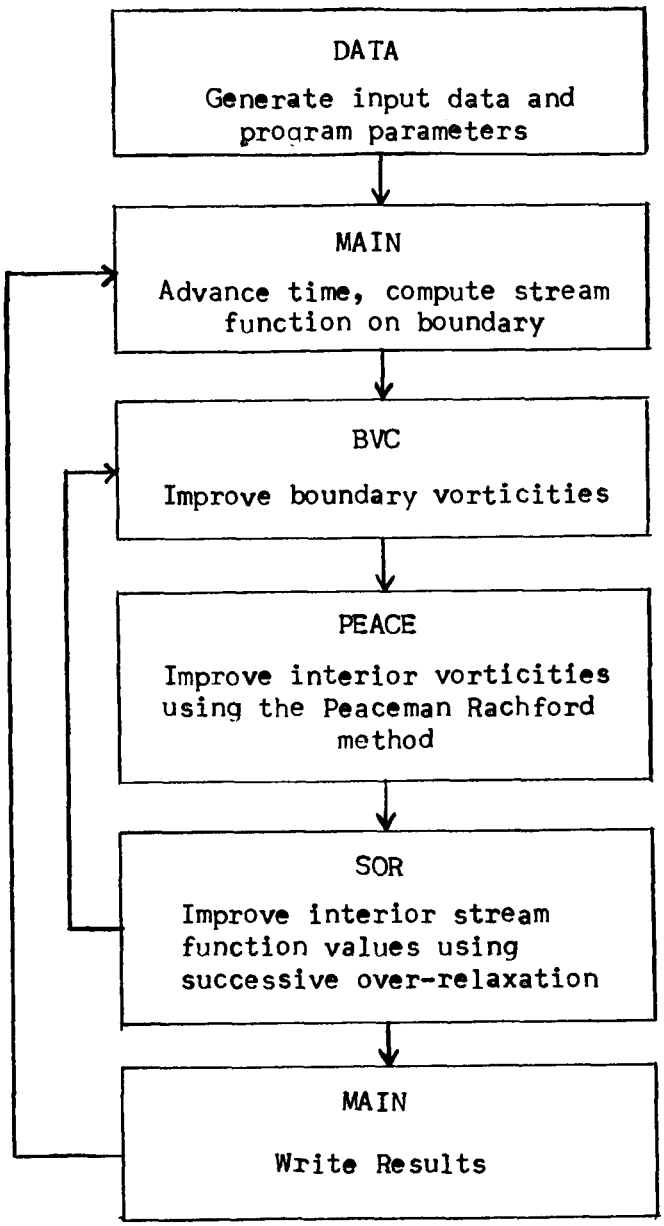

Figure 1.1-5

FORTRAN PROGRAM STRUCTURE

CHART

Table 1.1-1

FORTRAN Program

for

Numerical Solution

of

Time-Dependent Incompressible

Two-Dimensional Navier-Stokes

Equations

```
      DIMENSION PSN(61,31),PSO(61,31),PSM1(61,31),VN(61,31),VO(61,31),
     DIMENSION PSN(61,31),PSO(61,31),PSM1(61,31),VN(61,31),VO(61,31),
     1VM1(61,31),VMS(61,31),VT(61,31),BPSL(31),BPSR(31),BPSB(61),BPST(61
     2),BPSNL(31),BPSNR(31),BPSNB(61),BPSNT(61)
      COMMON PSN,PSO,PSM1,VN,VO,VMS,AB,AC,AD,AE,AF,AG,AH,N,NM1,NM2,NM3,M
     1,MM1,MM2,MM3,K5,K6,K7,NI,IIM2,NP,NDT,NDTF,CX,DT,TMAX,C,CO,COA,DAP,
     2DAP2,DAV2,NORUN,NORUNS,BPSL,BPSR,BPSB,BPST,BPSNL,BPSNR,BPSNB,BPSNT
     3,ALPHA,PI,VM1,VT,R,T,JJ,II,DAPP,DX2
      PI=3.14159265
      NORUN=0
      NORUNS=1
      IF (SENSE LIGHT 1) 900,900
  900 NORUN=NORUN+1
      IF(NORUN-NORUNS)901,901,902
  902 CALL EXIT
  901 CALL DATA
  910 NM1=N-1
      NM2=N-2
      NM3=N-3
      NSP=(N-1)/10
      MM1=M-1
      MM2=M-2
      MM3=M-3
      MSP=(M-1)/20
      DX=1./FLOATF(NM1)
      PI2=PI*PI
      DX2=DX*DX
      A=DT/DX2
      AB=C*A/(8.*(1.+A))
      AC=0.5*AB
      AD=A/(2.*(1.+A))
      AE=1./(1.+A)
      COSPH=(COSF(PI/FLOATF(MM1)))**2
      AP=2.*(1.-SQRTF(1.-COSPH))/CCSPH
      AF=0.5*DX2*AP
      AG=1.-AP
      AH=0.25*AP
  930 KK=0
      KKF=0
      T=0.
      WRITE OUTPUT TAPE 6,932,N,DT,CC,COA,C
  932 FORMAT(/////7H   N = I5,6H DT = E14.7,6H CC = E14.7,7H COA = E14.7
     1,5H C = E14.7)
      WRITE OUTPUT TAPE 6,933,DAP,DAP2,DAV2,IIM2,NI,K5,K6,K7,ALPHA,R,M
  933 FORMAT(//7H DAP = E14.7,8H DAP2 = E14.7,8H DAV2 = E14.7,8H IIM2 =
     1  I7, 6H NI = I6/6H K5 = I6,6H K6 = I5,6H K7 = I5, 7H ALPHA=E14.7,
     23H R=E14.7,3H M=I3)
      WRITE OUTPUT TAPE 6,934,DX,AP,A,AB,AC,AD,AE,AF,AG,AH,PI,PI2,TMAX
  934 FORMAT(// (6E16.8))
    1 JJ=0
      JJS=0
      T=T+DT
    2 IF(T-TMAX)3,3,900
    3 DO 5 J=1,N
      DO 4 I=1,M
      TR1=PSM1(I,J)
      TR2=VM1(I,J)
```

```
      DIMENSION PSN(61,31),PSO(61,31),PSM1(61,31),VN(61,31),VO(61,31),
     PSM1(I,J)=PSO(I,J)
     VM1(I,J)=VO(I,J)
     PSO(I,J)=PSN(I,J)
     VO(I,J)=VN(I,J)
     PSN(I,J)=3.*PSO(I,J)-3.*PSM1(I,J)+TR1
   4 VN(I,J)=3.*VO(I,J)-3.*VM1(I,J)+TR2
   5 CONTINUE
   6 KK=KK+1
     NP=2-XMINOF(1,XMODF(KK,NDT))
     NPF=2-XMINOF(1,XMODF(KK,NDTF))
     TF=1.-EXPF(-ALPHA*T)
  20 DO 21 I=1,M
     PSN(I,1)=TF*BPSB(I)
     PSM1(I,1)=TF*BPSNB(I)
     PSN(I,N)=TF*BPST(I)
  21 PSM1(I,N)=TF*BPSNT(I)
     DO 27 J=2,NM1
     PSN(1,J)=TF*BPSL(J)
     PSM1(1,J)=TF*BPSNL(J)
     PSN(M,J)=TF*BPSR(J)
  27 PSM1(M,J)=TF*BPSNR(J)
     DAPP=DAP
  95 DO 96 J=1,N
     DO 96 I=1,M
  96 VT(I,J)=VN(I,J)
 600 CALL BVC
 100 CALL PEACE
 180 GO TO (200,181),NP
 181 WRITE OUTPUT TAPE 6,182,JJ
 182 FORMAT(/16H   ITERATION NO.I4,12H VORTICITIES)
 200 CALL SOR
     IF(SENSE LIGHT 1 ) 900,400
 400 JJ=JJ+1
 601 JJS=JJS+II
     EEV=0.
     DO 405 J=1,N
     DO 405 I=1,M
 405 EEV=MAX1F(EEV,ABSF(VN(I,J)-VT(I,J)))
 450 IF(DAV2-EEV)456,501,501
 456 IF (NI-JJ) 457,457,95
 457 WRITE OUTPUT TAPE 6,458,JJ,EEV
 458 FORMAT(////15H WARNING AFTER I5,19H ITERATIONS, EEV = E14.7,20H FA
    1IL TO MEET SPEC. )
 501 WRITE OUTPUT TAPE 6,502,T,JJ,JJS
 502 FORMAT(22H1STEP COMPLETED FOR T=E12.4,5XI5,2X11HITERATIONS,2XI5,2X
    17HSWEEPS.)
 503 GO TO (1,504),NPF
 504 CONTINUE
     DIMENSION KOUT(21)
     BIG=0.
     DO 521 I=1,M
     DO 521 J=1,N
 521 BIG=MAX1F(BIG,ABSF(VN(I,J)))
     L=XINTF(.434294482*LOGF(BIG))
     IF(XSIGNF(1,L))522,527,523
 523 L=L+1
```

```
      DIMENSION PSN(61,31),PSO(61,31),PSM1(61,31),VN(61,31),VO(61,31),
  522 LM4=L-4
      WRITE OUTPUT TAPE 6,528,LM4,(I,I=1,M,MSP)
  528 FORMAT(12HOVORTICITY,E13//2X4HJ I=21(I2,4X))
      DO 525 J=1,N,NSP
      DO 524 I=1,M,MSP
  524 KOUT(I)=XINTF(VN(I,J)*10.**(4-L)+.5*SIGNF(1.,VN(I,J)))
  525 WRITE OUTPUT TAPE 6,526,J,(KOUT(I),I=1,M,MSP)
  526 FORMAT(/1XI2,21(I6))
  527 CONTINUE
      BIG=0.
      DO 531 I=1,M
      DO 531 J=1,N
  531 BIG=MAX1F(BIG,ABSF(PSN(I,J)))
      L=XINTF(.43429448Z*LOGF(BIG))
      IF(XSIGNF(1,L))532,537,533
  533 L=L+1
  532 LM4=L-4
      WRITE OUTPUT TAPE 6,538,LM4,(I,I=1,M,MSP)
  538 FORMAT(18HOSTREAM FUNCTION,E13//2X4HJ I=21(I2,4X))
      DO 535 J=1,N,NSP
      DO 534 I=1,M,MSP
  534 KOUT(I)=XINTF(PSN(I,J)*10.**(4-L)+.5*SIGNF(1.,PSN(I,J)))
  535 WRITE OUTPUT TAPE 6,526,J,(KOUT(I),I=1,M,MSP)
  537 CONTINUE
      GO TO 1.
      END(1,0,0,0,0,1,1,0,0,1,0,0,0,0,0)
```

```
      SUBROUTINE BVC

      SUBROUTINE BVC
      DIMENSION PSN(61,31),PSO(61,31),PSM1(61,31),VN(61,31),VO(61,31),
     1VM1(61,31),VMS(61,31),VT(61,31),BPSL(31),BPSR(31),BPSB(61),BPST(61
     2),BPSNL(31),BPSNR(31),BPSNB(61),BPSNT(61)
      COMMON PSN,PSO,PSM1,VN,VO,VMS,AB,AC,AD,AE,AF,AG,AH,N,NM1,NM2,NM3,M
     1,MM1,MM2,MM3,K5,K6,K7,NI,IIM2,NP,NDT,NDTF,DX,DT,TMAX,C,CO,COA,DAP,
     2DAP2,DAV2,NORUN,NORUNS,BPSL,BPSR,BPSB,BPST,BPSNL,BPSNR,BPSNB,BPSNT
     3,ALPHA,PI,VM1,VT,R,T,JJ,II,DAPP,DX2
  600 DO 602 J=2,NM1
      H2LP=4.*PSN(2,J)-.5*PSN(3,J)+PSN(1,J+1)+PSN(1,J-1)
     1 -5.5*PSN(1,J)-3.*DX*PSM1(1,J)
      VN(1,J)=(1.-COA)*(-.5*(H2LP)/DX2) + COA*VN(1,J)
  602 VMS(1,J)=.5*(VN(1,J)+VO(1,J))
      DO 603 I=2,MM1
      H2LP=4.*PSN(I,2)-.5*PSN(I,3) + PSN(I-1,1)+PSN(I+1,1)
     1-5.5*PSN(I,1)-3.*DX*PSM1(I,1)
      VN(I,1)=(1.-COA)*(-.5*H2LP/DX2)+COA*VN(I,1)
  603 VMS(I,1) =.5*(VN(I,1)+VO(I,1))
      DO 605 I=2,MM1
      H2LP=4.*PSN(I,NM1)-.5*PSN(I,NM2)+PSN(I-1,N)+PSN(I+1,N)
     1 - 5.5*PSN(I,N)-3.*DX*PSM1(I,N)
      VN(I,N)=(1.-COA)*(-.5*H2LP/DX2)+COA*VN(I,N)
  605 VMS(I,N)=.5*(VN(I,N)+VO(I,N))
      DO 606 J=2,NM1
      H2LP=4.*PSN(MM1,J)-.5*PSN(MM2,J)+PSN(M,J+1)+PSN(M,J-1)
     1-5.5*PSN(M,J)-3.*DX*PSM1(M,J)
      VN(M,J)=(1.-COA)*(-.5*H2LP/DX2)+COA*VN(M,J)
  606 VMS(M,J)=.5*(VN(M,J)+VO(M,J))
      RETURN
      END(1,0,0,0,0,1,1,0,0,1,0,0,0,0,0)
```

```
      SUBROUTINE DATA
      SUBROUTINE DATA
      DIMENSION PSN(61,31),PSO(61,31),PSM1(61,31),VN(61,31),VO(61,31),
     1VM1(61, 1),VMS(61,31),VT(61,31),BPSL(31),BPSR(31),BPSB(61),BPST(61
     2),BPSNL(31),BPSNR(31),BPSNB(61),BPSNT(61)
      COMMON PSN,PSO,PSM1,VN,VO,VMS,AB,AC,AD,AE,AF,AG,AH,N,NM1,NM2,NM3,M
     1,MM1,MM2,MM3,K5,K6,K7,NI,IIM2,NP,NDT,NDTF,DX,DT,TMAX,C,CO,CCA,DAP,
     2DAP2,DAV2,NORUN,NORUNS,BPSL,BPSR,BPSB,BPST,BPSNL,BPSNR,BPSNB,BPSNT
     3,ALPHA,PI,VM1,VT,R,T,JJ,II,DAPP,DX2
      IF(NORUN-1)11,11,12
   11 NORUNS=1
      N=11
      NM1=N-1
      M=21
      DT=.01
      TMAX=.1
      NDT=500
      NDTF=1
      CO=0.
      COA=.8
      C=1.
      R=100.
      DAP=.00016*R
      DAP2=.000016*R
      DAV2=.004*R
      IIM2=100
      NI=50
      ALPHA=20.
   12 DO 13 J=1,N
      BPSL(J)=0.
      BPSR(J)=0.
      BPSNL(J)=0.
      BPSNR(J)=0.
      DO 13 I=1,M
      PSN(I,J)=0.
      PSO(I,J)=0.
      PSM1(I,J)=0.
      VN(I,J)=0.
      VO(I,J)=0.
   13 VM1(I,J)=0.
      DO 14 I=1,M
      BPSB(I)=0.
      BPST(I)=0.
      BPSNB(I)=0.
   14 BPSNT(I)=0.
      GO TO (1,2),NORUN
    1 RC=.6*R/PI
      DO 21 I=1,M
   21 BPST(I)=RC
      N3=N/3
      DO 22 J=2,NM1
      BPSL(J)=RC/2.*(1.-COSF(PI*MINOF(J-1,N3)/FLOATF(N3)))
   22 BPSR(J)=BPSL(J)
      RETURN
    2 RETURN
      END(1,0,0,0,0,1,1,0,0,1,0,0,0,0,0)
```

```
      SUBROUTINE PEACE
```

```
      SUBROUTINE PEACE
      DIMENSION PSN(61,31),PSO(61,31),PSM1(61,31),VN(61,31),VO(61,31),
     1VM1(61,31),VMS(61,31),VT(61,31),BPSL(31),BPSR(31),BPSB(61),BPST(61
     2),BPSNL(31),BPSNR(31),BPSNB(61),BPSNT(61)
      DIMENSION PRA(61),PRB(61),PRC(61),PRC(61),PRE(61),PRF(61)
      COMMON PSN,PSO,PSM1,VN,VO,VMS,AB,AC,AD,AE,AF,AG,AH,N,NM1,NM2,NM3,M
     1,MM1,MM2,MM3,K5,K6,K7,NI,IIM2,NP,NDT,NDTF,DX,DT,TMAX,C,CO,COA,DAP,
     2DAP2,DAV2,NORUN,NORUNS,BPSL,BPSR,BPSB,BPST,BPSNL,BPSNR,BPSNB,BPSNT
     3,ALPHA,PI,VM1,VT,R,T,JJ,II,DAPP,DX2
105   DO 109 J=2,NM1
      DO 106 I=2,MM1
      PSAST=AC*(PSN(I,J+1)+PSO(I,J+1)-PSN(I,J-1)-PSO(I,J-1))
      PRA(I)= -AD - PSAST
      PRC(I)= -AD + PSAST
106   PRD(I)=AE*VO(I,J)+AD*(VO(I,J+1) - 2.*VO(I,J)+VO(I,J-1))
     1+AB*(VO(I,J+1)-VO(I,J-1))*(PSO(I+1,J) - PSO(I-1,J))
      PRD(2)=PRD(2)-PRA(2)*VMS(1,J)
      PRD(MM1)=PRD(MM1)-PRC(MM1)*VMS(M,J)
      PRB(2)=PRC(2)
      PRE(2)=PRD(2)
      DO 107 K=3,MM2
      PRB(K)=PRC(K)/(1.-PRA(K)*PRB(K-1))
107   PRE(K)=(PRD(K)-PRA(K)*PRE(K-1))/(1.-PRA(K)*PRB(K-1))
      VMS(MM1,J)=(PRD(MM1)-PRA(MM1)*PRE(MM2))/(1.-PRA(MM1)*PRB(MM2))
      DO 108 K=1,MM3
      L=MM1-K
108   VMS(L,J)=PRE(L)-PRB(L)*VMS(L+1,J)
109   CONTINUE
110   DO 115 I=2,MM1
      DO 111 J=2,NM1
      PSNP1=AB*(PSN(I+1,J)-PSN(I-1,J))
      PRA(J)=-AD+PSNP1
      PRC(J)=-AD-PSNP1
111   PRD(J)= AE*VMS(I,J)+AD*(VMS(I+1,J)-2.*VMS(I,J)+VMS(I-1,J))
     1-AC*(VMS(I+1,J)-VMS(I-1,J))*(PSN(I,J+1)+PSO(I,J+1)-PSN(I,J-1)
     2-PSO(I,J-1))
      PRD(2)=PRD(2)-PRA(2)*VN(I,1)
      PRD(NM1)=PRD(NM1)-PRC(NM1)*VN(I,N)
      PRB(2)=PRC(2)
      PRE(2)=PRD(2)
      DO 112 K=3,NM2
      PRB(K)=PRC(K)/(1.-PRA(K)*PRB(K-1))
112   PRE(K)=(PRD(K)-PRA(K)*PRE(K-1))/(1.-PRA(K)*PRB(K-1))
      PRF(NM1)=(PRD(NM1)-PRA(NM1)*PRE(NM2))/(1.-PRA(NM1)*PRB(NM2))
      DO 113 K=1,NM3
      L=NM1-K
113   PRF(L)=PRE(L)-PRB(L)*PRF(L+1)
      DO 114 J=2,NM1
114   VN(I,J)=CO*VN(I,J)+(1.-CO)*PRF(J)
115   CONTINUE
      RETURN
      END(1,0,0,0,0,1,1,0,0,1,0,0,0,0)
```

```
      SUBROUTINE SOR
      SUBROUTINE SOR
      DIMENSION PSN(61,31),PSO(61,31),PSM1(61,31),VN(61,31),VO(61,31),
     1VM1(61,31),VMS(61,31),VT(61,31),BPSL(31),BPSR(31),BPSB(61),BPST(61
     2),BPSNL(31),BPSNR(31),BPSNB(61),BPSNT(61)
      COMMON PSN,PSO,PSM1,VN,VO,VMS,AB,AC,AD,AE,AF,AG,AH,N,NM1,NM2,NM3,M
     1,MM1,MM2,MM3,K5,K6,K7,NI,IIM2,NP,NDT,NDTF,DX,DT,TMAX,C,CO,COA,DAP,
     2DAP2,DAV2,NORUN,NORUNS,BPSL,BPSR,BPSB,BPST,BPSNL,BPSNR,BPSNB,BPSNT
     3,ALPHA,PI,VM1,VT,R,T,JJ,II,DAPP,DX2
  200 II=0
  201 EE=0.
      DO 208 J=2,NM1
      DO 207 I=2,MM1
      PSNEW=AG*PSN(I,J)+AH*(PSN(I-1,J)+PSN(I+1,J)+PSN(I,J-1)
     1+PSN(I,J+1))+AF*VN(I,J)
      EE=MAX1F(EE,ABSF(PSN(I,J)-PSNEW))
  207 PSN(I,J)=PSNEW
  208 CONTINUE
      II=II+1
  260 IF(EE-DAPP) 265,265,261
  261 IF (II-500) 201,201,262
  262 WRITE OUTPUT TAPE 6,263,T,JJ,EE
  263 FORMAT(27H SOR FAILS TO CONVERGE, T= E14.6,8H    JJ = I4,8H    EE =
     1 E14.6)
      SENSE LIGHT 1
      RETURN
  265 IF(II-1)296,296,299
  296 IF(DAPP-DAP2-.0000001)299,299,297
  297 DAPP=DAP2
  298 GO TO 201
  299 GO TO (254,266),NP
  266 WRITE OUTPUT TAPE 6,267,JJ,EE,II
  267 FORMAT (  /14H ON ITERATION I4,24H,     THE TOLERANCE EE = E14.7,
     1 15H WAS MET AFTER I4,8H SWEEPS.)
  254 RETURN
      END(1,0,0,0,0,1,1,0,0,1,0,0,0,0,0)
```

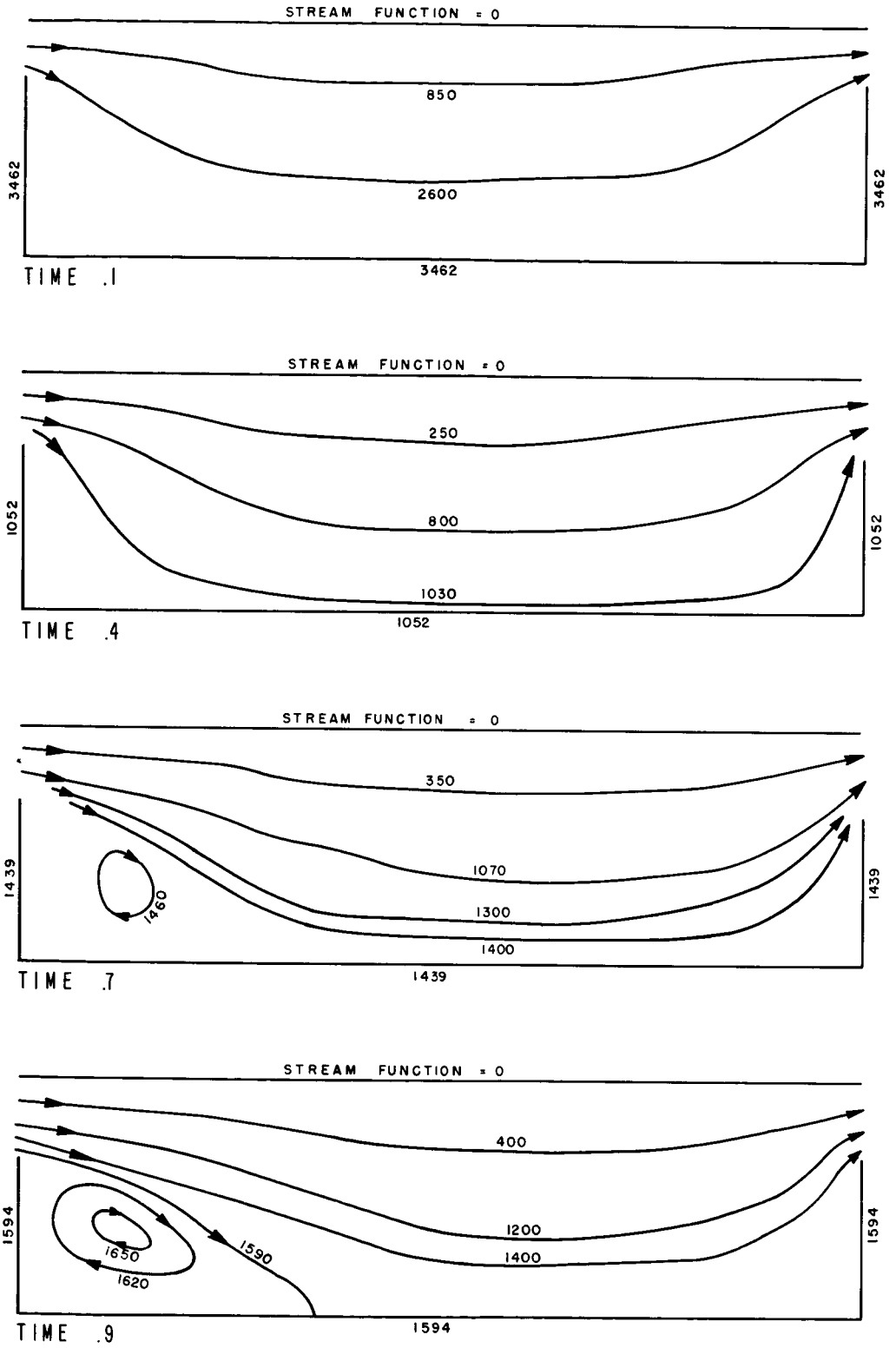

FIG. I.I-6 STREAMLINE PATTERN FROM NUMERICAL SOLUTION

(APPENDIX II)

1.2 Proposed Dynamic Test Standards for NOR and NAND Fluid Digital Amplifiers with Some Preliminary Experimental Results

1.2.1 Introduction

There is a scarcity of dynamic test data for digital fluid amplifiers in the literature; furthermore, such test data as are available are not based on accepted test standards, which would allow correlation of results and computation of dimensionless parameters such as some form of Strouhal Number. (See 1.2.2.2.5 for Strouhal Number definition.) For digital amplifiers, unlike proportional amplifiers, it has not been found possible to predict dynamic effect (such as encountered in a complex active circuit) by testing the component in a purely passive circuit; this is due to the very high range of frequencies which are excited by the fast switching transient. A quasi-steady-state lumped parameters analysis cannot yield adequate information under such conditions, while it appears to be useful for much slower analog amplifiers and circuits. Standard test procedures must be arrived at, whereby realistic transient conditions are imposed on the test unit, both on the input and on the output side. Since the transient effects can feedback upstream and propagate downstream, it is considered necessary that a minimum of two active levels be present both upstream and downstream of the test component, to bring out any complex dynamic and acoustic effects which may be present. Furthermore jet Mach Number and Reynolds Number must be presented, to correlate steady-state flow parameters with the dynamic time data.

1.2.2 Proposed Dynamic Test Standards

Dynamic test standards are proposed in this paper for a limited class of digital fluid amplifiers, i.e., NOR and NAND active amplifiers with a maximum fan-in of three and a maximum fan-out of four. The fan-in and fan-out limitation has been imposed arbitrarily in order to reduce the experimental complexity until sufficient experimental data have been accumulated. The proposed test circuits are shown in Figures 1.2.2-1, 1.2.2-2 and 1.2.2-3 for a fan-in of one, two and three respectively. A visual inspection of the test circuits shows that there are always two active amplifiers both upstream and downstream of the test unit; all units are meant to be identical, operating at the same supply pressure. Also, if a fan-in of one (for example) is intended for the test unit, then all units have a fan-in of one; if a fan-out of three (for example) is intended for the test unit, then all units have a fan-out of three. When multiple fan-in is used, as in Figure 1.2.2-2 and 1.2.2-3, only one input is used dynamically, while the others are kept ON or OFF in steady-state. For a fan-in of one and a fan-out up to four, seventeen amplifiers are required by the test circuit, as seen in Figure 1.2.2-1. For a fan-in of two and a fan-out up to four, twenty-one amplifiers are required by the test circuit, as seen in Figure 1.2.2-2. For a fan-in of three and a fan-out up to four, twenty-five amplifiers are required by the test circuit, as seen in Figure 1.2.2-3.

1.2.2.1 Test Procedure. The following procedures are common to all three test circuits:

a) Operate fluid pulse generator at variable pulse frequency f, 50% duty cycle.

b) Interconnecting lines: constant length L and diameter D for all lines.

c) Measure supply weight flow W.

d) Measure supply chamber pressure P_s and dump pressure P_a; also corresponding temperatures T_s and T_a.

1.2.2.1.1 Standard Test Circuit I - Fan-in of one (Figure 1.2.2-1).

a) Test first with fan-out of 1, omitting components 2, 3, 4, 6, 7, 8, 10, 11, 12, 14, 15 and 16.

Next test with fan-out of 2, omitting components 2, 3, 6, 7, 10, 11, 14 and 15.

Next test with fan-out of 3, omitting components 2, 6, 10 and 14.

Finally test with fan-out of 4, including all components as shown.

b) Before each test, determine that circuit 1-5-9-13-17 is working properly with the fluid pulses supplied by fluid pulse generator; display on oscilloscope hot-wire signal from flow meters 1 and 8. Determine maximum operable pulse frequency, f_M. for each condition of fan-out.

c) For each test, display hot-wire signals from flow meters 2 and 6, 2 and 5, 2 and 4, 2 and 3, on oscilloscope and record on film. Employ several pulse frequencies, f, up to f_M.

d) From calibrated oscilloscope film, translate voltage vs time plots into flow rate vs time plots (using hot-wire calibration curve). Test data may be fed directly to a computer, which then would perform the functions below:

Determine 10% and 90% flow points on the time scale.
Determine switch-ON time, t_n, from 10% input to 90% output flow.
Determine rise-time, t_r, from 10% output to 90% output flow.
Determine switch-OFF time, t_f, from 90% input to 10% output flow.
Determine decay time, t_d, from 90% output to 10% output flow.

Note that the above applies to inverse amplifiers.

Use data from flowmeters 2 and 6, provide that 3, 4 and 5 are in reasonable agreement.

1.2.2.1.2 Standard Test Circuit II - Fan-in of Two (Figure 1.2.2-2).

a) Test first with fan-out of 1, omitting components 6, 7, 8, 10, 11, 12, 14, 15, 16, 18, 19 and 20.

Next test with fan-out of 2, omitting components 6, 7, 10, 11, 14, 15, 18 and 19.

Next test with fan-out of 3, omitting components 6, 10, 14 and 18.

Finally, test with fan-out of 4, including all components as shown.

b) For NOR gates, components 2, 3, 4 and 5 must be kept in OFF conditon; corresponding solenoid valves must be OPEN, allowing input flow to the respective components. For NAND gates, components 2, 3, 4 and 5 must be kept in ON condition; corresponding solenoid valves must be CLOSED.

c) Before each test, determine that circuit 1-9-13-17-21 is working properly with the fluid pulses supplied by the fluid pulse generator; display on oscilloscope hot-wire signal from flowmeters 1 and 9. Determine maximum operable pulse frequency, f_M, for each condition of fan-out.

d) For each test, display hot-wire signals from flowmeters 2 and 6, 2 and 5, 2 and 4, 2 and 3 on oscilloscope and record on film. Check flowmeter 7 for steady-state input (zero for NOR gates, positive for NAND gates). Employ several pulse frequencies f up to f_M.

e) From calibrated oscilloscope film, translate voltage vs time plots into flow-rate vs time plots (using hot-wire calibration curve). Test data may be fed directly to a computer, which then would perform the functions below:

Determine 10% and 90% flow points on the time scale.
Determine switch-ON time, t_n, from 10% input to 90% output flow.
Determine rise-time, t_r, from 10% output to 90% output flow.
Determine switch-OFF time, t_f, from 90% input to 10% output flow.
Determine decay-time, t_d, from 90% output to 10% output flow.

Note that the above applies to inverse amplifiers.

Use data from flowmeters 2 and 6, provided that 3, 4 and 5 are in reasonable agreement.

f) For NOR gates, keep component 3 on ON condition (solenoid valve closed) and check output transient on flowmeter 6 against input pulse on flowmeter 2. Transient is deemed to be negligible if output of component 17 on flowmeter 8 is not affected by it. For NAND gates, keep component 3 in OFF condition (solenoid valve open) and check output transient on flowmeter 6 against input pulse on flowmeter 2. Transient is deemed to be negligible if output of component 17 on flowmeter 8 is not affected by it.

1.2.2.1.3 Standard Test Circuit III - Fan-in of Three (Figure 1.2.2-3).

a) Test first with fan-out of 1, omitting components 10, 11, 12, 14, 15, 16, 18, 19, 20, 22, 23 and 24.

Next test with fan-out of 2, omitting components 10, 11, 14, 15, 18, 19, 22 and 23.

Next test with fan-out of 3, omitting components 10, 14, 18 and 22.

Finally test with fan-out of 4, including all components as shown.

b) For NOR gates, components 2, 3, 4, 5, 6, 7, 8 and 9 must be kept in the OFF condition; corresponding solenoid valves must be OPEN, allowing input flow to the respective components. For NAND gates, components 2, 3, 4, 5, 6, 7, 8 and 9 must be kept in the ON condition; corresponding solenoid valves must be CLOSED.

c) Before each test, determine that circuit 1-13-17-21-25 is working properly with the fluid pulses supplied by the fluid pulse generator; display on oscilloscope hot-wire signal from flowmeters 1 and 10. Determine maximum operable pulse frequency, f_M, for each condition of fan-out.

d) For each test, display hot-wire signals from flowmeters 2 and 6, 2 and 5, 2 and 4, 2 and 3 on oscilloscope and record on film. Check flowmeters 7 and 8 for steady-state inputs (zero for NOR gates, positive for NAND gates). Employ several pulse frequencies, f, up to f_M.

e) From calibrated oscilloscope film, translate voltage vs time plots into flow-rate vs time plots (using hot-wire calibration curve).

Test data may be fed directly to a computer, which then would perform the functions below:

Determine 10% and 90% flow points on the time scale.
Determine switch-ON time, t_n, from 10% input to 90% output flow.
Determine rise-time, t_r, from 10% output to 90% output flow.
Determine switch-OFF time, t_f, from 90% input to 10% output flow.
Determine decay time, t_d, from 90% output to 10% output flow.

Note that the above applies to inverse amplifiers.

Use data from flowmeters 2 and 6, provided that 3, 4 and 5 are in reasonable agreement.

f) For NOR gates, keep component 4 in ON condition (solenoid valve closed) and check output transient on flowmeter 6 against input pulse on flowmeter 2. Repeat with components 4 and 5 in ON condition. Transient is deemed to be negligible if output of component 21 on flowmeter 9 is not affected by it.

For NAND gates, keep component 4 in OFF condition (solenoid valve open) and check output transient on flowmeter 6 against input pulse on flowmeter 2. Repeat with components 4 and 5 in OFF condition. Transient is deemed to be negligible if output of component 21 on flowmeter 9 is not affected by it.

1.2.2.2 Presentation of Data

1.2.2.2.1 Steady-state flow data:

Supply pressure	P_s
Dump pressure	P_a

1.2.2.2.1 Steady-state flow data: (continued)

Supply temperature	T_s
Dump temperature	T_a
Weight flow	W

1.2.2.2.2 Fluid Characteristics:

Name of gas	
Absolute viscosity @ dump	μ_a
Ratio of specific heats	γ
Gas constant	R
Mass density @ dump	ρ_a

1.2.2.2.3 Steady-state Flow Parameters:

Speed of sound	$C = \sqrt{\gamma R T_a}$
Pressure ratio	P_s/P_a
Temperature ratio	T_s/T_a
Jet Mach Number	$M_j = \frac{W\sqrt{T_s}}{gA_jP_s} \quad \frac{P_s}{P_a} \quad \sqrt{\frac{T_a}{T_s}} \quad \sqrt{\frac{R}{\gamma}}$
Jet velocity	$U_j = M_j\, c$
Jet Reynolds Number	$Re = \frac{u_j b \rho_a}{\mu_a}$
Adiabatic Fluid Power	$AFP = W \frac{R\,T_a}{\frac{\gamma-1}{\gamma}} \left[\left(\frac{P_s}{P_a} \right)^{\frac{\gamma-1}{\gamma}} - 1 \right]$

It is to be noted that the jet velocity, with its concomitant Reynolds Number and Mach Number, is the primary reference quantity for the correlation of time data, rather than the mere supply pressure P_s or the pressure ratio P_s/P_a.

1.2.2.2.4 Dynamic Time Data:

a. Fan-in of One

Line Length L = ...
Line Diameter D = ...

Fan-out	Times	Pulse Frequency				
		f_1	f_2	f_3	f_4	f_M
1	t_n					
	t_r					
	t_f					
	t_d					
2	t_n					
	t_r					
	t_f					
	t_d					
3	t_n					
	t_r					
	t_f					
	t_d					
4	t_n					
	t_r					
	t_f					
	t_d					

b. Fan-in of Two

L = ...
D = ...

Same as above.

c. Fan-in of Three

L = ...
D = ...

Same as above.

1.2.2.2.5 Dynamic Time Parameters: The dynamic time parameters will be expressed in the form of Strouhal Numbers, with time or frequency (as appropriate), jet velocity and jet width.

$$St = \frac{U_j t}{b}$$

$$Sf = \frac{bf}{U_j}$$

Depending on the results of the dynamic test data above, a summary table of time parameters will be presented below. For instance, assuming that the times have negligible dependence on fan-out, the following table will be compiled:

Summary Table - Dynamic Parameters

Fan-in	Times	Pulse Frequency					
		Sf_1	Sf_2	Sf_3	Sf_4	Sf_5	Sf_M
1	St_n						
	St_r						
	St_f						
	St_d						
2	St_n						
	St_r						
	St_f						
	St_d						
3	St_n						
	St_r						
	St_f						
	St_d						
					Line Length L/b:		
					Line Diameter D/b:		

1.2.3 Preliminary Experimental Results

A preliminary experimental investigation has been carried out to explore the usefulness and practicability of the proposed test standards, using fifteen identical NOR amplifiers and twin DISA hot-wire anemometers.

1.2.3.1 Axisymmetric Focussed-Jet NOR Amplifier. The NOR device used in the investigation is the axisymmetric focussed-jet amplifier developed prior to this contract by the Sperry Utah Company (patent pending). A thin jet is made to issue from an annular slot of very high aspect ratio $\frac{\pi d}{b} > 200$ at an inward angle with a base plate; an axisymmetric Coanda effect takes place, forcing the jet to adhere to the baseplate and to issue forth as a central "focussed" stream. Figure 1.2.3.1 shows the detail of the fluid interaction region: the jet width is approximately only 0.010" and the control width is also 0.010"; the jet angle to the base plate is about 30^0. The flow is picked up by the flared output tube and then split into several output leads. Figure 1.2.3-2 presents a typical four-unit assembly with a common supply duct and chamber; the multiple input and output tubes are built-in and need only to be interconnected by Tygon tubing. Many units can be built in extremely rugged multiple assemblies, without problems of sealing and dirt contamination; the annular slot has proved to be highly self-cleaning under adverse conditions of supply and environment.

1.2.3.2 Test Procedure. The test circuit used in this preliminary investigation is shown in Figure 1.2.3-3. It is a simplified version of the proposed Standard Test Circuit III (fan-in of three) shown in Figure 1.2.2-3 do to the availability of only fifteen amplifiers. The fan-out of three and the multiple fan-in is limited to the test unit (#7) above. Unit #1 if fed a train of fluid pulses @ 15 cps from a mechanical slotted-disc-and-jet signal generator. The amplitude of the pulse is that just sufficient to cause switching. Unit #1 fans out into #2, #3 and #4; in its turn, unit #4 fans out into #5, #6 and #7. Now unit #7 is the fluid amplifier under test; it is provided with three inputs, from #4 (as shown before) and also from units #14 and #15. These units are both kept either ON or OFF in steady-state by solenoid-controlled inputs. Thus unit #7 has a pulsed input from #4 and steady-state inputs from #14 and #15. Downstream, unit #7 fans out into #8, #9 and #10. Unit #9 in its turn fans out into #11, #12 and #13. All the interconnecting tubing lengths are 18" of 1/8" I.D. Tygon; all the outputs of all the units are provided with an 18" length of tubing; the required outputs are connected to the respective inputs, while the unneeded outputs dump to atmosphere. No special provisions or "tuned" resistances are used in the interconnecting lines. For all test the common air supply pressure was held at 5 PSIG with atmospheric dump and a temperature of 72^0F. Hot-wire stations 1-A, 2-A, 3-A and 4-A are connected to one DISA anemometer through a DISA 4-way switch; hot-wire stations 1-B, 2-B, 3-B and 4-B are connected to the second DISA anemometer through another DISA 4-way switch; thus any A hot-wire may be displayed on the oscilloscope against any B hot-wire.

1.2.3.3 Test Results. The first test is from hot-wire station 1-A to station 4-B, i.e., across the entire chain of logic; Figure 1.2.3-4 displays the hot-wire oscilloscope photos, with units #14 and #15 ON and also with #14 and #15 OFF. It is seen that the operation is correct, i.e., with #14 and #15 OFF, the pulses go through with good waveform fidelity, while with #14 and #15 ON, the output at station 4B is ON in steady state. The leading edge of the pulse appears to be

clean and devoid of wave reflection, while the trailing edge of the pulses seems to be always accompanied by a wave-decay pattern. The damping is high at station 1-A and lower at station 4-B.

Figure 1.2.3-5 presents the traces of hot-wire stations 3-A and 3-B, across test unit #7. With units #14 and #15 in the OFF state, there is a normal input pulse (3-A) and output pulse (3-B); both pulses are much noisier than in the proceding figure. However, with units #14 and #15 ON, the input pulse (3-A) has disappeared, because there is an upstream directed flow feedback from #14 and #15 which is bucking the downstream-directed input pulse; there are only negative spikes at the leading and trailing edges of the input pulse. The output (3-B), which is steady-state ON, shows a very high level of fluctuations and a slight flow decrease at the time-location of the input pulse; such fluctuations, however, do not affect the downstream unit #9 (as demonstrated by Figure 1.2.3-4). By definition since the downstream unit #9 is not affected, such fluctuations may be termed negligible.

Since the #4 output into #7 was affected by the feedback from #14 and #15, when #14 and #15 are ON, the question arises whether all output from #4 are so affected. Figure 1.2.3-6 shows the traces of hot-wire stations 4-A and 3-B and it is seen that output from #4 into #6 (station 4-A) is not affected by #14 and #15; the SUCO amplifier is not disturbed by output feedback in the manner of some other pure fluid devices.

Figure 1.2.3-7 shows the traces of hot-wire stations 3-A and 1-B, to demonstrate the feedback into unit #14 from the input pulses at 3-A. The feedback is felt only as a transient negative spike at the leading edge and trailing edge of the pulse, with causing switching of #14.

Finally, Figure 1.2.3-8 shows a time display of the pulses from 1-A to 4-B and from 1-A to 2-A. From 1-A to 4-B across four amplifiers, there is a time of 8 milliseconds (ms), yielding 2 ms per amplifier plus 1.5 feet of tubing. This result is confirmed by the trace from 1-A to 2-A. Taking 1.5 ms delay time for 1.5 feet of tubing (velocity of sound), the net switching time for the amplifier is of the order of 0.5 ms.

Because the hot-wire measuring stations have not yet been calibrated against total flow, exact times are not reported.

1.2.4 Conclusions

It appears that the proposed test circuits would be operable, at least with the axisymmetric focussed-jet NOR amplifier, and that useful and realistic results can be achieved. In regard to the time data, it should be possible to determine accurately the 10% and 90% flow point on the leading edge of the pulse, while on the trailing edge the 90% flow point will be easy to determine but the 10% flow point will present quite some difficulties. These difficulties are due to the presence of reflected waves which decay with varying amounts of damping.

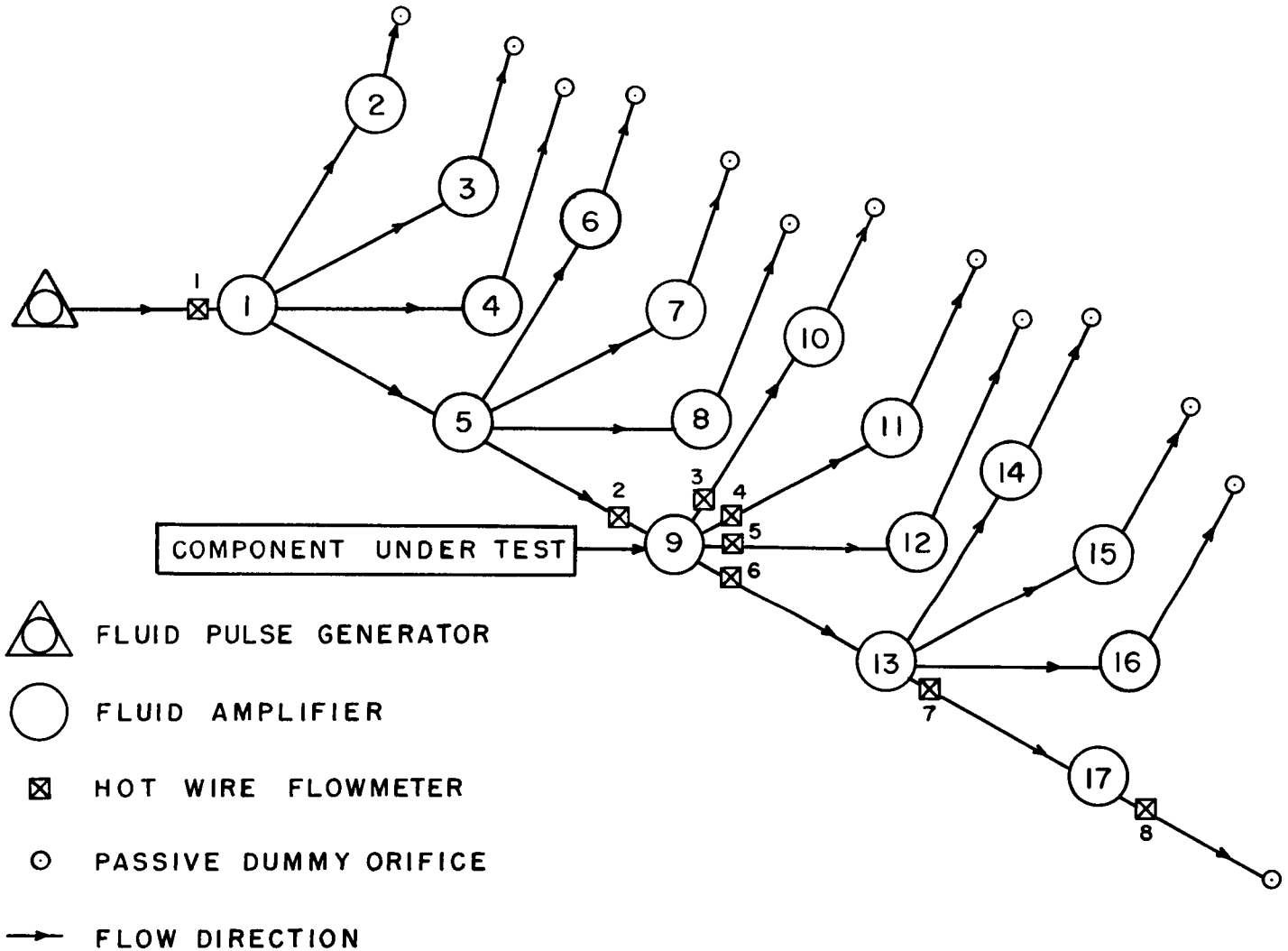

FIG. 1.2.2-1 STANDARD TEST CIRCUIT I
FAN-IN OF ONE - NOR AND NAND FLUID GATES

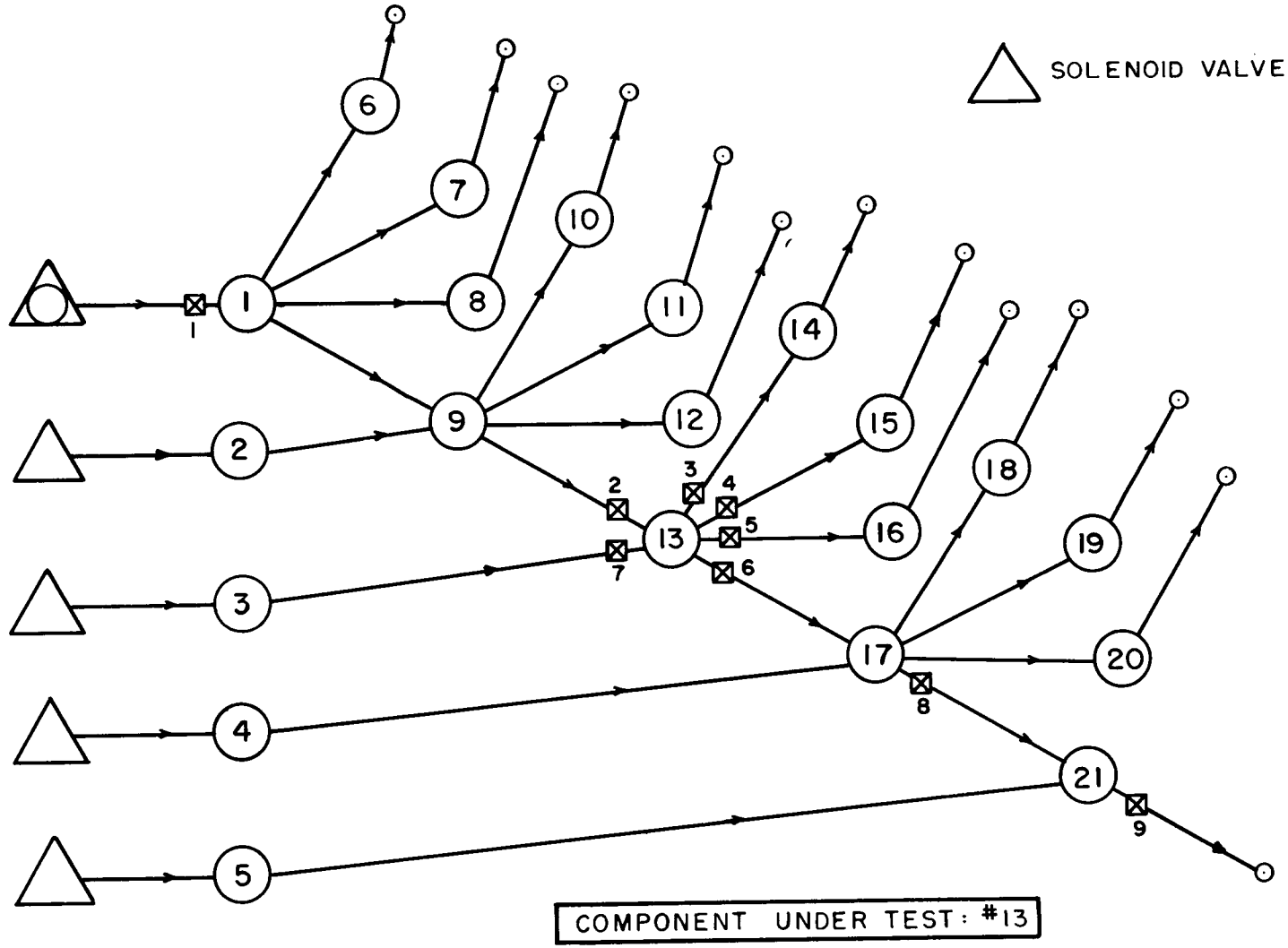

FIG. 1.2.2-2

STANDARD TEST CIRCUIT II

FAN-IN OF TWO-NOR AND NAND FLUID GATES

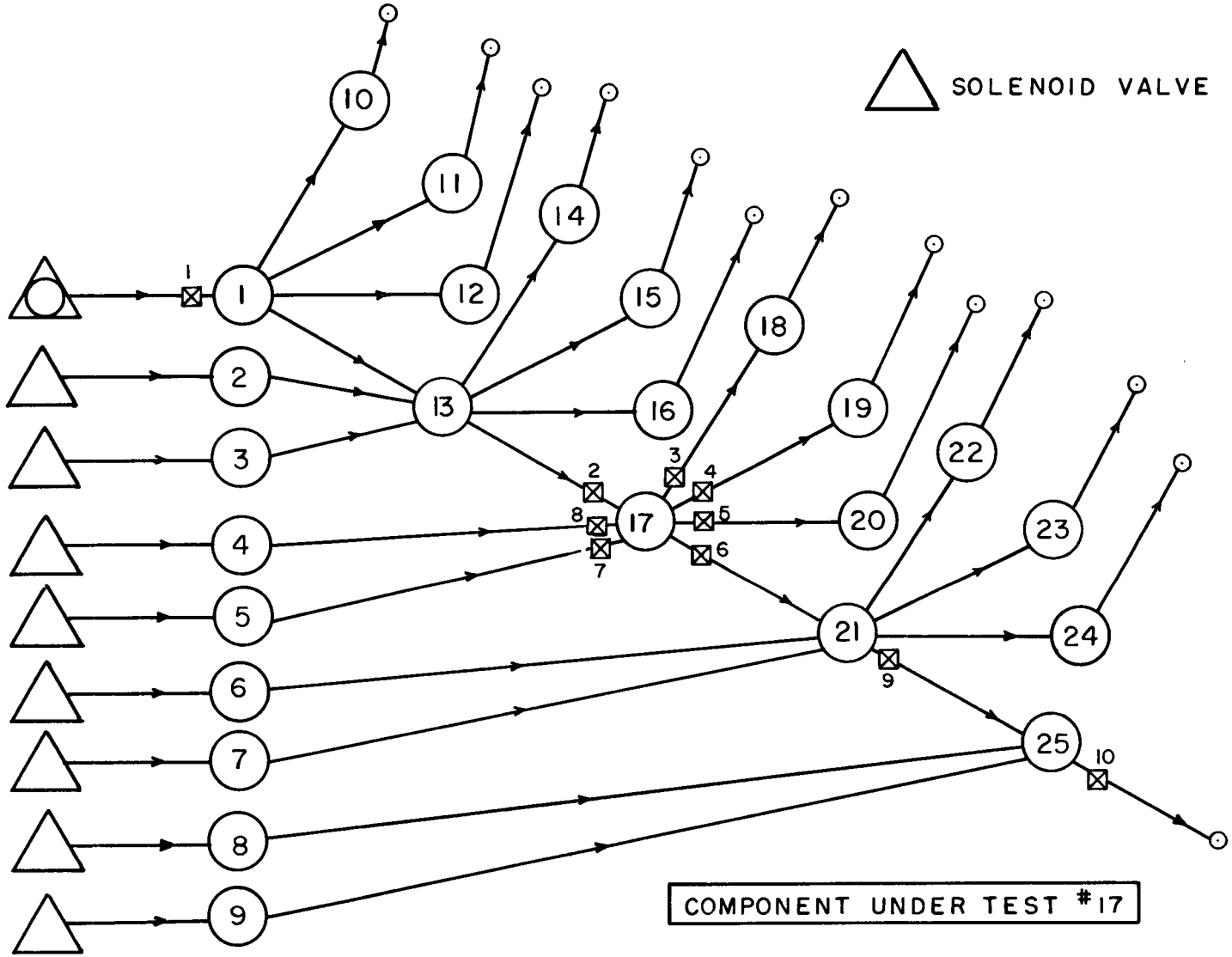

FIG. 1.2.2-3

STANDARD TEST CIRCUIT III

FAN-IN OF THREE- NOR AND NAND FLUID GATES

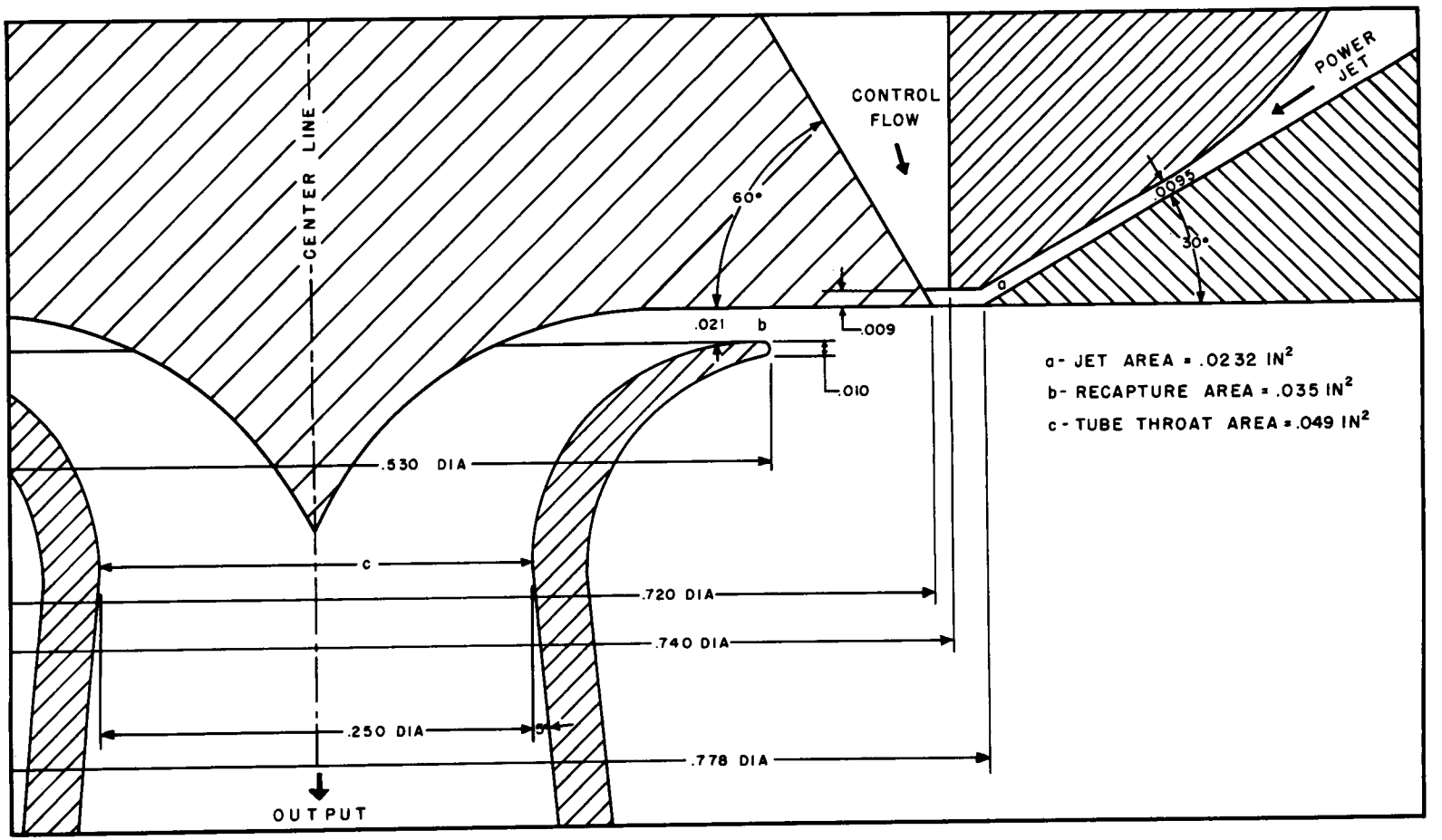

FIG. 1.2.3-1 AXISYMMETRIC FOCUSSED-JET INVERSE FLUID AMPLIFIER
DETAIL OF INTERACTION REGION

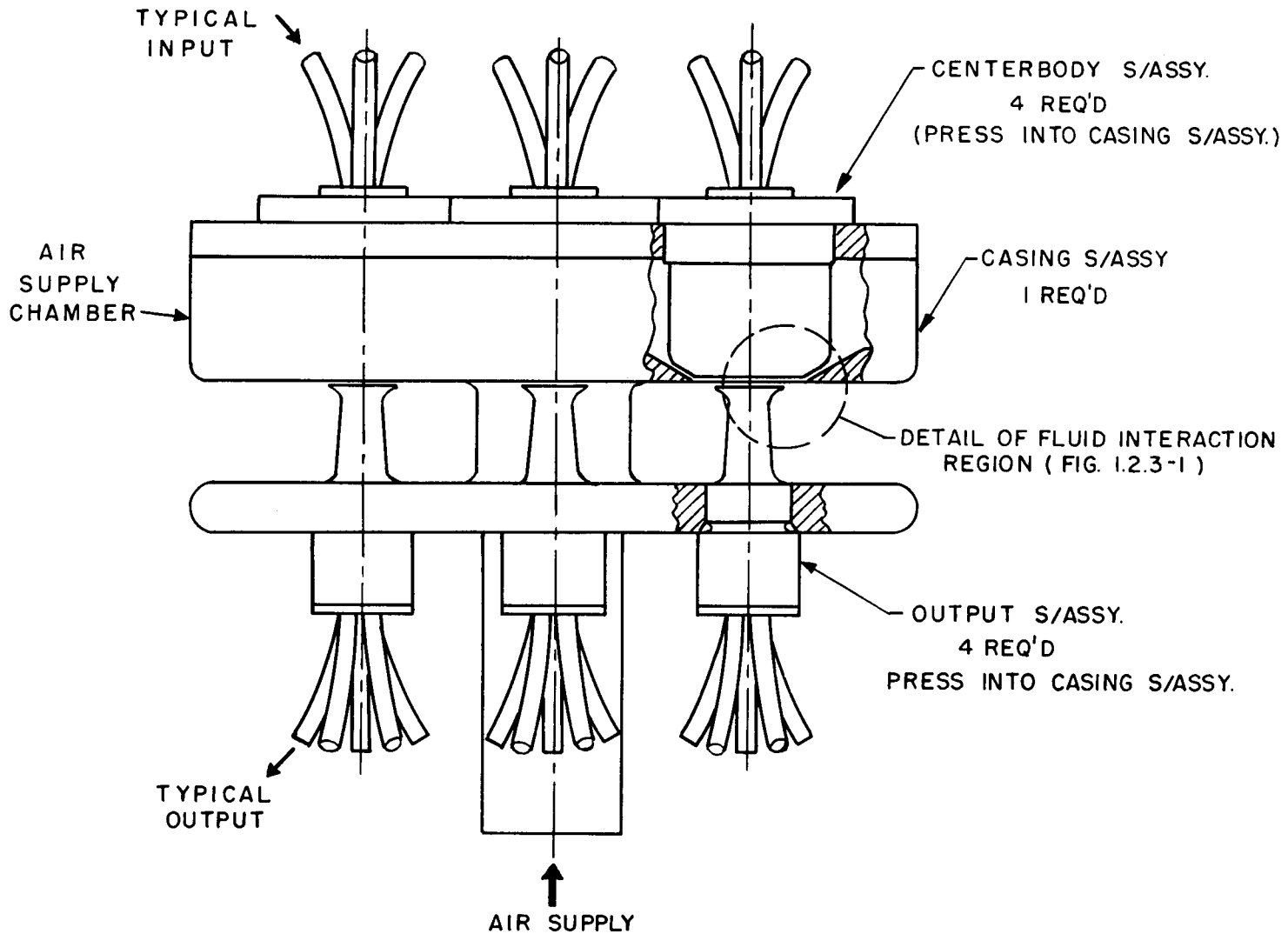

FIG. 1.2.3-2 FOUR-UNIT AXISYMMETRIC AMPLIFIER ASSY., MARK I

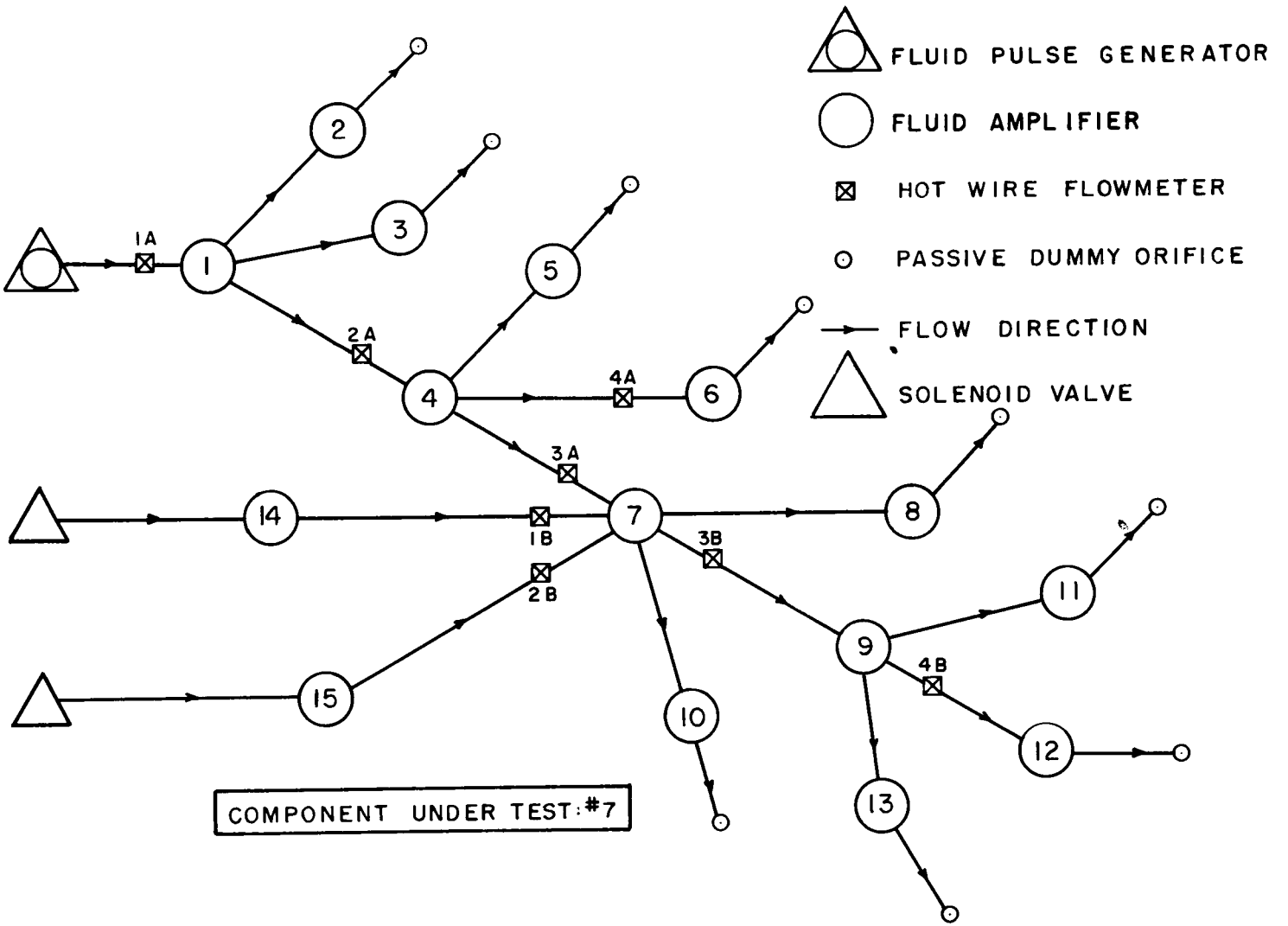

FIG. 1.2.3-3

NOR TEST CIRCUIT
FAN-IN OF 3, FAN-OUT OF 3

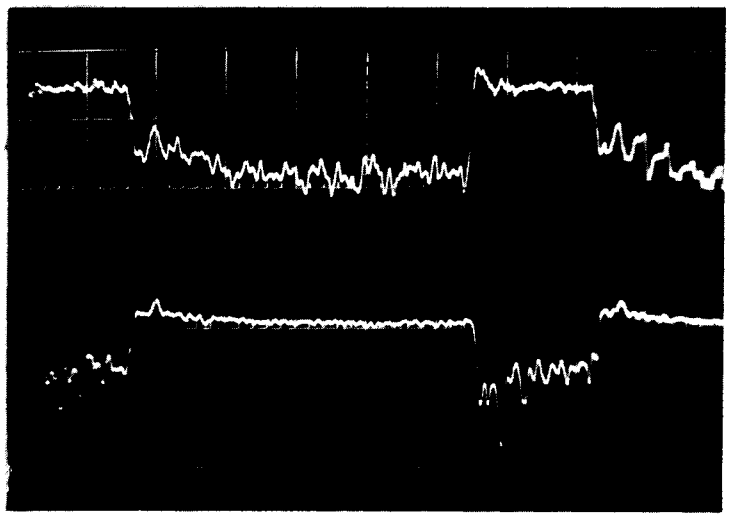

UPPER: HOT-WIRE 3-A
LOWER: HOT-WIRE 3-B
NO. 14 AND NO. 15 OFF STEADY-STATE
HORIZONTAL SWEEP: 10 ms/cm
VERTICAL SWEEP: 2 v/cm

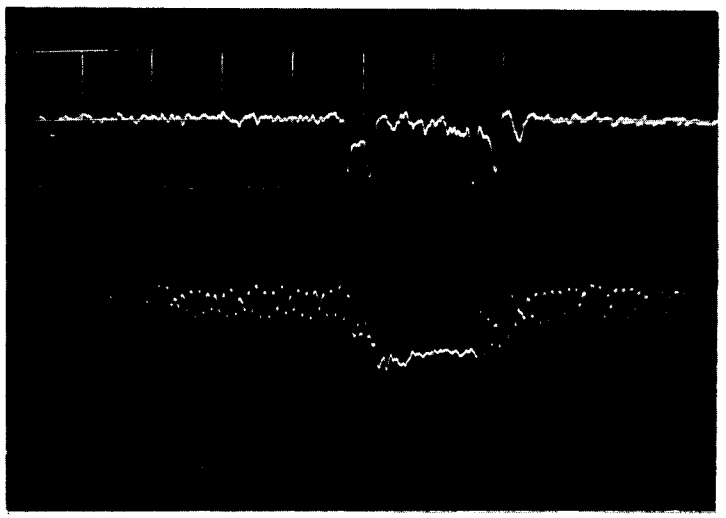

UPPER: HOT-WIRE 3-A
LOWER: HOT-WIRE 3-B
NO. 14 AND NO. 15 ON STEADY-STATE
HORIZONTAL SWEEP: 10 ms/cm
VERTICAL SWEEP: 2 v/cm

Figure 1.2.3-4
Preliminary Test Results -- Hot-wire Oscilloscope Photos.

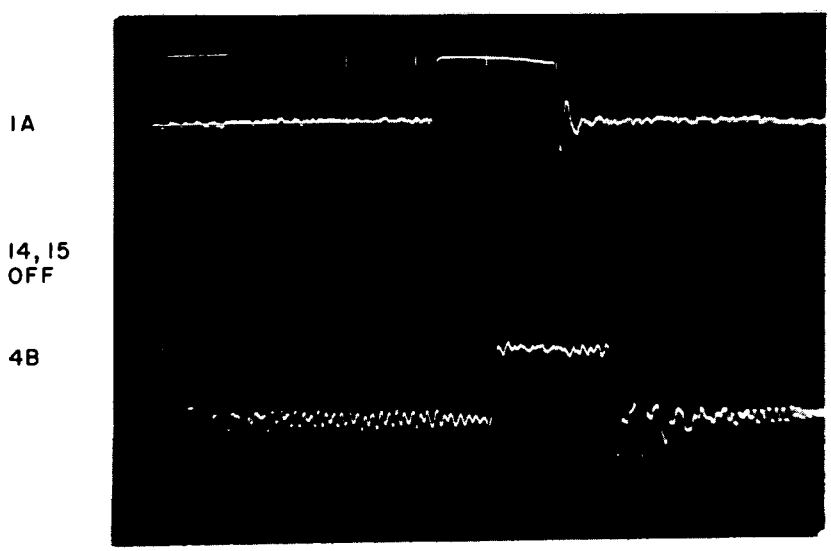

UPPER: HOT-WIRE 1-A
LOWER: HOT-WIRE 4-B
NO. 14 AND NO. 15 OFF STEADY-STATE
HORIZONTAL SWEEP: 10 ms/cm
VERTICAL SWEEP: 2 v/cm

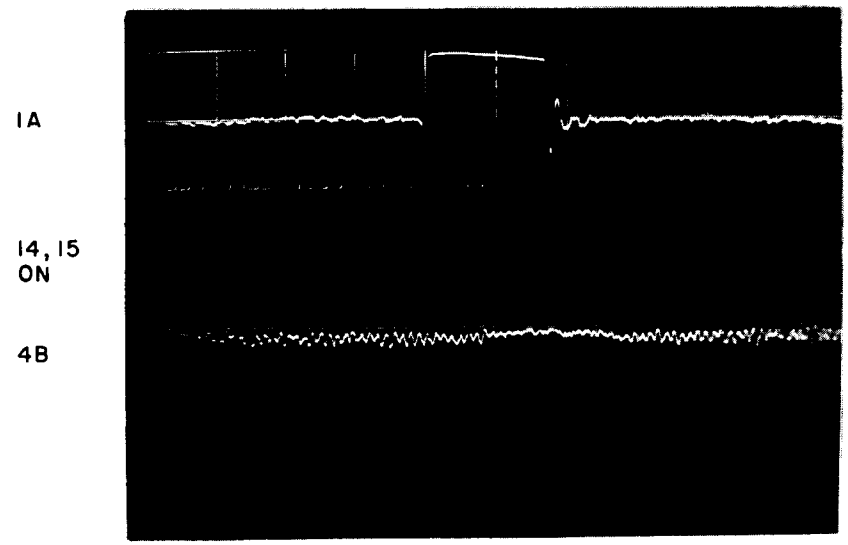

UPPER: HOT-WIRE 1-A
LOWER: HOT-WIRE 4-B
NO. 14 AND NO. 15 ON STEADY-STATE
HORIZONTAL SWEEP: 10 ms/cm
VERTICAL SWEEP: 2 v/cm

Figure 1.2.3-5
Preliminary Test Results -- Hot-wire Oscilloscope Photos.

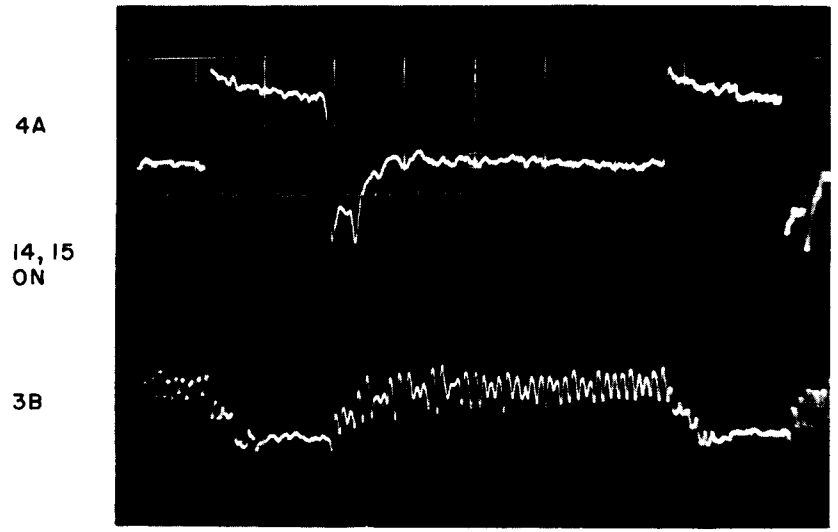

UPPER: HOT-WIRE 4-A
LOWER: HOT-WIRE 3-B
NO. 14 AND NO. 15 ON STEADY-STATE
HORIZONTAL SWEEP: 10 ms/cm
VERTICAL SWEEP: 2 v/cm

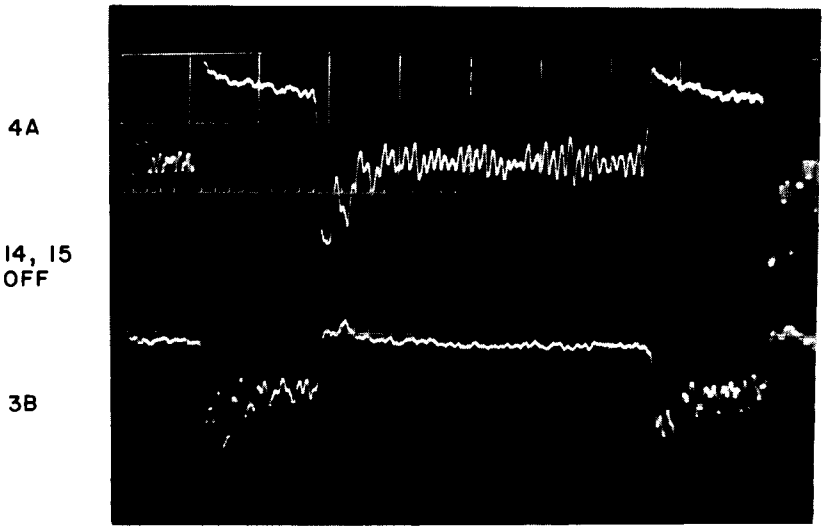

UPPER: HOT-WIRE 4-A
LOWER: HOT-WIRE 3-B
NO. 14 AND NO. 15 OFF STEADY-STATE
HORIZONTAL SWEEP: 10 ms/cm
VERTICAL SWEEP: 2 v/cm

Figure 1.2.3-6
Preliminary Test Results -- Hot-wire Oscilloscope Phots.

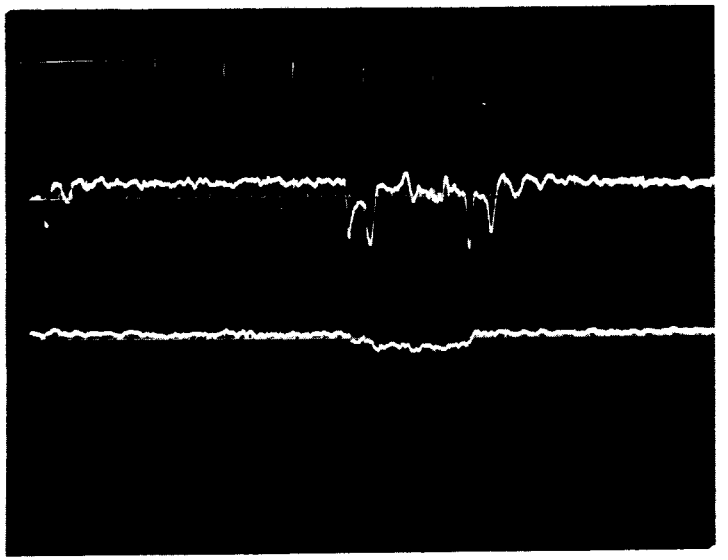

UPPER: HOT-WIRE 3-A
LOWER: HOT-WIRE 1-B
NO. 14 AND NO. 15 ON STEADY-STATE
HORIZONTAL SWEEP: 10 ms/cm
VERTICAL SWEEP: 2 v/cm

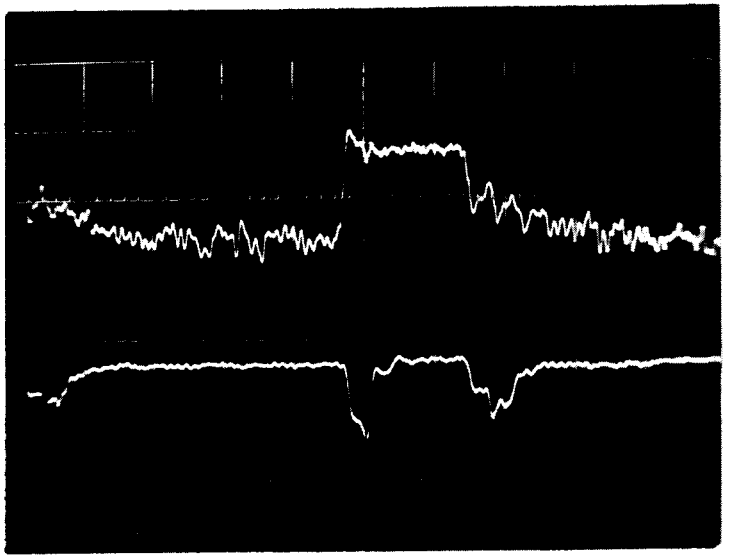

UPPER: HOT-WIRE 3-A
LOWER: HOT-WIRE 1-B
NO. 14 AND NO. 15 OFF STEADY-STATE
HORIZONTAL SWEEP: 10 ms/cm
VERTICAL SWEEP: 2 v/cm

Figure 1.2.3-7

Preliminary Test Results -- Hot-wire Oscilloscope Photos.

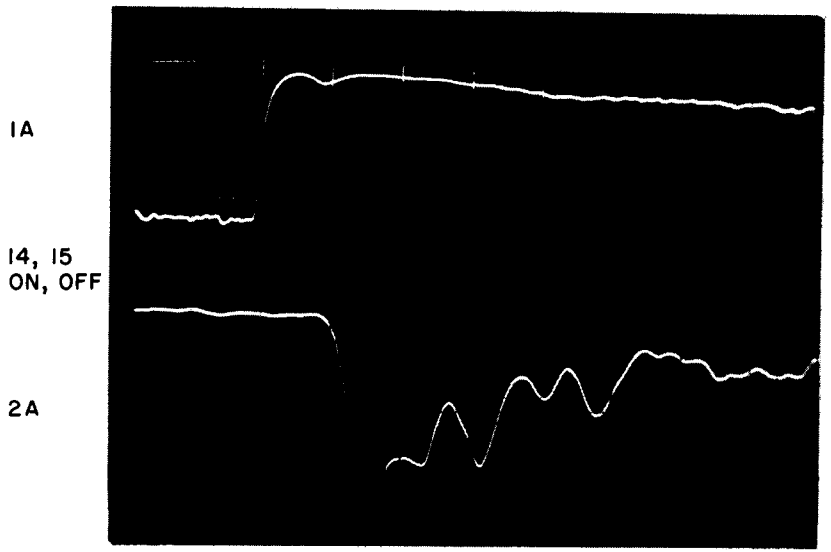

UPPER: HOT-WIRE 1-A
LOWER: HOT-WIRE 2-A
NO. 14 AND NO. 15 EITHER ON OR OFF STEADY-STATE
HORIZONTAL SWEEP: 2 ms/cm
VERTICAL SWEEP: 2 v/cm

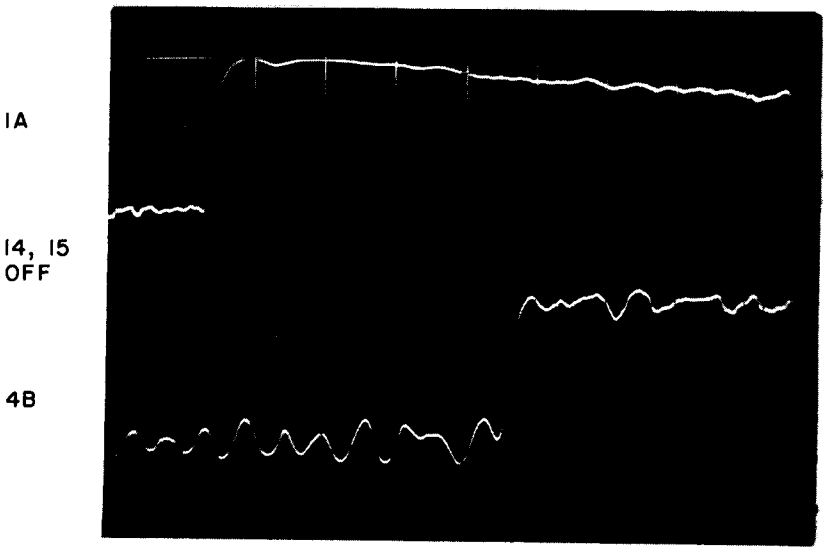

UPPER: HOT-WIRE 1-A
LOWER: HOT-WIRE 4-B
NO. 14 AND NO. 15 OFF STEADY-STATE
HORIZONTAL SWEEP: 2 ms/cm
VERTICAL SWEEP: 2 v/cm

Figure 1.2.3-8

Preliminary Test Results -- Hot-wire Oscilloscope Photos.

1.3 List of References

1. H. Schlichting, "Boundary Layer Theory," Fourth Edition, 1960, McGraw Hill Book Company

2. J. E. Fromm and F. H. Harlow, "Numerical Solution of the Problem of Vortex Street Development," Physics of Fluids, 6, 1963, p. 975

3. J. E. Fromm, "A Method for Computing Nonsteady Incompressible Viscous Fluid Flows," Los Alamos Scientific Laboratory, Report LA-2910, UC-32, September 1963

4. C. E. Pearson, "A Computational Method for Two-Dimensional Time-Dependent Viscous Flow Problems," Sperry Rand Research Center Report SRRC-RR-64-8, 1964

5. D. M. Dix, "The Magnetohydrodynamic Flow Past a Non-Conducting Flat Plate in the Presence of a Transverse Magnetic Field," J. Fluid Mechanics, 15, 1963, p. 449

6. R. B. Payne, "A Numerical Method for Calculating the Starting and Perturbation of a Two-Dimensional Jet," Aero Res. Council R. & M. No. 3047, June 1956

7. J. D. Hellums and S. W. Churchill, "Computation of Natural Convection by Finite Difference Methods," Proc. International Heat Transfer Conference, 1961, p. 985

8. J. D. Hellums and S. W. Churchill, "Transient and Steady State, Free and Natural Convection, Numerical Solutions," A.I. Ch. E. Journal, November 1962, p. 690

9. J. O. Wilkes, "The Finite Difference Computation of Natural Convection in an Enclosed Rectangular Cavity," Ph.D. thesis, University of Michigan, 1963

10. C. E. Pearson, "Numerical Solutions for the Time-Dependent Viscous Flow Between Two Rotating Coaxial Discs," Sperry Rand Research Center Report SRRC-RR-64-41.

11. R. E. Esch, "An Alternative Method of Handling Boundary Conditions and Various Computational Experiments in the Numerical Solution of Time-Dependent Viscous Flow Problems," Sperry Rand Research Center Report SRRC-RR-64-64

1.4 List of Symbols

		Dimensions
A_j	Jet cross-sectional area	$[ft^2]$
AFP	Adiabatic Fluid Power	$\left[\frac{ft\ lb}{sec}\right]$
b	Jet width	$[ft]$
C	Local speed of sound	$[ft/sec]$
c	Control width	$[ft]$
d	Control jet offset	$[ft]$
D	Interconnecting line diameter	$[ft]$
f	Pulse frequency, 50% duty cycle	$\left[\frac{1}{sec}\right]$
f_m	Maximum operable pulse frequency	$\left[\frac{1}{sec}\right]$
L	Interconnecting line length	$[ft]$
M_j	Jet Mach Number	$[0]$
P_s	Supply chamber pressure (abs)	$[lb/ft^2]$
P_a	Dump (ambient) pressure (abs)	$[lb/ft^2]$
R	Gas constant	$[ft/^oR]$
Re	Reynolds Number	$[0]$
St	Strouhal Number (based on time)	$[0]$
Sf	Strouhal Number (based on frequency)	$[0]$
t_n	Switch-ON time - 10% input to 90% output	$[sec]$
t_r	Rise time - 10% output to 90% output	$[sec]$
t_f	Switch-OFF time - 90% input to 10% output	$[sec]$
t_d	Decay time - 90% output to 10% output	$[sec]$
T_s	Supply chamber temperature (abs)	$[^oR]$
T_a	Dump (ambient) temperature (abs)	$[^oR]$
U_j	Power Jet Velocity	$[ft/sec]$
u	Control velocity	$[ft/sec]$

List of Symbols (continued)		Dimensions
θ	Angle of power jet	[degrees]
γ	Ratio of specific heats	[0]
ρ	Fluid mass density	[lb sec^2/ft^4]
ν	Fluid kinematic viscosity	[ft^2/sec]
μ	Fluid absolute viscosity	[lb sec/ft^2]

NOTE: The dimensional notation lb refers to pound force.

DYNAMIC ANALYSIS OF PASSIVE CIRCUITS

2.1. Introduction

The dynamic analysis of passive circuits can become extremely complex in fluid dynamics even at low excitation frequency. Because of such complexity, a very simple passive circuit has been chosen for analysis to illustrate the procedure and to explain the analogous relationships to electrical networks; it has been selected both because the analysis will be comparatively straightforward and because the experimental check will allow accurate measurements. The passive circuit comprises a large pipe, a tube and a closed chamber, as shown below:

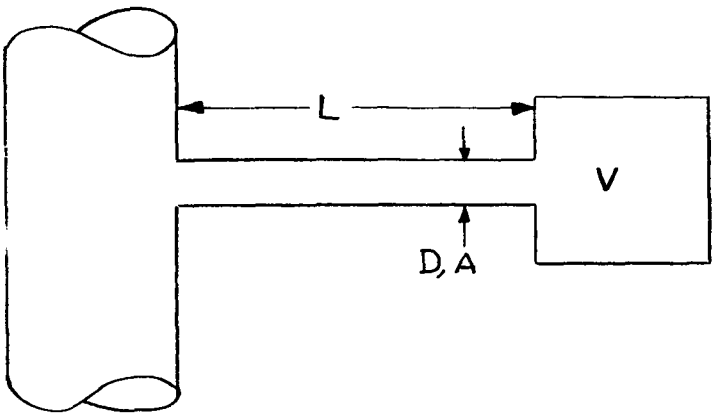

The large pipe applies a sinusoidal oscillatory pressure to the entrance of the tube; the tube, which transmits the pressure, is characterized by a constant cross-sectional area and by its length; the closed chamber is characterized only by its volume. It is assumed that the walls of tube and chamber are completely rigid. The theory will be valid for any gas, however it will be developed first as an elementary theory and then as a more realistic theory comprising fluid compressibility effects, finite pressure variations, fluid acceleration, finite length of tubing and also heat conduction, following the analysis of Iberall[1].

2.2. Elementary Theory

In deriving the elementary theory it is assumed that the steady-state laminar pipe-flow (Poiseuille) law holds at each point in the tube (quasi-steady-state assumption); that the fluid is incompressible in the tube; that the sinusoidal pressure oscillations at the beginning of the tube are of small amplitude compared to the mean absolute pressure (infinitesimal-perturbation assumption); and that, if the fluid is a gas (as against a liquid) it expands and contracts in the chamber isothermally.

These above assumptions applied to a truly incompressible fluid (i.e., liquid) lead to the conclusion that there is no loss of amplitude or phase lag as the liquid would not expand or contract in the chamber.

For the Poiseuille law we may write:

$$\frac{\partial p}{\partial x} = - \frac{128}{\pi} \frac{\mu_o}{D^4} Q \qquad (1)$$

and for continuity:

$$\frac{\partial M}{\partial x} = - A \frac{\partial \rho}{\partial t} \qquad (2)$$

(The subscript o refers to mean conditions)
We infer from continuity and from the incompressibility assumption for the tube (i.e., $\frac{\partial e}{\partial t} = 0$) that the mass flow and the volumetric flow do not vary along the tube with X but vary only with time (the fluid motion is piston-like). By differentiation of eq.1 it is obtained:

$$\frac{\partial^2 p}{\partial x^2} = 0 \quad \text{along the tube.} \qquad (3)$$

Our boundary conditions are that at X = 0 :

$$p = p_o + \Delta p e^{j\omega t} \qquad (4)$$

and that at X = L (entrance to the chamber) :

$$\left.\begin{aligned} Q &= \frac{V}{Po} \frac{\partial p}{\partial t} \quad \text{(isothermal assumption)} \\ \frac{\partial p}{\partial x} &= - \frac{128}{\pi} \frac{\mu_o}{D^4} Q \end{aligned}\right\} \qquad (5)$$

The first line of eq.5 expresses the rate at which a compressible fluid entering a rigid volume builds up pressure isothermally, whereas the second line of eq.5 states that the flow into the volume is limited by the pressure gradient at the end of the tube.

It is convenient to introduce a new variable ξ, the fractional pressure increment, defined as

$$\xi = \frac{p - Po}{Po} \qquad (6)$$

so that eqs. 3, 4 and 5 become respectively:

$$\frac{\partial^2 \xi}{\partial x^2} = 0 \qquad (7)$$

at X = 0 $$\xi = \xi_0 e^{j\omega t} \tag{8}$$

at X = L $$\frac{\partial \xi}{\partial x} = -\frac{128}{\pi} \frac{\mu_o}{p_o} \frac{V}{D^4} \frac{\partial \xi}{\partial t}$$

$$\frac{\partial \xi}{\partial x} = -\frac{\lambda_o}{L} \frac{\partial \xi}{\partial t} \tag{9}$$

where $$\lambda_o = \frac{128}{\pi} \frac{\mu_o}{p_o} \frac{L}{D^4} V$$

$$\lambda_o = 32 \frac{\mu_o}{p_o} \left(\frac{L}{D}\right)^2 \frac{V}{AL} \tag{10}$$

The parameter λ_o is to be interpreted as a time constant of the system since it has the dimensions of time (sec); it comprises the ratio of chamber volume to tube volume, the ratio of tube length to diameter and the ratio of absolute fluid viscosity to mean pressure. It is of further convenience to separate the pressure increment ξ into a part that varies with X and a part that varies with time.

Let $$\xi = \bar{\xi} e^{j\omega t} \tag{11}$$

where $\bar{\xi}$ is the maximum amplitude of the pressure increment at any point in the tube. Our eqs. then become:

$$\frac{d^2 \bar{\xi}}{dx^2} = 0 \tag{12}$$

at X = 0 $$\bar{\xi} = \xi_0 \tag{13}$$

and at X = L $$\frac{d\bar{\xi}}{dx} = -\frac{\lambda_o \omega}{L} j \bar{\xi} \tag{14}$$

The solution of eq. 12, which satisfies eq. 13 and 14 is:

$$\bar{\xi} = \xi_0 \frac{1 + \lambda_o \omega (1 - \frac{X}{L}) j}{1 + \lambda_o \omega j} \tag{15}$$

The ratio of the amplitudes of the pressure increment at the end of the tube to that at the beginning of the tube is then given by:

$$\frac{\bar{\xi}_L}{\xi_0} = \frac{1}{1 + \lambda_o \omega j}$$

$$= \frac{1}{1 + \chi_o j} \tag{16}$$

where: $\chi_o = \lambda_o \omega$ (17)

and is to be interpreted as an attenuation factor for the amplitude ratio.

$\bar{\xi}_L$ is the maximum amplitude of the pressure increment at the chamber volume.

The real part of eq. 16 is the attenuation in amplitude of the pressure increment, whereas the imaginary part is the phase lag δ_o:

$$\left| \frac{\bar{\xi}_L}{\xi_0} \right| = \frac{1}{\left[1 + \chi_o^2\right]^{\frac{1}{2}}} \qquad (18)$$

$$\tan \delta_o = \chi_o$$

The above eq. 18 is the elementary solution of the problem, subject to the restrictive assumptions described above. Also to be noted is that the tube Reynolds Number $R_e = \frac{Q}{D\nu_0}$ must be less than 1500 for the tube flow to be laminar. It indicates that a volume-terminated tube is characterized by a time constant λ_o, which can be computed from the tube dimensions, the chamber volume and the average fluid conditions, and by an attenuation factor χ_o for each angular frequency, yielding the amplitude ratio and phase lag against frequency (Bode plot).

The main defect of this elementary solution is that it does not provide quantitative criteria for the limits of its applicability; discrepancies between experimental results and theoretical predictious are difficult to explain in terms of any one factor.

2.3. Corrected Theory

2.3.1. The assumptions made in the elementary theory are quite restrictive and in this section they will be modified, one at a time, until a complete solution is arrived at, which takes into account all first-order phenomena. The factors that must be taken into account are:

2.3.1.1. Compressible flow in the tube:

The effect of fluid compressibility is to introduce a time constant and corresponding attenuation factor depending on the tube volume in addition to the one depending on the chamber volume.

2.3.1.2. Finite pressure increment

The effect of the application of a finite pressure increment to a compressible fluid in a transmission tube is to introduce harmonic distortion and to modify the mean pressure. However, the attenuation of the fundamental is essentially independent of the magnitude of the pressure increment. The percentage of distortion is approximately proportional to the applied pressure increment.

2.3.1.3. Fluid Acceleration

The effects of fluid inertia is to modify the time constants of the system. Both the attenuation of the fundamental and the magnitude of harmonic distortion are affected. A dimensionless parameter "S" analogous to the "Q" of an electrical system characterizes the fluid regime and determines whether fluid inertia may or may not be neglected.

When fluid inertia is negligible, a tube acts like a highly damped system; when fluid inertia is large, a tube acts as an undamped system and elementary acoustic theory is applicable.

Elementary acoustic theory itself has a limit of application in regard to frequency, i.e., the onset of transverse acoustic waves.

2.3.1.4. Finite length of tube

The effect of fluid acceleration at the ends of the tube results in a further distortion of wave form, which must be taken into account for short tubes.

2.3.1.5. Heat conduction

If there were no heat transfer from outside the tube or chamber to inside, the oscillatory processes would take place adiabatically; if there were perfect heat transfer into and through the tube and chamber, the processes would take place isothermally. The effects of finite heat conduction, which may well vary from one servosystem installation to another, is to make the real processes occur in between the ideal extremes in a rather complex manner.

2.3.2. Correction Steps.

In this section, the several theoretical correction steps will be developed and presented in logical order. A complete solution of the problem is not obtained. All first-order effects are treated to the point where the solution is correct to frequencies well in the sonic region.

2.3.2.1. Thermodynamic equation of state.

In the case of an oscillatory variation of fluid flow, the equation relating the thermodynamic parameters of the fluid lie between the adiabatic and the isothermal equations of state. For high frequencies, as in sound waves, it is well known that the adiabatic condition holds. However, for viscously damped motion the adiabatic relation is not attained in general. Such an "inbetween" condition is termed "polytropic" and is characterized by a constant exponent n in the expression:

$$p = c\rho^n$$

$$1 + \xi = \eta^n \qquad (19)$$

with $\quad 1 \leq |n| \leq \gamma$

where n = exponent of polytropic expansion in tube

γ = ratio of specific heats

η = density ratio = $\dfrac{\rho}{\rho_o}$

$\xi = \dfrac{p - p_o}{p_o}$ = pressure increment ratio

The absolute viscosity of gases μ is substantially independent of the pressure and, as an approximation, proportional to the absolute temperature. The more rigorous approximation is that:

$$\mu \sim \frac{T^{\frac{1}{2}}}{1 + \frac{c}{T}}$$

This, however, does not need to be taken into account over small temperature differentials, provided that a mean μ_o value is obtained accurately.

Therefore:

$$\left.\begin{aligned} \mu &= c\,T \\ \frac{\mu}{\mu_0} &= (1+\xi)^{\frac{n-1}{n}} \\ \frac{\mu}{\mu_0} &= \eta^{n-1} \end{aligned}\right\} \qquad (20)$$

Eqs. 19 and 20 thus express the variation of viscosity, density and pressure in a polytropic process in a gas. For liquids, we assume that the polytropic equation of state is given by:

$$\rho = \rho_0 + C\,p^n \qquad \text{where} \quad 1 \leq |n| \leq \gamma \qquad (21)$$

For liquids, however, γ lies so close to unity that we may satisfactorily assume $n = 1.0$.
Eq. 21 can then be written in the form:

$$\eta = 1 + b\,\xi \qquad (22)$$

where b is a liquid compressibility factor at average conditions in the tube. The variation of viscosity μ in a liquid over a small temperature range can be neglected, so that:

$$\mu = \mu_0 \qquad (23)$$

Actually, the implications of eqs. 22 and 23 are that, in a liquid-filled tube, conditions are substantially isothermal.

It is also necessary to discuss the heat transfer conditions at the chamber. For an isothermal process with a gas, it was previously assumed (eq. 5) that $Q = \frac{V}{p_o}\frac{\partial p}{\partial t}$ represents the influx of fluid into the chamber. If instead, a polytropic process is assumed, characterized by an exponent (heat transfer may vary from tube to chamber, so that m is not necessarily equal to n), then eq. 5 should be modified to:

$$\underline{\text{Gases}} \qquad \left.\begin{aligned} Q &= \frac{V}{mp}\frac{\partial p}{\partial t} \\ Q &= \frac{n}{m}\frac{V}{\rho}\frac{\partial \rho}{\partial t} \end{aligned}\right\} \qquad (24)$$

It will be shown later that these polytropic exponents modify the time constants of the tube and chamber.

2.3.2.2. Polytropic Compressibility Correction
(Infinitesimal pressure increments).

In this step, polytropic fluid compressibility is introduced both for the tube (previously incompressible) and for the chamber (previously isothermal). The assumptions are the Poiseuille law of laminar pipe flow (quasi-steady-state), infinitesimal pressure increments and that density, pressure and viscosity are related by the polytropic equation of state.

For gases it can be written:

$$\left.\begin{aligned} \frac{\partial p}{\partial x} &= -\frac{128}{\pi}\frac{\mu}{D^4}Q \\ \text{or } \frac{\rho}{\mu}\frac{\partial p}{\partial x} &= -\frac{128}{\pi}\frac{\mu}{D^4}M \end{aligned}\right\} \text{ Poiseuille law} \qquad (1)$$

$$\text{and } \frac{\partial M}{\partial x} = -A\frac{\partial p}{\partial t} \qquad \text{Continuity} \qquad (2)$$

The mass flow M can be eliminated to obtain:

$$\frac{\partial}{\partial x}\left(\frac{\rho}{\mu}\frac{\partial p}{\partial x}\right) = \frac{32}{D^2}\frac{\partial e}{\partial t} \qquad (25)$$

Because of the assumption of infinitesimal pressure increments and the equations of state (eq. 19 and 20), the differentiation of $\frac{\rho}{\mu}$ can be disregarded in eq. 25 and can be replaced by its mean value. Eq. 25 then becomes:

$$\left.\begin{aligned} \frac{\partial^2 p}{\partial x^2} &= \frac{32\mu_o}{n\,p_o\,D^2}\frac{\partial p}{\partial t} \\ \text{or} \quad \frac{\partial^2 \xi}{\partial x^2} &= \frac{32\mu_o}{n p_o D^2}\frac{\partial \xi}{\partial t} \end{aligned}\right\} \qquad (26)$$

Utilizing the previous definition of λ_o (eq. 10), eq. 26 becomes:

$$\left.\begin{aligned} \frac{\partial^2 \xi}{\partial x^2} &= \left(\frac{AL}{V}\frac{\lambda_o}{n}\right)\frac{1}{L^2}\frac{\partial \xi}{\partial t} \\ \text{or} \quad \frac{\partial^2 \xi}{\partial x^2} &= \frac{\lambda_{To}}{L^2}\frac{\partial \xi}{\partial t} \end{aligned}\right\} \qquad (27)$$

where $\lambda_{To} = \frac{AL}{V} \quad \frac{\lambda_o}{n}$

or $\lambda_{To} = \left(\frac{L}{D}\right)^2 \quad \frac{\mu_o}{npo} \; 32$ (28)

The significance of the new time constant λ_{To} can be seen by inspection of eq. 28; the chamber volume V does not enter it anymore and it depends entirely on the tube dimensions L and D.

If, as in the elementary solution, we separate our pressure variables into a space and time part

$$\xi = \bar{\xi} e^{j\omega t} \tag{11}$$

eq. 27 becomes

$$\frac{\partial^2 \bar{\xi}}{\partial x^2} = \frac{\lambda_{To} \omega}{L^2} j \bar{\xi}$$

or $$\frac{\partial^2 \bar{\xi}}{\partial x^2} = \frac{\chi_{To}}{L^2} j\bar{\xi} \tag{29}$$

where $$\chi_{To} = \lambda_{To} \omega \tag{30}$$

The quantity χ_{To} is an attenuation factor based on the tube dimensions.

Eq. 29 may be compared with the corresponding eq. 12 of the elementary solution; in order for the elementary solution to be valid and the tube compressibility to be neglected χ_{To} must be small in comparison to L^2. It may be stated that

$$\frac{32 \omega \mu_o}{D^2 \, n \, po} \leq \frac{1}{100} \tag{31}$$

for the tube compressibility to be negligible; this provides one limiting criterion for the elementary theory. Referring now to eq. 29, the boundary conditions are:

$$\text{at } X = 0 \qquad \bar{\xi} = \xi_o \tag{13}$$

$$\text{and at } X = L \qquad \frac{d\bar{\xi}}{dx} = -\left(\frac{\lambda_o \omega}{m}\right) j \frac{\bar{\xi}}{L} \tag{32}$$

(see eqs. 5,9 and 24)

We may redefine a time constant and attenuation factor for the chamber volume, taking into account the polytropic process as:

$$\left.\begin{aligned} \lambda_{Io} &= \frac{\lambda_o}{m} \\ \chi_{Io} &= \lambda_{Io}\,\omega \end{aligned}\right\} \qquad (33)$$

at X = L, eq. 32 therefore becomes

$$\frac{d\,\bar{\xi}}{dx} = -\frac{\chi_{Io}}{L}\, j\,\bar{\xi} \qquad (34)$$

The solution to eq. 29, which satisfies the boundary conditions (eq. 13 and 34) is:

$$\frac{\bar{\xi}}{\xi_o} = \frac{e^{-\psi_{To}}(\psi_{To} - \psi_{Io})e^{\psi_{To}\frac{X}{L}} + e^{\psi_{To}}(\psi_{To} + \psi_{Io})e^{-\psi_{To}\frac{X}{L}}}{e^{\psi_{To}}(\psi_{To} + \psi_{Io}) + e^{-\psi_{To}}(\psi_{To} - \psi_{Io})} \qquad (35)$$

$$\left.\begin{aligned} \text{where } \psi_{To} &= \left[\frac{\chi_{To}}{2}\right]^{\frac{1}{2}}(1 + j) \\ \psi_{Io} &= j\,\chi_{Io} \end{aligned}\right\} \qquad (36)$$

The new ψ's, which shall be termed attenuation parameters are:

ψ_{To} attenuation factor depending on tube volume

ψ_{Io} attenuation factor depending on chamber volume

The ratio of the fractional pressure increment at the end of the tube $\bar{\xi}_L$ to that at the beginning of the tube ξ_o is then:

$$\frac{\bar{\xi}_L}{\xi_o} = \frac{\psi_{To}}{\psi_{To}\cosh\psi_{To} + \psi_{Io}\sinh\psi_{To}} \qquad (37)$$

For small ψ_{To} values, the attenuation approaches

$$\frac{\bar{\mathcal{E}}_L}{\mathcal{E}_o} = \frac{1}{1+\psi_{Io}} = \frac{1}{1+j\chi_{Io}} \qquad (38)$$

which is the same result as in eq. 16 of the elementary theory.

For small values of both ψ_{To} and ψ_{Io} the attenuation approaches

$$\frac{\bar{\mathcal{E}}_L}{\mathcal{E}_o} = \frac{1}{1+\frac{\chi_{To}}{2}j} \qquad (39)$$

The form of eqs. 38 and 39 is similar; in fact for small values of both ψ_{To} and ψ_{Io} it is possible to define a composite attenuation factor χ by the relation:

$$\left.\begin{aligned} \chi &= \chi_{Io} + \frac{\chi_{To}}{\sqrt{6}} \\ \text{or} \\ \lambda &= \lambda_{Io} + \frac{\lambda_{To}}{\sqrt{6}} \end{aligned}\right) \qquad (40)$$

such that the real magnitude of the attenuation is approximately:

$$\left|\frac{\bar{\mathcal{E}}_L}{\mathcal{E}_o}\right| = \frac{1}{\left[1+\chi^2\right]^{\frac{1}{2}}} \qquad (18)$$

which preserves the form of the elementary solution. Eq. 18 can be interpreted as meaning that the "proper" time constant of the system can be obtained by adding to the n weighted chamber volume, $\frac{1}{\sqrt{6}}$ of the m weighted volume of the tube, and substituting this in the elementary formula. In principle, for larger values of the ψ parameters, a more general coupling coefficient could be introduced which would vary somewhat with the magnitude of ψ, to preserve the elementary form.

2.3.2.3. Finite pressure increments correction.

In this section, the effects of finite pressure increments on the attenuation in a tube will be discussed. It will be shown that the effect of finite pressure increments is as follows:

Excitation of higher harmonics
Distortion of wave form
Increase of mean pressure along the tube

The only assumption used will be that of Poiseuille velocity distribution in the tube (Quasi-steady-state).
The method of solution selected will be that of expansion in harmonic series in which the excitation of sum frequencies only is considered and the difference frequencies are neglected.
The second order term in the variation of the mean pressure will be estimated separately. For convenience, the equations will be derived on a density basis; density and pressure are related by the equation of state.
For gases, we start from:

$$\frac{\partial}{\partial x}\left(\frac{\rho}{\mu}\frac{\partial p}{\partial x}\right) = \frac{32}{D^2}\frac{\partial \rho}{\partial t} \qquad (25)$$

Using eqs. 19 and 20 to eliminate viscosity and pressure, a non-linear partial differential equation is obtained in terms of density ratio η:

$$\frac{\partial}{\partial x}\left(\eta\frac{\partial \eta}{\partial x}\right) = \frac{\lambda\, To}{L^2}\frac{\partial \eta}{\partial t}$$

$$\text{or}\quad \frac{\partial^2 \eta^2}{\partial x^2} = \frac{2\lambda\, To}{L^2}\frac{\partial \eta}{\partial t} \qquad (41)$$

The following series expansion is assumed as solution for the density ratio η:

$$\eta = 1 + \eta_1 e^{j\omega t} + \eta_2 e^{2j\omega t} + \eta_3 e^{3j\omega t} + \ldots \qquad (42)$$

For the sake of brevity, the extremely lengthy series solution is omitted and the results presented.

If an input pressure wave is given by:

$$\xi = \xi_0 e^{j\omega t} + \xi_1 e^{2j\omega t} + \ldots . \qquad (43)$$

The wave at the end of the tube will be given by:

$$\xi = \left[\xi_o \frac{\psi_{To}}{\psi_{To} \cosh \psi_{To} + \psi_{Io} \sinh \psi_{To}} \right] e^{j\omega t} + \ldots . \quad (44)$$

The increase in mean pressure in the chamber volume is given by the following:

$$\frac{\xi_o \Delta_P \left[1 + \left| \frac{\bar{\xi}_{OL}}{\xi_o} \right|^2 \right]}{4} \quad (45)$$

2.3.2.4. Fluid Acceleration Correction

Here the main restrictive assumption will be removed, i.e. the quasi-steady-state assumption of Poiseuille velocity distribution in the tube. In order to achieve this, it is required to return to the basic Navier-Stokes equations of viscous flow. It is possible to take the Navier-Stokes eqs. and combine them with the mass continuity equation and the thermodynamic equation of energy balance, to arrive at the Kirchoff eqs. of sound, which are valid to first order. This procedure was followed, making no assumption as to the form of the equation of state for the fluid and the following results were obtained for the attenuation parameter and the velocity in an infinite tube:

$$\left[\frac{\psi_T}{L} \right]^2 = -\frac{\omega}{C}^2 \frac{1 + 2(\gamma - 1) \frac{J_1(g \frac{D}{2})}{g \frac{D}{2} J_o (g \frac{D}{2})}}{1 - \frac{2 J_1 (h \frac{D}{2})}{h \frac{D}{2} J_o (h \frac{D}{2})}} \quad (46)$$

where $g\frac{D}{2} = (1-j)\frac{D}{2}\left[\frac{\omega \delta_o}{2\nu_o}\right]^{\frac{1}{2}}$

$h\frac{D}{2} = (1-j)\frac{D}{2}\left[\frac{\omega}{2\nu_o}\right]^{\frac{1}{2}}$ (47)

and $Q = -\frac{\pi D^2}{4j\omega\rho_o}\left(1 - \frac{2J_1(h\frac{D}{2})}{h\frac{D}{2}J_o(h\frac{D}{2})}\right)\frac{\partial p}{\partial x}$ (48)

The attenuation parameter ψ_T is to be interpreted as before in eq. 35.

For small values of g and h (Bessel function arguments) eqs. 46 and 48 become:

$$\left[\frac{\psi_T}{L}\right]^2 = \frac{32\, j\omega\nu_o\gamma}{c^2 D^2}$$

$$Q = -\frac{\pi D^4}{128\mu_o}\frac{\partial p}{\partial x} \qquad (49)$$

which are precisely the results assumed in eqs. 1 and 29 under the condition in eq. 29 that the "polytropic" coefficient is unity. This is so because $\frac{c^2}{\gamma}$ in eq. 49 is the square of the velocity of sound, which for gases is P_o/ρ_o
Eqs. 46 and 48, which take into account the heat conduction, thus demonstrate that, when the previous results are valid, the equation of state is the isothermal. At higher frequencies, the modifying term in eq. 46 may be regarded as the "polytropic" coefficient. To bring this out explicitly, eqs. 46 and 48 may be rewritten:

$$\left(\frac{\psi_T}{L}\right)^2 = \frac{32\, j\omega\nu_o\gamma}{c^2 D^2}\left[\frac{\frac{\left(h\frac{D}{2}\right)^2}{8}}{\frac{2J_1(h\frac{D}{2})}{h\frac{D}{2}J_o(h\frac{D}{2})} - 1}\right]\left[\frac{1 + \frac{2(\gamma-1)J_1(g\frac{D}{2})}{g\frac{D}{2}J_o(g\frac{D}{2})}}{\gamma}\right]$$

$$Q = \frac{\pi D^4}{128\mu_o}\frac{\partial p}{\partial x}\left[\frac{\frac{2J_1(h\frac{D}{2})}{h\frac{D}{2}J_o(h\frac{D}{2})} - 1}{\frac{(h\frac{D}{2})^2}{8}}\right] \qquad (50)$$

Eq. 50 may be regarded as an extended definition of the attenuation parameter ψ_T and of the modified flow law that replaces Poiseuille's law. It is therefore used without the zero subscript, which denotes results based on the quasi-steady-state assumption of Poiseuille's law.
Bringing in the boundary condition at X = L:

$$Q = \frac{V}{mpo} \frac{\partial p}{\partial t} \tag{24}$$

it is obtained for a gas:

$$\frac{d\bar{\Xi}}{dx} = -\frac{128\mu_o \, Vj\omega}{\pi D^4 \, mpo} \left[\frac{\frac{(h\frac{D}{2})^2}{8}}{\frac{2\,J_1(h\frac{D}{2})}{h\frac{D}{2}\,J_o(h\frac{D}{2})} - 1} \right] \bar{\Xi} \tag{51}$$

Let

$$\chi_I = \frac{128\,\mu_o \, V\omega L}{\pi D^4 \, mpo} \left[\frac{\frac{(h\frac{D}{2})^2}{8}}{\frac{2\,J_1(h\frac{D}{2})}{h\frac{D}{2}\,J_o(h\frac{D}{2})} - 1} \right] \tag{52}$$

We have thus extension of our definition of χ_I to cover high frequencies; the limiting value of χ_I for small arguments obviously becomes the previous χ_{IO}.

Since the only modification has been to extend the definitions of ψ_T and ψ_I without changing the form of the equations to be solved, eqs. 29 and 34, the previous result of eq. 37 is strictly valid. The results however are now correct for frequencies well in the audio range, subject to the well-known limitation of the advent of transverse acoustic waves.
The first transverse wave mode is known to occur for

$$\frac{\omega D}{C} = 3.68 \tag{53}$$

and therefore this is the limit of application of the above results.

2.3.2.5. Finite Tube Length Correction.

Since the tube is of finite length and it takes an appreciable length to set up the Poiseuille velocity distribution in the tube, the tube end-effects must be considered for completeness of the analysis. The character of the entrance flow is that the axial velocity is flat at the entrance, gradually developing an approximately parabolic velocity profile with a core of uniform velocity, until the parabolic velocity profile fills the entire tube.

Going back to the Navier-Stokes eqs. the following assumptions are made:

The entrance flow is incompressible (low Mach Number)
Radial pressure variation is negligible
Quadratic velocity terms negligible in the entrance flow
Uniform central velocity core conforms to potential (inviscid) flow.

The equation of motion of the central core may be written for our purposes simply as:

$$\frac{\partial u_p}{\partial t} + u_p \frac{\partial u_p}{\partial x} = -\frac{1}{\rho_o} \frac{\partial p}{\partial x} \qquad (54)$$

where u_p is the axial velocity in the central core.

$$\text{Let } u_p = \frac{\partial \phi}{\partial x} \qquad (55)$$

where ϕ is the velocity potential; then

$$\left.\begin{aligned} &\frac{\partial}{\partial x}\left(\frac{\partial \phi}{\partial t}\right) + \tfrac{1}{2}\frac{\partial u_p^2}{\partial x} + \frac{1}{\rho_o}\frac{\partial p}{\partial x} = 0 \\ \text{or } &\frac{\partial \phi}{\partial t} + \tfrac{1}{2} u_p^2 + \frac{p}{\rho_o} = f(t) \end{aligned}\right\} \qquad (56)$$

where f (t) is an arbitrary function of time. The boundary conditions are a prescribed pressure variation at X=0 with a flat velocity profile ($\bar{u}_p = \bar{u}$) average velocity) and a parabolic velocity profile somewhere downstream at $X = \ell$.

The assumption of incompressibility makes $\bar{u}$ equal at both sections. These conditions lead to the result

$$p(0, t) = p(\ell, t) + \frac{3}{2}\rho_o \bar{u}^2 + \frac{\partial \phi}{\partial t}(\ell, t) - \frac{\partial \phi}{\partial t}(0, t) \qquad (57)$$

Referring to the physical discussion given by Goldstein[2] for the steady-state case, it is found that

$$p(0) = p(\ell) + \frac{3}{2}\rho_o \bar{u}^2 + \frac{16\rho_o \bar{u}^2}{\frac{D}{2} R_e}\left(\ell - 0.0575 \frac{D}{2} R_e\right) \qquad (58)$$

Where R_e is the tube Reynolds Number. It follows from these two equations that the leading term for the entrance loss in the oscillatory case is the usual $\rho_o \bar{u}^2$ loss. Therefore the effect of the entrance is to cause an additional pressure drop given by:

$$\Delta p = 1.2 \rho_o \bar{u}^2 \qquad (59)$$

The pressure increment ξ' just inside the tube, due to this loss, will be given approximately by:

$$\xi^1 = \xi_o e^{j\omega t} - \frac{jD^2\omega}{32\nu_o}\left[\frac{\psi_{To} \tanh \psi_{To} + \psi_{Io}}{\psi_{To} + \psi_{Io} \tanh \psi_{To}}\right]^2 \xi_o^2 \, e^{2j\omega t} \qquad (60)$$

Eq. 60 is the desired result; it shows that the approximate effect of the entrance is to distort each input harmonic. It can be interpreted as meaning that the effect of the entrance is the same as if it did not exist, but with the fundamental harmonic generator replaced by a fundamental and a second harmonic generator. The first-order terms are thus left unaffected and only the second harmonic attenuation requires modification.

2.3.3. Summary of Corrected Theory.

2.3.3.1 Complex attenuation of the fundamental frequency:

$$\frac{\bar{\xi}_{OL}}{\xi_o} = \frac{\psi_T}{\psi_T \cosh \psi_T + \psi_I \sinh \psi_T} \qquad (61)$$

where ξ_{OL} is the complex amplitude of the fractional pressure increment of the fundamental at the end of the tube and the subscript O refers to the fundamental. Eq. 61 is valid if

$$\frac{\nu_o}{CD} < 1$$
$$\frac{\nu_o \omega}{c^2} < 1 \qquad (62)$$

2.3.3.2. Attenuation parameters: have been defined (eq. 36) as

$$\psi_T^2 = j\chi_T$$
$$\psi_I = j\chi_I \qquad (63)$$

The attenuation factors have been defined most generally

$$\chi_T = \frac{32\,\nu_o\omega}{C_T^2}\left(\frac{L}{D}\right)^2 \left[\frac{1 + \dfrac{2(\gamma-1)J_1\left(q\frac{D}{2}\right)}{g\frac{D}{2}\,J_o\left(g\frac{D}{2}\right)}}{\gamma}\right]\left[\frac{\dfrac{\left(h\frac{D}{2}\right)^2}{8}}{\dfrac{2\,J_1\left(h\frac{D}{2}\right)}{h\frac{D}{2}\,J_o\left(h\frac{D}{2}\right)} - 1}\right] \qquad (64)$$

HIGH FREQUENCY

$$\chi_I = \frac{32\,\nu_o\omega}{C_I^2}\left(\frac{L}{D}\right)^2 \frac{V}{AL}\left[\frac{\dfrac{\left(h\frac{D}{2}\right)^2}{8}}{\dfrac{2\,J_1\left(h\frac{D}{2}\right)}{h\frac{D}{2}\,J_o\left(h\frac{D}{2}\right)} - 1}\right]$$

The Bessel arguments are defined as

$$g\frac{D}{2} = (1 - j)\frac{D}{2}\left[\frac{\omega\,\sigma_o}{2\,\nu_o}\right]^{\frac{1}{2}}$$
$$h\frac{D}{2} = (1 - j)\frac{D}{2}\left[\frac{\omega}{2\,\nu_o}\right]^{\frac{1}{2}}$$

While for quasi-steady-state Poiseuille flow they are defined as:

$$\chi_{T_o} = \frac{32\,\nu_o \omega}{C_T^2}\left(\frac{L}{D}\right)^2 \qquad (65)$$

LOW FREQUENCY

$$\chi_{I_o} = \frac{32\,\nu_o \omega}{C_I^2}\left(\frac{L}{D}\right)^2 \frac{V}{AL}$$

Here C_T is the velocity of sound appropriate to the tube and C_I the velocity of sound appropriate to the chamber volume.

$$C_T = \left(\frac{p_o}{\rho_o}\right)^{\frac{1}{2}} \qquad (66)$$

$$C_I = \left(\frac{m p_o}{\rho_o}\right)^{\frac{1}{2}}$$

For computational purposes, introduce functions $F_1\left(h\frac{D}{2}, \gamma\right)$ and $F_2\left(h\frac{D}{2}, \gamma\right)$ such that:

$$\chi_T = \chi_{To} F_1 = \frac{32\,\mu_o \omega}{p_o}\left(\frac{L}{D}\right)^2 F_1 \qquad (67)$$

$$\chi_I = \chi_{Io} F_1 F_2 = \frac{32\,\mu_o \omega}{m p_o}\left(\frac{L}{D}\right)^2\left(\frac{V}{AL}\right) F_1 F_2$$

$$F_1 = \left[\frac{1 + \dfrac{2(\gamma - 1) J_1\left(h\frac{D}{2}\right)}{h\frac{D}{2} J_o\left(h\frac{D}{2}\right)}}{\gamma}\right]\left[\frac{\dfrac{\left(h\frac{D}{2}\right)^2}{8}}{\dfrac{2 J_1\left(h\frac{D}{2}\right)}{h\frac{D}{2} J_o\left(h\frac{D}{2}\right)} - 1}\right] \qquad (68)$$

$$F_2 = \left[\frac{\gamma}{1 + (\gamma - 1)\dfrac{2 J_1\left(h\frac{D}{2}\right)}{h\frac{D}{2} J_o\left(h\frac{D}{2}\right)}}\right] \qquad (69)$$

2.3.3.3. Computation of real attenuation ratio and of phase angle.

2.3.3.3.1. A low-frequency, high-damping fluid regime may be defined by the Stokes Number S ranging from zero to unity, where:

$$S = \frac{D^2 \omega}{4 \nu_o} \qquad (70)$$

This regime starts from steady-state flow and presupposes the validity of quasi-steady-state flow in the tube. The attenuation factors are χ_{To} and χ_{Io} of eqs. 65 and 66.

The real pressure increment attenuation ratio is given by:

$$\left| \frac{\Im_{oL}}{\xi_o} \right|_o = \frac{2}{\cosh\left[2\chi_{To}\right]^{\frac{1}{2}} + \cos\left[2\chi_{To}\right]^{\frac{1}{2}} + \left[\frac{\chi_{Io}}{\chi_{To}}\right]\left[2\chi_{To}\right]^{\frac{1}{2}}\left[\sinh\left[2\chi_{To}\right]^{\frac{1}{2}} - \sin\left[2\chi_{To}\right]^{\frac{1}{2}}\right] + \left(\frac{\chi_{Io}}{\chi_{To}}\right)^2 \chi_{To}\left[\cosh\left[2\chi_{To}\right]^{\frac{1}{2}} - \cos\left[\chi_{To}\right]^{\frac{1}{2}}\right]} \qquad (71)$$

and the phase angle:

$$\left|\tan\delta_o\right|_o = \frac{\tanh\left[\frac{\chi_{To}}{2}\right]^{\frac{1}{2}} \tan\left[\frac{\chi_{To}}{2}\right]^{\frac{1}{2}} + \left(\frac{\chi_{Io}}{\chi_{To}}\right)\left(\frac{\chi_{To}}{2}\right)^{\frac{1}{2}}\left[\tanh\left(\frac{\chi_{To}}{2}\right)^{\frac{1}{2}} + \tan\left(\frac{\chi_{To}}{2}\right)^{\frac{1}{2}}\right]}{1 + \left(\frac{\chi_{Io}}{\chi_{To}}\right)\left(\frac{\chi_{To}}{2}\right)^{\frac{1}{2}}\left[\tanh\left(\frac{\chi_{To}}{2}\right)^{\frac{1}{2}} - \tan\left(\frac{\chi_{To}}{2}\right)^{\frac{1}{2}}\right]} \qquad (72)$$

The independent parameters are seen to be:

χ_{To} frequency parameter

$r = \chi_{Io}/\chi_{To}$ volume ratio

2.3.3.3.2. A <u>high-frequency, low-damping</u> fluid regime may be defined, ranging between a value of $S \geq 100$ and a value of the parameter $\frac{\omega D}{C_T}$ below 3.68 (onset of transverse acoustic waves).
This regime is the undamped longitudinal acoustic regime. Digital fluid circuitry is expected to fall in this regime.
Defining a new frequency parameter (in a Strouhal Number Form):

$$Z = \frac{\omega L}{C} = \left[\frac{\chi_{To}\, S}{8\gamma}\right] \qquad (73)$$

and a volume ratio r:

$$r = \gamma \frac{\chi_{Io}}{\chi_{To}} = \gamma \frac{m}{n} \frac{V}{AL} \qquad (74)$$

The real pressure increment attenuation is given by:

$$\left|\frac{\xi_{oL}}{\xi_o}\right| = \left[\frac{2}{1 + \cos 2Z - 2\, r\, Z \sin 2\, Z + \frac{r^2}{4}(2Z)^2(1 - \cos 2\, Z)}\right] \qquad (75)$$

and the phase angle:

$$\tan \delta_o = \left[\frac{\gamma\, \chi_{To}}{16}\right]^{\frac{1}{2}} \frac{\left(1 + r\left(\frac{2-\gamma}{\gamma}\right)\right)\tan Z + r\, Z}{1 - r\, Z \tan Z} \qquad (76)$$

The independent parameters are seen to be:

Z frequency parameter
r volume ratio

2.3.3.3.3. <u>An intermediate-frequency, intermediate-damping</u> fluid regime may be defined, ranging between S = 1 and S = 100.

Most practical applications of proportional fluid control circuitry are expected to fall in this intermediate regime.

The attenuation factors χ_I and χ_T are in the most general form; all the theoretical corrections are accounted for and therefore these results are valid for all frequencies (Z values). It is to be noted that for very low S $\leqq$ 1) or very high Z values Z $\geq$ 100) the preceding eqs. are simpler and easier to compute.

The real pressure increment attenuation is given by:

$$\left|\frac{\Delta p_{oL}}{\Delta p_o}\right| = \left[\frac{2}{\cosh 2C_1 + \cos 2C_2 + 2C_3 \sinh 2C_1 - 2C_4 \sin 2C_2 + (C_3^2 + C_4^2)(\cosh 2C_1 - \cos 2C_2}\right]^{\frac{1}{2}} \quad (77)$$

The phase angle is given by:

$$\tan \delta_o = \frac{\tanh C_1 \tan C_2 + C_3 \tan C_2 + C_4 \tanh C_1}{1 + C_3 \tanh C_1 - C_4 \tan C_2} \quad (78)$$

where

$$C_1 = \left[1 - \sin C_5\right]^{\frac{1}{2}} \left[\frac{\chi_{To}}{2} \left|F_1\right|\right]^{\frac{1}{2}} \quad (79)$$

$$C_2 = \left[1 + \sin C_5\right]^{\frac{1}{2}} \left[\frac{\chi_{To}}{2} \left|F_1\right|\right]^{\frac{1}{2}} \quad (80)$$

$$C_3 = \left(\cos C_6 \left[1 - \sin C_5\right]^{\frac{1}{2}} - \sin C_6 \left[1 + \sin C_5\right]^{\frac{1}{2}}\right) \left[\frac{\chi_{To}}{2} \left|F_1\right|\right]^{\frac{1}{2}} \frac{\chi_{Io}}{\chi_{To}} \left|F_2\right| \quad (81)$$

$$C_4 = \left(\cos C_6 \left[1 + \sin C_5\right]^{\frac{1}{2}} - \sin C_6 \left[1 - \sin C_5\right]^{\frac{1}{2}}\right) \left[\frac{\chi_{To}}{2} \left|F_1\right|\right]^{\frac{1}{2}} \frac{\chi_{Io}}{\chi_{To}} \left|F_2\right| \quad (82)$$

$$F_1 = f_1 + g_1 j \quad (83)$$

$$F_2 = f_2 + g_2 j \quad (84)$$

$$\cos C_5 = \frac{f_1}{|F_1|} \tag{85}$$

$$\sin C_5 = \frac{g_1}{|F_1|} \tag{86}$$

$$\cos C_6 = \frac{f_2}{|F_2|} \tag{87}$$

$$\sin C_6 = \frac{g_2}{|F_2|} \tag{88}$$

2.3.3.4. Graphical presentation of results.

The results of the analysis may be presented graphically by three sets of curves for the high-damping, intermediate and low-damping regimes, yielding the amplitude attenuation and the phase angle of the fundamental frequency.

If S lies between 0 and 1.0, use Figs. 2.3.3-1 and 2.3.3-2; if it is over 100, use Figs. 2.3.3-3 and 2.3.3-4. An intermediate set of curves has been computed for S= 6.25 which are shown in Figs. 2.3.3-5 and 2.3.3-6
Figs. 2.3.3-1, 2.3.3-2, 2.3.3-5 and 2.3.3-6 use the attenuation factor χ_{To} as the frequency index; Figs. 2.3.3-3 and 2.3.3-4 use the parameter Z as the frequency index.

2.4 Classification of Fluid Regimes and Similarity Rules.

2.4.1. Classification of Dynamic Regimes.

It is very important to understand the dynamic classification of fluid regimes and the physical factors entering such classification criterion.

It is well known that the classic Reynolds Number supplies the criterion for the steady-state classification of fluid regimes. Creeping flow, laminar flow, transitional flow, turbulent flow can be denoted by appropriate numerical values of the Reynolds Number.

Similarly, it has been shown that the dimensionless Stokes Number $S = \frac{\omega D^2}{4\gamma_0}$ classifies the fluid regimes in regard to dynamic conditions; it is in the nature of a dynamic damping index. Frequency, tube diameter and fluid kinematic viscosity enter into the parameter; it clearly demonstrates that frequency alone is not sufficient to denote a dynamic state in fluid dynamics, as it seems to be in electricity.

Three basic dynamic fluid regimes can be identified, as will be discussed below.

2.4.1.1. High Damping Regime.

This area comprises the S - range from 0 to 1.0; at S = 0, of course, there is steady-state flow. Here it is essential to have similarity for both R_e and S, since the steady-state flow is the boundary of the area and quasi-steady-state flow may be assumed for the mathematical solution.

The elementary solution may be used, if tube compressibility may be neglected and the chamber processes are isothermal. A criterion for the neglect of tube compressibility is as follows:

$$\frac{32\omega\mu_o}{D^2 n\, p_o} \leqq \frac{1}{100} \qquad (31)$$

Generally, the corrected theory should be used, with the attenuation and phase angle given by eqs. 71 and 72.

2.4.1.2. Intermediate - damping Area.

This area comprises the S - range from 1.0 to 100; most practical applications of proportional fluid control circuitry are expected to fall in this area.

The elementary solution should not be used in this area since tube compressibility will be important and the chamber processes will be approaching adiabatic. The corrected theory should be used, with the attenuation and phase angle given by eqs. 77 and 78.

2.4.1.3. Low-damping Area.

This area comprises the S - range above 100; the upper limit is not defined by a S value, but by another parameter, i.e. $\frac{\omega D}{C} = 3.68$. This area may be also termed the elementary longitudinal acoustic area and its upper limit of applicability is given by the onset of transverse acoustic waves. When such waves occur, the full three-dimensional analysis is required. The corrected theory should be used, with the attenuation and given by eqs. 75 and 76.

2.4.2. Similarity Rules.

2.4.2.1. Dimensionless Parameters

The theory developed in the preceding sections has shown that the amplitude attenuation ratio and the phase angle is dependent on the following dimensionless parameters:

$$S = \frac{\omega D^2}{\nu} \tag{70}$$

$$\chi_{To} = \omega \frac{\mu_o}{n\, p_o} \left(\frac{L}{D}\right)^2 = \omega \frac{\nu_o}{C^2} \left(\frac{L}{D}\right)^2 \tag{30}$$

$$\frac{\chi_{Io}}{\chi_{To}} = \frac{V}{AL} \quad \frac{m}{n}$$

$$Z = \frac{\omega L}{C} \tag{73}$$

In addition, the classic Reynolds Number $R_e = \frac{UD}{\nu}$ should also be considered, to account for steady-state similarity in the tube (pressure-loss and transverse velocity distribution).

The geometric similarity parameters are $\frac{L}{D}$ and $\frac{V}{AL}$. The heat transfer similarity parameters are $\frac{m}{n}$ explicitly and also implicitly in the velocity of sound; they will be neglected explicitly in the following dimensional analysis.

If in addition to the Reynolds Number R_e and the Stokes Number S (both basic parameters which can be derived directly from the fluid equations of motion), another Reynolds Number is considered, with the form: $R_{ea} = \frac{CD}{\nu}$ (89)

then it will be shown that χ_{To} and Z can be expressed in terms of S and R_{ea}.

Indeed $$\chi_{To} = \frac{\omega\nu}{C^2}\left(\frac{L}{D}\right)^2 = \left[\frac{\omega D^2}{\nu}\right]\left[\frac{\nu^2}{C^2D^2}\right]\left[\frac{L}{D}\right]^2$$

thus $$\chi_{To} = \frac{S}{R_{e_a}^2}\left(\frac{L}{D}\right)^2 \qquad (90)$$

also $$Z = \frac{\omega L}{C} = \frac{\omega L D^2 \nu}{C\, D^2 \nu} = \left[\frac{\omega D^2}{\nu}\right]\left[\frac{\nu}{CD}\right]\left[\frac{L}{D}\right]$$

thus $$Z = \frac{S}{R_{ea}}\left(\frac{L}{D}\right) \qquad (91)$$

2.4.2.2. Similarity Rules.

From the above considerations it has appeared that to insure both steady-state and dynamic similarity between two geometrically similar circuits (equal $\frac{L}{D}$ and $\frac{V}{AL}$), it is necessary that R_e, S and R_{e_a} be constant.

Using subscript 1 to denote one circuit and subscript 2 to denote the second circuit, it can be written:

$$R_e = \frac{U_1 D_1 \rho_1}{\mu_1} = \frac{U_2 D_2 \rho_2}{\mu_2} \qquad (92)$$

$$R_{e_a} = \frac{C_1 D_1 \rho_1}{\mu_1} = \frac{C_2 D_2 \rho_2}{\mu_2} \qquad (93)$$

$$S = \frac{W_1 D_1^2 \rho_1}{\mu_1} = \frac{\omega_2 D_2^2 \rho_2}{\mu_2} \qquad (94)$$

From eq. (92):

$$\frac{\mu_2}{\mu_1} = \frac{U_2}{U_1}\frac{D_2}{D_1}\frac{\rho_2}{\rho_1} \qquad (95)$$

From eq. (93):

$$\frac{\mu_2}{\mu_1} = \frac{C_2}{C_1}\ \frac{D_2}{D_1}\ \frac{\rho_2}{\rho_1} \tag{96}$$

From eq. (94):

$$\frac{\mu_2}{\mu_1} = \frac{\omega_2}{\omega_1}\ \frac{D_2^2}{D_1^2}\ \frac{\rho_2}{\rho_1} \tag{97}$$

Since all three eqs. must be valid by definition:

$$\frac{U_2}{U_1}\ \frac{D_2}{D_1}\ \frac{\rho_2}{\rho_1} = \frac{C_2}{C_1}\ \frac{D_2}{D_1}\ \frac{\rho_2}{\rho_1} = \frac{\omega_2}{\omega_1}\ \frac{D_2^2}{D_1^2}\ \frac{\rho_2}{\rho_1}$$

Therefore

$$\frac{U_2}{U_1} = \frac{C_2}{C_1} = \frac{\omega_2}{\omega_1}\ \frac{D_2}{D_1}$$

and

$$\left.\begin{aligned}
&\frac{U_2}{U_1} = \frac{C_2}{C_1} = \frac{\omega_2}{\omega_1}\ \frac{D_2}{D_1} \\
&\frac{C_2}{C_1} = \frac{U_2}{U_1}\ \frac{\omega_2}{\omega_1}\ \frac{D_2}{D_1} \\
&\frac{\omega_2}{\omega_1} = \frac{C_2}{C_1}\ \frac{D_1}{D_2} = \frac{U_2}{U_1}\ \frac{D_1}{D_2} \\
&\frac{D_2}{D_1} = \frac{U_2}{U_1}\ \frac{\omega_1}{\omega_2} = \frac{C_2}{C_1}\ \frac{\omega_1}{\omega_2}
\end{aligned}\right\} \quad \begin{array}{l}\underline{\text{STOKES-REYNOLDS}} \\ \underline{\text{SIMILARITY LAWS}} \\ \underline{\text{FOR}} \\ \underline{\text{CONSTANT FLUID}} \\ \underline{\text{VISCOSITY}}\end{array} \tag{98}$$

Again from eq. (92):

$$\frac{D_2}{D_1} = \frac{U_1}{U_2}\ \frac{\rho_1}{\rho_2}\ \frac{\mu_2}{\mu_1} \tag{99}$$

and from eq. (93):

$$\frac{D_2}{D_1} = \frac{C_1}{C_2}\ \frac{\rho_1}{\rho_2}\ \frac{\mu_2}{\mu_1} \tag{100}$$

and from eq. (94):

$$\frac{D_2^2}{D_1^2} = \frac{\omega_1}{\omega_2}\ \frac{\rho_1}{\rho_2}\ \frac{\mu_2}{\mu_1} \tag{101}$$

Since all three must be valid by definition:

$$\frac{U_1}{U_2}\ \frac{\rho_1}{\rho_2}\ \frac{\mu_2}{\mu_1} = \frac{C_1}{C_2}\quad \frac{\rho_1}{\rho_2}\ \frac{\mu_2}{\mu_1} = \left[\frac{\omega_1}{\omega_2}\right]^{\frac{1}{2}}\left[\frac{\rho_1}{\rho_2}\right]^{\frac{1}{2}}\left[\frac{\mu_2}{\mu_1}\right]^{\frac{1}{2}}$$

Therefore

$$\frac{U_1}{U_2}\left[\frac{\rho_1}{\rho_2}\right]^{\frac{1}{2}}\left[\frac{\mu_2}{\mu_1}\right]^{\frac{1}{2}} = \frac{C_1}{C_2}\left[\frac{\rho_1}{\rho_2}\right]^{\frac{1}{2}}\left[\frac{\mu_2}{\mu_1}\right]^{\frac{1}{2}} = \left[\frac{\omega_1}{\omega_2}\right]^{\frac{1}{2}}$$

Thus

$$\frac{U_2}{U_1} = \frac{C_2}{C_1} = \left[\frac{\omega_2}{\omega_1}\right]^{\frac{1}{2}}\left[\frac{\rho_1}{\rho_2}\right]^{\frac{1}{2}}\left[\frac{\mu_2}{\mu_1}\right]^{\frac{1}{2}}$$

$$\frac{C_2}{C_1} = \frac{U_2}{U_1} = \left[\frac{\omega_2}{\omega_1}\right]^{\frac{1}{2}}\left[\frac{\rho_1}{\rho_2}\right]^{\frac{1}{2}}\left[\frac{\mu_2}{\mu_1}\right]^{\frac{1}{2}}$$

$$\frac{\omega_2}{\omega_1} = \left[\frac{U_2}{U_1}\right]^2 \frac{\rho_2}{\rho_1}\ \frac{\mu_1}{\mu_2} = \left[\frac{C_2}{C_1}\right]^2 \frac{\rho_2}{\rho_1}\ \frac{\mu_1}{\mu_2}$$

$$\frac{\mu_2}{\mu_1} = \left[\frac{U_1}{U_2}\right]^2 \frac{\omega_1}{\omega_2}\ \frac{\rho_2}{\rho_1} = \left[\frac{C_2}{C_1}\right]^2 \frac{\omega_1}{\omega_2}\ \frac{\rho_2}{\rho_1}$$

$$\frac{\rho_2}{\rho_1} = \left[\frac{U_1}{U_2}\right]^2 \frac{\omega_2}{\omega_1}\ \frac{\mu_2}{\mu_1} = \left[\frac{C_1}{C_2}\right]^2 \frac{\omega_2}{\omega_1}\ \frac{\mu_2}{\mu_1}$$

STOKES-REYNOLDS SIMILARITY LAWS FOR CONSTANT TUBE DIAMETER (102)

Eqs. 98 and 102 prescribe the correct scaling procedure for the case of constant fluid viscosity μ and constant tube diameter D respectively.

2.4.3. Conclusions.

In this section the entire range of dynamic fluid regimes has been discussed and classified, from steady-state viscous flow to the onset of transverse acoustic waves.

The dimensionless parameters, which underlie the theoretical results of this chapter, have been presented and discussed as to their relation to the basic Stokes and Reynolds Numbers.

Complete similarity rules have been derived and presented, for the case of constant fluid viscosity and for the case of constant tube diameter.

2.5 Electrical Analogy to Fluid Theory.

There are some useful analogies to be made between electrical networks and fluid circuits; these analogies are useful only because they allow the extensive electrical network theory to be exploited for the rapid approximate solution of fluid circuit problems. However, the analogy must be carefully defined, with its restriction of validity and its limits of application.

2.5.1. Analogy to Elementary Fluid Theory.

The simplest electrical analog to the passive circuit under study may be drawn as follows:

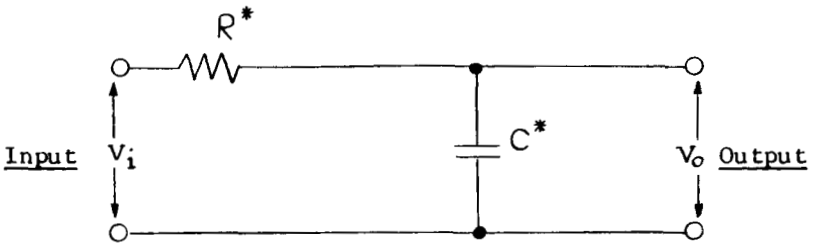

The real attenuation ratio is given by:

$$\left|\frac{v_o}{v_i}\right| = \frac{1}{\left[1 + (R^* C^* \omega)^2\right]^{\frac{1}{2}}} \qquad (103)$$

where R^* is the electrical resistance and C^* is the electrical capacitance and the phase angle is given by:

$$\tan \delta_o = R^* C^* \omega \qquad (104)$$

These expressions may be compared with eq. 18:

$$\left|\frac{\bar{\xi}_L}{\xi_o}\right| = \frac{1}{\left[1 + \chi_o^2\right]^{\frac{1}{2}}} \qquad (18)$$

$$\tan \delta_o = \chi_o$$

It is readily seen that there is an analogy between $R^* C^* \omega$ and χ_o.

Furthermore, eq. 17 shows that: $\chi_o = \lambda_o \omega$ (17)

and therefore there is a direct analogy between the electrical and fluid quantities

$$R^* C^* \equiv \lambda_o \qquad (105)$$

It remains to interpret the resistance quantity and the capacitance quantity from the R^*C^* product.
From eq. 10:

$$\lambda = \frac{128}{\pi} \frac{\mu_o}{\rho o} \frac{L}{D^4} V \qquad (10)$$

However $\frac{128}{\pi} \frac{\mu_o}{D^4} = \frac{\partial p}{\partial x}_{/Q}$ from eq. 1.

Therefore $$R^*C^* = \left[\frac{\partial p}{\partial x} \frac{L}{Q}\right] \left[\frac{V}{\rho o}\right] \qquad (106)$$

The quantity $\frac{\partial p}{\partial x}_L$ is the total steady-state pressure differential over the tube length L, thus it must be that

$$R^* = \frac{\partial p}{\partial x} \frac{L}{Q} \qquad (107) \quad \frac{\text{lb sec}}{\text{ft}^5} \qquad \frac{\text{RESISTANCE}}{\text{(Volumetric flow)}}$$

and therefore the capacitance C* must correspond to:

$$C^* = \frac{V}{\rho o} \qquad (108) \quad \frac{\text{ft}^5}{\text{lb}} \qquad \frac{\text{CAPACITANCE}}{\text{(Volumetric flow)}}$$

It is to be noted that volume flow Q as the analog "current" is used for the resistance; laminar incompressible flow was assumed in the tube and for this type of flow the pressure drop is proportional to the viscous shear, which is due to velocity gradient and viscosity. On the other hand, the mass (or weight) flow ρQ (or $g \rho Q$) may be preferable as more generally convenient as the analog "current"; then the resistance must be divided by :

$$R^* \equiv \frac{\partial p}{\partial x} \frac{L}{\rho_o Q} = \frac{\partial p}{\partial x} \frac{L}{M} \qquad (109) \qquad \frac{\text{RESISTANCE}}{\text{(mass flow)}}$$

and therefore the capacitance C* must correspondingly be multiplied by to maintain λ_o unchanged:

$$C^* = \frac{V \rho_o}{\rho o} \qquad (110)$$

But since $\frac{p_o}{\rho_o}$ is the square of the isothermal velocity of sound in the chamber, then

$$C^* = \frac{V}{c^2} \qquad (111)$$

But since $c^2 = g\,RT$ (112)

where

$g = 32.2$ ft/sec^2 (acceleration of gravity)

$R =$ ft/^oF (gas constant)

then $C^* = \frac{V}{g\,RT}$ (113) $\frac{\text{CAPACITANCE}}{\text{(mass flow)}}$

ELECTRICAL ANALOGY TABLE I.

	Effort	Current	Resistance	Capacitance
Electric	v (volts)	I (amps)	R* (ohms)	C* (farads)
Fluid - Volume Flow	P (lb/ft^2)	Q (ft^3/sec)	$\frac{\partial P}{\partial x}\frac{L}{Q}\left(\frac{lb\ sec}{ft^5}\right)$	$\frac{V}{Po}\left(\frac{ft^5}{lb}\right)$
Fluid - Mass Flow	P (lb/ft^2)	M ($\frac{lb\ sec}{ft}$)	$\frac{\partial P}{\partial x}\frac{L}{M}\left(\frac{1}{ft\ sec}\right)$	$\frac{V}{gRT}$ (ft sec^2)
Fluid - Weight Flow	P (lb/ft^2)	W (lb/sec)	$\frac{\partial P}{\partial x}\frac{L}{W}\left(\frac{sec}{ft^2}\right)$	$\frac{V}{RT}$ (ft^2)

The above table summarizes the electrical analogy to the elementary fluid theory. It is to be well understood that there are three possible definitions of fluid parameters, depending on whether the volume flow, the mass flow or the weight flow is preferred for the "current". Each set of parameters is valid, but care must be taken to avoid interchanging parameters between the three sets. The choice of the "current" is up to the circuit designer and depends on the particular circuit and the fluid and pressure used. For liquids, the volume flow seems indicated; for compressible gases at substantial pressure ratios, the mass or weight flow would be probably used. In the dimensional notation, "lb." is intended as pound force. The tube contributes only a resistance and the only volume contribution is that of the chamber. While it may seem inconsistent that incompressible flow was assumed for the tube resistance and isothermal compressibility for the chamber, it must be noted that the fluid resistance mechanism is "incompressible" if the flow Mach Number is low (say 0.1 or 0.2), even if the fluid itself is a compressible

gas. A change of pressure along the tube will affect the local density and flow velocity and thus the local $\frac{\partial p}{\partial x}$, without introducing actual high Mach "compressibility" effects in the flow pattern.

In conclusion, there is an exact analogy between the elementary fluid theory and the simple lumped-parameter electrical circuit; the analogy will hold within the restrictive assumptions of the elementary theory.

It is expected that this analogy will be very useful for quick preliminary circuit synthesis and design.

2.5.2. Analogy to Corrected Fluid Theory.

In general, the simple electrical network discussed above is not an adequate analog to the corrected fluid theory. If, however, the electrical network is improved by introduction of distributed resistances and capacitances to represent the tube, then its basic usefulness is impaired by the growing complexity of the circuit; furthermore, there does not seem to be any clear cut manner to prescribe the number of distributed parameters required as the Stokes Number increases from 0 to 100 and higher.

2.5.2.1. Analogy to High-damping Regime.

First the analogy will be examined for the high-damping (small S) fluid regime, where the attenuation ratio approaches the elementary formula for small values of the attenuation parameters.

For small ψ_{To}, the attenuation approaches:

$$\frac{\bar{\xi}_L}{\xi_o} = \frac{1}{1 + \psi_{Io}} = \frac{1}{1 + j\chi_{Io}} \qquad (38)$$

and for both ψ_{Io} and ψ_{To} small, the attenuation approaches:

$$\frac{\bar{\xi}_L}{\xi_o} = \frac{1}{1 + \frac{\psi^2_{To}}{2}} = \frac{1}{1 + j\frac{\chi_{To}}{2}} \qquad (39)$$

The two above equations are to be compared with the elementary solution

$$\frac{\bar{\xi}_L}{\xi_o} = \frac{1}{1 + j\chi_o} \qquad (18)$$

and it is seen that they possess the same form. For the case of small values of both ψ_{To} and ψ_{Io} it is possible to define a composite attenuation factor χ by the relation

$$\chi = \chi_{Io} + \frac{\chi_{To}}{\sqrt{6}}$$

$$\text{or } \lambda = \lambda_{Io} + \frac{\lambda_{To}}{\sqrt{6}} \qquad (40)$$

For the analogy then, for small ψ_{To} and ψ_{Io} values:

$$R^*C^* = \lambda = \lambda_{Io} + \frac{\lambda_{To}}{\sqrt{6}} \qquad (114)$$

Now: $\lambda_{Io} = \frac{\lambda_o}{m} = \frac{128}{\pi} \frac{\mu_o}{m p_o} \frac{L}{D^4} V$

$$\lambda_{To} = \frac{\pi D^2 L}{4 V} \frac{\lambda_o}{n} \qquad (115)$$

$$\lambda = \frac{\lambda_o}{m} + \frac{\pi D^2 L}{4\sqrt{6}\ V} \frac{\lambda_o}{n}$$

As before $\lambda_o = \left(\frac{\partial p}{\partial x} \frac{L}{Q}\right) \left(\frac{V}{p_o}\right)$ (116)

Therefore

$$\lambda = \left(\frac{\partial p}{\partial x} \frac{L}{Q}\right) \left[\frac{V}{p_o m} + \frac{V}{p_o n} \frac{\pi D^2 L}{4\sqrt{6}\ V}\right] \qquad (117)$$

and finally

$$\lambda = \left[\frac{\partial p}{\partial x} \frac{L}{Q}\right] \left[\frac{V}{p_o m} + \frac{AL}{\sqrt{6}\ p_o n}\right] \qquad (118)$$

where $A = \frac{\pi D^2}{4}$

and AL = volume of tube

As was done before

$$R^* \equiv \frac{\partial p}{\partial x} \frac{L}{Q} \qquad (119)$$

and $$C^* \equiv \frac{V}{p_o m} + \frac{AL}{\sqrt{6}\, p_o n} = \frac{V}{p_o}\left[\frac{1}{m} + \frac{AL}{V}\,\frac{1}{\sqrt{6}\, n}\right] \qquad (120)$$

or $$C^* = C_o^*\left[\frac{1}{m} + \frac{AL}{V}\,\frac{1}{n\sqrt{6}}\right]$$

where C_o^* is the elementary theory capacitance

The resistance analogy has remained unchanged, but the capacitance analogy has changed to include polytropic exponents and to include a contribution from the tube volume.

If $\frac{AL}{V}$ is small, then the only change to the elementary theory capacitance is the inclusion of the polytropic chamber exponent m.

A summary table for the analogy is shown below, similar to that for the elementary theory.

ELECTRICAL ANALOGY TABLE II.

	Effort	Current	Resistance	Capacitance
Electric	v	I	R*	C*
Fluid-Volumetric Flow	P	Q	$\frac{\partial p}{\partial x}\,\frac{L}{Q}$	$\frac{V}{po}\left[\frac{1}{m} + \frac{AL}{V}\,\frac{1}{n\sqrt{6}}\right]$
Fluid - Mass Flow	P	M	$\frac{\partial p}{\partial x}\,\frac{L}{M}$	$\frac{V}{gRT}\left[\frac{1}{m} + \frac{AL}{V}\,\frac{1}{n\sqrt{6}}\right]$
Fluid - Weight Flow	P	W	$\frac{\partial p}{\partial x}\,\frac{L}{W}$	$\frac{V}{RT}\left[\frac{1}{m} + \frac{AL}{V}\,\frac{1}{n\sqrt{6}}\right]$

The dimensional notation is the same used in Table I.

The polytropic exponents m and n (for chamber and tube respectively) are not necessarily equal; their values range from 1.0 (isothermal) to γ (adiabatic). It is suggested as a first approximation that a linear relation be assumed for m and n against the parameter S, i.e. $m = n = 1.0$ @ $Z = 0$ and $m = n = \gamma$ @ $Z = 100$. For $S > 100$, it is certainly true that $m = n = \gamma$.

Actually m and n should be determined by experiment for the prevailing operational conditions.

It remains to discuss the meaning of the assumed condition that ψ_{Io} and ψ_{To} are both small. When this condition is violated, then the simple electrical analogy seems to break down.

For the attenuation parameters ψ's to be small, the attenuation factor χ's must be small.

$$\chi_{Io} = \frac{128}{\pi} \frac{\mu_o}{mpo} \frac{L V \omega}{D^4} \qquad (121)$$

Thus $\pi mp.D^4 \gg 128 \mu_o L V W$

$$\text{or} \quad \boxed{\frac{mpo}{\omega \mu_o} \gg 40 \frac{LV}{D^4}} \qquad (122) \quad \underline{\text{LIMITATION CRITERION}} \text{ I}$$

On the right side are all the geometric quantities, on the left side are all the fluid, thermodynamic and dynamic quantities.

$$\chi_{To} = \left(\frac{L}{D}\right)^2 \frac{\mu_o \omega 32}{n p_o} \qquad (123)$$

Thus $D^2 np_o \gg L^2 \mu_o \omega 32$

$$\text{or} \quad \boxed{\frac{npo}{\mu_o \omega} \gg 32 \frac{L^2}{D^2}} \qquad (124) \quad \underline{\text{LIMITATION CRITERION}} \text{ II}$$

Thus it may be stated that for the simple electrical analogy to be valid even in the high-damping fluid regime, the above criteria I and II must generally hold. The practical limitation of the $\gg$ symbol can only be made clear by abundant experimental data. Certainly the left-side quantity should be at least one order of magnitude greater than the right-side quantity.

Since only the high-damping regime was considered, where $S \leq 1$, then the total restrictive set of criteria is summerized below (assuming $m \equiv n$):

$$\frac{npo}{\omega\mu_o} \gg 40\left(\frac{L}{D}\right)^2 \qquad (124)$$

LIMITATION CRITERIA FOR APPLICABILITY OF SIMPLE ELECTRICAL ANALOGY.

$$\frac{npo}{\omega\mu_o} \gg 40\left(\frac{L}{D}\right)^2\left(\frac{V}{D^2L}\right) \qquad (122)$$

$$\frac{\omega D^2}{4\nu_o} \leq 1.0 \qquad (70)$$

Whenever the electrical analogy is applied, it is recommended that the above criteria be computed and recorded, so as to build up a body of experimental data to verify the accuracy of the analogy and the applicability of the above criteria.

2.5.2.2. Analogy to Low and Intermediate Damping Regimes.

Since the simple electrical analogy is limited within the high-damping regime, it is clearly not applicable to the intermediate and low damping fluid regimes. A more complex electrical analogy must be made, by the introduction of distributed resistances and capacitances to represent the tube. There does not seem to be any clear cut manner to prescribe the number of distributed parameters required as S increases from 1.0 to 100 and higher.

In any event, the usefulness of the simple electric analogy for preliminary circuit design work is certainly impaired by the growing complexity of the electrical circuit.

In the very low damping (acoustic) regime for $S \gg 100$, an analogy may be made between the electrical "telephone" equations and the longitudinal (one-dimensional) flow equations when the fluid viscosity is assumed to be negligible ($\mu o \equiv 0$). This analogy is described in Appendix III, "On the Usefulness of the Analogy Between Acoustical and Electric Circuits".

In all cases, whether it is the simple lumped-parameter analogy, the distributed-parameter analogy or the telephone-line analogy, the analogy is not an identity; its qualifications and limitations must be clearly understood.

2.6. LIST OF REFERENCES.

1. A. S. Iberall, "Attenuation of Oscillatory Pressures in Instrument Lines". NBS Research Paper RP 2115 1950

2. S. Goldstein, "Modern Developments in Fluid Mechanics" Vol. I. pp. 299 - 308. Oxford Clarendon Press 1950

2.7. LIST OF SYMBOLS

			Dimensions
A	=	tube cross-sectional area	$[ft^2]$
C	=	velocity of sound	$[ft/sec]$
C_T	=	velocity of sound in tube	
C_I	=	velocity of sound in chamber	
C*	=	electrical capacitance	[farads]
D	=	inside diameter of tube	[ft]
F_1, F_2	=	correction functions	[0]
J_o, J	=	Bessel functions	
L	=	tube length	[ft]
M	=	mass flow	$\left[\frac{lb\ sec}{ft.}\right]$
Q	=	volumetric flow	$[ft^3/sec]$
r	=	volume ratio	[0]
R	=	gas constant	$[ft/^oF]$
R*	=	electrical resistance	[ohms]
R_e	=	Reynolds Number	[0]
U	=	Mean velocity in tube	$[ft/sec]$
Z	=	frequency parameter	[0]
T	=	absolute temperature	$[^oF]$
V	=	chamber volume	$[ft^3]$
W	=	weight flow	[lb/sec]
b	=	compressibility factor for liquids	[0]
c	=	arbitrary constant	[0]
f	=	arbitrary function	[0]
g, h	=	Bessel function arguments	[0]
ℓ	=	entrance length of tube	[ft]
m	=	exponent of polytropic expansion of chamber	[0]

n	=	exponent of polytropic expansion of tube	$[0]$
p	=	pressure	$[lb/ft^2]$
t	=	time	$[sec]$
u	=	axial velocity	$[ft/sec]$
x	=	axial distance along tube	$[ft]$
S	=	Stokes Number	$[0]$
γ	=	ratio of specific heats	$[0]$
δ	=	phase angle	$[0]$
η	=	density ratio	$[0]$
λ	=	time constant	$[sec]$
μ	=	absolute fluid viscosity	$[lb\ sec/ft^2]$
ν	=	Kinematic fluid viscosity	$[ft^2/sec]$
ξ	=	fractional pressure increment	$[0]$
ρ	=	fluid mass density	$[lb\ sec^2/ft^4]$
ϕ	=	velocity potential	$[0]$
χ	=	attenuation factor	$[0]$
ψ	=	attenuation parameter	$[0]$
ω	=	angular frequency	$\left[\frac{1}{sec}\right]$

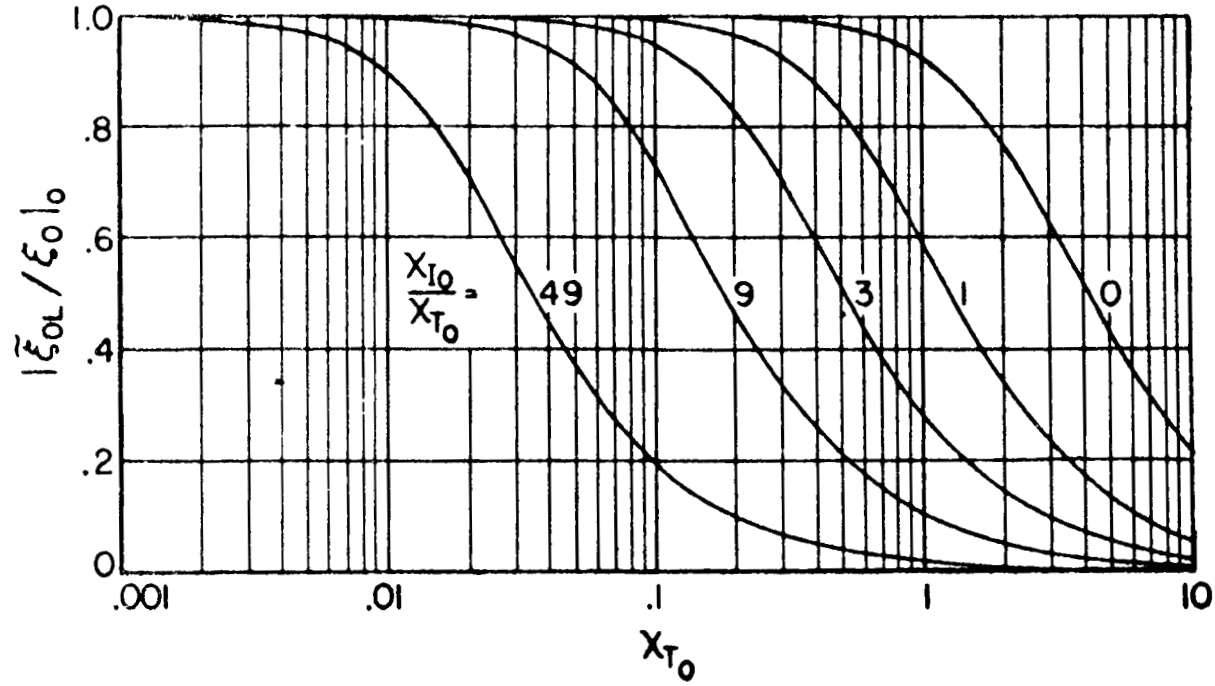

Real amplitude ratio vs. attenuation factor, for several ratio of chamber to tube volumes. High-damping regime ($S \leq 1.0$).

FIGURE 2.3.3-1

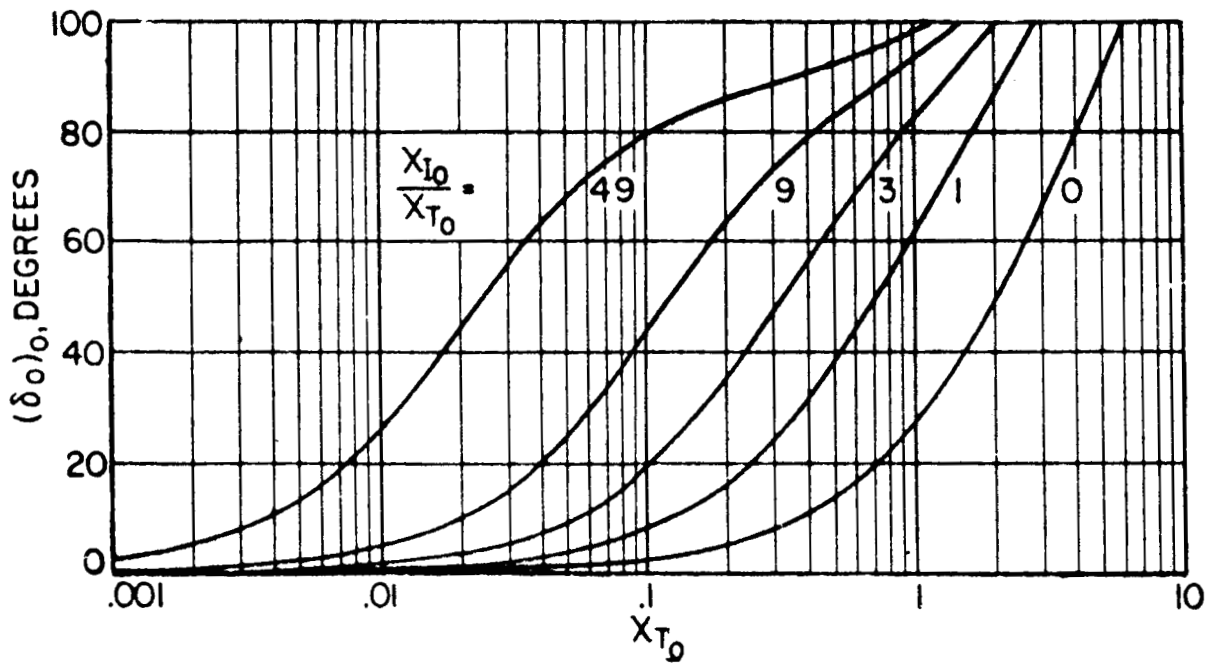

Phase lag vs. attenuation factor, for several ratios of chamber to tube volumes. High-damping regime ($S \leq 1.0$).

FIGURE 2.3.3-2

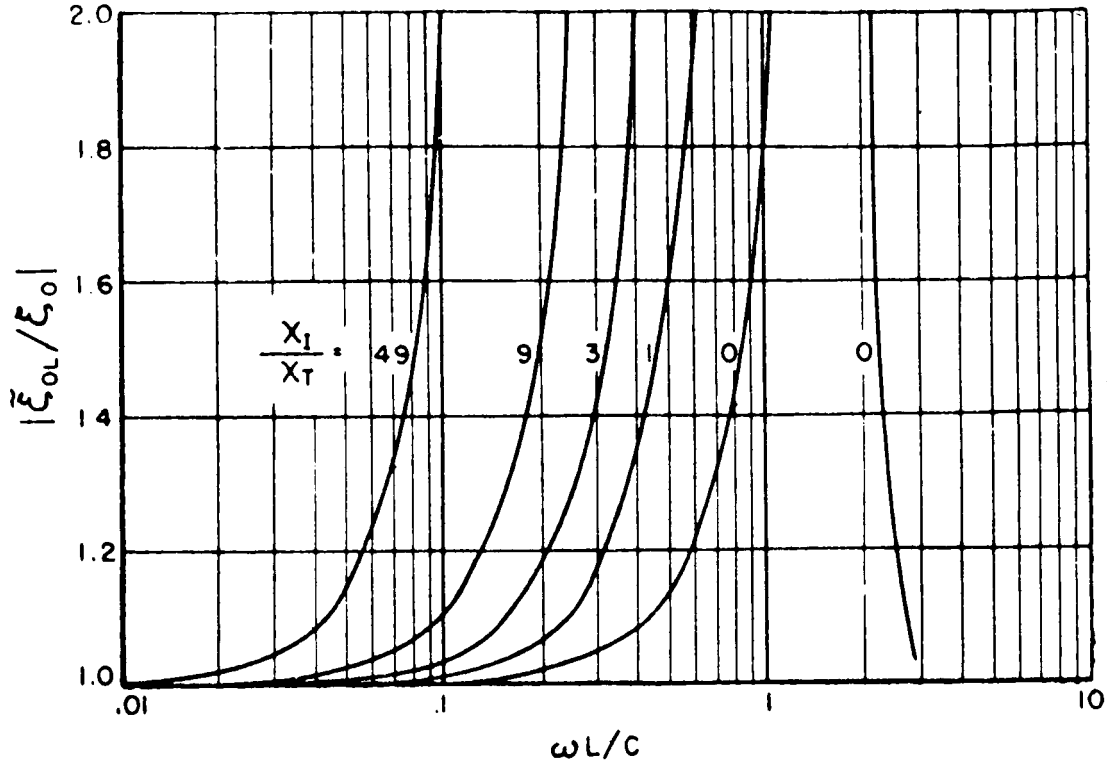

Real amplitude ratio vs. frequency parameter Z for several ratio of chamber to tube volumes. Low-damping regime (S≤100).

FIGURE 2.3.3-3

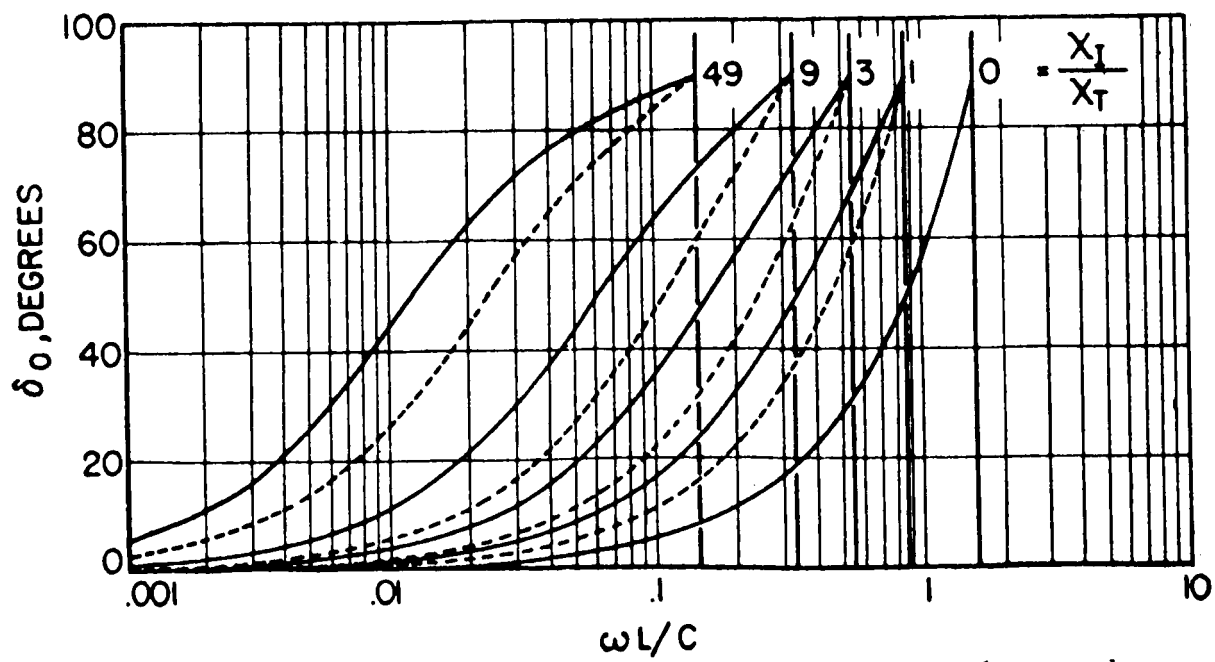

Phase lag vs. frequency parameter Z for several ratios of chamber to tube volumes. Low-damping regime (S ≤100), for γ = 1.0 (solid line) and γ = 2.0 (dashed line). Vertical lines are for limit case of zero damping.

FIGURE 2.3.3-4

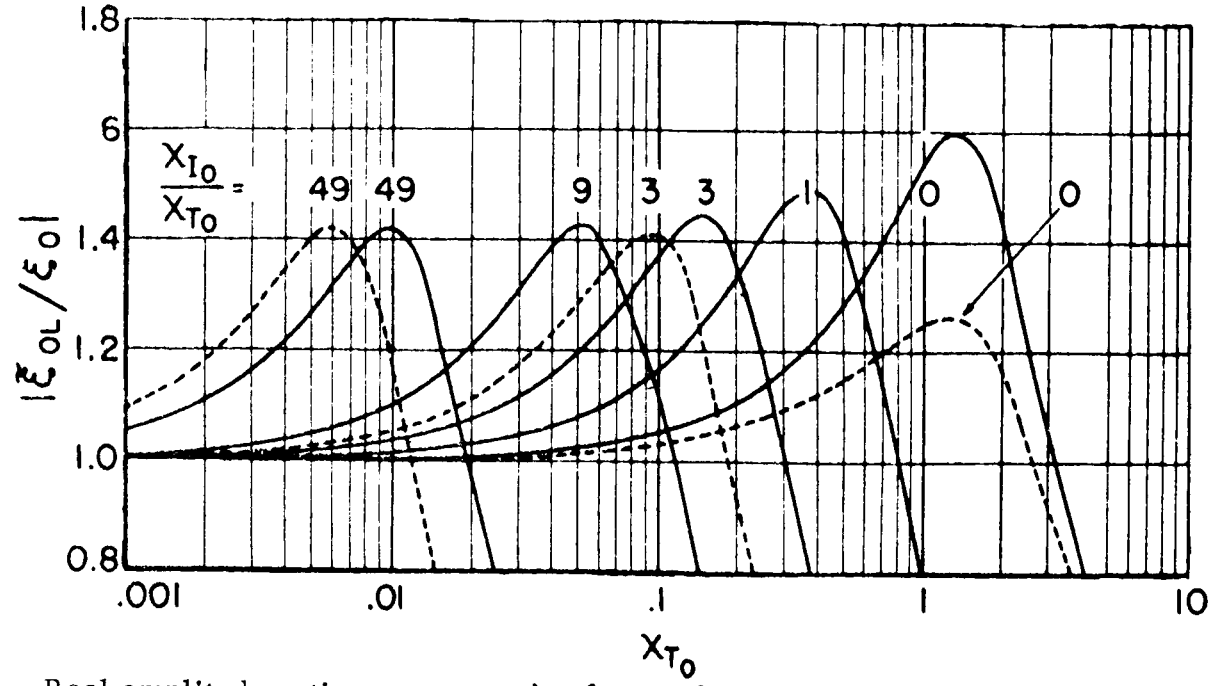

Real amplitude ratio vs. attenuation factor, for several ratios of chamber to tube volumes. Intermediate damping regime (S = 6.25), for γ = 1.0 (solid line) and γ = 2.0 (dashed line).

FIGURE 2.3.3-5

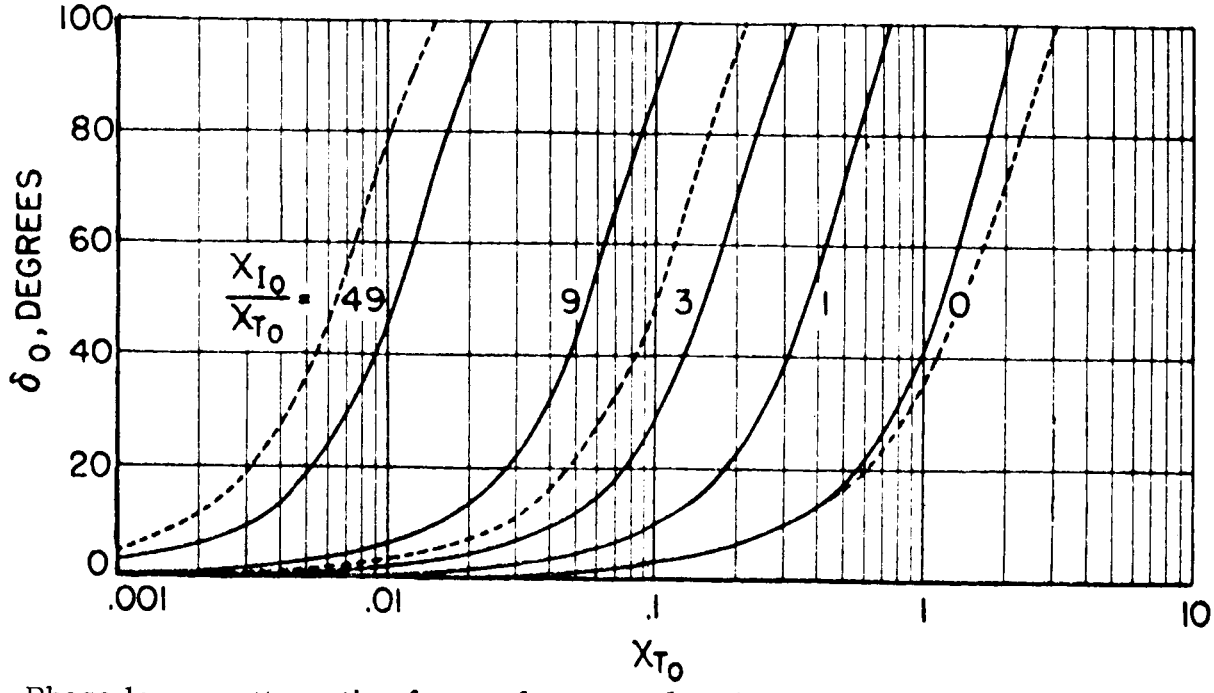

Phase lag vs. attenuation factor, for several ratios of chamber to tube volumes. Intermediate-damping regime (S = 6.25), for γ = 1.0 (solid line) and γ = 2.0 (dashed line).

FIGURE 2.3.3-6

FEASIBILITY STUDY OF A THRUST-VECTOR-CONTROL SERVOSYSTEM

3.1. Introduction

The new technology of pure fluid amplification deserves careful consideration for use in selected NASA programs because of the potential high reliability of operation under adverse environmental conditions. A particularly promising application is the use of a fluid servo system in thrust vector control of large boosters. The environmental conditions of temperatures ranging from LH_2 (-250^{o} F) to combustion chamber temperatures (5000^{o} F), extremely high acoustic levels, and severe vibration levels, all of which are found in large rocket boosters, may require fluid control systems. One promising future fluid servosystem for thrust vector control could operate with commands from the upper stage but upon stage separation the fluid servosystem would utilize fluid inertial components to serve as the control system for booster recovery.

The ultimate objective of this program is the development of prototype hardware utilizing the inherent high reliability of pure fluid systems and which would be applicable to servosystem requirements in selected NASA programs. The thrust vector control of Saturn class vehicles has been chosen as a typical application for this preliminary development effort.

A fluid hybrid system connotates the use of components other than pure fluid in addition to certain pure fluid components. In any system requiring a controlled movement of a mechanical part (such as the gimballed nozzle), the system cannot be a pure fluid system. However, if thrust vector control is accomplished by the use of secondary injection of gases from the combustion chamber into the nozzle, then a pure fluid TVC system can be designed. The table 3.1-1 illustrates three types of hybrid and pure fluid systems which could be designed around the basic thrust vector control problem.

The servosystem problem involves the control of a gimballed nozzle in response to electrical commands from the Saturn upper stage guidance computer. It will be noted that the system requires an electrical to fluid input transducer, a pure fluid servo-amplifier containing a summing junction, a servovalve, an actuator, and a position feedback transducer.

The best proportional pure fluid component (yet developed) to be used as the basis for high gain servo-amplifier functions, summing and differencing functions, and servo-shaping functions is the Impact Modulator developed by Johnson Service Company. Sperry Utah Company under exclusive arrangements with Johnson Service Company has utilized the Transverse Impact Modulator to perform the required fluid control functions.

TABLE 3.1-1

CLASSIFICATION OF THRUST VECTOR CONTROL SYSTEMS

SYSTEM ELEMENTS	PURE FLUID TYPE SYSTEM	HYBRID I TYPE SYSTEM	HYBRID II TYPE SYSTEM
THRUST CONTROL	SECONDARY GAS INJECTION	GIMBALLED NOZZLE	GIMBALLED NOZZLE
ACTUATOR	NONE	PNEUMO-MECHANICAL OR HYDRAULIC	PNEUMO-MECHANICAL OR HYDRAULIC
SERVOVALVE	PURE FLUID	PURE FLUID	MECHANICAL
COMMAND	ELECTRIC-FLUID TRANSDUCER	ELECTRIC-FLUID TRANSDUCER	ELECTRIC-FLUID TRANSDUCER
POSITION FEEDBACK TRANSDUCER	SENSED THROUGH GUIDANCE INERTIAL COMPONENTS	PURE FLUID	PURE FLUID
SUMMING AMPLIFIER	PURE FLUID	PURE FLUID	PURE FLUID
MECHANICAL MOVING PARTS	NONE	NOZZLE & ACTUATOR	NOZZLE, ACTUATOR, SERVOVALVE
OPERATING FLUIDS	HOT GAS SECONDARY INJECTION (2000° F) EITHER HOT OR COLD GAS FOR AMPLIFIERS	COLD GAS (CAN USE LH_2 BOIL OFF) (-250° F) & EITHER GAS OR HYDRAULIC FOR ACTUATORS	COLD GAS (CAN USE LH_2 BOIL OFF) (-250° F) & EITHER GAS OR HYDRAULIC FOR ACTUATORS

3.2. General Description of NASA Nozzle-Gimballing Servosystem.

A specific class of nozzle-gimballing TVC servosystems for Saturn-type vehicles has been considered for this feasibility study. The type of servosystem will be a Hybrid Type II, as defined above in Table 3.1-1, where the actuator and the servovalve are of conventional design.

3.2.1. NASA System Specifications.

The NASA system information has been derived from NASA "Pneumatic Actuator Thrust Vector Control Specification" of 12-9-63, Dwg 50M35026. The available fluid is cold gaseous hydrogen at -250° F and at a nominal maximum pressure of $800 \begin{smallmatrix} +50 \\ -100 \end{smallmatrix}$ PSIG. The vehicle space environment is expected to be near vacuum. The actuator stroke is to be 3.0" and the gimballed-nozzle angular range is to be $\pm$ 7.5°.

The closed-loop maximum actuator force is to be 34,800 lb. Rated load is to be 23,200 lb, consisting of 7300 lb dry friction and an inertia load of 1400 slugs.

The gas consumption shall be not greater than 3.0 lb/min with the system cycling at 0.3 cps with the input magnitude corresponding to 1/3 max. actuator displacement.

The quiescent flow consumption shall be limited to 0.08 lb/min.

The maximum closed-loop actuator velocity under rated load shall be not less than 1.6 in/sec and the load acceleration shall be not less than 21 in/sec^2.

The transient response to a step input of 0.05" (0.25°) shall be within $\pm$ 2.5% of the steady-state value within 0.35 seconds, as shown in Fig. 3.2-1.

The closed-loop frequency response of the entire servosystem as shown in Fig. 4.2-2 shall have no greater than 20° phase lag at 1 cps and a peak amplitude ratio not greater than 1.5. The system shall be stable with at least 30° and 6 db phase margin and gain margin respectively.

The system shall have a bandwidth of at least 8 cps.

The linearity of the position feedback transducer shall meet the requirements shown in Fig. 3.2-3.

3.2.2. Definition of Two Subsystems and of Interface.

For this feasibility study effort, a Hybrid Type II servosystem is considered.

The first reason for this choice is that a pure fluid servovalve has not yet been developed and the second reason is that no known pure fluid servovalve can meet the stated requirements of very small quiescent flow.

All pure fluid servovalve are characterized by a more or less constant fluid demand. It is believed that 20% of maximum flow is the best that could be achieved with the present state of the art with a pure fluid vortex throttling valve.

The complete servosystem of Fig. 3.2-2 can be redrawn as a hybrid fluid-mechanical system as shown in Fig. 3.2-4; it comprises a Fluid Bridge, an Operational Amplifier with Shaping Circuits, Fluid Bellows, a conventional Servovalve and a conventional Actuator.

For convenience of analysis and development, the hybrid servosystem may be subdivided into two parts, i.e. the Fluid Control Subsystem and the Power Subsystem, as indicated in Fig. 3.2-4. The interface between the two subsystems is given by the fluid bellows, which accept the fluid output of the Operational Amplifier and provides the force input to the conventional servovalve.

The Fluid Control Subsystem comprises the electric/fluid command transducer, the fluid position-feedback transducer (mounted on the actuator shaft), the operational amplifier and the fluid bellows.

The Power Subsystem comprises the fluid bellows, the servovalve, the actuator and the load.

The bellows are listed with both subsystems because they form the interface.

3.3. Program Goals.

The program goals under this contract comprise the feasibility study and demonstration of the Fluid Control Subsystem.

First the steady-state performance of the components was developed and demonstrated, with particular attention to linearity and repeatability; then the entire subsystem was tested, from electric command input to output pressure into the fluid bellows.

Dynamic analysis was performed for all components and for the subsystem; from these results shaping requirements were determined, on the basis of the servo analysis of the complete system (including load) and of the NASA specifications.

3.4 Power Subsystem.

Some knowledge of the servovalve and actuator package is required in order to design the Fluid Control Subsystem output properly.

A tentative selection has been made, on the basis of the Gemini Rotary Actuator package, which was developed by the Vickers Division of Sperry Rand Corporation for North American Aviation under contract to NASA.

The package characteristics have been found to be approximately satisfactory for the system considered, with the addition of a lead screw or similar mechanism to convert rotary into linear motion.

The dynamic characteristics of the servovalve-actuator assembly have been studied by Vickers at some length.

Figure 3.4-1 gives a simplified simulation diagram of the Gemini Actuator Assembly for force input, which is the applicable input from the fluid bellows. The required force input is ± 15 lbs and the required bellows displacement has to be ± 0.015"; these data are sufficient to design the output of the Fluid Control Subsystem.

Other selections may be made later, on the basis of different hardware, at the option of NASA personnel.

3.5 Fluid Control Subsystem.

3.5.1. Introduction.

Considering Fig. 3.2-4, the Fluid Control Subsystem comprises an electric-to-fluid command transducer, a fluid position-feedback transducer (mounted on the actuator output shaft), an operational amplifier with associated shaping circuits as required, and fluid bellows.

The gross requirements imposed on the subsystem are as follows:

NASA Specs	Output Shaft Displacement	0" - 3.0"
	Max. Electric Input to Servovalve	250 mw.
Gemini Actuator-Assembly Specs	Bellows Force	± 15 lb.
	Bellows Displacement	± 0.015"

The fluid-dynamics analysis of the subsystem for this program has been directed toward room-temperature air as the working fluid and std. atmosphere as the dump conditions.

The first fluid problem is the selection of a supply pressure common to all fluid elements, which would be as low as possible, to minimize flow and power requirements.

As will be shown later in detail for each component, the minimum common supply pressure is 20.0 PSIG.

One of the subsystem fluid parameters which was investigated is the effect of supply pressure variation and therefore the supply - dump pressure regulation requirements. This pressure regulation, which is taken for granted in the laboratory, may well prove to be one of the major problems in a space system.

The second fluid problem of the subsystem is the flow-and-pressure matching of the electric transducer to the feedback transducer and the matching of both to the operational amplifier.

Finally the operational amplifier must have a sufficient flow and pressure output to operate the bellows fast enough and to yield the required force. The maximum pressure differential across the bellows should be at least 10 PSI and the flow into the bellows should be of the order of 1/3 CFM.

3.5.2. Electric/Fluid Command Transducer.

The electric-to-fluid command transducer has been selected to be the Johnson Service Company Model N-6800, which was originally developed for temperature control of industrial installations. The device is shown in Fig. 3.5-1; it was designed to convert a 0 to 15 volt DC input signal into a linear 0 to 20 PSI output pressure. The instrument has a factory calibrated sensitivity setting of 1.33 PSI/volt; a calibrating set screw is provided for adjusting the sensitivity to any value within a 0.5 to 4.0 PSI/volt. range.

A change in the voltage input to the transducer electro-magnetic coil changes the position of the transfer lever in relation to a control port. This actuates a pneumatic flapper-valve relay and produces an output pressure which is linear to the input voltage.

Pneumatic feedback is incorporated to provide maximum accuracy and stability between the input voltage and the output pressure. On electric power failure, the output pressure will be zero (shut-off flow).

The coil resistance is 1000 ohms, so that the current is 0-15 ma DC for an input range from 0-15 volts DC, yielding a maximum input power of 225 mw, which is below the specified 250 mw.

In this application, the N-6800 transducer has been employed in a particular manner, i.e. the flow has been by-passed to atmosphere through a fixed orifice and the fluid output has been tapped off the chamber comprised between the fixed orifice and the electrically controlled valve. This was done in order to reduce the output pressure range from 20 PSI to 1.5 PSI, which was desired for the operational amplifier input.

In this manner of operation, the electric input has been limited from 0.2 to 0.8 volts DC, with consequent reduction of the maximum electric input power to about 1 mw, which is extremely low and two orders of magnitude less than the allowed 250 mw. The steady-state calibration of the modified transducer is shown in Fig. 3.5-2, for a supply pressure of 20.0 PSIG against atmospheric dump. The linearity of output-pressure against input voltage is seen to be good, the repeatability is also satisfactory.

It is to be noted, however, that the transducer is sensitive to supply pressure changes, the output pressure being directly proportional to the supply pressure; also, in its present form, the transducer is susceptible to shock and vibration and its frequency response is quite low, being limited to about 5 cps. The N-6800 transducer has been satisfactory for a feasibility demonstration of the Fluid Control Subsystem; however, for actual space application, it must be redesigned to make the device more rugged, increase the bandwidth to be flat to at least 50 cps and increase the natural frequency high enough to preserve system stability. Also its sensitivity to supply pressure must be decreased by an appropriate feedback loop.

3.5.3. Position-Feedback Transducer.

The fluid position-feedback transducer must yield a fluid pressure which is linearly proportional to a linear or rotary displacement.

One approach to the problem is a linear variable resistance; a second approach is the nozzle-flapper arrangement. Since the first approach would be quite difficult to apply to a rotary displacement, it was decided to employ the second approach as the more general and as possessing ample technical background.

Fleckenstein[1] presents a method for determining the Laplace transform of a pneumatic nozzle-flapper combination.

Norwood[2] has conducted extensive studies on nozzle-flapper valves. Pawlak[3] also has investigated the nozzle-flapper.

Much work has been done at the Dynamic Analysis and Control Laboratory, MIT under contract to the US Air Force Basic Research and Development in Fluid Power Control.

The mode of operation chosen for the position transducer was to keep the upstream orifice always supercritical and the downstream nozzle flow always subsonic for all flapper positions. In this manner, for a constant supply conditions, the weight flow passing through the nozzle would be constant for all flapper positions, assuring more accurate pressure output and faster operation.

The dimensioning of the device was dictated by the requirement to have a nozzle flow very much greater than the flow tapped off to the operational amplifier, so that the chamber pressure would not be disturbed.

The upstream orifice diameter was set at 0.048" and the nozzle diameter at 0.125".

The flow rate at 20 PSIG was 1.22 CFM (std. atm.)
The flow rate at 25 PSIG was 1.37 CFM (std. atm.)
The flow rate at 30 PSIG was 1.54 CFM (std. atm.)

Since linear or rotary displacement was to be sensed, the flapper takes the form of a cam, so shaped by empirical development as to yield a linear relationship between displacement and chamber pressure.

It has been found that different flow patterns occur at different gap ratios so that the cam profile is probably dependent on the nozzle Reynolds Number.

Since the nozzle flow is constant, Re can be defined by the nozzle diameter, the average nozzle flow velocity and the fluid kinematic viscosity at ambient conditions.

Also it has been found that several layers of fine screen were required in the chamber to dissipate the pressure fluctuations due to the sonic jet issuing from the orifice into the chamber.

Two cams have been developed, one for a linear 0"-3.0" displacement and another for an angular 0°-75° displacement. The profiles of the two cams are similar, though not identical because of the curvature; they are shown in Fig. 3.5-3. The minimum gap for both cases is between 0.0205" and 0.021" and the maximum gap is between 0.045" and 0.055".

The steady-state calibration is presented in Fig. 3.5-4 showing the output pressure against displacement, at 20.0 PSIG supply pressure against atmospheric dump. It is seen that the linearity is excellent over the entire displacement range and that both transducers are perfectly matched; this is a significant achievement in fluid control technology. The effect of supply pressure changes is to affect the output pressure to the square of supply pressure ratio. Here again good supply pressure regulation is required.

The two transducers are displayed in Fig. 3.5-5 as mounted on a lathe cross-feed carriage and on a precision turn-table respectively, for steady-state bench testing.

3.5.4. Operational Amplifier Development

The operational amplifier has been designed and developed at the Research Division of the Johnson Service Company on the basis of the "Transverse Impact Modulator" proportional amplifier. The desired input and output characteristics of the amplifier have been specified by Sperry Utah early in the program on the basis of expected position transducer and electric transducer performance (pressure vs. displacement and volts vs. pressure).

The Impact Modulator is described by B. G. Bjornsen[4]; proportional circuitry applications are given by T. J. Lechner and P. H. Sorenson[5].

3.5.4.1. Operational Amplifier Theory.

An operational amplifier is a linear amplifier capable of multiplying the incoming signal by a constant, the value of which is selected by the ratio of a set of summing resistors. Figure 3.5-6a shows a schematic representation of an electronic operational amplifier which is idealized because it assumes the high gain amplifier in the forward leg has an infinite input impedance. While the electronic amplifier input impedance is not truly infinite it is many decades higher than the summing resistors and can be considered as such. In the pneumatic version of the operational amplifier the input impedance to the forward leg is not negligible and must be considered in the analysis, such that the schematic of Figure 3.5-6b must be used.

3.5.4.1.1. Analysis.

In order to design an operational amplifier, the input characteristics of the amplifier must be prescribed. It is further assumed that the output power range of this amplifier be sufficient to drive the summing resistors that are to be used; that is, the one or more in its own feedback and the inputs to several other operational amplifiers. These prescribed characteristics can be found in reference 6, section I, where the necessary ones are summarized below.

Input-output equations

$$P_o = P_R - K_o(P_A - P_B) \qquad (1)$$

Input impedance

$$R_A = 2\sqrt{P_B}/\beta \qquad (2)$$

Input flow (perturbation) equation

$$Q_A = \beta \sqrt{P_B} + \frac{1}{R_A} P_A \qquad (3)$$

Consider an operational amplifier having n inputs (one or several of which may be set points), each input possessing a particular gain with respect to the output, where it is desired that these gains be the resistance ratios of the feedback to forward resistance. Figure 3.5-7 shows the basic design of the operational amplifier where an elevated pressure P_L (above standard atmosphere) is used as zero reference in order to facilitate positive and negative signals.

Summing the flows in Figure 3.5-7 we find,

$$Q_A = \sum_{k=1}^{n} \frac{1}{R_k} (P_k - P_A) + \frac{1}{R_f} (P_o - P_A) \qquad (4)$$

Introducing the zero pressure level P_L we can write the pressures in equation (4) in terms of the pressures that exist at the zero reference, and the variational values around this level, that is,

$$p_k = P_k - P_L \qquad k = (1,2,3....n) \qquad (5a)$$

$$p_o = P_o - P_L \qquad (5b)$$

$$P_A = P_A - P_A(ave) \cong P_A - P_B^* \qquad (5c)$$

---

* Note that when the amplifier output is at P_L the amplifier input pressure P_A is not quite equal to P_B but rather

$$P_A(ave) = P_B - \frac{P_L - P_R}{k_o}$$

but since the gain (K_o) is very high in the limit

$$\text{Lim } P_A(ave) = P_B$$

$$K_o \rightarrow \infty$$

Substituting equation set 5 into 4

$$Q_A = \sum_{k=1}^{n} \frac{1}{R_k} (p_k + P_L - p_A - P_B) + \frac{1}{R_f} (p_o + P_L - P_A - P_B) \qquad (6)$$

Substituting (3) into (6)

$$\beta \sqrt{P_B} + \frac{1}{R_A} p_A = \sum_{k=1}^{n} \frac{1}{R_k} (p_k + P_L - p_A - P_B) + \frac{1}{R_f} (p_o + p_L - p_A - p_B) \qquad (7)$$

This equation consists of two parts, the steady terms, and the variational terms, each of which must be a separate equation. If we now define,

$$\text{(Total Conductance)} \quad G_T = \sum_{k=1}^{n} \frac{1}{R_k} + \frac{1}{R_f}$$

then equation (7) breaks into the following two equations,

Steady equation:

$$\beta \sqrt{P_B} = \sum_{k=1}^{n} \frac{1}{R_k} (P_L - P_B) + \frac{1}{R_f} (P_L - P_B) = G_T (P_L - P_B) \qquad (8)$$

Variational equation:

$$\frac{1}{R_A} p_A = \sum_{k=1}^{n} \frac{1}{R_k} (p_k - p_A) + \frac{1}{R_f} (p_o - p_A) \qquad (9)$$

The steady equation (8) gives the value of pressure P_B when all variational pressures are zero. Equation (8) is plotted in Figure 3.5-8 and with this value of P_B equation (2) can be used to find the amplifier input impedance, see Figure 3.5-9. In both of these figures P_L is taken to be 5 psig, as this is the value used in our amplifier design.

The variational equation (9) is the equation of main interest and from it the transfer function will result, expanding (9) we find:

$$\left(\frac{1}{R_A} + G_T\right) p_A = \sum_{k=1}^{n} \frac{1}{R_k} p_k + \frac{1}{R_f} p_o \qquad (10)$$

From equation (1) it can be seen that the variational change in p_o is related to p_A by

$$p_o = -K_o p_A$$

or,
$$p_A = \frac{p_o}{-k_o} \tag{11}$$

Substituting (11) into (10)

$$\left(\frac{1}{R_f} + \frac{1}{K_o R_A} + \frac{G_T}{K_o}\right) p_o = -\sum_{k=1}^{n} \frac{1}{R_k} p_k$$

or,
$$p_o = \sum_{k=1}^{n} \frac{-\left(\frac{R_f}{R_k}\right)p_k}{\left(1 + \frac{R_f}{K_o R_A} + \frac{R_f G_T}{K_o}\right)} \cong \sum_{k=1}^{n} -\left(\frac{R_f}{R_k}\right) p_k \tag{12}$$

In order for the closed loop gain to be equal to the resistance ratio $\frac{R_f}{R_k}$, the denominator in equation (12) must equal unity, that is:

$$\frac{R_f}{K_o}\left(\frac{1}{R_A} + G_T\right) = 0 \tag{13}$$

If equation (13) is not zero its value is approximately the error (ϵ) of gain prediction, so that

$$\epsilon\,\% = \frac{R_f}{K_o}\left(\frac{1}{R_A} + G_T\right) \times 100\% \tag{14}$$

Expanding:

$$\frac{\epsilon\,\%}{100\%} = \epsilon = \left(\frac{R_f}{K_o}\frac{1}{R_A} + \frac{1}{R_f} + \sum_{k=1}^{n} \frac{1}{R_k}\right)$$

$$= \frac{1}{K_o}\left(\frac{R_f}{R_A} + 1 + \sum_{k=1}^{n} \frac{R_f}{R_k}\right)$$

Let K_T define one plus the sum of the operational amplifier gains, i.e.,

$$K_T = 1 + \sum_{k=1}^{n} \frac{R_f}{R_k} \quad , \text{ then}$$

$$\epsilon = \left(\frac{R_f}{K_o R_A} + \frac{K_T}{K_o} \right) \tag{15}$$

Three equations then, must be considered for the amplifier design.

$$(2) \qquad R_A = \frac{2\sqrt{P_B}}{\beta}$$

$$(8) \beta\sqrt{P_B} = G_T(P_L - P_B) = \frac{K_T}{R_f}(P_L - P_B) \tag{16}$$

$$(15) \quad K_o \epsilon = R_f/R_A + K_T$$

Elimination of P_B and R_A from the above equations gives:

$$\frac{K_o \epsilon}{K_T} = 1 + \frac{1}{4}\left(\frac{R_f}{K_T}\right)\left(\frac{\beta}{\sqrt{P_L}}\right)\left\{\left[\left(\frac{R_f}{K_T}\right)\left(\frac{\beta}{\sqrt{P_L}}\right) + \sqrt{\left[\left(\frac{R_f}{K_T}\right)\left(\frac{\beta}{\sqrt{P_L}}\right)\right]^2 + 4}\right]\right\} \tag{17}$$

This equation is plotted in Figure 3.5-10 where the deviation between the amplifier gain and that predicted by R_f/R_i can be directly determined by knowing the amplifier characteristics (K_o, β, P_L) and the desired parameters (K_T, R_f).

Normalizing the unknowns in equation set (16) by letting

$$y = \frac{K_o \epsilon}{K_T}, \quad z = \frac{R_f}{K_T}, \quad w = \frac{\beta}{P_L}, \quad u = \sqrt{\frac{P_B}{P_L}}, \quad R_A = R_A$$

and solving we find

$$y = 1 + \frac{zw}{4}\left[zw + \sqrt{z^2w^2 + 4}\right]$$

$$z = \frac{2(y-1)}{w\sqrt{2y-1}} \qquad (18)$$

$$u = \left(\frac{w}{2z}\right) + \sqrt{\left(\frac{w}{2z}\right)^2 + 1}$$

$$R_A = \frac{2u}{w}$$

3.5.4.1.2. Experimental Verification.

Figure 3.5-11a shows the comparison between the calculated and actual gains computed from equation (12) where only one input was used. From this it can be seen that the equation is a true representation of the amplifier gain. It is, however, desirable that the gain be independent of the active elements such that for a given amplifier the graph of Figure 3.5-11a must be consulted to assure the prediction error is below the desired value. Figure 3.5-11b shows the gain range of the operational amplifier.

A double input amplifier designed with these considerations is shown in schematic form in Figure 3.5-12. The performance curves are illustrated in Figures 3.5-13 and 3.5-14. Corning resistors were used, and the numbers placed on the schematic are the Corning number, representing resistance values of that number x 10^6 #f sec/ft^5.

There was little time to perform frequency response data but the cutoff frequency of the amplifier is probably in the neighborhood of 10-20 cps. The reason for this low cutoff frequency is two-fold; first, the capacitance at the error junction coupled with the high values of summing resistors slowed the system down, and second the active elements were of relatively low power which were affected by capacitive loads. A more detailed discussion of this subject is presented later.

3.5.4.2. Operating Specifications and Circuit Design of Summing Amplifier for Fluid Control Subsystem.

The Fluid Control Sub-System is shown in Figure 3.2-4. The command signal (P_{c2}) is obtained from an electric-to-pneumatic transducer. This signal causes an unbalance in the differential input and thus the outputs of the amplifier which actuates the final operator. The operator alters the actuator position until the output shaft (which is connected to the actuator) is repositioned such that the amplifier inputs are again nulled.

The summing amplifier has an input range of 0.5 to 1.4 psig on each leg while the output range is 0-10 psig on each leg. When the inputs are equal the outputs are equal at 5 psig. Thus the equations relating static operation of the amplifier becomes:

$$P_{o1} = 5.0 + 11.0\ (P_{c2}-P_{c1})\ \text{psig}$$

$$P_{o2} = 5.0 - 11.0\ (P_{c2}-P_{c1})\ \text{psig} \qquad (19)$$

If the system were to operate at an elevated level (where the sink or reference pressure were P_r), the generalized operating equations become:

$$(P_{o1}-P_r) = 5.0 + 11.0\ (P_{c2}-P_{c1})\ \text{psid}$$

$$(P_{o2}-P_r) = 5.0 - 11.0\ (P_{c2}-P_{c1})\ \text{psid} \qquad (20)$$

The maximum flow which can be drawn from the pneumatic bridge is 9 in^3/min at 1.4 psid, defining the input resistance (R_i) of each leg as:

$$R_i \geq \frac{1.4}{9.0} = 0.155\ \frac{\#f\ \text{min}}{in^5} \qquad (21)$$

To insure a fast response time of the amplifier the short circuit output flow of 700 in^3/minute is required on each leg.

The supply pressure to the complete pneumatic system is 20 psig.

Based on the analysis of section 4.5.4.1, a schematic of the push-pull difference amplifier is illustrated in Figure 3.5-15, see photos of Figure 3.5-16. The lower amplifier in the schematic is a single output difference amplifier with a 11.0 gain on each leg. The equations governing this circuit are:

$$P_{o1} = 5.0 + \frac{R_f}{R_2} P_{c2} - \frac{R_f}{R_1} P_{c1}$$

$$P_{o2} = 10 - P_{o1} \qquad (22)$$

where $R_1 = R_2 = 0.5$ #f min/in^5

$R_f = 5.5$ #f min/in^5

so that equation (22) reverts to that of (19). The upper amplifier is a unity gain inverter used to obtain the double or push-pull outputs. Figure 3.5-17 shows the output difference versus input difference of that amplifier. Figure 3.5-18 shows the pressures required on each input in order to balance the outputs at 5.0 psig.

The amplifier frequency response was of the order of 15 to 20 cps, but can be increased to at least 50 to 75 cps with proper design. The reason for the low cut-off frequency of this unit is due to the non-optimum manifolding of the last stage.

As can be seen from Figure 3.2-4, the upper input to the summing amplifier is in the forward leg of the control sub-system, while the lower input is in the feedback leg. This means that proper phasing can be incorporated into either the forward or feedback leg or both.

Because of its unique feature of having positive and negative gains, we have the capability of adding or subtracting any number of signals. Such capabilities make it possible to perform differentiation, integration or combinations thereof on each of the nulling inputs.

Bootstrap integration is attained by trying a feedback connection to one of the positive inputs together with a parallel capacitor to ground. Thus we can attain pure integration as shown in Figure 3.5-19, or integration plus proportional action.

Pure differentiation is obtained by having the negative and positive gains equal, while derivative plus proportional action is achieved by having unequal gains. Examples of derivative control with increasing amounts of proportionality is illustrated in Figure 3.5-20.

3.5.5. Fluid Bridge.

The Fluid Bridge comprises the electric/fluid command transducer and the position-feedback transducer (either linear or angular); the bridge compares the signals and produces a pressure differential which is linearly proportional to the signal difference. The absolute level of the pressures, however, varies with the position along the displacement, as seen in Figs. 3.5-2 and 3.5-4; at X = 0 (or X = 0^{o}), the output pressure is low while at X = 3.0 (or X = 75^{o}) the pressure is high; the pressure differential, on the other hand, depends only upon the difference between the X - position (or θ^{o} position) and the electric command signal.

The bench testing layout of the fluid bridge can be seen in Fig. 3.5-21, where the complete Fluid Control Subsystem is shown.

The steady-state calibration of the Fluid Bridge is shown in Fig. 3.5-22, where the electric input signal (volts) is plotted directly against displacement, at 20 PSIG supply pressure against atmospheric dump. The linearity is seen to be good, as well as the repeatability, demonstrating the satisfactory matching of the two transducers into a Fluid Bridge.

The bridge calibration was tested with and without the operational amplifier, with undetectable changes in pressure. This demonstrates that the flow being tapped off into the amplifier is sufficiently small in comparison to the supply flow to the transducers.

The effect of supply pressure changes has been checked and has been found to unbalance the null between the electric and either position transducer, while no effect can be seen on the null between the two position transducers when connected against each other in a bridge.

It is highly desirable that the null be independent of supply pressure; if it can be achieved between the two position transducers, it can also be achieved between the electric transducer and the position transducer by proper redesign of the former. It can also be conceived that the angular position transducer (0^{o}-75^{o}) be used as a command transducer through a Selsyn (or similar device) for angular cam positioning. This device could be extremely accurate in steady-state; the Selsyn being easily capable of $\pm$ 0.25^{o}; the output displacement could be regulated to $\pm$ 0.01".

3.5.6. Complete Subsystem Tests.

The complete Fluid Control Subsystem was bench tested in steady-state, according to the test layout of Fig. 3.5-21. Either the Angular position or the Linear position transducer can be connected into a Fluid Bridge against the Electric Input Transducer and the corresponding pressure differential measured on the water-gage U-manometers.

The pressure which would exist in the fluid bellows is measured by the Output Pressure Gages; the electric command signal is measured by the Input Voltmeter.

The final results are shown in Figure 4.5-23, using the angular position transducer. The test procedure was as follows:

1. Command and position transducers were nulled out at 0^{o}; with the command signal unchanged, the position transducer was moved forward stepwise up to 40^{o}.

2. The command and position transducers were nulled out at 37.5^{o} (mid point); with the command signal unchanged, the position transducer was moved stepwise backward to 0^{o} and forward to 75^{o}.

3. The command and position transducers were nulled out at 75^{o}; with the command signal unchanged, the position transducer was moved stepwise backward to 35^{o}.

The linearity of push-pull output pressure against displacement is excellent from 20^{o} to 75^{o}; in the area between 0^{o} and 20^{o} there is some deviation, which is due to pressure mismatch between transducer and operational amplifier. This mismatch may be easily cured by increasing the output pressure level of the position transducer to 0.5 PSIG @ 0^{o}; this can be done by increasing the supersonic orifice diameter by a small amount.

In conclusion, it is shown that there is a linear relationship between the position-error signal and a force by push-pull fluid bellows.

Bellows area of the order of 2 in^2 would be sufficient to produce the 15 lb force required by the Vickers Gemini servovalve; the electrical input power (1 mw), on the other hand, is two orders of magnitude lower than that allowed by NASA specifications for the conventional electrically-operated servovalve (250 mw).

The steady-state feasibility of the Fluid Control Subsystem is demonstrated satisfactorily.

3.6. Servo Analysis of Idealized Control System.

A block diagram of the control system is shown in Figure 3.2-4. In this Figure, the closed loop which is to be analyzed for stability consists of a valve-actuator package, the load, the linear position feedback transducer, and the operational amplifier with its bellows output.

The position feedback transducer and the operational amplifier part of the loop have been tested and built. In order to analyze the loop stability, typical transfer functions for the other elements shall be assumed. Since this is a preliminary analysis, highly simplified approximations of the actual transfer functions shall be used. This is particularly true in the case of the pneumatic Gemini valve and motor.

The transfer function of a pneumatic valve-motor combination which is suitable for the intended nozzle actuation system was obtained from the Vickers Division of the Sperry Rand Corporation, and was discussed in Section 3.4. This transfer function is shown in Figure 3.4-1 and gives the output rpm as a function of the input force in pounds. The first block shows a dead-band of plus and minus 5 pounds with a maximum input of 15 pounds. This, in the equivalent circuit, is transformed into an effective force which feeds a block with a transfer function of 19,200 RPM/sec-lb. The output of this block is an angular acceleration. This is integrated, giving an angular velocity which feeds into a dead-band of $\pm$1,650 rpm. The output of this is the output rpm of the motor. There is feedback around the integrator and the angular velocity dead-band as shown in Figure 3.4-1.

This transfer function, while not complex, includes dead-bands and an accurate analysis would require an analog computer simulation. For our purposes, the circuit analysis will be simplified by ignoring the dead-bands. This is not too unrealistic. The first dead-band, that is the effective force dead-band, is caused by springs in the valve and overlap of the valve; this dead-band could be reduced as much as desired by small changes in the design. Simply lapping the valve closer would be one such change. At the time of this writing it is not known what physically contributes to the rpm dead-band.

In this analysis the dead-bands shall be ignored and the resulting continuous transfer functions shall be used. The 19,200 rpm block is reduced to 320 revolutions/sec^2 -lb, revolutions/sec^2 being a more convenient unit to use than RPM/sec.

The resultant equivalent circuit of the valve-motor combinations is shown in Figure 3.6-1. It is readily seen that the overall transfer functions between θ and F of Figure 3.6-1 is given by

$$\frac{\theta}{F} = \frac{1.33}{s(\tau_2 s + 1)} \quad \frac{\text{rev}}{\text{lb}} \tag{1}$$

where τ_2 is equal to 1/24th of a second. This corresponds to a break frequency of 3.8 cycles/second.

The motor will be used to drive (through gearing) a leadscrew, which will actuate the nozzle. The leadscrew must have a three-inch travel. A 5-threads/inch thread size has been tentatively selected and used in the analysis.

From considerations of power requirements and maximum speed requirements, a reasonable gear ratio of between the actuator and the leadscrew was found to 3/16. Let x be the linear travel of the leadscrew. It follows that

$$x = \frac{3}{80}\ \theta \tag{2}$$

which is the transfer function between the linear output motion and the angular travel (in revolutions) of the motor. From this equation, and equation (1) above, the transfer function can be found between the input force which is applied to the valve and the displacement of the leadscrew. This is found to be:

$$\frac{x}{F} = \frac{.05}{s(\tau_2 S + 1)}\ \frac{\text{inch}}{\text{lb}} \tag{3}$$

The position feedback transducer is discussed in Section 4.5.3 of Volume II. As shown in that section, the equivalent circuit is a simple RC network whose transfer function is:

$$G(s) = \frac{A}{1 + \tau_1 s} \tag{4}$$

where the gain constant A is 0.346 psi/inch.

The time constant τ_1 depends upon the bandwidth of the circuit. Considering the worst case, namely the narrowest bandwidth, the time constant τ_1 is found to be 0.00061 seconds. The transfer function is hence

$$G(s) = \frac{0.346}{1 + 0.00061s}\ \text{psi/inch} \tag{5}$$

The closed loop gain of the operational amplifier is 11. As shown in Volume II, the output impedance of a typical impact modulator is roughly 10^5 fluid ohms. The definition of fluid ohm is given and discussed in Vol. II, Section 2.2. The output impedance of the operational amplifier will then be 10^5 fluid ohms divided by 11 or 9,100 fluid ohms.

Tests at the Johnson Service Company have shown that the bandwidth of an operational fluid amplifier is determined to a large extent by the load applied to the amplifier. In the particular case under consideration, the load is a metal bellows. A typical value for the volume of the bellows would be 0.1 cubic inch. The output circuit of the operational amplifier then becomes a 9,100 ohm

resistor feeding a capacity representing the 0.1 cubic inch volume. The break frequency of this circuit is 59 cycles per second. This corresponds to a time constant of 0.0027 seconds.

The force output of the bellows will depend upon the pressure within the bellows and the area of the bellows. Considering a bellows area of 2 square inches, the transfer function of the operational amplifier and the bellows becomes

$$G(s) = \frac{22}{1 + .0027s} \quad \text{lbf/psi} \qquad (6)$$

The simplified equivalent block diagram of the control circuit is given in Figure 3.6-2. The block containing K_1 is the transfer function of the flapper-valve transducer. The frequency response characteristics of the operational fluid amplifier and the bellows is given by the block containing K_2. The valve-actuator and load transfer function is represented by the block which is fed by the output of the mechanical summer.

The phase-gain characteristics of the transfer function for the open loop is plotted in Figure 3.6-3. It is seen from this plot that the circuit, as it stands, will have a gain margin of 46 db. and a phase margin of 80 degrees. This however, is a highly idealized approximation. No rate feedback is shown in the control loop of Figure 3.6-2. Without a rate feedback of some sort, the response characteristics of the system would be unsatisfactory.

A rate feedback pressure signal could be taken from the Gemini motor exhaust; however, it would be load-resistive and therefore not entirely suitable.

However, rate feedback can be obtained by differentiating the output of the position feedback transducer and then summing this differentiated signal with the direct output of the transducer as shown in Fig. 3.6-4. Examples of differential plus proportional control achieved by Impact Modulator Operational Amplifiers is shown in Fig. 3.5-20. It is seen that varying degrees of control may be achieved, from pure differential to differential plus substantial proportional control. It is to be noted that the fluid summing circuit shown in Fig. 3.6-4 would actually be achieved by applying multiple inputs to the Operational Amplifier.

3.7. List of References.

1. J. E. Fleckenstein - Method for Determining the Laplace Transform of a Pneumatic Nozzle-Flapper Combination. ASME Paper 62-WA-15 1962.

2. R. E. Norwood - Pneumatic Flapper Valve Study First International Congress - International Federation of Automatic Control, Moscow, June 1960.

3. R. J. Pawlak - Continued Study of Pneumatic Flapper Valves. S. M. Thesis, ME Dept. MIT 1959.

4. B. J. Bjornsen - The Impact Modulator Proceedings of the Second Fluid Amplification Symposium. Vol. II pp. 5 - 32 Harry Diamond Laboratories May 1964.

5. T. J. Lechner and P. H. Sorenson - Some Properties and Applications of Direct and Transverse Impact Modulators. Proceedings of the Second Fluid Amplification Symposium. Vol. II pp. 33 - 59 Harry Diamond Laboratories May 1964.

6. Johnson Service Co. Research Division Staff. - Impact Modulators, Impact Modulator Amplifiers with Feedback and Systems Applications. Final Report - Contract DA-49-186-AMC-28(x) U. S. Army, Harry Diamond Laboratories.

3.8. List of Symbols.

		Dimensions
d	Input orifice diameter	$\left[\text{in}\right]$
G_p	Pressure gain	$\left[0\right]$
G_T	Total conductance	$\left[\frac{\text{in}^5}{\text{lb min}}\right]$
K_o	Slope of experimental curve	$\left[0\right]$
K_T	Sum of Operational Amplifier Gains plus one	$\left[0\right]$
m	Polytropic exponent	$\left[0\right]$
P_1, P_2	Supply pressures	$\left[\frac{\text{lb}}{\text{in}^2}\right]$
P_A	Input pressure	$\left[\frac{\text{lb}}{\text{in}^2}\right]$
P_B	Input bias	$\left[\frac{\text{lb}}{\text{in}^2}\right]$
P_R	Recovery pressure	$\left[\frac{\text{lb}}{\text{in}^2}\right]$
P_o, P_{o1}, P_{o2}	Output pressures	$\left[\frac{\text{lb}}{\text{in}^2}\right]$
P_L, P_r	Reference pressures (above atm.)	$\left[\frac{\text{lb}}{\text{in}^2}\right]$
$p_K = P_K - P_L$	Differential pressure	$\left[\frac{\text{lb}}{\text{in}^2}\right]$
$p_o = P_o - P_L$	Differential output pressure	$\left[\frac{\text{lb}}{\text{in}^2}\right]$
$p_A = P_A - P_A(\text{ave})$	Differential input pressure	$\left[\frac{\text{lb}}{\text{in}^2}\right]$
P_{1c}, P_{2c}	Differential inputs to operational amplifier	$\left[\frac{\text{lb}}{\text{in}^2}\right]$

Q_A	Input flow	$\left[\frac{in^3}{min}\right]$
Q_O	Output flow	$\left[\frac{in^3}{min}\right]$
R_K	Resistance	$\left[\frac{lb\ min}{in^5}\right]$
R_A	Input impedance	$\left[\frac{lb\ min}{in^5}\right]$
R_i	Input resistance	$\left[\frac{lb\ min}{in^5}\right]$
R_f	Feedback resistance	$\left[\frac{lb\ min}{in^5}\right]$
V	Volume	$\left[in^3\right]$
X	Linear displacement of actuator output	$\left[in\right]$
Y, Z, U	Dimensionless computational parameters	$\left[0\right]$
β	Input orifice diameter multiplier	$\left[0\right]$
ϵ	Error of gain prediction	$\left[0\right]$
θ	Angular displacement of actuator output	$\left[degrees\right]$

Notes: 1. The dimensional notation lb. refers to pound force.

2. The electrical analogy in Section 3.5.4 is based on the following self-consistent set of definitions:

Current	Volumetric Flow Q	$\left[\frac{in^3}{min}\right]$
Effort	Pressure P	$\left[\frac{lb}{in2}\right]$
Resistance	$\frac{\Delta P}{Q}$	$\left[\frac{lb\ min}{in^5}\right]$
Capacitance	$\frac{V}{mP}$	$\left[\frac{in^5}{lb}\right]$

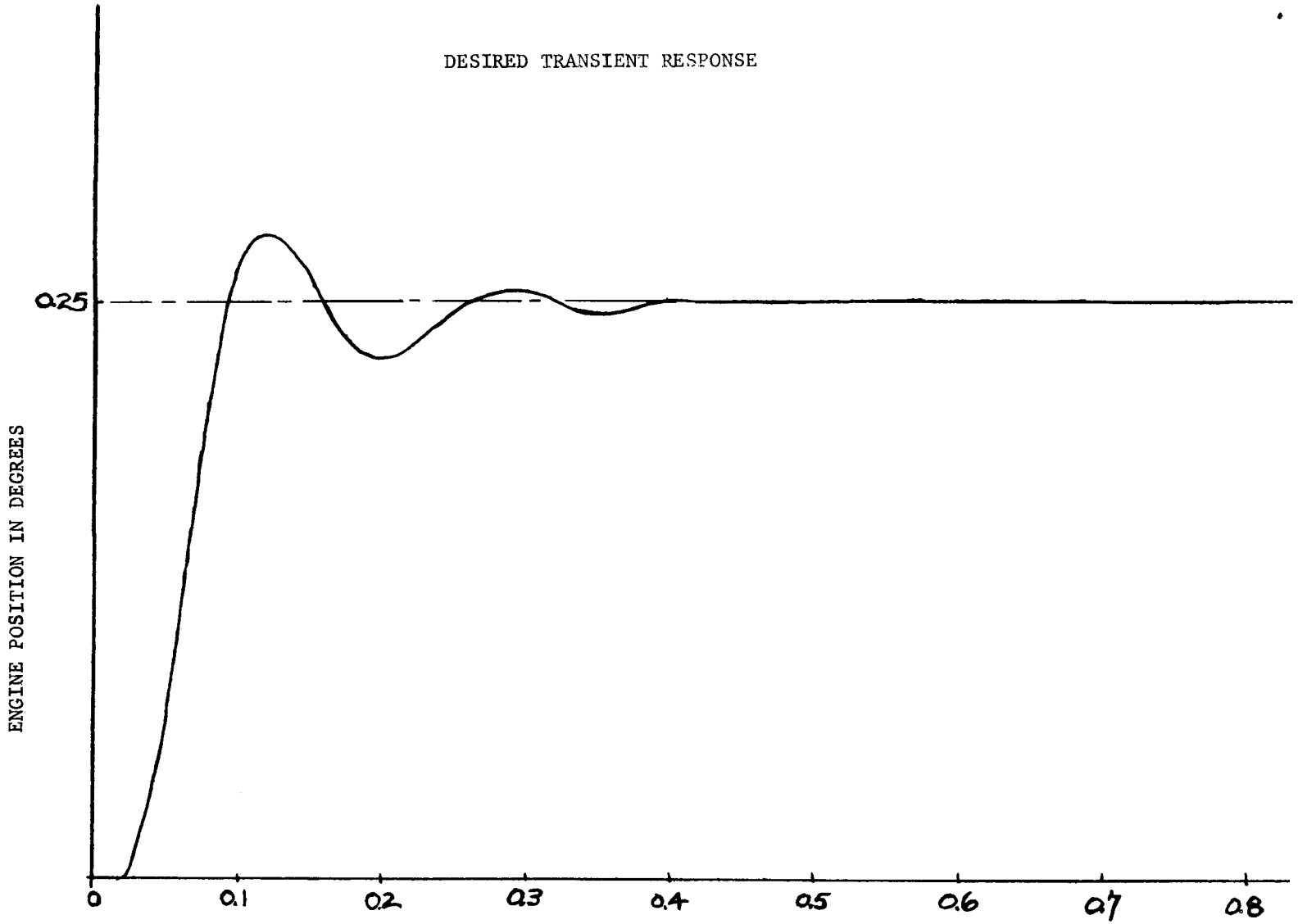

TRANSIENT RESPONSE

FIGURE 3.2-1

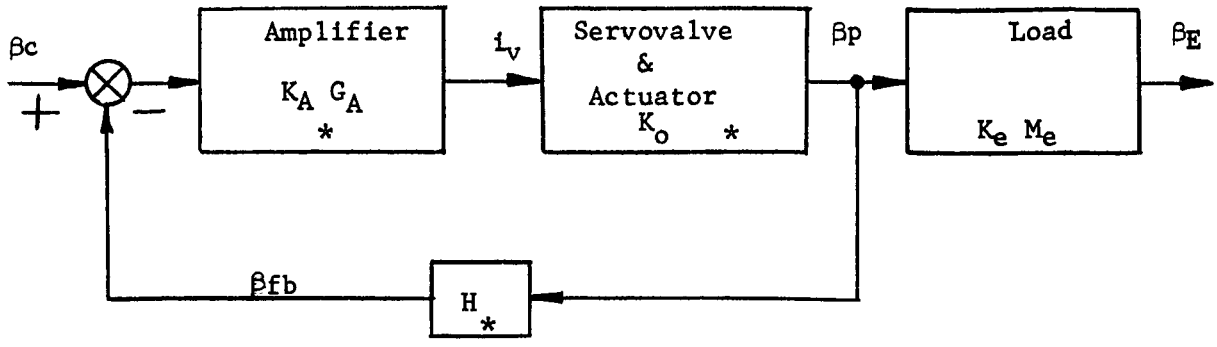

β_c = Input Signal = (VOLTS), equivalent to ± 0.05 inches

β_p = Piston Displacement = (IN.)

β_E = Engine Displacement = (DEG.)

β_{fb} = Feedback Signal = (VOLTS)

H = Feedback Scale Constant = $\frac{\text{VOLTS}}{\text{IN.}}$

K_A = Amplifier Static Gain = $\frac{\text{MA}}{\text{VOLTS}}$

G_A = $-\frac{1}{\tau S + 1}$

$\tau = \frac{1}{\omega}$

ω = $2\pi 30$ radians/second

i_v = Valve signal Current = (MA)

K_e = Equivalent Spring Constant of Engine and Structure = 300,000 (LB/IN)

M_e = Equivalent Mass of Engine to the Actuator = 1400 slugs

K_0 = Spring Constant of working fluid and Actuator = (LB/IN)

* Shaping permitted as necessary (electrical least desirable)

FIGURE 3.2-2 System Block Diagram

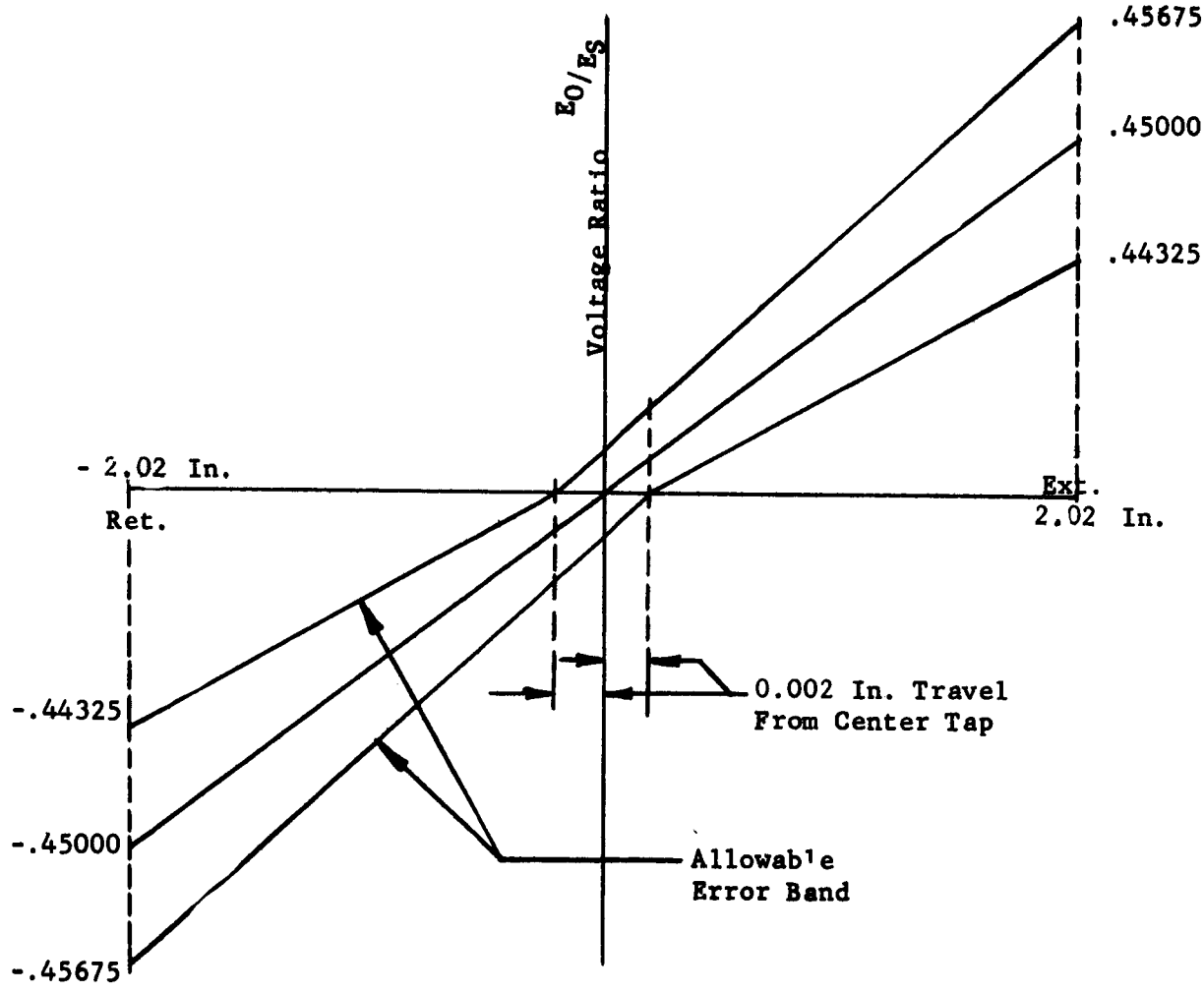

FIGURE 3.2-3 Potentiometer Linearity

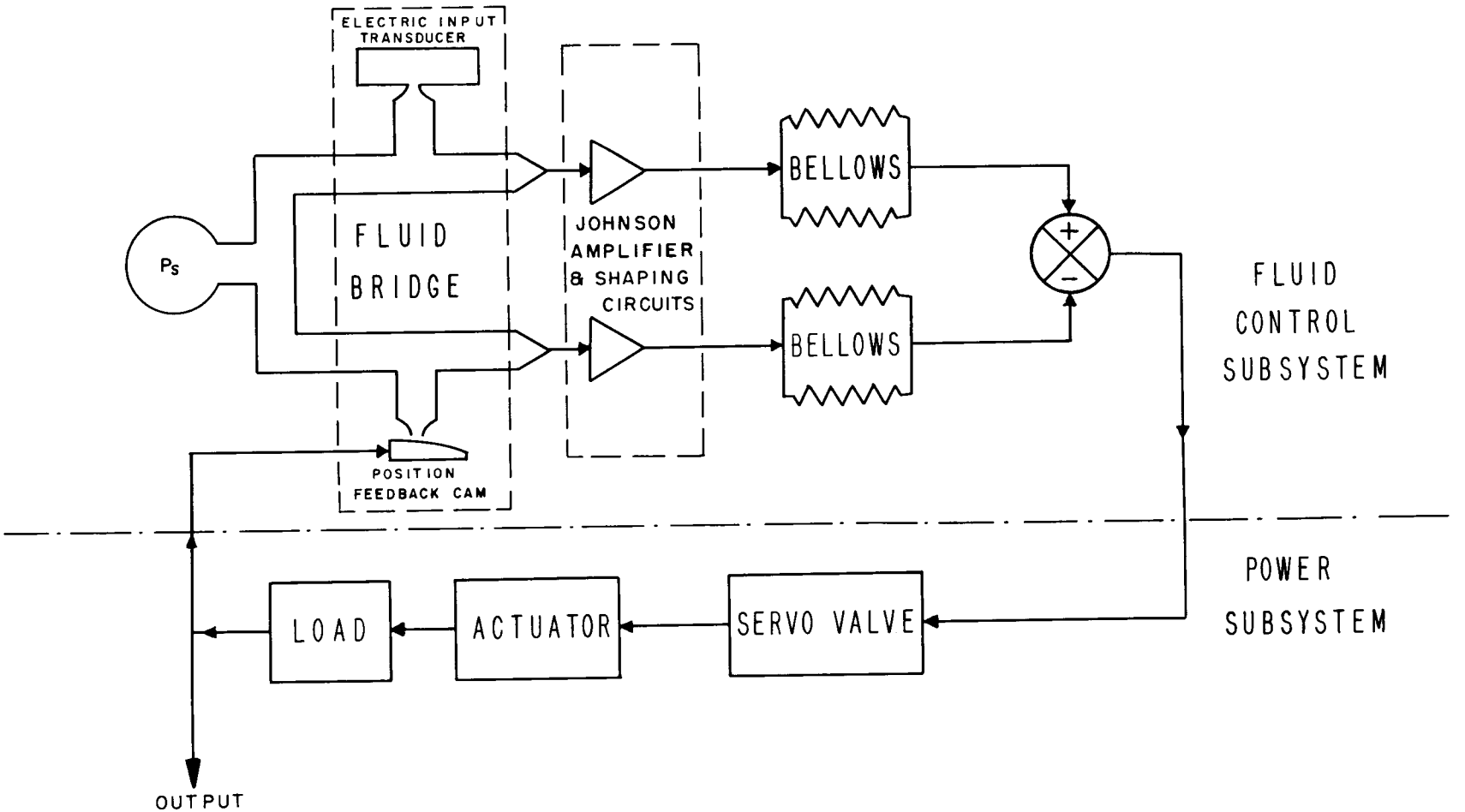

FIG. 3.2-4 SERVOSYSTEM SCHEMATIC

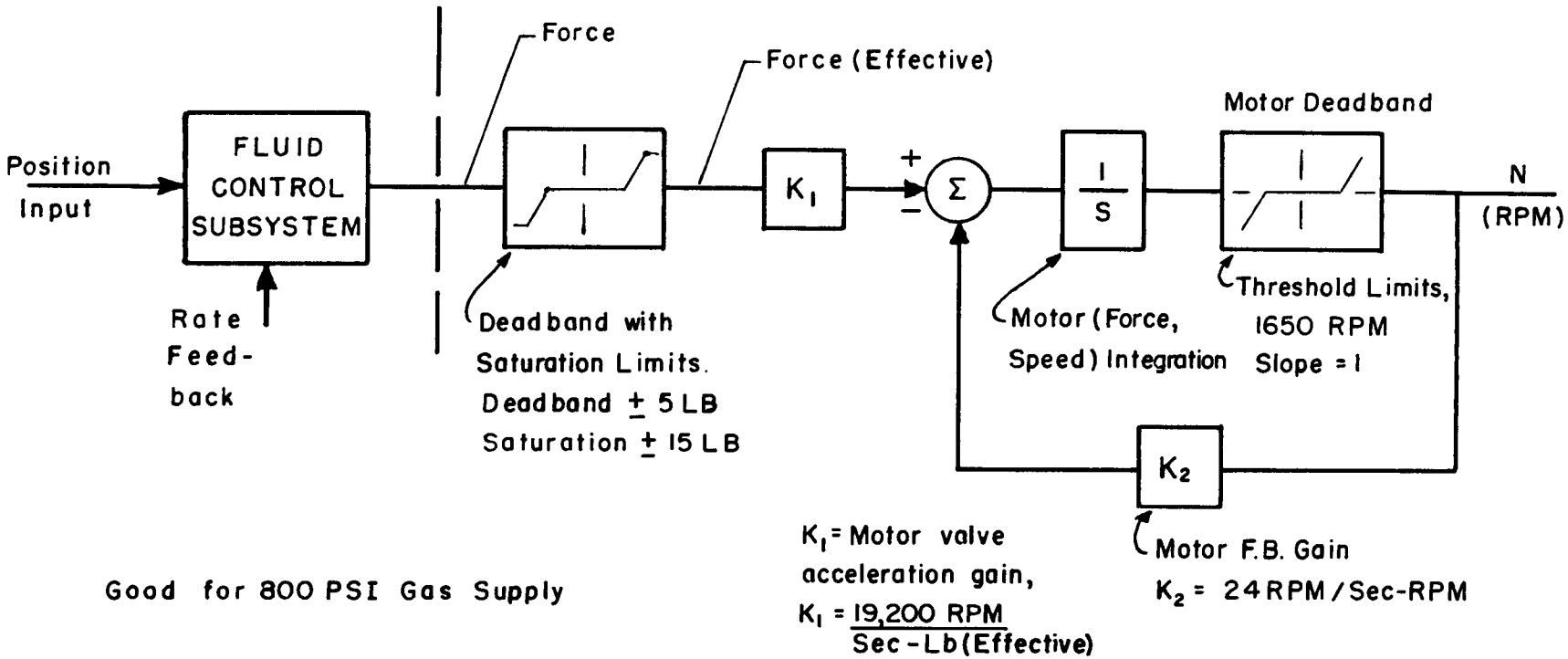

FIG. 3.4-1 GEMINI PNEUMATIC ACTUATOR SIMULATION

(FORCE INPUT)

ELECTRIC-TO-PNEUMATIC TRANSDUCER

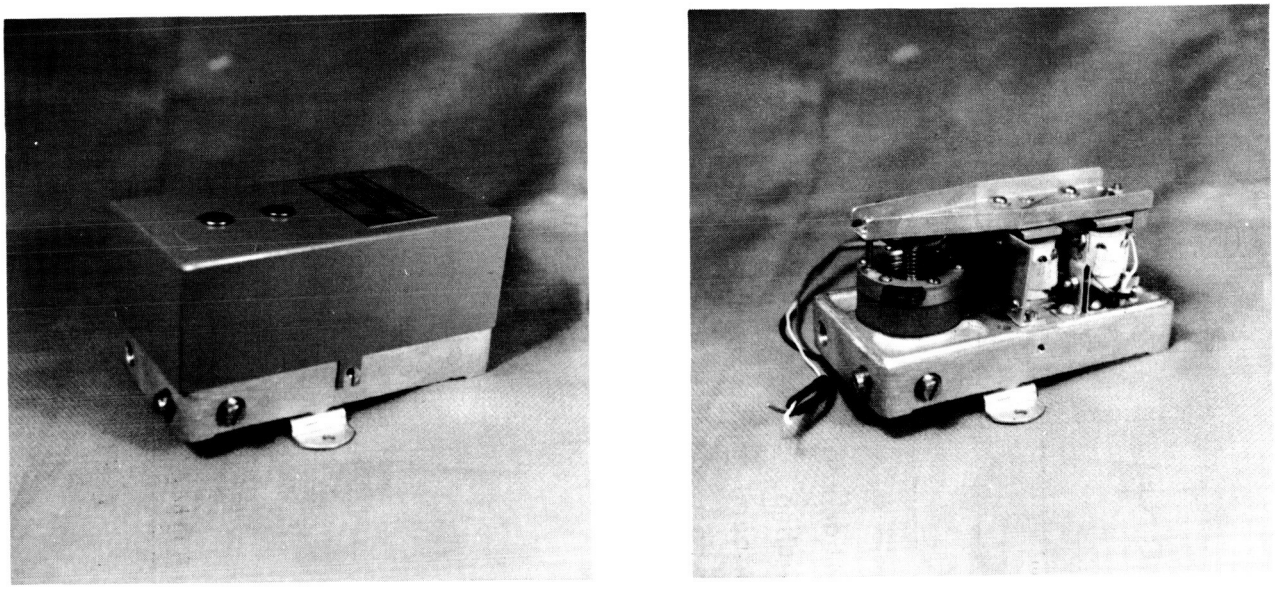

FIGURE 3.5-1

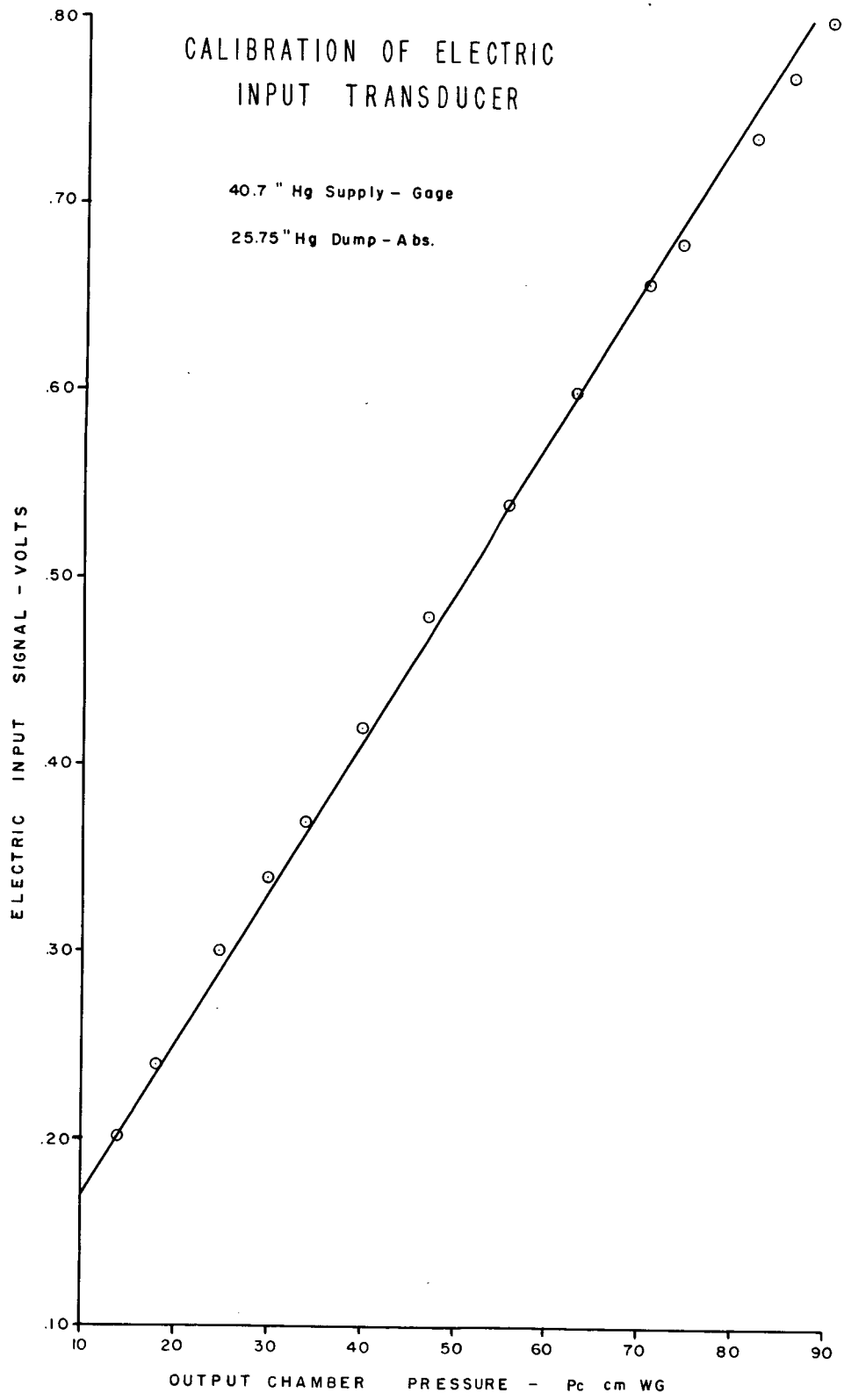
CALIBRATION OF ELECTRIC
INPUT TRANSDUCER
40.7 " Hg Supply - Gage
25.75" Hg Dump - Abs.
ELECTRIC INPUT SIGNAL - VOLTS
.80
.70
.60
.50
.40
.30
.20
.10
10
20
30
40
50
60
70
80
90
OUTPUT CHAMBER PRESSURE - Pc cm WG

FIG. 3.5-2

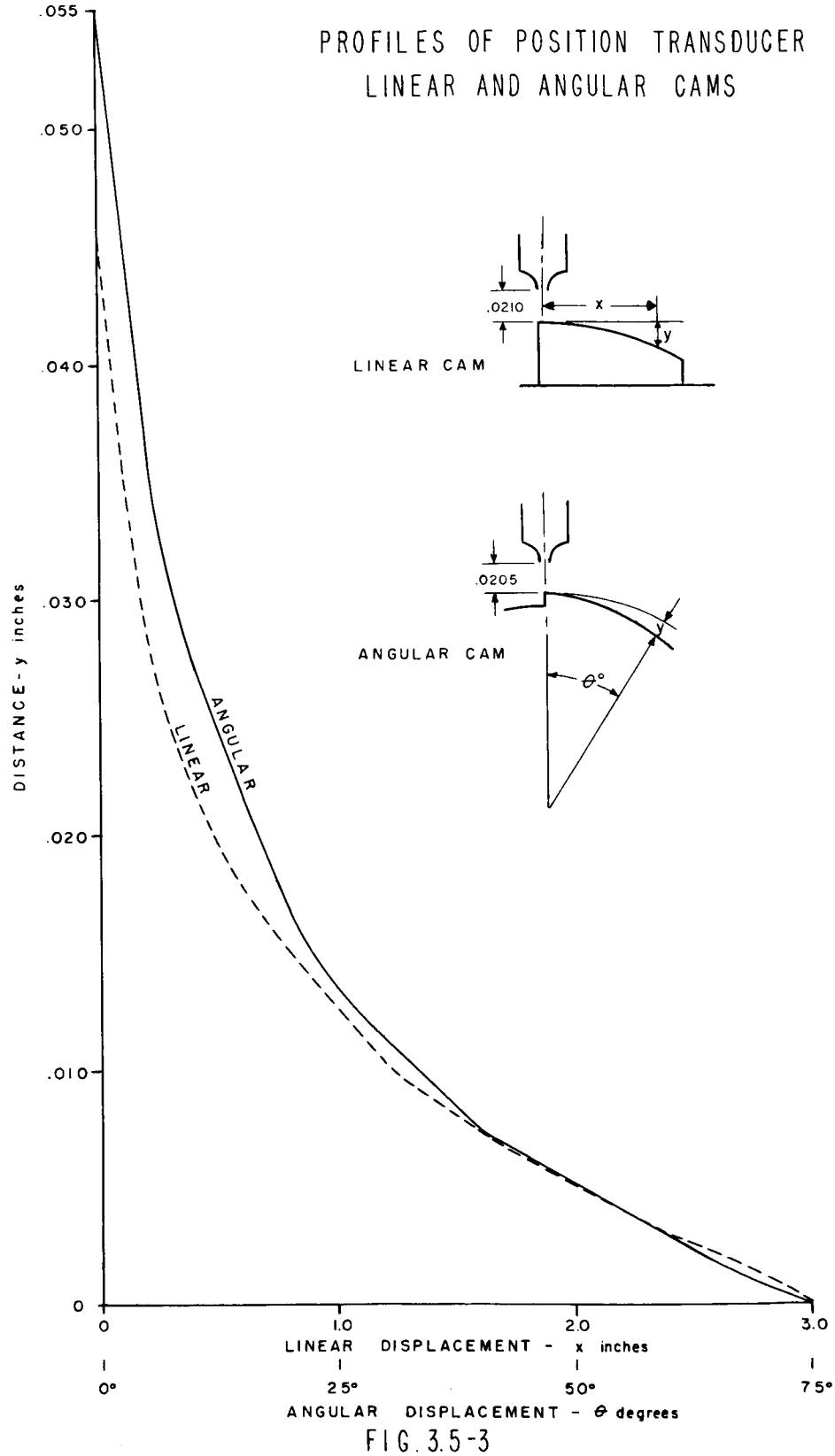
PROFILES OF POSITION TRANSDUCER
LINEAR AND ANGULAR CAMS
LINEAR CAM
.0210
x
y
ANGULAR CAM
.0205
θ°
DISTANCE - y inches
.055
.050
.040
.030
.020
.010
0
ANGULAR
LINEAR
0
1.0
2.0
3.0
LINEAR DISPLACEMENT - x inches
0°
25°
50°
75°
ANGULAR DISPLACEMENT - θ degrees

FIG. 3.5-3

CALIBRATION OF FLUID POSITION TRANSDUCERS

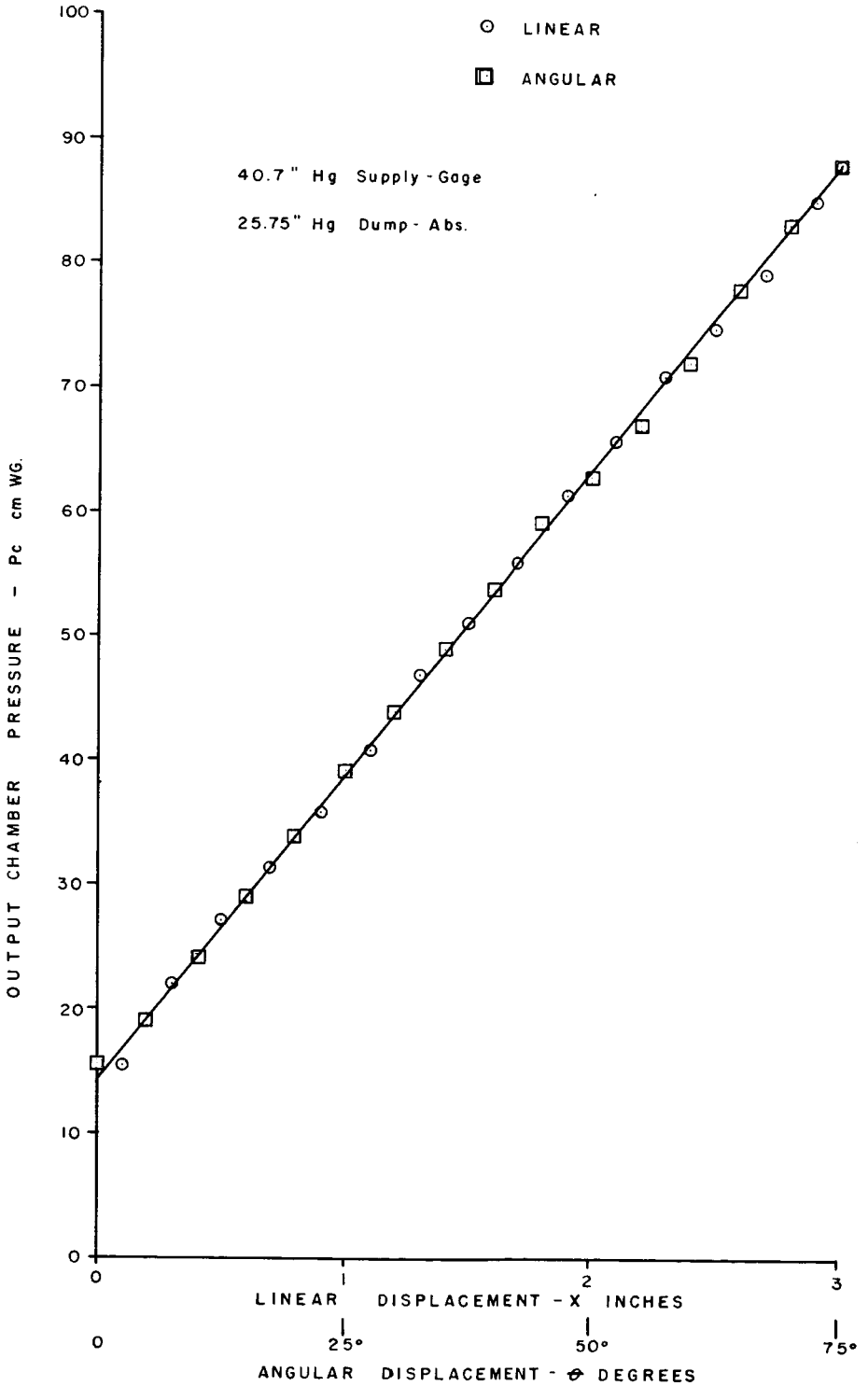

FIG. 3.5-4

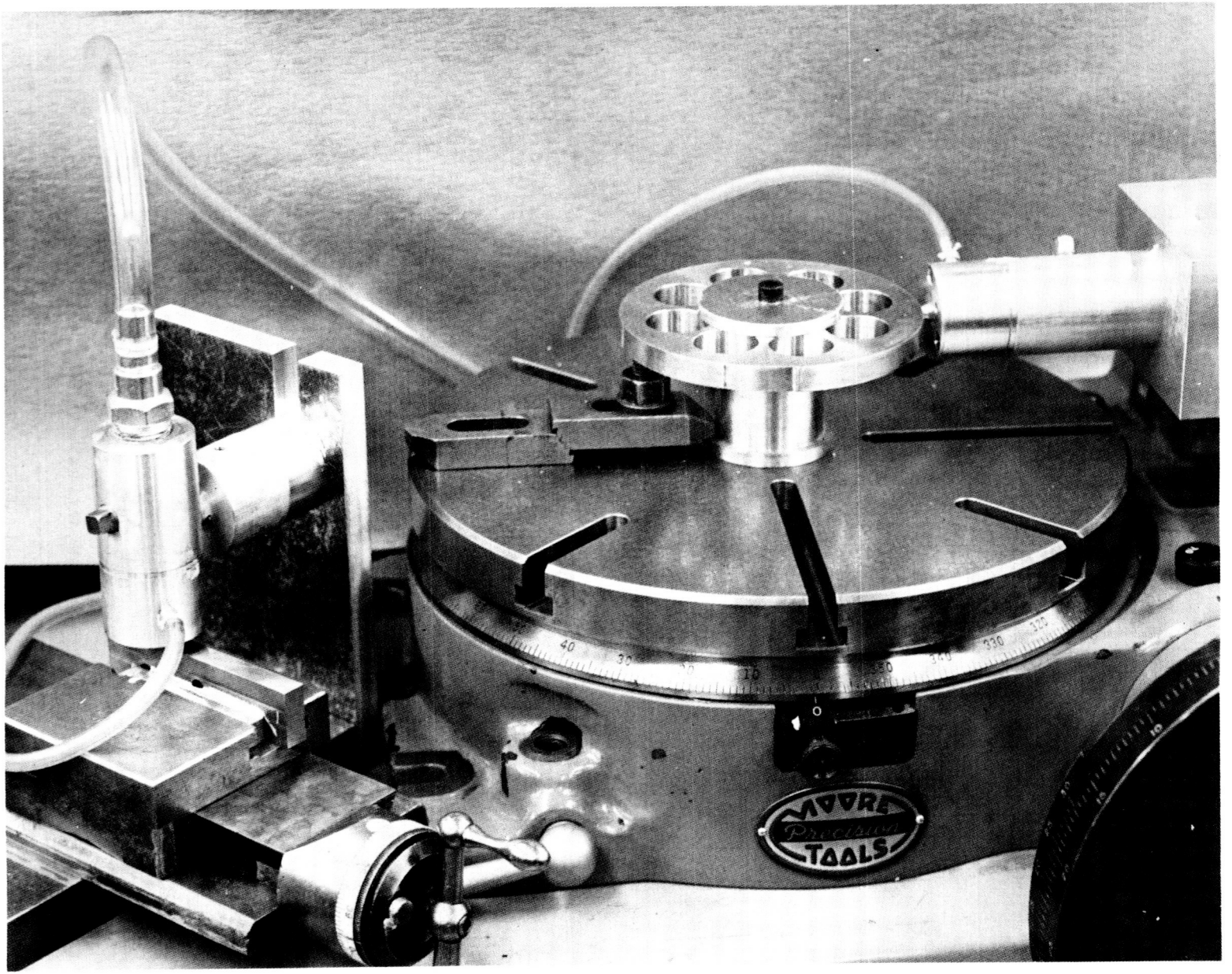

FIGURE 3.5-5 Linear and Angular Position Transducers on Test Bench.

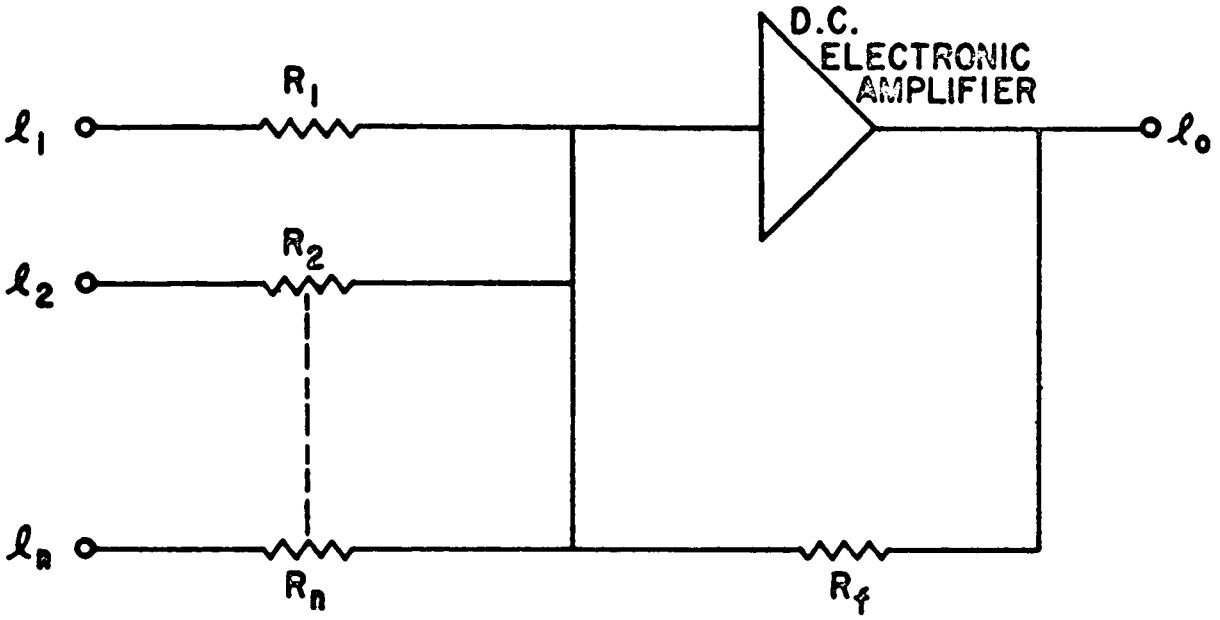

$$\ell_o = \sum_{k=1}^{n} \frac{R_f}{R_k} \ell_k$$

ELECTRONIC OPERATIONAL AMPLIFIER (a)

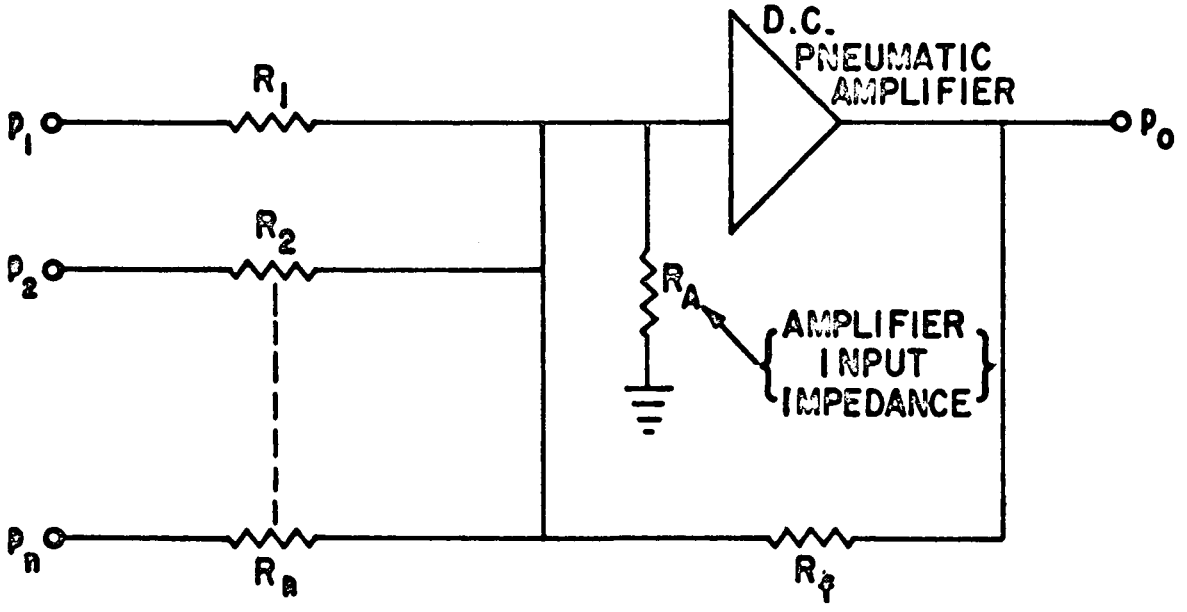

PNEUMATIC OPERATIONAL AMPLIFIER (b)

FIGURE 3.5-6

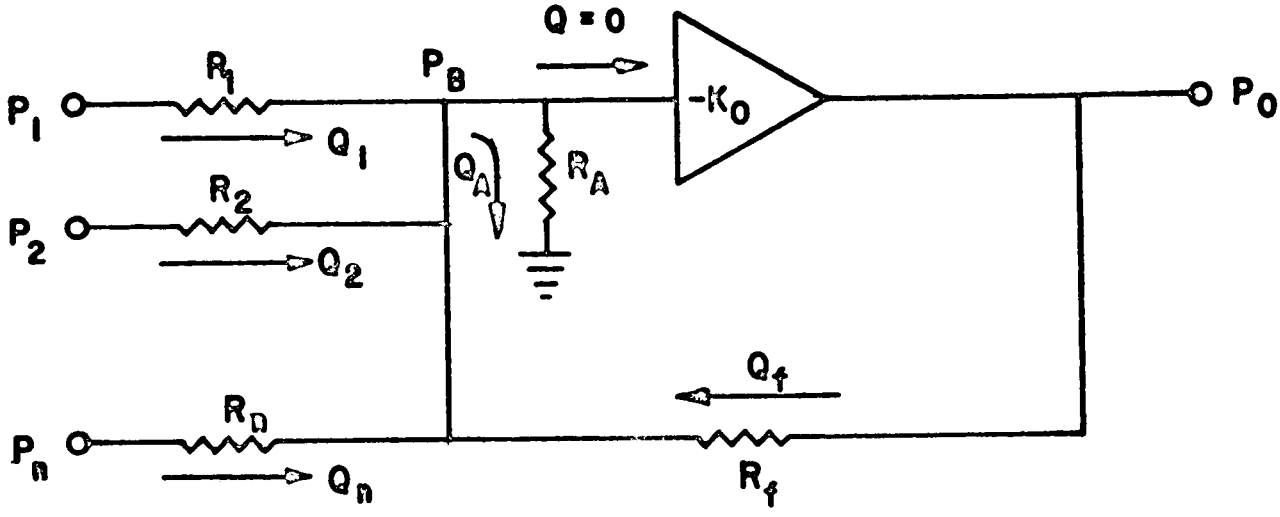

$$Q_A = \sum_{k=1}^{n} Q_k + Q_f$$

PNEUMATIC AMPLIFIER SHOWING FLOW SUMMATION

FIGURE 3.5-7

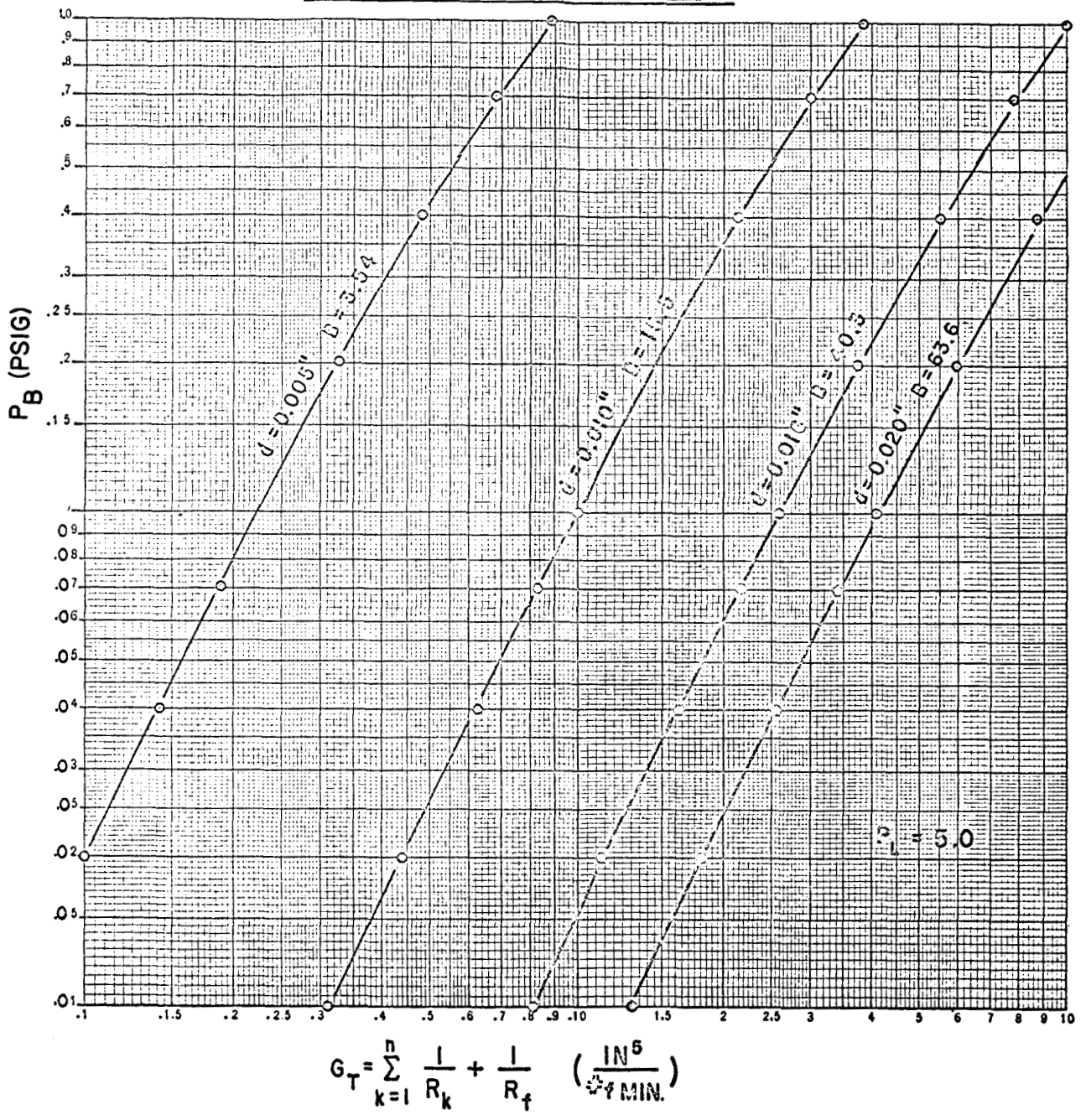
AMPLIFIER PRESSURE
V.S.
TOTAL CONDUCTANCE
P_B (PSIG)
d=0.005" B=3.54
d=0.010" B=14.5
d=0.016" B=40.3
d=0.020" B=63.6
P_L = 5.0
$G_T = \sum_{k=1}^{n} \frac{1}{R_k} + \frac{1}{R_f}$ $\left(\frac{IN^5}{\#\ MIN.}\right)$

FIGURE 3.5-8

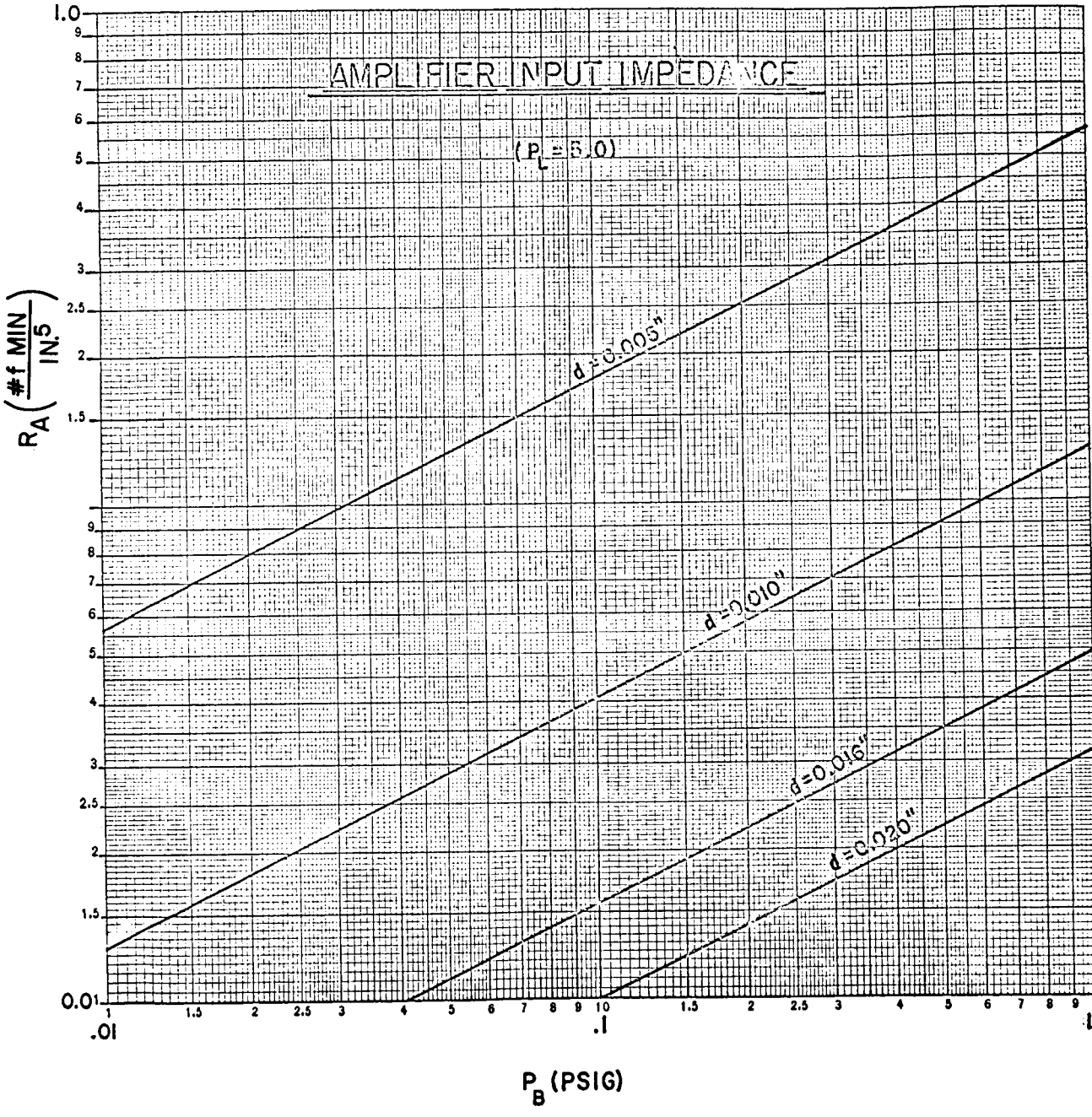
AMPLIFIER INPUT IMPEDANCE
(P_L = 5.0)
$R_A\left(\frac{\#f\ MIN}{IN.^5}\right)$
d = 0.005"
d = 0.010"
d = 0.016"
d = 0.020"
1.0
9
8
7
6
5
4
3
2.5
2
1.5
0.01
.01
.1
1.0
1
1.5
2
2.5
3
4
5
6
7
8
9
10
P_B (PSIG)

FIGURE 3.5-9

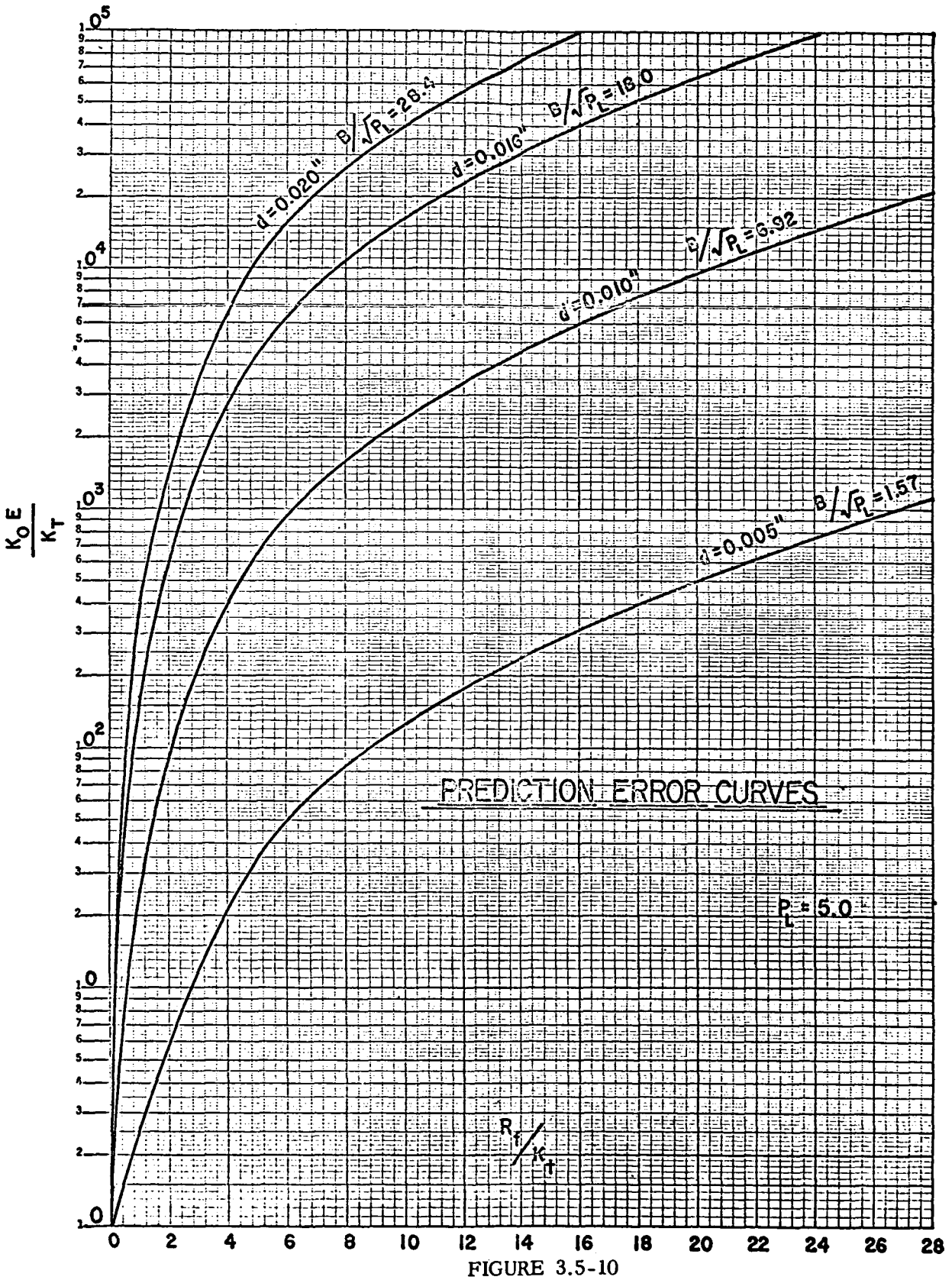
$\frac{K_O E}{K_T}$
10^5
10^4
10^3
10^2
10
1
d=0.020"
$B/\sqrt{P_L}=28.4$
d=0.016"
$B/\sqrt{P_L}=18.0$
d=0.010"
$B/\sqrt{P_L}=6.92$
d=0.005"
$B/\sqrt{P_L}=1.57$
PREDICTION ERROR CURVES
$P_L = 5.0$
R_f/K_t
0 2 4 6 8 10 12 14 16 18 20 22 24 26 28

FIGURE 3.5-10

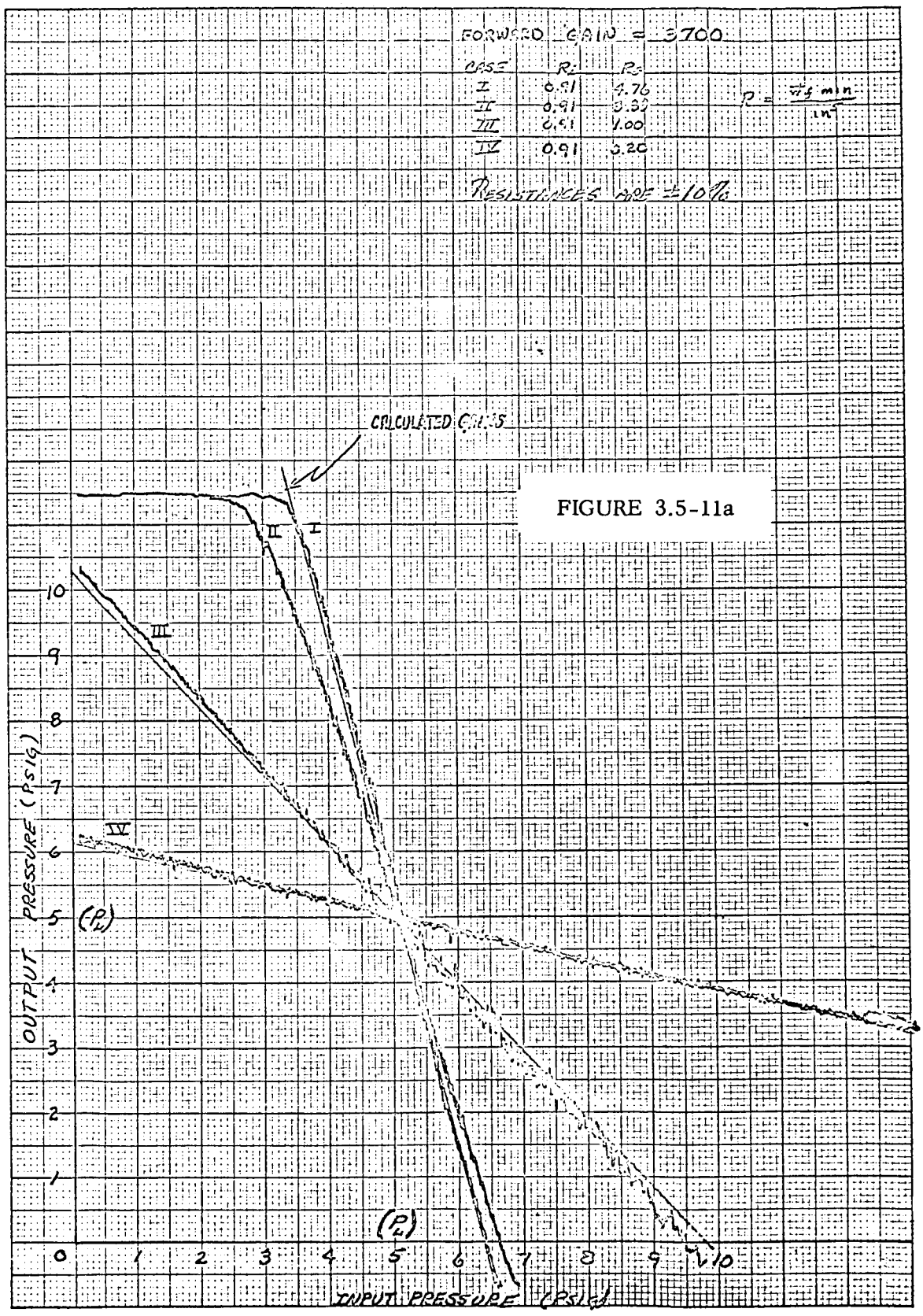

FIGURE 3.5-11a

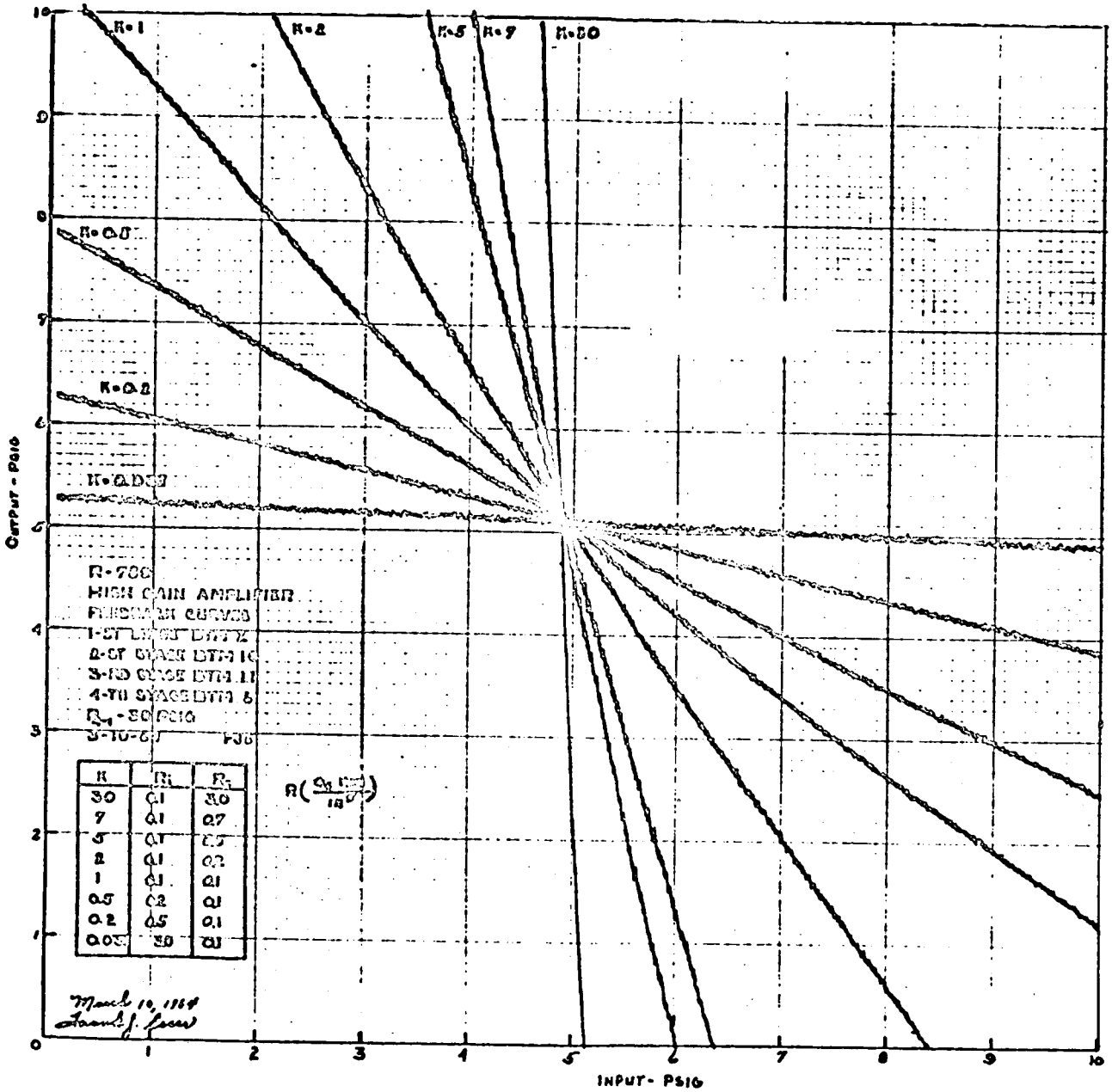

FIGURE 3.5-11b

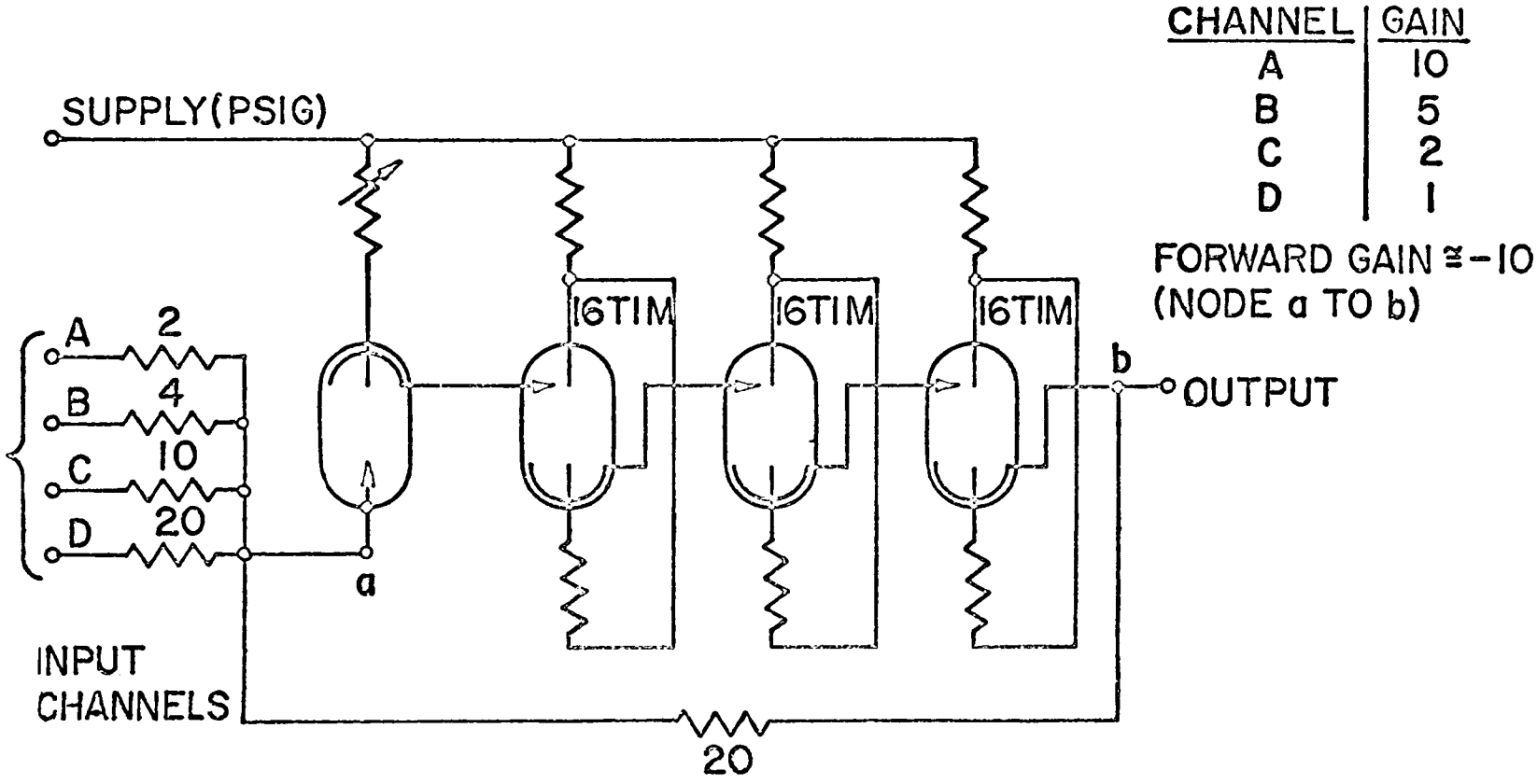

"PURE FLUID SUMMING AMPLIFIER"

FIGURE 3.5-12

"PURE FLUID OPERATIONAL AMPLIFIER CHARACTERISTIC"

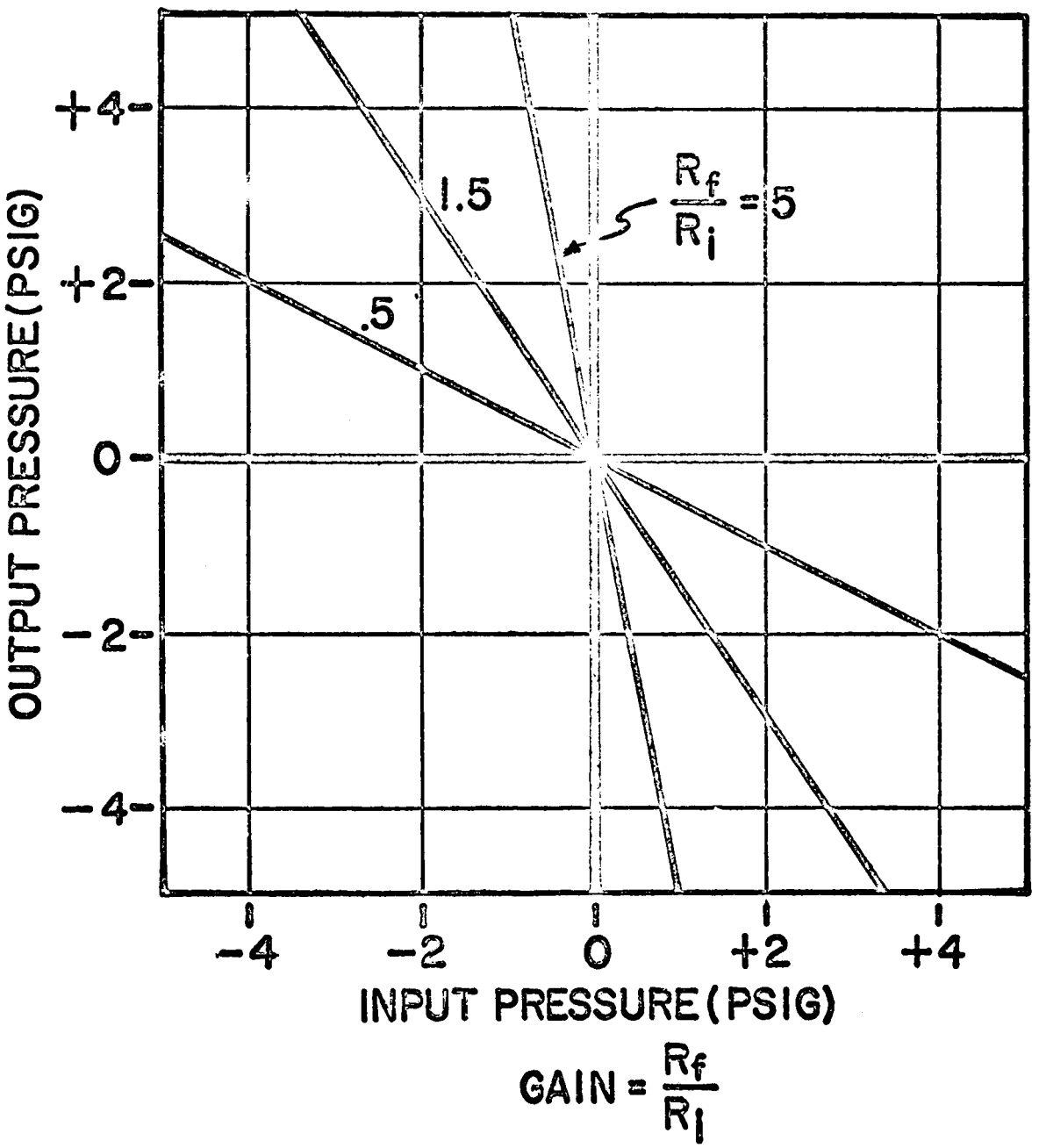

FIGURE 3.5-13

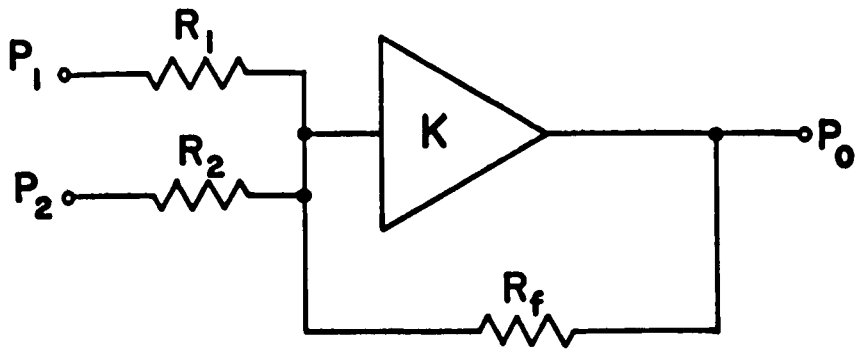

$\frac{R_f}{R_1} = 3$

$\frac{R_f}{R_2} = 5$

$P_0 = 3P_1 + 5P_2$

"PURE FLUID OPERATIONAL AMPLIFIER CHARACTERISTIC"

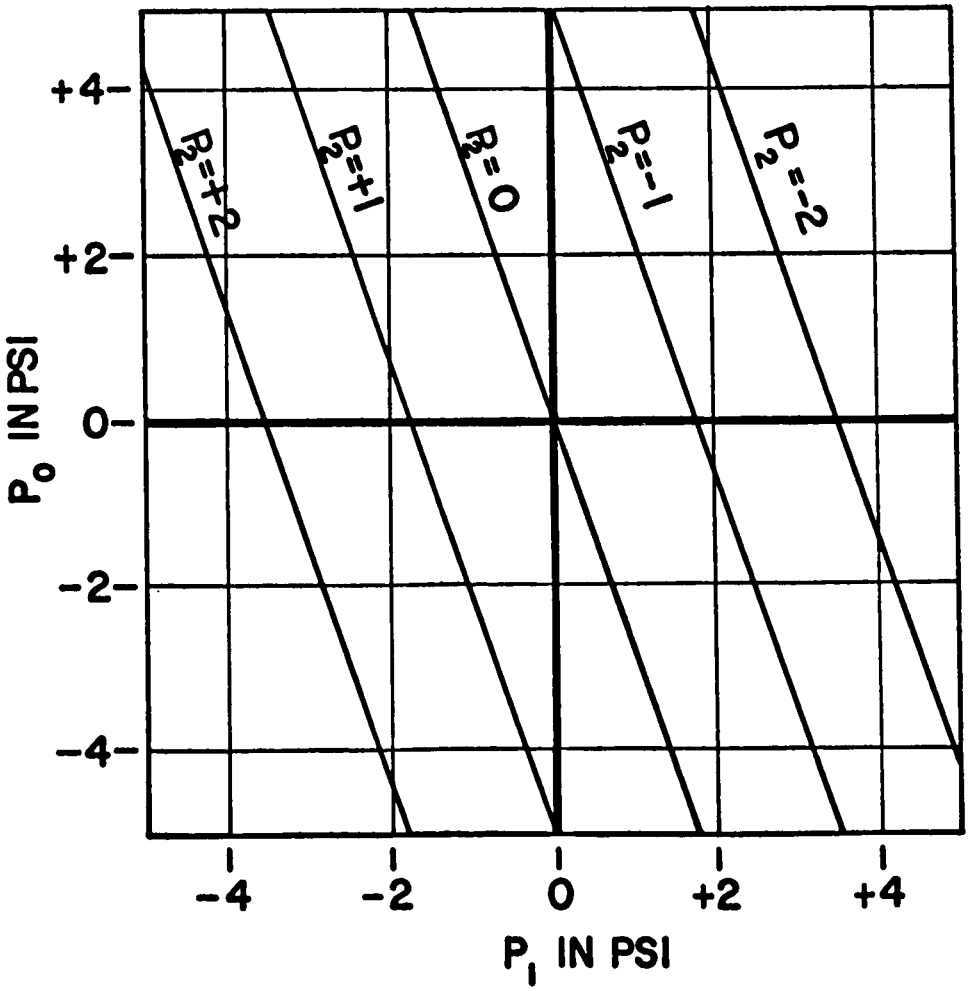

FIGURE 3.5-14

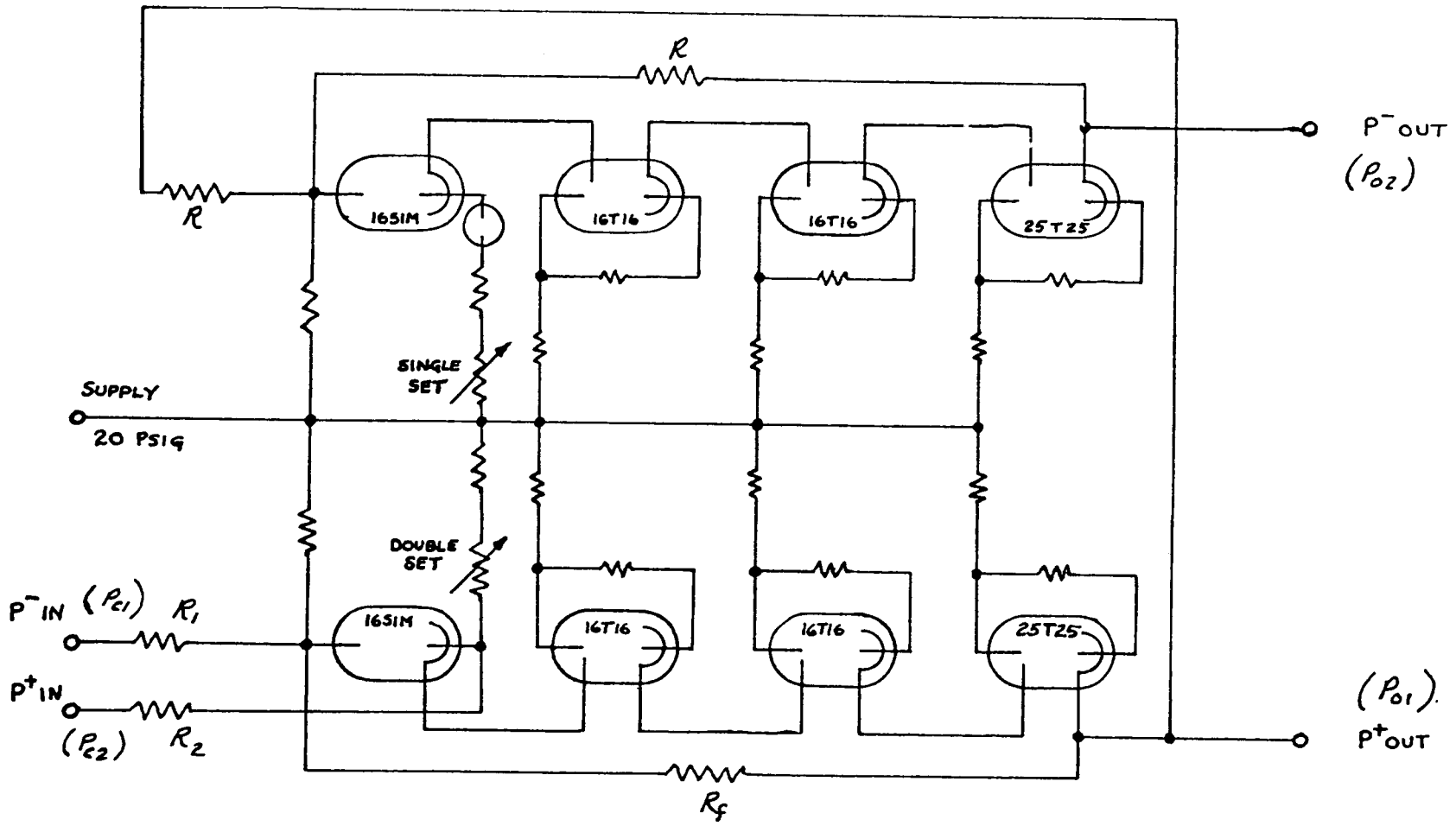

Push Pull Difference Amplifier

FIGURE 3.5-15

AMPLIFIER ASSEMBLY

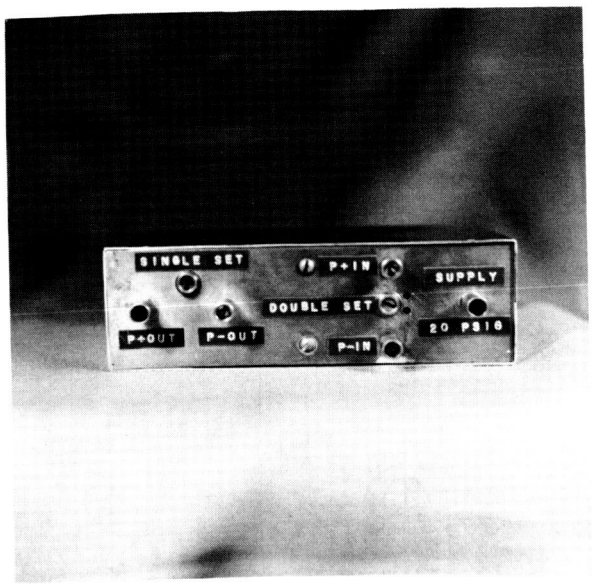

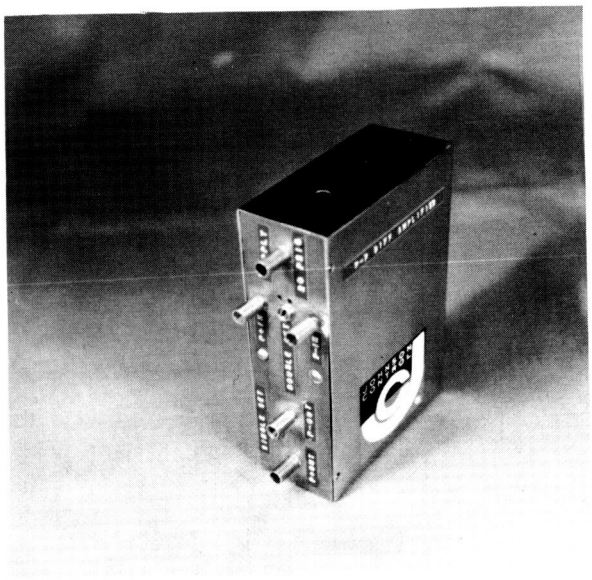

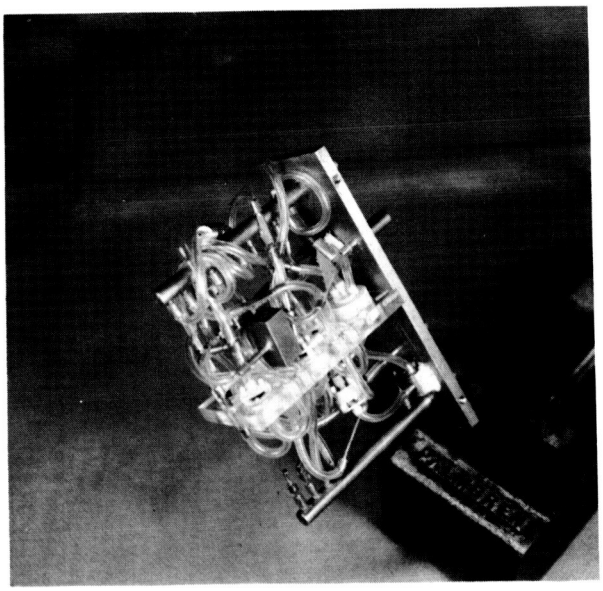

FIGURE 3.5-16

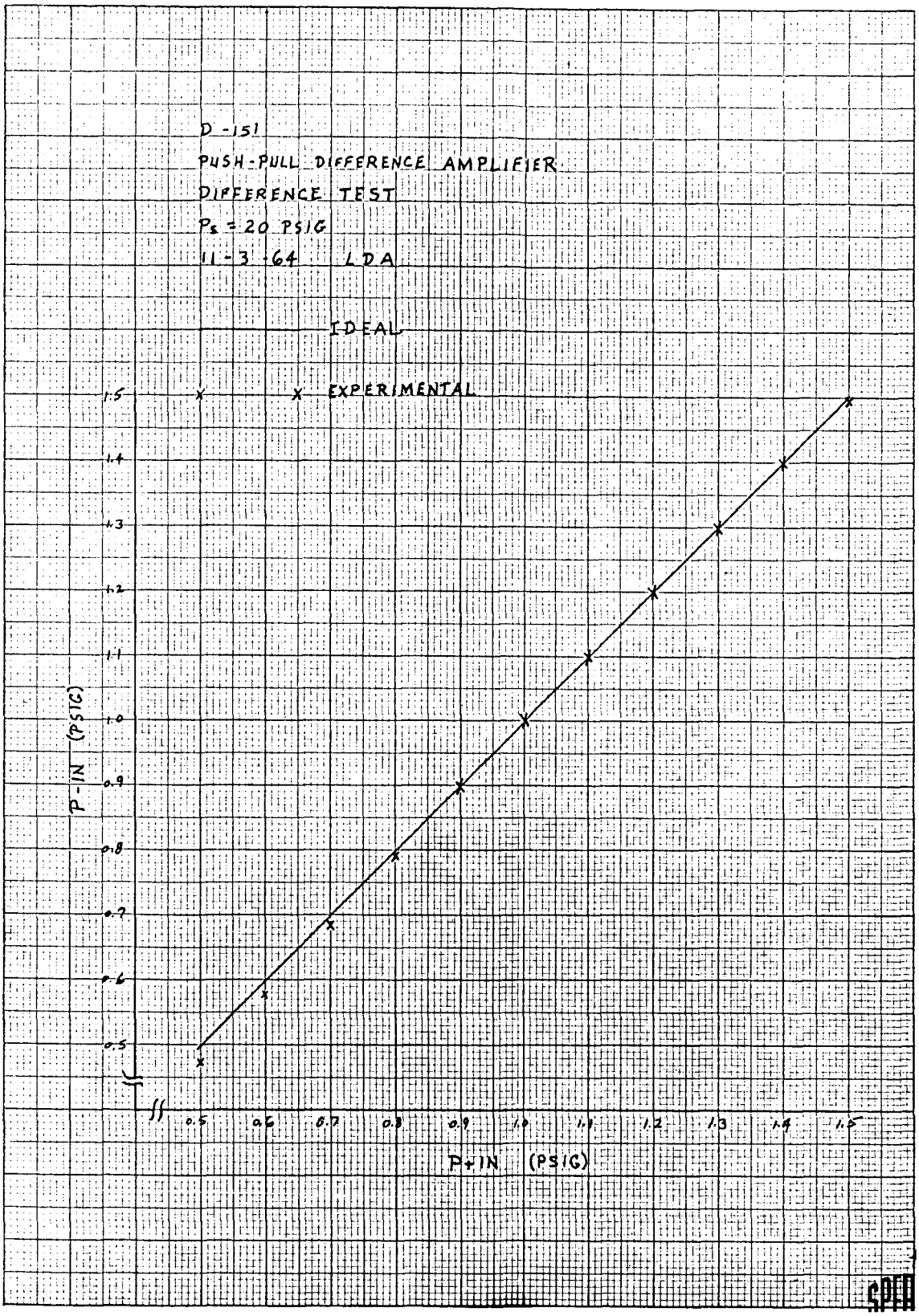
D-151
PUSH-PULL DIFFERENCE AMPLIFIER
DIFFERENCE TEST
P_s = 20 PSIG
11-3-64 LDA
IDEAL
EXPERIMENTAL
P-IN (PSIG)
P+IN (PSIG)
0.5
0.6
0.7
0.8
0.9
1.0
1.1
1.2
1.3
1.4
1.5

FIGURE 3.5-17

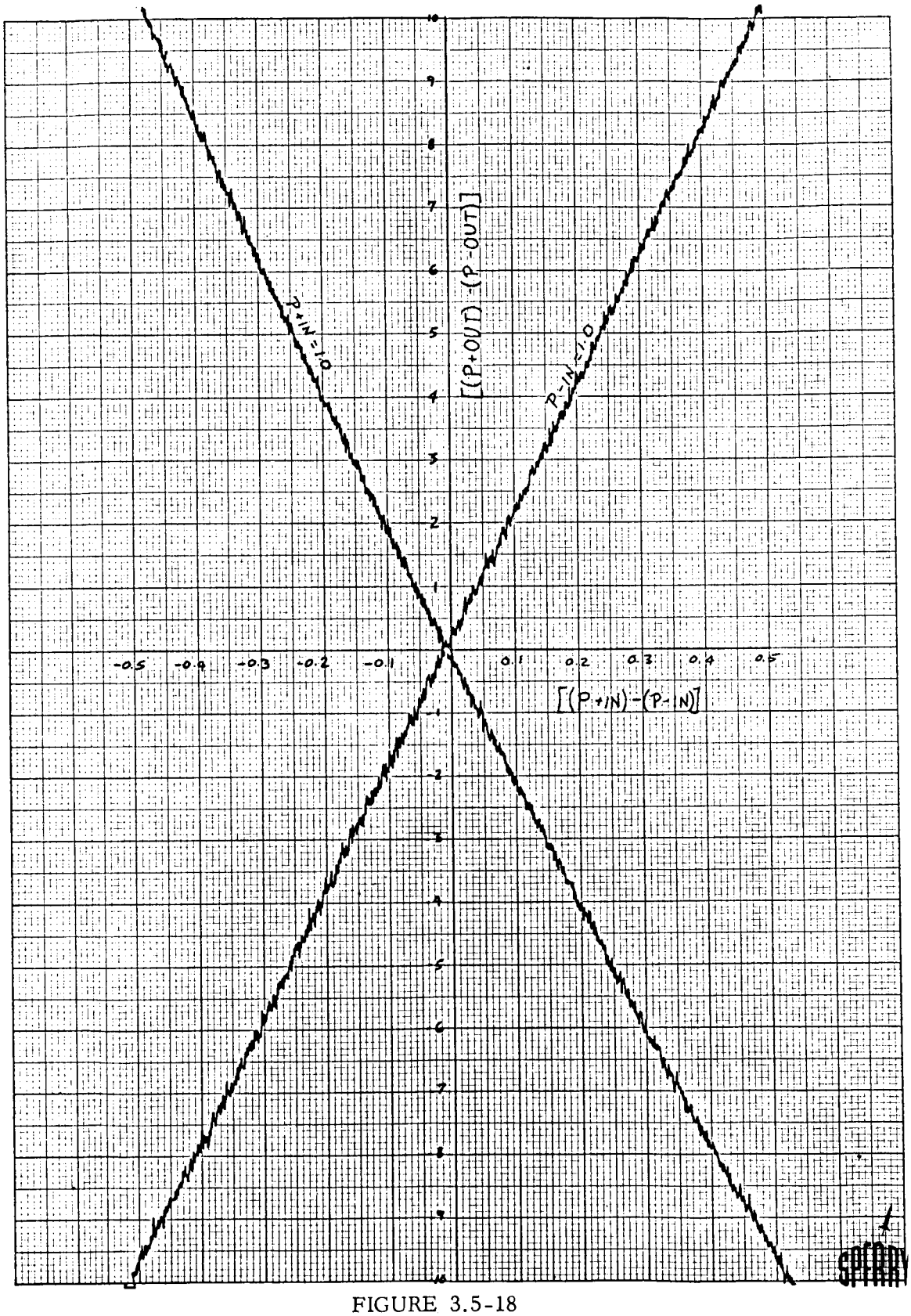
P+IN=1.0
P-IN=1.0
[(P+OUT)-(P-OUT)]
[(P+IN)-(P-IN)]
-0.5
-0.4
-0.3
-0.2
-0.1
0.1
0.2
0.3
0.4
0.5
10
9
8
7
6
5
4
3
2
1
-1
-2
-3
-4
-5
-6
-7
-8
-9
-10

FIGURE 3.5-18

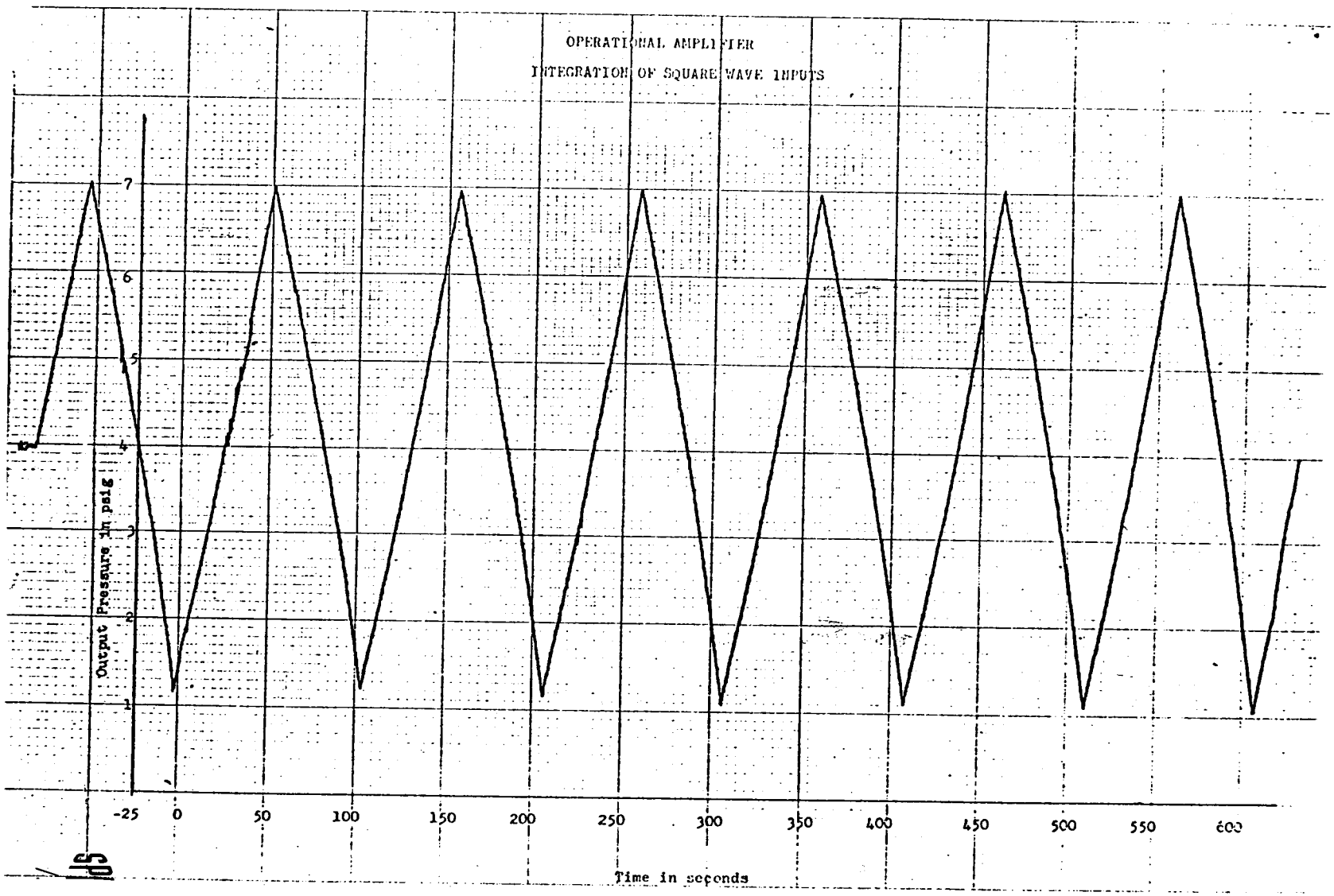
OPERATIONAL AMPLIFIER
INTEGRATION OF SQUARE WAVE INPUTS
Output Pressure in psig
7
6
5
4
3
2
1
-25
0
50
100
150
200
250
300
350
400
450
500
550
600
Time in seconds

FIGURE 3.5-19

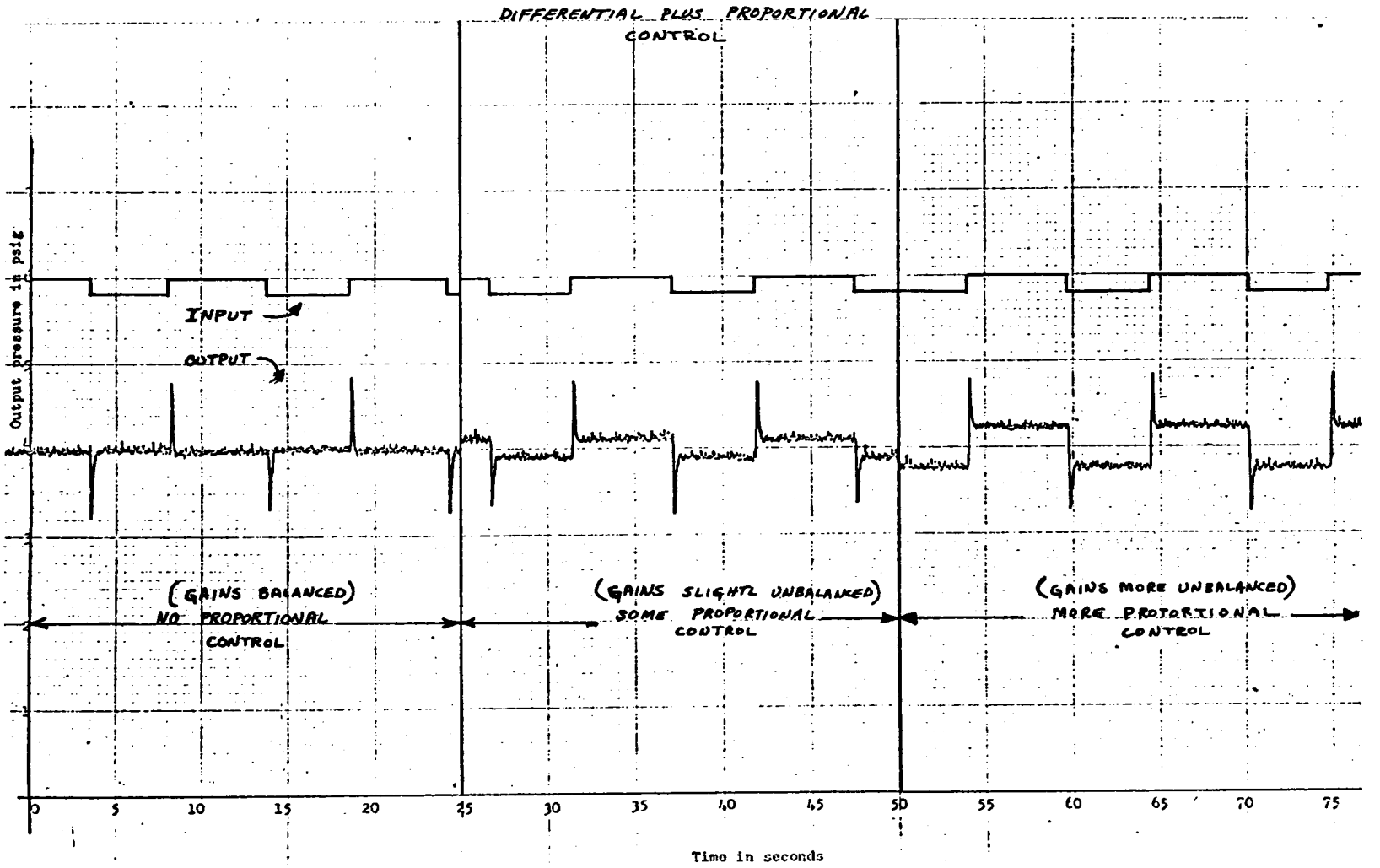
DIFFERENTIAL PLUS PROPORTIONAL CONTROL
Output pressure in psig
INPUT
OUTPUT
(GAINS BALANCED)
NO PROPORTIONAL CONTROL
(GAINS SLIGHTL UNBALANCED)
SOME PROPORTIONAL CONTROL
(GAINS MORE UNBALANCED)
MORE PROPORTIONAL CONTROL
0 5 10 15 20 25 30 35 40 45 50 55 60 65 70 75
Time in seconds

FIGURE 3.5-20

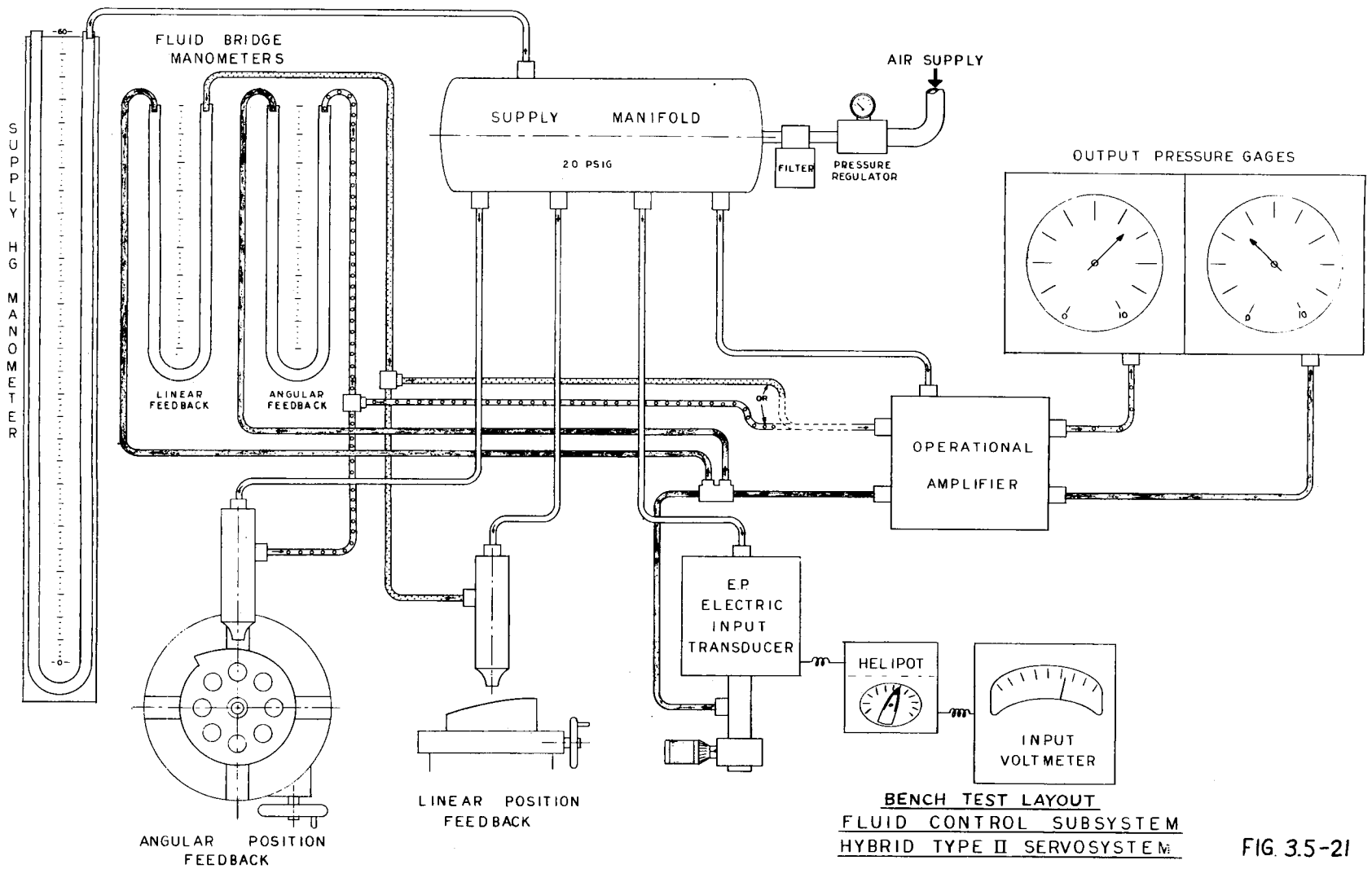

BENCH TEST LAYOUT
FLUID CONTROL SUBSYSTEM
HYBRID TYPE II SERVOSYSTEM

DWG. NO. 250-365

FIG. 3.5-21

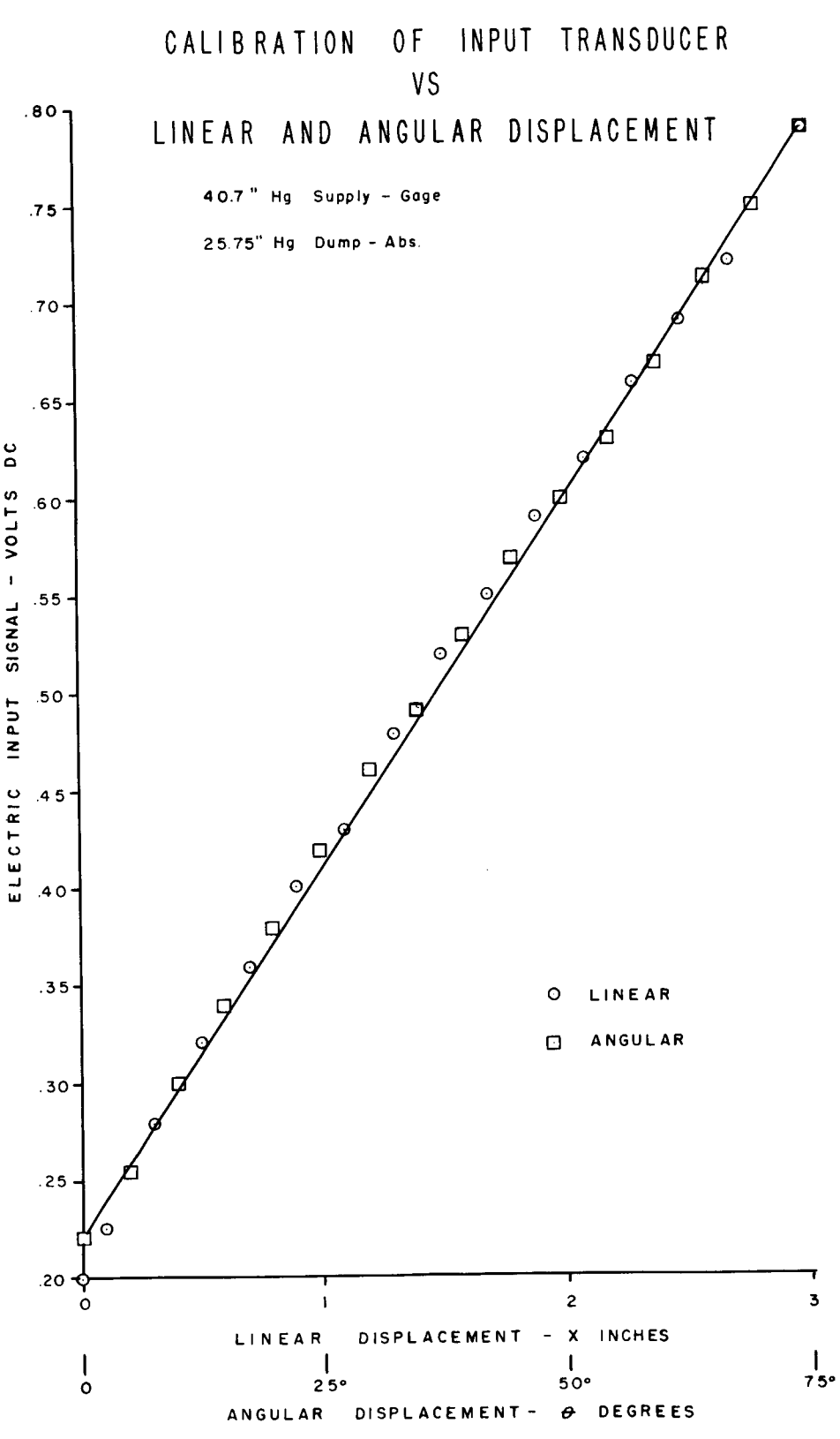
CALIBRATION OF INPUT TRANSDUCER
VS
LINEAR AND ANGULAR DISPLACEMENT
40.7" Hg Supply - Gage
25.75" Hg Dump - Abs.
ELECTRIC INPUT SIGNAL - VOLTS DC
.80
.75
.70
.65
.60
.55
.50
.45
.40
.35
.30
.25
.20
LINEAR
ANGULAR
0
1
2
3
LINEAR DISPLACEMENT - X INCHES
0
25°
50°
75°
ANGULAR DISPLACEMENT - θ DEGREES

FIG. 3.5-22

FLUID CONTROL SUBSYSTEM
OUTPUT LEGS PRESSURE
VS
ANGULAR TRANSDUCER DISPLACEMENT

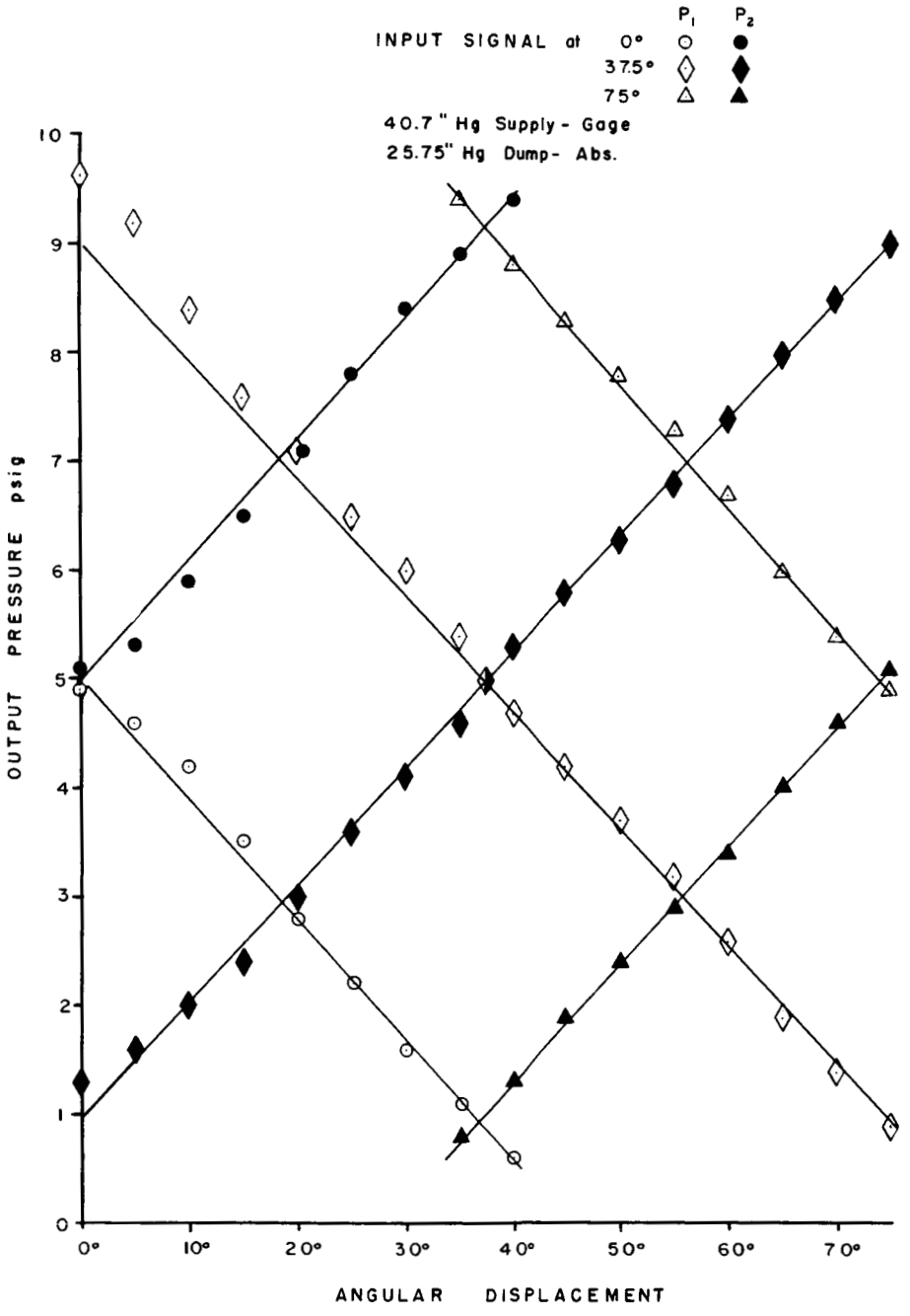

FIG. 3.5-23

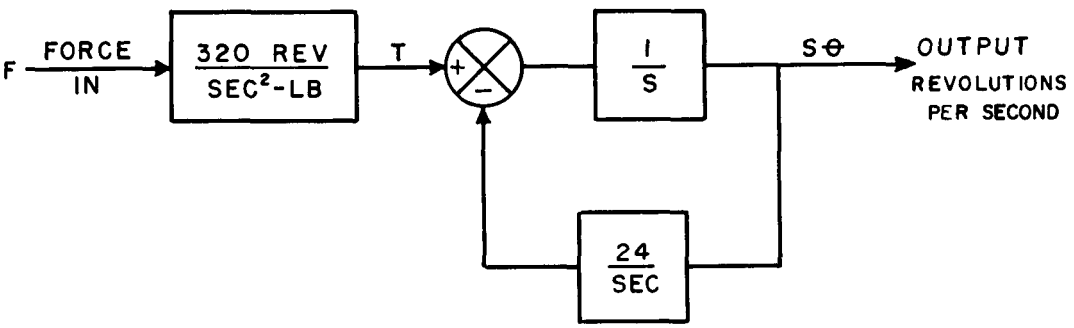

FIG. 3.6-1 EQUIVALENT CIRCUIT OF VALVE-MOTOR ASSEMBLY

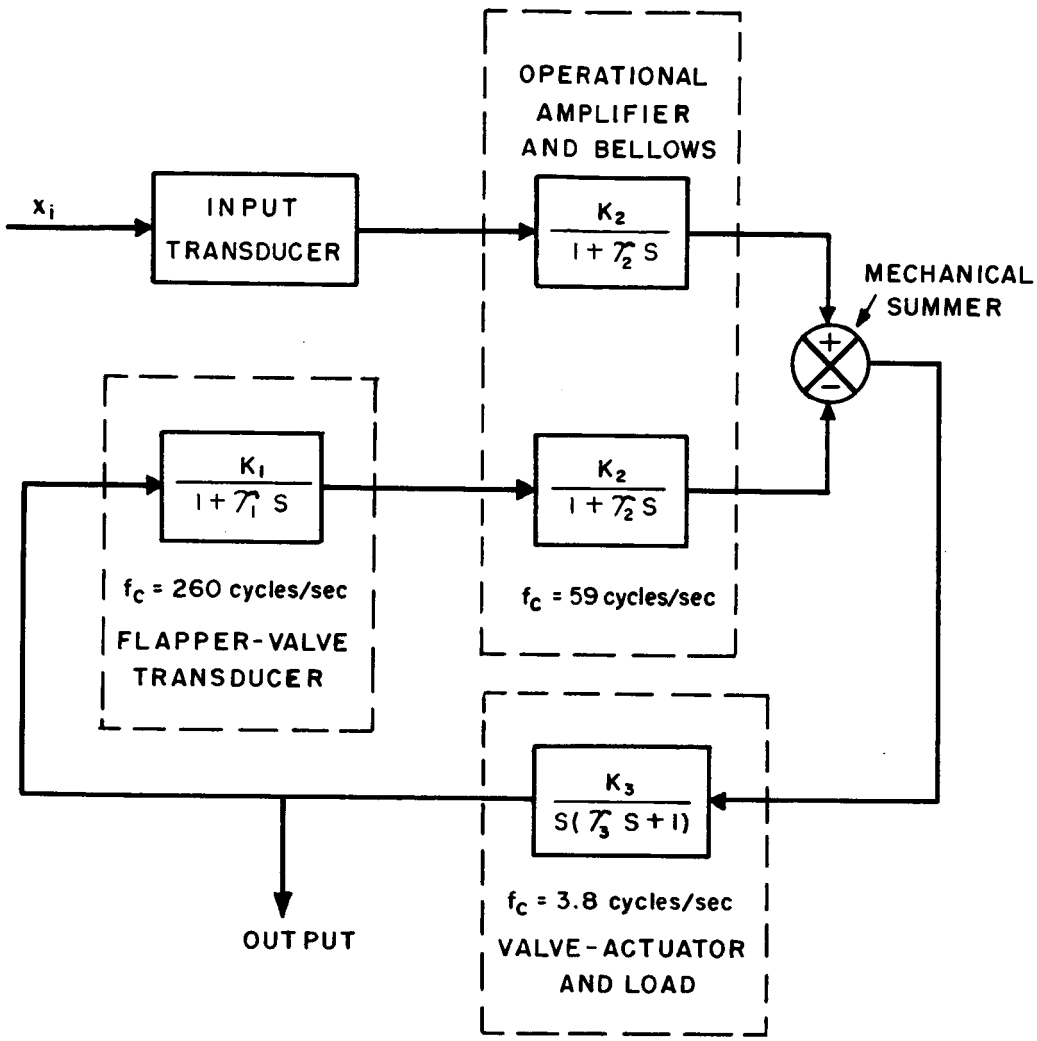

K_1 = 0.364 psi/inch
K_2 = 22 lbf/psi
K_3 = 0.5 in/lbf

τ_1 = 0.00061 sec
τ_2 = 0.0027 sec
τ_3 = 0.416 sec

FIG. 3.6-2 SIMPLIFIED EQUIVALENT BLOCK DIAGRAM

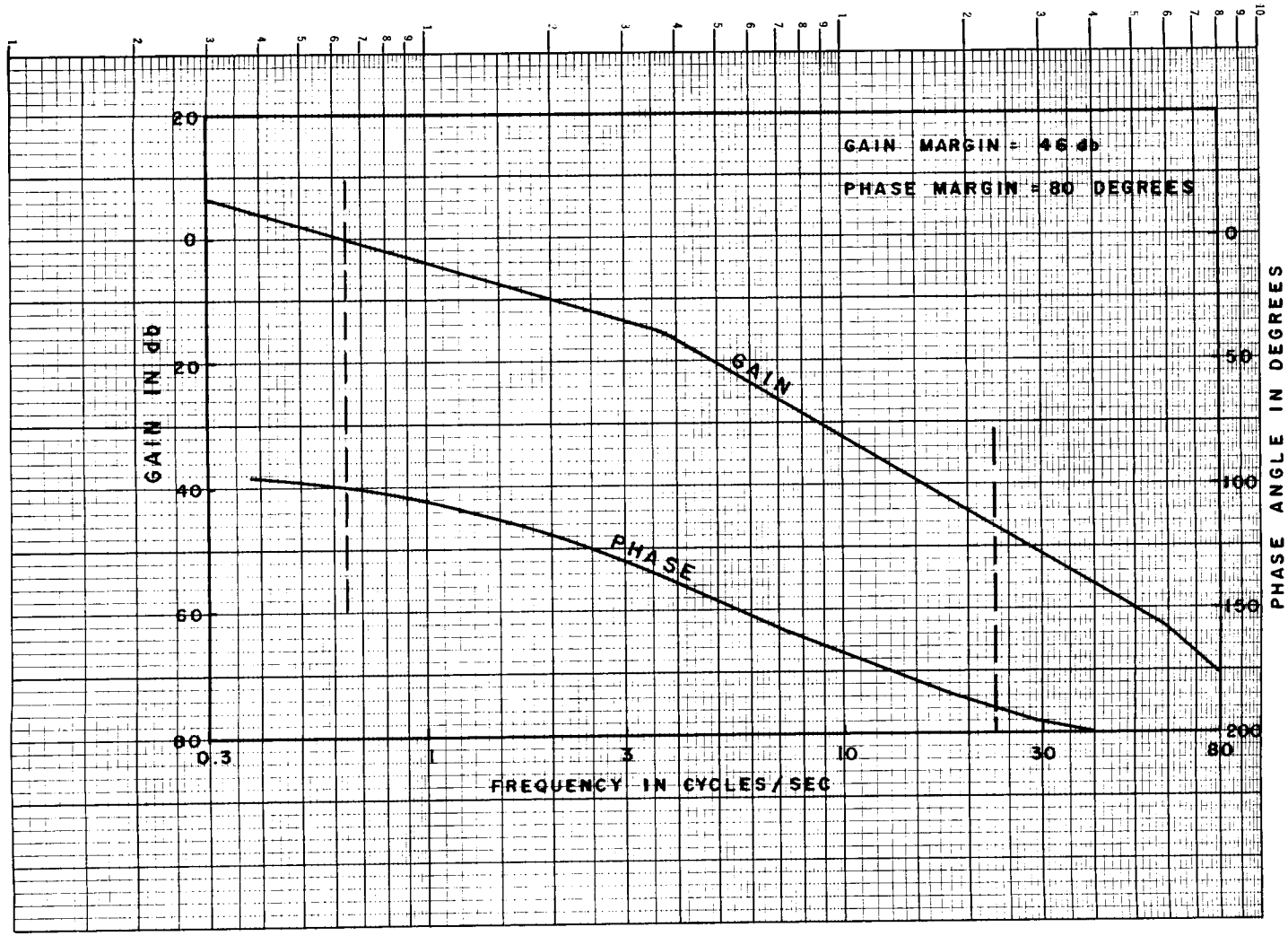

FIG. 3.6-3 PHASE-GAIN CHARACTERISTICS OF OPEN-LOOP TRANSFER FUNCTION

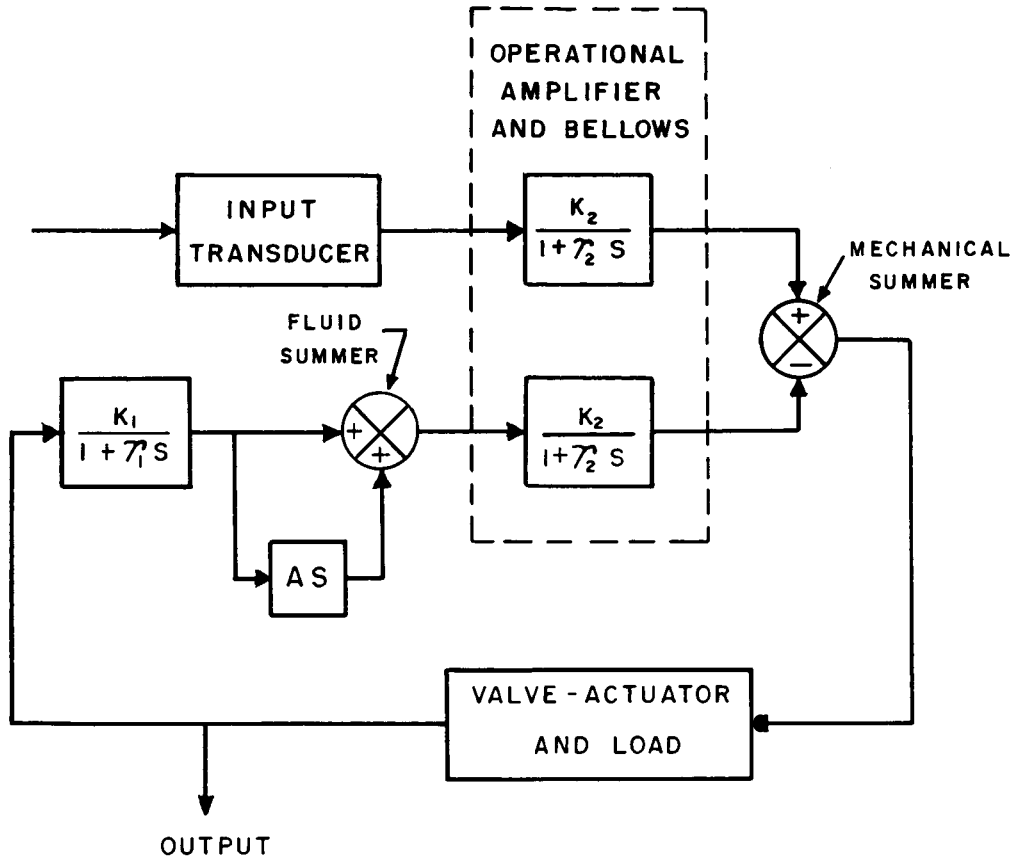

FIG. 3.6-4 SIMPLIFIED EQUIVALENT BLOCK DIAGRAM WITH RATE FEEDBACK

APPENDIX I

A SUMMARY OF ANALYTICAL FLUID INVESTIGATIONS PERFORMED AT SPERRY RAND RESEARCH CENTER AND SPERRY UTAH COMPANY

Prepared by
R. L. Blosser
SPERRY UTAH COMPANY
Division of Sperry Rand Corporation
Salt Lake City, Utah

April 1964

SYMBOLS

u^1 = radial component of velocity

v^1 = tangential component of velocity

w^1 = axial component of velocity

(r^1, θ, z^1) = cylindrical coordinates

(u, v, w) = normalized velocity components

a = viscosity

p = density

δ = boundary layer thickness

v_δ = tangential velocity at boundary layer

$\eta = \frac{z}{\delta}$ = normalized axial component of velocity

A SUMMARY OF ANALYTIC FLUID INVESTIGATIONS PERFORMED AT SPERRY RAND RESEARCH CENTER AND SPERRY UTAH

Recent advances in computer hardware coupled with sophisticated numerical techniques have led to significant advances towards accurate, reliable and physically interpretable solutions of the complete two dimensional fluid flow problem.

The numerical methods follow the usual technique of a superpositioning a grid upon the region of interest and applying a difference equation which is derived from the differential equation. The unknown values of the stream function and vorticity are obtained at all grid points. The grid may be rectangular, elliptial, or circular, depending upon the geometry of the problem to be solved.

Three inherent problems arise in the use of numerical methods: the stability of the solution, the amount of computer time required, and the accuracy of the solution.

Slighting or failing to overcome any of these three obstacles invites failure: loss of stability and the computational program will not approach a solution in a reasonable time; lack of accuracy and the obtained values are not physically meaningful; and finally, inordinate amounts of computer time may result in both of the above, plus storage and memory problems, as long problems require large memories. The numerical techniques developed at Sperry have circumvented these problems and allowed adequate numerical solutions to two dimensional fluid flow problems. A critical study was made on the mathematics of a vortex (Ref. 1). This effort was performed in house at Sperry Utah. A Univac-490, Real-Time, computer was used. The purpose of this study was investigations of boundary layer flow and other parameters observed in incompressible viscous flow in a vortex chamber.

Since, the vortex chamber is a cylinder, and the vortex itself has cylindrical symmetry, writing the Navier-Stokes equations in cylindrical coordinates allows a more forceful attack on the vortex chamber problem than if the usual rectangular coordinates were used. An abbreviated synopsis of Sperry Utah's work follows.

The applicable Navier-Stokes equations in cylindrical coordinates (r', θ, z') are:

$$u'\frac{\partial u'}{\partial r'} + w'\frac{\partial u'}{\partial z'} - \frac{v'^2}{r'} = -\frac{1}{p}\frac{\partial p'}{\partial r'} + a\left[\frac{\partial^2 u'}{\partial r'^2} + \frac{\partial}{\partial r'}\left(\frac{u'}{r'}\right) + \frac{\partial^2 u'}{\partial z'^2}\right] \tag{1}$$

$$u'\frac{\partial v'}{\partial r'} + u'\frac{\partial v'}{\partial z'} + \frac{u'v'}{r} = \left[\frac{\partial^2 v'}{\partial r'^2} + \frac{\partial}{\partial r'}\left(\frac{v'}{r'}\right) + \frac{\partial^2 v'}{\partial z'^2}\right] \tag{2}$$

$$u'\frac{\partial w'}{\partial r'} + \frac{w'\partial w'}{\partial z} = -\frac{1}{p}\frac{\partial p'}{\partial z'} + a\left[\frac{\partial^2 w'}{\partial r'^2} + \frac{1}{r}\frac{\partial w'}{\partial r'} + \frac{\partial^2 w'}{\partial z'^2}\right] \tag{3}$$

$$\frac{\partial u'}{\partial r'} + \frac{\partial w'}{\partial z'} + \frac{u'}{r'} = 0 \tag{4}$$

Where a is the viscosity, p the density, and u', v' and w' are the radial, tangential and axial components of the velocity, respectively.

It is physically reasonable to assume that the radial derivates are an order of magnitude smaller than those in the z, or longitudinal, direction. It is also assumed that w is an order of magnitude larger than u and v .

Thus, the equations become

$$u'\frac{\partial u'}{\partial r'} + w'\frac{\partial u'}{\partial z'} - \frac{v'}{r'} = -\frac{1}{p}\frac{\partial p'}{\partial r'} + a\frac{\partial u'^2}{\partial z'} \tag{5}$$

$$u'\frac{\partial v'}{\partial r'} + w'\frac{\partial v'}{\partial z'} + \frac{u'v'}{r'} = a\frac{\partial v^2}{\partial z^2} \tag{6}$$

$$\frac{\partial u'}{\partial r'} + \frac{\partial u'}{\partial z'} + \frac{u'}{r'} = 0 \tag{7}$$

Introducing

$$u = \frac{u'}{v_1'},\ v = \frac{v'}{v_1'},\ w = \frac{w'}{\sqrt{a\theta_1}},\ r = \frac{r'}{r_1'},\ z = z'\sqrt{\frac{\theta'}{a}},\ \theta_1' = \frac{v'}{a}$$

and calculating the necessary derivatives.

$$\frac{\partial u'}{\partial r'},\ \frac{\partial u'}{\partial r_1'},\ \frac{\partial u'}{\partial z'} \text{ ---------- } w'\frac{\partial v'}{\partial z'}$$

The above equations become:

$$u\frac{\partial u}{\partial r}+w\frac{\partial u}{\partial z}-\frac{v^2}{r}+\frac{v_\delta^2}{r}=\frac{\partial^2 u}{\partial z^2} \tag{8}$$

$$u\frac{\partial v}{\partial r}+w\frac{\partial v}{\partial z}+\frac{uv}{r}=\frac{\partial^2 v}{\partial z^2} \tag{9}$$

$$\frac{\partial (ru)}{\partial r}+\frac{\partial (rw)}{\partial z}=0 \tag{10}$$

For convenience, (8) and (9) are written in a slightly different form

$$\frac{\partial}{\partial r}(ru^2)+r\frac{\partial}{\partial z}(uw)+v_\delta^2-v^2=r\frac{\partial u^2}{\partial z^2} \tag{11}$$

$$\frac{\partial}{\partial r}(r^2uv)+r^2\frac{\partial}{\partial z}(vw)=r^2\frac{\partial v^2}{\partial z^2} \tag{12}$$

Integrating (11) and (12) with respect to z from 0 to δ, where δ, a function of r, is the boundary layer thickness, gives

$$\frac{d}{dr}\left(r\int_0^\delta u^2 dz\right)+r\frac{d}{dz}\int_0^\delta uw\,dz+\int_0^\delta\left(v_\delta^2-v^2\right)dz=-r\frac{\partial u}{\partial z}\Big|_{z=0} \tag{13}$$

$$\frac{d}{dr}\left(r^2\int_0^\delta (uv\,dz)\right)+r^2\frac{d}{dz}\left(\int_0^\delta vw\,dz\right)=-r^2\frac{\partial v}{\partial z}\Big|_{z=0} \tag{14}$$

The boundary conditions,

1. $z=0$ $\quad u=0$, $v=0$
2. $z=\delta$ $\quad u=0$, $\frac{\partial u}{\partial z}=0$, $\frac{\partial v}{\partial z}=0$

and the introduction of the further change of variables,

$$\eta = \frac{z}{\delta} \tag{15}$$

yields,

$$\frac{d}{dr}\left(\delta r \int_0^1 u^2\, d\eta\right) + \delta \int_0^1 \left(v_\delta^2 - v^2\right) d\eta = -\frac{r}{\delta}\left.\frac{\partial u}{\partial \eta}\right|_{\eta=0} \tag{16}$$

$$\frac{d}{dr}\left(\delta r^2 \int_0^1 uv\, d\eta\right) - r v_\delta \frac{d}{\delta dr}\left(\delta r \int_0^1 u\, d\eta\right) = -\frac{r^2}{\delta}\left.\frac{\partial v}{\partial \eta}\right|_{\eta=0} \tag{17}$$

The velocity components can be written as

$$u(r,\eta) = v_\delta(r)\, E(r)\, f(\eta) \tag{18}$$

$$v(r,\eta) = v_\delta(r)\, g(\eta) \tag{19}$$

Where $f(\eta)$ is the radial velocity profile and g(y) is the tangential velocity and E(r) is to be determined, boundary conditions on f and y are

$$f(0) = f(1) = 0 \qquad \left.\frac{\partial u}{\partial \eta}\right|_{\eta=0} = v_\delta(r)\, E(r)\, f'(0)$$

$$g(0) = 0$$

$$g(1) = 1 \qquad \left.\frac{\partial v}{\partial \eta}\right|_{\eta=0} = v_\delta\, g'(0) \tag{20}$$

If we apply these boundary conditions to (16) and (17) we have

$$\frac{d}{dr}\left(\delta r\, v_\delta^2 E^2\right) \int_0^1 f^2 d\eta + v_\delta^2 \delta \int_0^1 (1-g^2) d\eta = -\frac{1}{\delta}\, r v_\delta f'(0) \tag{21}$$

$$\frac{d}{dr}\left(\delta r^2 v_\delta^2 E\right) \int_0^1 fg\, d\eta - \left(r v_\delta \frac{d}{dr}\left(\delta r\, v_\delta E\right) \int_0^1 f\, d\eta\right) = -\frac{1}{\delta}\, r^2 v_\delta\, g'(0) \tag{22}$$

We define the various f and g intergals as follows

$$I_1 = \int_0^1 f\, d\eta\,, \quad I_2 = \int_0^1 f^2 d\eta\,, \quad I_3 = \int_0^1 (1-g^2)\, d\eta\,, \quad I_4 = \int_0^1 fg\, d\eta \tag{23}$$

To simplify further take

$$A=\frac{I_3}{I_2}, \quad B=\frac{I_1-2I_4}{I_1-I_4}, \quad C=\frac{f'(0)}{I_2}, \quad D=\frac{g'(0)}{I_1-I_4} \tag{24}$$

The two primary equations then become

$$\frac{d}{dr}(rv_\delta^2 \delta E^2) + Av_\delta^2 \delta = -Crv_\delta \frac{E}{\delta} \tag{25}$$

$$\frac{d}{dr}(\delta E) + B\left[\frac{1}{rv_\delta}\frac{d}{dr}(rv_\delta)\right]\delta E = \frac{D}{v_\delta}\frac{1}{\delta} \tag{26}$$

After a substantial amount of manipulation, these equations can be put in the form

$$\frac{d}{dr}(E\delta^2) - \frac{3}{2}\delta E\frac{d\delta}{dr} = -\frac{1}{2}E\delta^2\frac{d}{dr}(\ln rv_\delta^2) - \frac{A\delta^2}{2rE} - \frac{C}{2v_\delta} \tag{27}$$

$$\frac{d}{dr}(E\delta^2) - \delta E\frac{d\delta}{dr} = -BE\delta^2\frac{d}{dr}(\ln rv_\delta) + \frac{D}{v_\delta} \tag{28}$$

Assuming velocity distributions of the form $v_\delta(r) = r^{-N}$, where N is a constant, equations (27) and (28) become

$$\frac{dE^2}{dr} = 2E^2\left[N-(1-N)(1-B)\right] + \frac{2A}{r} - \frac{2(C+D)E^2 r^N}{E\delta^2} \tag{29}$$

or

$$\frac{d}{dr}(E\delta^2) = E\delta^2\left[N+(1-N)(3B-1)\right] + \frac{A}{r}\frac{E\delta^2}{E^2} + (C+3D)r^N \tag{30}$$

Equations (29) and (30) must be solved by numerical methods since the $\frac{E^2}{E\delta^2}$ and $\frac{E\delta^2}{E}$ terms introduce singularities as $r \to 1$. We overcome this difficulty by requiring that E^2, δ^4, $\frac{E^2}{\delta^2}$, and $\frac{\delta^2}{E}$ have the same behavior at $r = 1$. It can be established that

$$E \sim (1-r)^{\frac{1}{2}}$$

$$\delta \sim (1-r)^{\frac{1}{4}} \tag{31}$$

for $r \lesssim 1$. Expanding E^2 and $E\delta^2$ in powers of $(1 - r)$, we have,

$$E^2 = a_1(1-r) + a_2(1-r)^2 + \text{----------}$$

$$E\delta^2 = b_1(1-r) + b_2(1-r)^2 + \text{----------} \tag{32}$$

It is found that

$$a_1 = \frac{4AD}{3C+5D}$$

$$b_1 = -\frac{4}{3}D$$

$$a_2 = \left[-b_1 + (C+D)\right] = \frac{b^2}{2}(a_1 - 2A) + a_2\left[(2-B)b_1 + (C+D)\right]N + b_1\left[(B-1)a_1 - A\right]$$

and so on.

Now defining f (n) and g (n) by

$$f(N) = N(1-N)^2 \qquad f'(0) = 1$$

$$f(N) = 1 - 4N + 3N^2$$

$$g(N) = 1 - (1-N)^2 \qquad g'(0) = 2$$

$$g(N) = 2 - 2N$$

Then $$I_1 = \int_0^1 (\eta - 2\eta^2 + \eta^3)\, d\eta = \frac{1}{12}$$

Similarly evaluating I_2, I_3 and I_4 yields

$$I_2 = 1/105 \qquad I_3 = 7/15 \qquad I_4 = 1/20$$

and in turn

$A = 40$

$B = .05$

$C = 105$

$D + 60$

for $N = .75$

We have $a_1 = 4AD/3C + 5D = 4(40)\,(60)/3(105) + 5(60) = 19.121$

$b_1 = -4(60)/3 = 80$

Similarly $a_2 = 21.3224$

$a_3 = 24.2589$

$b_2 = 37.8421$

$b_3 = 117.354$

With starting values of $r = .99$

we obtain from $E^2 = a_1(1-r) + a_2(1-r)^2$; $E = -.439$

and from $E\delta^2 = h_1(1-r) + h_2(1-r)^2$; $\delta = 1.345$

These are the starting values.

Let us for simplicity let $y = E^2$

$u = E\delta^2$

$y' = d_E 2/d_r 2$

$u' = d/d_r\,(E\delta^2)$

$y_0 = .193$

$u_0 = .796$

Thus our equations to be solved become

$$y' = \left(\frac{0.75}{r} - \frac{330 r^N}{u}\right) y - \frac{98}{r}$$
$$u' = \left(\frac{49}{ry} - \frac{125}{r}\right) y + 285 r^N \qquad (33)$$

A Runge Kutta Integration was performed on Sperry Utah Univac 490 real time computer. Figure 1 lists the solution for N = .75. The 490 solution allows us to examine flow rates and other fluid parameters of interest.

The axial component of velocity obtained by integration of the continuity equation its final form being

$$w_\delta = -I_1\left[\frac{E\delta(1-N)(1-B)}{r^{(1+N)}} + \frac{D}{\delta}\right] \qquad (34)$$

A plot of this is given in Figure 2 for N = 0.75

The tangential stress and radial stress are given by

$$T_r = \frac{1}{\delta}\left[v_\delta(r)\right] E(r)\, F'(0)$$
$$T_t = \frac{1}{\delta}\left[v_\delta(r)\right] g'(0) \qquad (35)$$

Plots of these are given in Figure 3. Figures 4 and 5 show plots of the boundary layer thickness and the maximum layer thickness developed for maximum outer flow.

To still more briefly summarize the Sperry Utah effort, an axially symmetric case was considered. It was assumed that the derivatives in Z^1 direction were larger than those in r^1 direction, and that w^1 was an order of magnitude smaller than u^1 and v^1. After non-dimensionalizing the Navier-Stokes equations with the aid of the $\eta = \frac{\delta}{Z}$ substitution, and the velocity profiles $u(r_1\eta) = v_\delta(r)\, E(r) f(\eta)$, $v(r_1\eta) = v_\delta\, g(\eta)$, the equations were rewritten in terms of E^2 and $E\delta^2$. By the use of the Runge Kutta method on the Sperry Utah Company's Univac 490 computer, the various fluid parameters such as stress, velocity, and flow were obtained.

The result was not an exact solution of the Navier-Stokes equations and various areas need to be developed further, particularly in the behavior of w_δ and the boundary thickness at the end wall of the cylinder.

Table D-1. Solution When $\mu = 0.75$

r	$v^{(.75)}$	$E(r)$	$\delta(r)$
0.99	0.992491	0.460652	1.314446
0.95	0.962261	1.000500	1.971714
0.90	0.924021	1.440625	2.276093
0.85	0.885246	1.800417	2.443223
0.80	0.845897	2.124265	2.542880
0.75	0.805927	2.429794	2.599825
0.70	0.765285	2.726720	2.625929
0.65	0.723910	3.021506	2.627825
0.60	0.681731	3.319172	2.609565
0.55	0.638663	3.624169	2.573697
0.50	0.594603	3.940939	2.521830
0.45	0.549425	4.274342	2.454892
0.40	0.502972	4.630065	2.373264
0.35	0.455040	5.015287	2.276833
0.30	0.405359	5.439550	2.164907
0.25	0.353552	5.916367	2.036050
0.20	0.299068	6.466158	1.887680
0.15	0.241027	7.122591	1.715064
0.10	0.177826	7.948761	1.508484
0.05	0.105735	9.093289	1.241430
0.01	0.031620	10.617895	0.882042

Figure 1. Runge-Kutta Integration

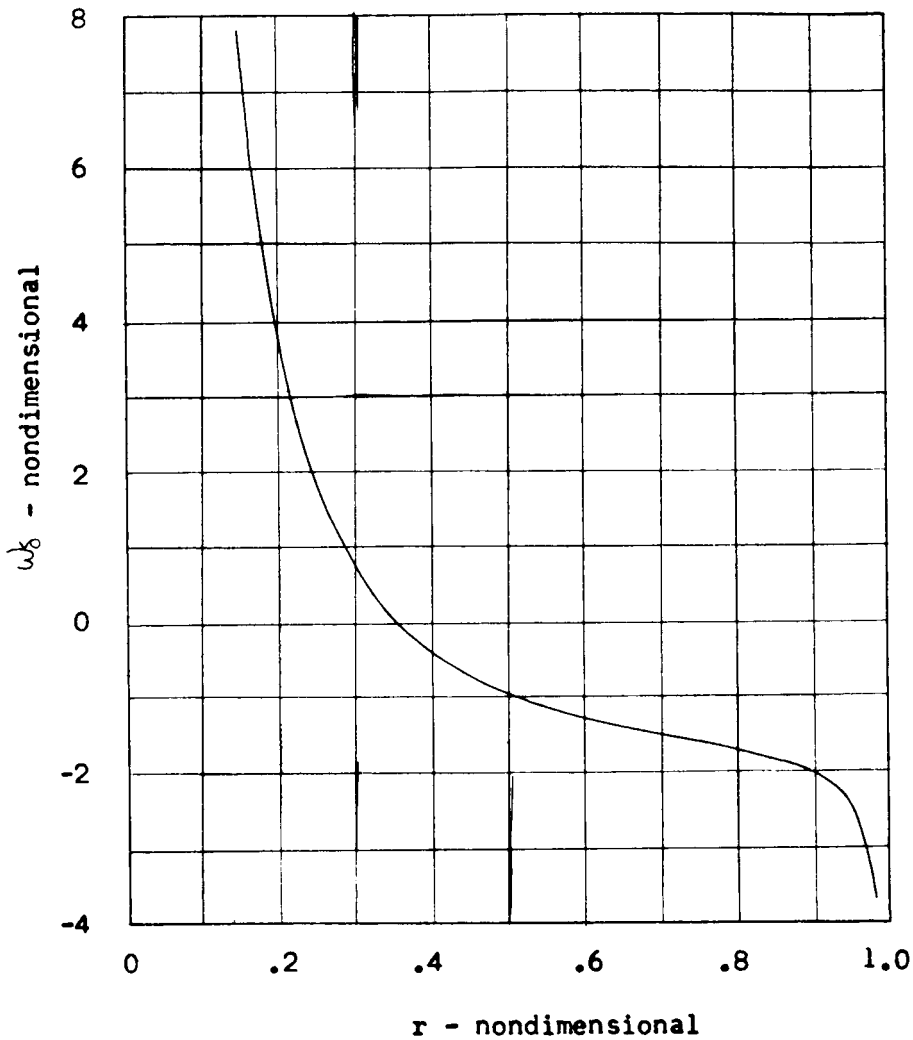

Figure 2. Axial Component of the Velocity as the Flow Enters and Leaves the Boundary Layer for Chamber I (n = .75)

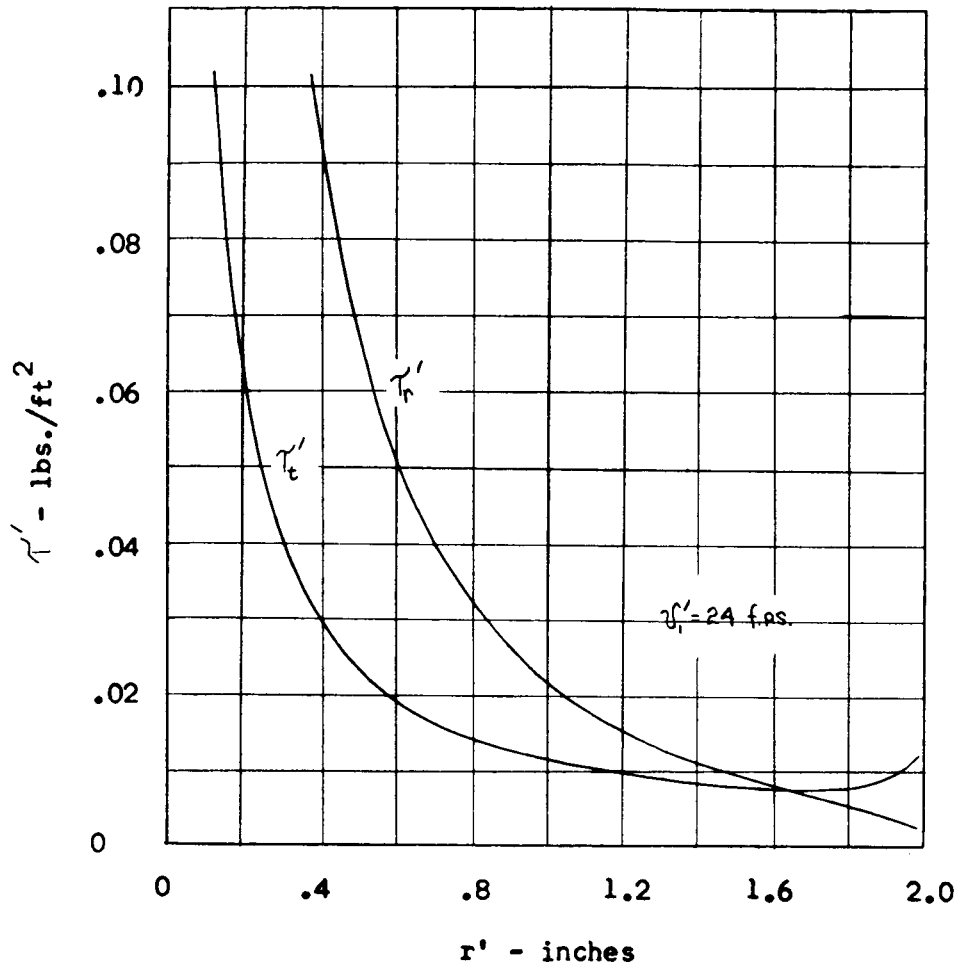

Figure 3 The radial and Tangential Components of the Shearing Stress of the Flow in the End Wall Boundary Layer for Chamber I (n = .75)

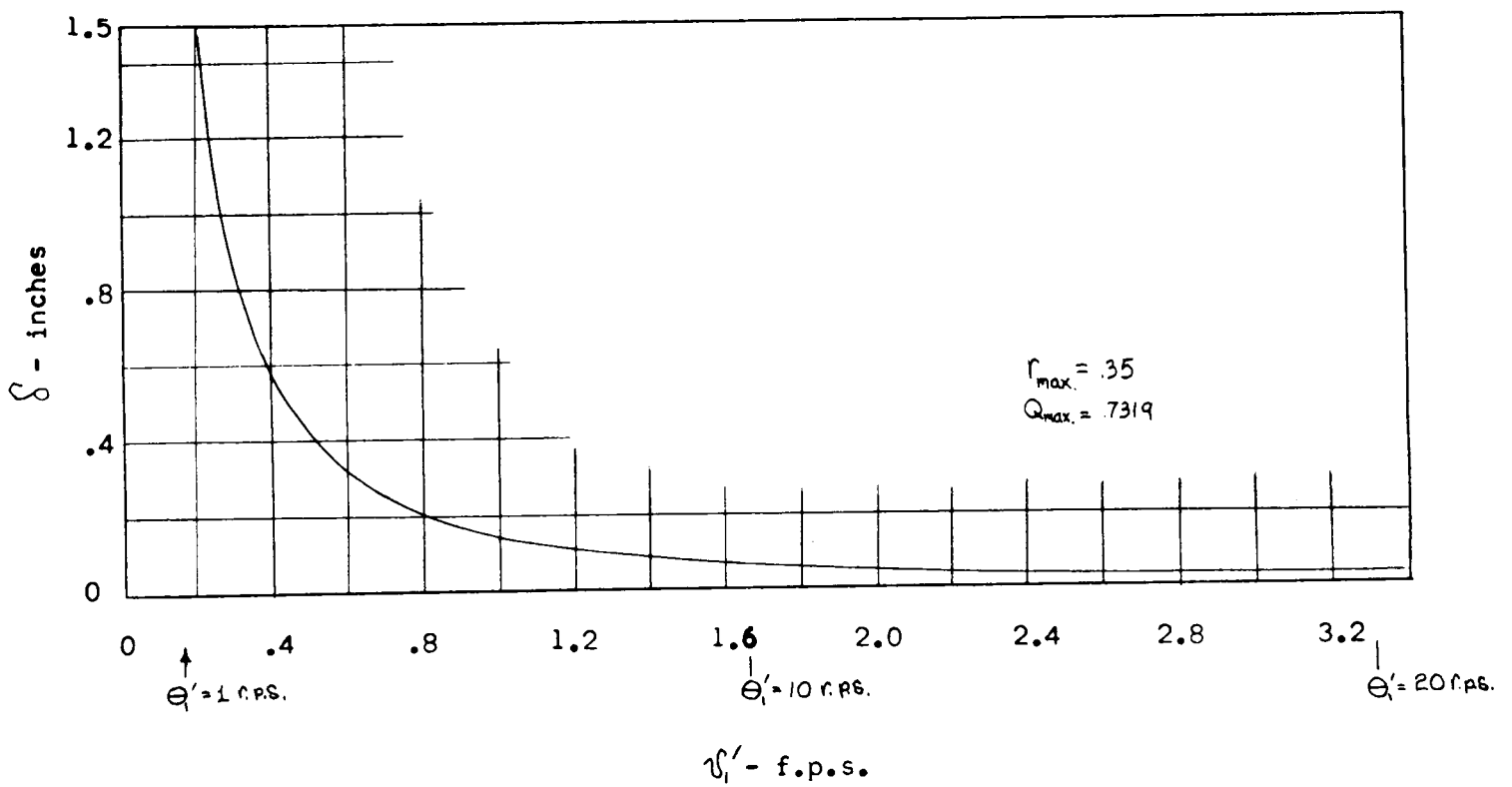

Figure 4 Boundary Layer Thickness on the End Wall of Chamber I for Various Tangential Outer Flow Velocities

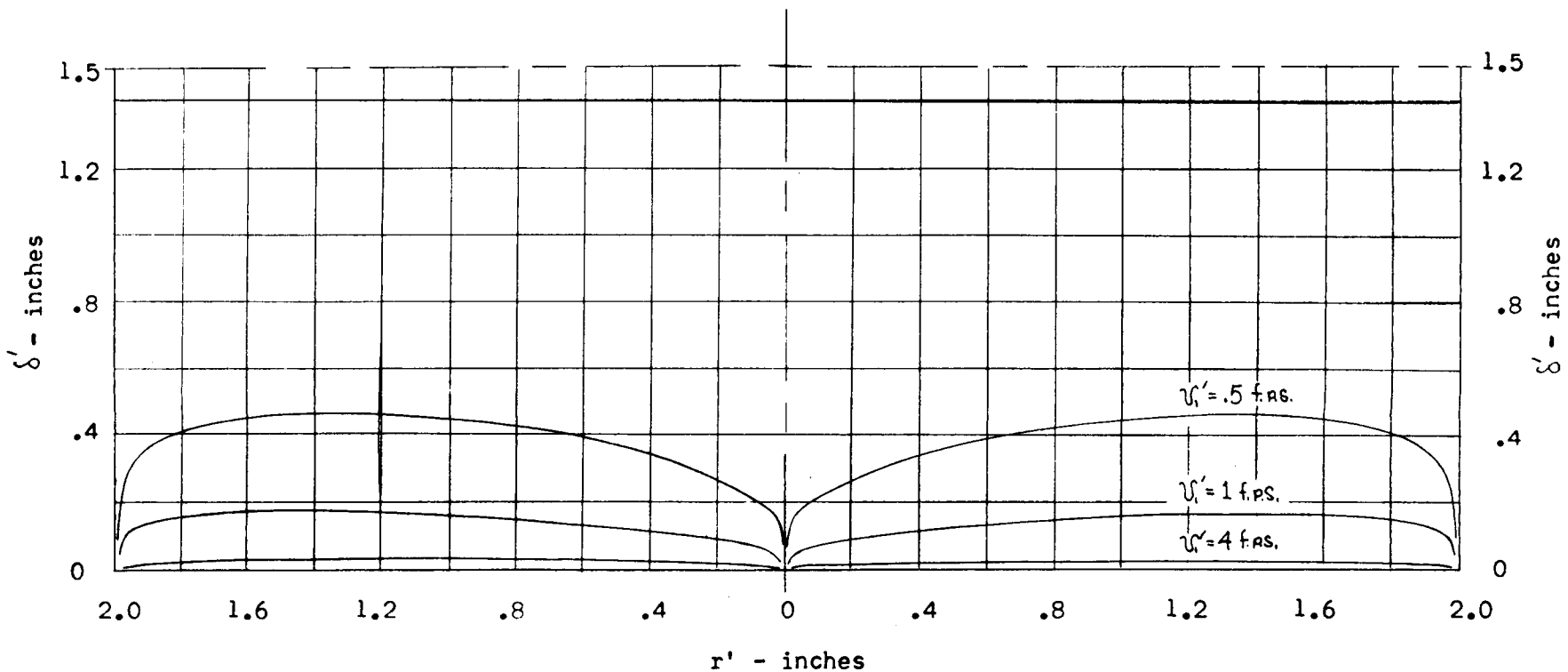

Figure 5 Boundary Layer Thickness Evaluated at the Maximum $Q'(r)$ in Terms of the Tangential Outer Flow Velocity

During the empirical portion of the Sperry Utah fluid vortex effort, several interesting phenomena were observed. First, matter waves were observed to move up and down on the vortex column. Secondly, some connection (as observed by smoke phenomena in the transparent vortex chamber) existed between the boundary layer and the core; and finally, when the driving jet was increased a well defined tornado column was apparent in the vortex chamber.

The Sperry Rand Research Center was informed of Sperry Utah's efforts and an interchange of material was begun and is continuing at this time. Two problems, namely spin-up or spin-down, and the diffusion of material have been under direct investigation by the Sperry Rand Research Center (Ref. 1).

To summarize the Sperry Rand Research Center effort, the equations governing the time dependent motion of a viscous incompressible fluid for an axially symmetric vortex were written. Coordinates (r_1, θ, z) were used.

Again symmetry conditions allow the three dimensional problem to be considered two-dimensionally. After simplification and reducing to a dimensionless form, the Navier-Stokes equation becomes:

$$\frac{1}{R}\left(\frac{\partial^2}{\partial z^2} - \frac{\partial}{\partial t}\right) v - \frac{\partial}{\partial z}\phi = 0 \tag{36}$$

$$\left(\frac{1}{R}\frac{\partial}{\partial z^2} - \frac{\partial}{\partial t}\right)\frac{\partial^2 \phi}{\partial z^2} + \frac{\partial v}{\partial z} = 0$$

Where ϕ and v are defined by

$$v = 1 \quad \phi = \frac{\partial \phi}{\partial z} = 0 \quad z = \pm 1$$

$$v = 0 \quad \phi = 0 \quad \text{for} \quad t \leq 0 \tag{37}$$

Boundary conditions are

$$\phi = \frac{\partial \phi}{\partial z} = 0$$

$$\phi = 0$$

The Laplace transform was used effectively in this effort, and solutions obtained by residue theory.

The following conclusions were drawn from the Sperry Rand Research Center effort:

1. The centrifugal force produces an outward radial flux within the viscious boundary layer.

2. This is compensated for by flow from the interior region.

3. The spin-up time (the time needed for interior fluid to approach solid body rotation) is essentially a function of the Ekman layer.

4. The establishment of the Ekman layer begins immediately between the first and second revolutions of the fluid.

A concluding report (reference 3) on the spin-up phenomena investigation was generated by Sperry Rand Research Center. In essence it is an angular momentum examination of the rotating fluid. Significantly the report calls for advanced numerical programs on the two-dimensional vortex problem. Such an effort is now underway at Sperry Rand Research Center (Ref. 4).

Several methods for examining the time dependent two-dimensional incompressible viscous flow problem are being considered; the first portion of this effort was an evaluation of possible numerical methods by comparing accuracy of solution, stability, and computer time used on solutions of the one-dimensional diffusion equation, $Y_T = Y_{XX}$, where subscripts indicate differentiation. The boundary conditions are

$$y(1, T) = 0$$

$$y(1, T) = 0$$

and $$y(x, 0) = x - \sin x$$

The exact solution is compared to values obtained by the explicit, DuFort-Frankel, and implicit numerical methods. The stability and relaxation speed are compared for various time steps in chart form. An example is given in Figures 6, 7 and 8. It is through this comparison of exact and numerical approaches that the superiority of the implicit method rapidly becomes apparent.

At this time the fourth-order, Navier-Stokes, two-dimensional problem was attacked by separation into two coupled equations, one of which has a diffusion-equation character and one of which has a poisson-equation character.

(a) $N = 40,\ \Delta t = .0003125,\ A = \Delta t/\Delta x^2 = 0.5$

(Stability Limit for Explicit Method)

t	Explicit	DuFort-Frankel	Implicit
.005	2.03×10^{-4}	2.04×10^{-4}	1.01×10^{-4}
.010	2.47×10^{-4}	2.47×10^{-4}	1.23×10^{-4}
.015	2.26×10^{-4}	2.26×10^{-4}	1.13×10^{-4}
.020	1.84×10^{-4}	1.83×10^{-4}	9.23×10^{-5}
.025	1.40×10^{-4}	1.39×10^{-4}	7.09×10^{-5}
.030	1.03×10^{-4}	1.01×10^{-4}	5.24×10^{-5}
.035	7.29×10^{-5}	7.17×10^{-5}	3.78×10^{-5}
.040	5.08×10^{-5}	4.94×10^{-5}	2.69×10^{-5}
.045	3.47×10^{-5}	3.34×10^{-5}	1.90×10^{-5}
.050	2.35×10^{-5}	2.21×10^{-5}	1.34×10^{-5}
.055	1.57×10^{-5}	1.42×10^{-5}	9.57×10^{-6}
.060	1.03×10^{-5}	8.88×10^{-6}	6.92×10^{-6}
.065	6.72×10^{-6}	5.27×10^{-6}	5.13×10^{-6}
.070	4.31×10^{-6}	2.86×10^{-6}	3.94×10^{-6}
.075	2.71×10^{-6}	1.25×10^{-6}	3.16×10^{-6}
.080	1.66×10^{-6}	2.82×10^{-7}	2.64×10^{-6}
.085	9.68×10^{-7}	4.91×10^{-7}	2.30×10^{-6}
.090	5.16×10^{-7}	9.34×10^{-7}	2.07×10^{-6}
.095	2.23×10^{-7}	1.23×10^{-6}	1.92×10^{-6}
.100	6.12×10^{-8}	1.43×10^{-6}	1.83×10^{-6}

Figure 6 Comparison of Explicit, Dufort Frankel and Implicit Integrations

(d) $N = 40,\ \Delta t = .01,\ \frac{\Delta t}{\Delta x^2} = 16$ (Explicit Method Unstable)			(e) $N = 80,\ \Delta t = .01,\ \frac{\Delta t}{\Delta x^2} = 64$	
t	DuFort-Frankel	Implicit	DuFort-Frankel	Implicit
.005	9.76×10^{-2}	6.36×10^{-5}	1.06×10^{-1}	1.44×10^{-4}
.010	2.27×10^{-1}	7.11×10^{-5}	2.83×10^{-1}	1.61×10^{-4}
.015	3.37×10^{-1}	6.31×10^{-5}	4.87×10^{-1}	1.43×10^{-4}
.020	4.02×10^{-1}	5.05×10^{-5}	6.89×10^{-1}	1.15×10^{-4}
.025	4.14×10^{-1}	3.81×10^{-5}	8.69×10^{-1}	8.66×10^{-5}
.030	3.79×10^{-1}	2.77×10^{-5}	1.01	6.30×10^{-5}
.035	3.10×10^{-1}	1.96×10^{-5}	1.12	4.46×10^{-5}
.040	2.23×10^{-1}	1.35×10^{-5}	1.18	3.09×10^{-5}
.045	1.33×10^{-1}	9.22×10^{-6}	1.20	2.11×10^{-5}
.050	5.06×10^{-2}	6.18×10^{-6}	1.17	1.42×10^{-5}
.055	1.52×10^{-2}	4.09×10^{-6}	1.10	9.48×10^{-6}
.060	6.08×10^{-2}	2.64×10^{-6}	9.93×10^{-1}	6.25×10^{-6}
.065	8.59×10^{-2}	1.67×10^{-6}	8.61×10^{-1}	4.07×10^{-6}
.070	9.28×10^{-2}	1.02×10^{-6}	7.07×10^{-1}	2.62×10^{-6}
.075	8.56×10^{-2}	5.82×10^{-7}	5.39×10^{-1}	1.69×10^{-6}
.080	6.91×10^{-2}	3.12×10^{-7}	3.63×10^{-1}	1.03×10^{-6}
.085	4.79×10^{-2}	1.34×10^{-7}	1.87×10^{-1}	6.36×10^{-7}
.090	2.61×10^{-2}	6.32×10^{-8}	1.80×10^{-1}	3.75×10^{-7}
.095	6.73×10^{-3}	7.99×10^{-8}	1.39×10^{-1}	1.98×10^{-7}
.100	8.33×10^{-3}	1.37×10^{-7}	2.80×10^{-1}	1.02×10^{-7}

Figure 7 Comparison of Explicit, Dufort Frankel and Implicit Integrations

(b) $N = 40$, $\Delta t = .00125$, $\frac{\Delta t}{\Delta x^2} = 2$		(c) $N = 40$, $\Delta t = .0025$, $\frac{\Delta t}{\Delta x^2} = 4$	
(Explicit Method Unstable)		(Explicit Method Unstable)	
t	DuFort-Frankel	DuFort-Frankel	Implicit
.005	4.83×10^{-3}	9.97×10^{-5}	1.91×10^{-2}	9.33×10^{-5}
.010	5.90×10^{-3}	1.20×10^{-4}	2.50×10^{-2}	1.11×10^{-4}
.015	5.39×10^{-3}	1.10×10^{-4}	2.30×10^{-2}	1.01×10^{-4}
.020	4.36×10^{-3}	8.95×10^{-5}	1.84×10^{-2}	8.20×10^{-5}
.025	3.31×10^{-3}	6.84×10^{-5}	1.38×10^{-2}	6.25×10^{-5}
.030	2.41×10^{-3}	5.03×10^{-5}	9.88×10^{-3}	4.57×10^{-5}
.035	1.71×10^{-3}	3.60×10^{-5}	6.87×10^{-3}	3.26×10^{-5}
.040	1.18×10^{-3}	2.53×10^{-5}	4.67×10^{-3}	2.28×10^{-5}
.045	8.09×10^{-4}	1.76×10^{-5}	3.13×10^{-3}	1.57×10^{-5}
.050	5.45×10^{-4}	1.22×10^{-5}	2.07×10^{-3}	1.07×10^{-5}
.055	3.64×10^{-4}	8.45×10^{-6}	1.35×10^{-3}	7.24×10^{-6}
.060	2.41×10^{-4}	5.88×10^{-6}	8.79×10^{-4}	4.87×10^{-6}
.065	1.58×10^{-4}	4.14×10^{-6}	5.67×10^{-4}	3.28×10^{-6}
.070	1.03×10^{-4}	2.97×10^{-6}	3.63×10^{-4}	2.21×10^{-6}
.075	6.71×10^{-5}	2.21×10^{-6}	2.32×10^{-4}	1.50×10^{-6}
.080	4.34×10^{-5}	1.70×10^{-6}	1.47×10^{-4}	1.04×10^{-6}
.085	2.79×10^{-5}	1.37×10^{-6}	9.30×10^{-5}	7.39×10^{-7}
.090	1.76×10^{-5}	1.15×10^{-6}	5.86×10^{-5}	5.38×10^{-7}
.095	1.14×10^{-5}	1.01×10^{-6}	3.69×10^{-5}	4.12×10^{-7}
.100	7.19×10^{-6}	9.13×10^{-7}	2.31×10^{-5}	3.26×10^{-7}

Figure 8 Comparison of Explicit, Dufort Frankel and Implicit Intergrations

The splitting up of the fourth-order equation is especially attractive because of computer speed and stability of solutions. For a specific problem, a region in the upper half plan was examined. The viscous flow equation was found to be

$$\xi_t = \Delta\xi + \xi\phi\psi_x - \xi_x\psi_y \tag{38}$$

which has a solution of the form

$$\psi = e^{-2\pi^2 t}\cos(\pi x)\cos(\pi y) \tag{39}$$

This satisfies (38) but since our non-linear terms vanish identically we are not quite as close to a meaningful solution as we would like to be.

Here again the comparison of the implicit method with the explicit process showed the superiority of the implicit method. Despite the good results obtained when comparing to (39), the vorticity (ξ) was in error about 5% on the average and up to 50% on the boundary. By investigation of our usual numerical expression of certain quantities (expansions), a more accurate expression of ξ and ψ is obtained. The expression used was

$$\psi_2 = \psi_1' + \psi' \delta x + \frac{1}{2}\psi' \Delta x^2 \tag{40}$$

These second order terms removed the stated inacurracies. Accuracies of the order of 1/3 of 1% in ψ and 1/4 of 1% in ξ were then obtained. Time steps were consequently increased in size thus reducing computer time and cost.

From this effort the injection of viscous fluid into a rectangular geometry was considered. This essentially corresponds to the vortex problem mentioned in the first section of this paper except for a slightly different container geometry, and fluid flow.

The governing equations become

$$\begin{aligned} &\xi_t + \xi_x\psi_y - \xi_y\psi_x = \Delta\xi \\ &\xi = -\Delta\psi \end{aligned} \tag{41}$$

The region of interest is $0 \le x \le 1$, $0 \le y \le 1$ and the boundary conditions are $\psi = \psi_N = 0$ for all sides except the side $y = 0$.

The boundary condition chosen was $\psi = 10\left[\cos(2\pi x - 1)\right](1 - e^{-100t})$.

The modification of the afore used implicit method was used. The program used was the Peaceman-Rachford method. For small Reynolds numbers there is little to chose between the two as far as accuracy is concerned. For large Reynolds numbers associated with high velocities, the Peaceman-Rachford is definitely superior. This stems from the non-iteration requirement of the P-R method in comparison to the sometimes awkward iteration efforts needed with the highly accurate implicit method.

Non-linear terms and boundary coupling problems, the two main causes of instability, were obviated by choices of smoothing parameters. The values obtained were especially interesting. Such areas as the end wall vorticities and corner flows show good clarification. Typical stream contour plots are shown in Figure 9, 10 and 11. The closed contours indicate reverse flow. The numbers on the contour are values of ψ.

Summary: Through the cooperation efforts of Sperry Rand Research Center and Sperry Utah companies, extensions have been made to the approximate analytical methods previously available. Because of the progress made on the axially symmetric approach to fluid devices, Sperry Utah's in-house fabrication and research effort has been directed in this manner. Three dimensional generalizations exist for certain special cases, gut the problems of accuracy, computer size, solution construction and stability preclude more constructive effort in the three-dimensional areas at this time.

With the current effort under way in both the two-dimensional, theoretical, and experimental areas of fluid development, Sperry Utah is well grounded to enter into long range systems programs.

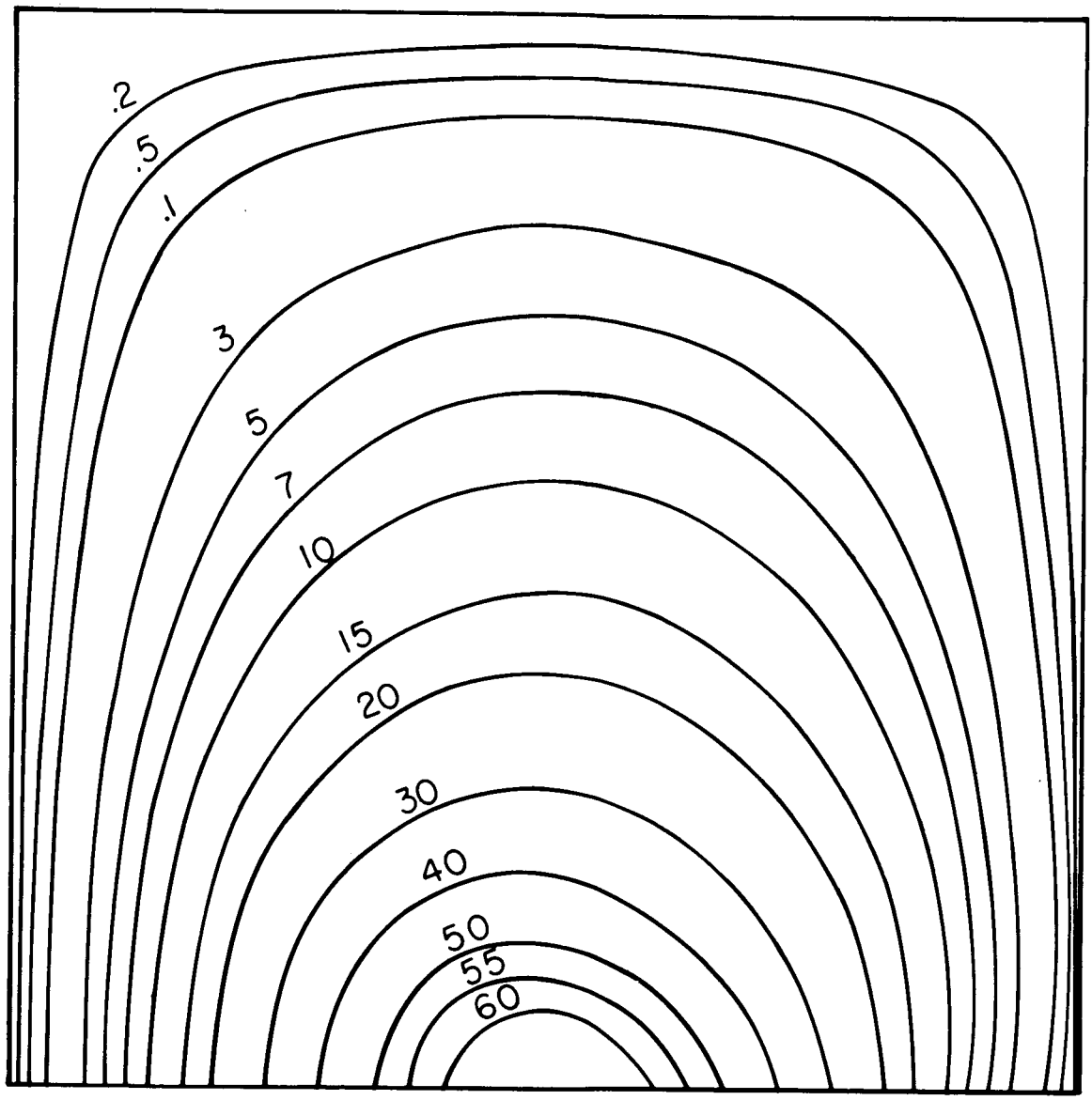

Fig. 9 Re-entrant viscous flow
Amplitude = 100
Time = .004

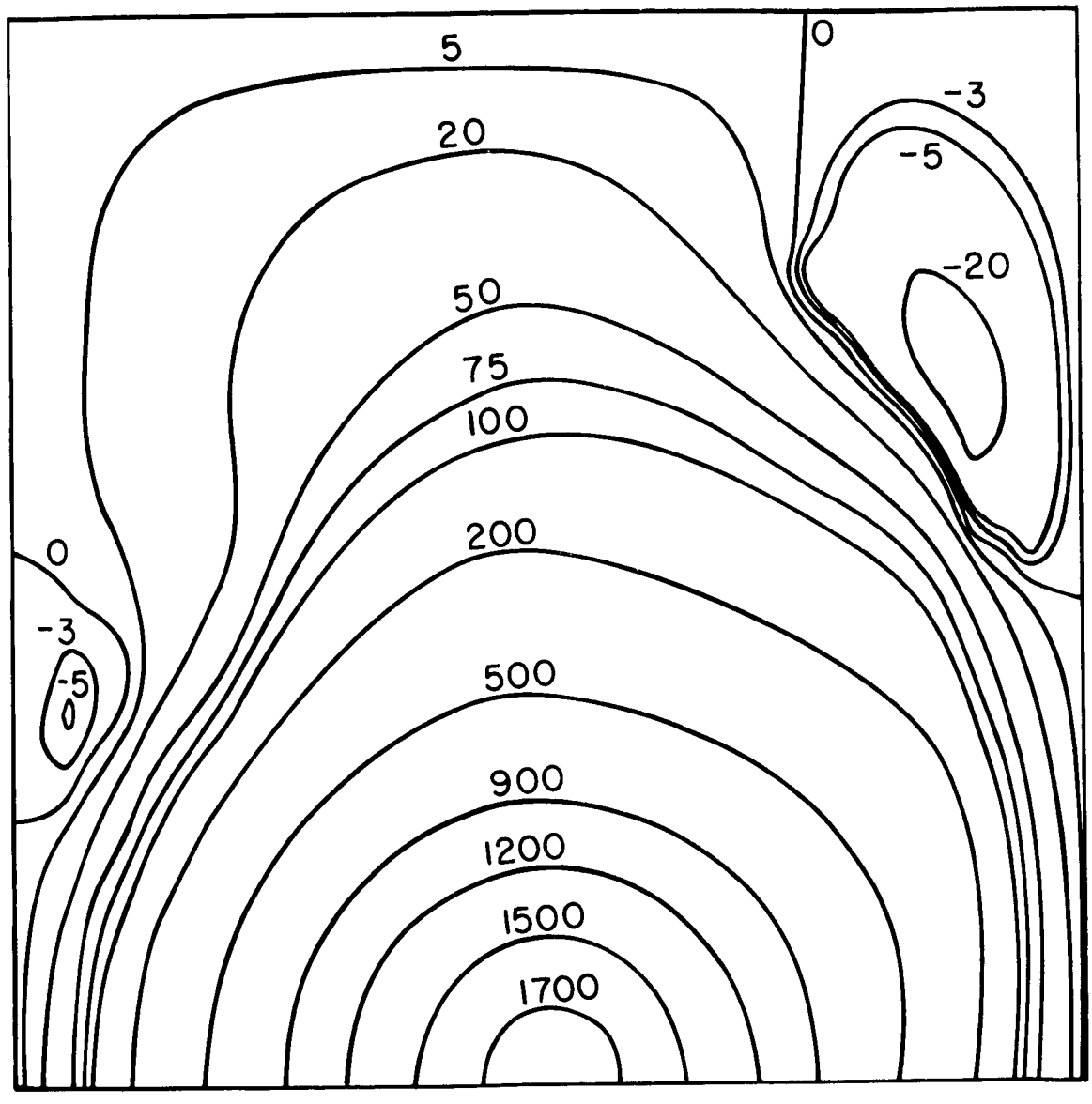

Fig. 10 Re-entrant viscous flow
Amplitude = 1000
Time = .022

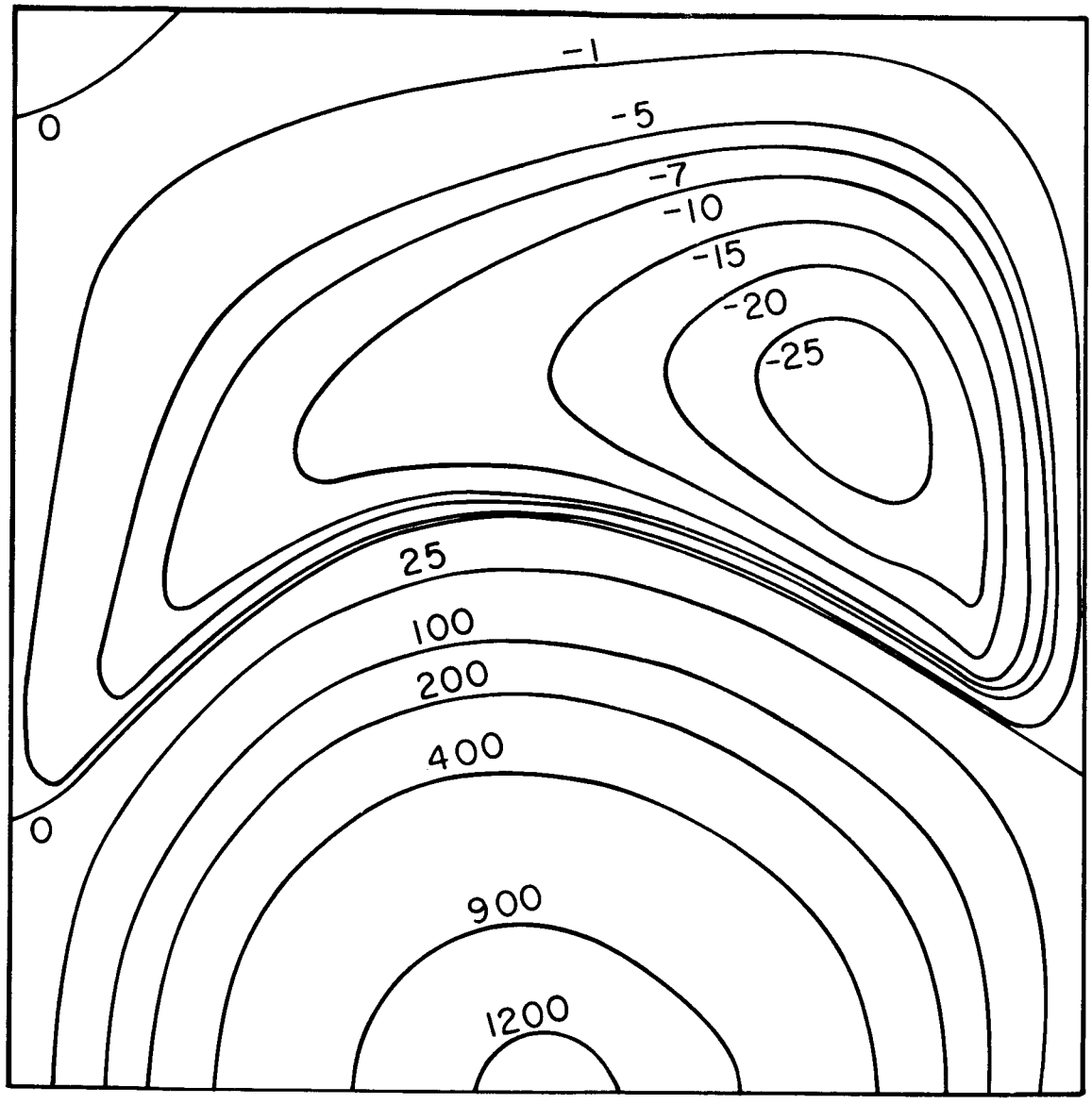

Fig. 11 Re-entrant viscous flow
Amplitude = 1000
Time = .01

TITLES AND AUTHORS OF RELEVANT REPORTS AND PAPERS

1. "High Reliability Elements for Missile or Space Vehicle Equipment", Final Report, March 31, 1963, Sperry Utah Company.

2. "On the Transient Motion of a Contained Rotating Fluid", January 1964, Sperry Rand Research Center SRRC-RR-64-7, H. P. Greenspan.

3. "A Boundary Layer Analysis of Spin-up Phenomenon", May 1963, Sperry Rand Research Center SRRC-RQ-63-24, H. P. Greenspan.

4. "A Computational Method for Time Dependent Two-Dimensional Incompressible Flow", February 1964, Sperry Rand Research Center SRRC-RR-64-17, C. E. Pearson.

APPENDIX II.

INITIAL COMPUTER RUN

OF

NUMERICAL SOLUTION OF TIME-DEPENDENT

INCOMPRESSIBLE TWO-DIMENSIONAL

NAVIER-STOKES EQUATIONS

FOR A VISCOUS JET.

SPERRY RAND RESEARCH CENTER

AUGUST - 1964

CONTRACT NAS 8-11236

FORTRAN PROGRAM - TABLE 1.1-1

STREAMLINE PLOTS- FIG. 1.1-6

```
BEGIN       END         NAME        ENTRY       COMMON

00144       00463       DATA        00151       41177
00464       00754       SQR         00472       41177
00755       02373       PEACE       00761       41177
02374       03016       BVC         02400       41177
03017       03041       (FPT)       03017       77461
03042       03231       COS         03045       77773
                        SIN         03046
03232       03420       (STH)       03244       77750
                        (STHM)      03252
                        (STHD)      03260
03421       03511       (WER)       03433       00000
                        (WTC)       03464
03512       05430       (IOH)       03514       77521
                        (FIL)       05244
                        (RTN)       05255
05431       06267       (EXEM)      05435       77750
06270       06310       EXIT        06271       00000
06311       06311       (TES)       06311       00000
06312       06440       (ICS)       06315       00000
                        (RDS)       06374
                        (WRS)       06375
                        (BSR)       06376
                        (WEF)       06377
                        (REW)       06400
                        (ETI)       06401
                        (RCH)       06402
                        (TEF)       06403
                        (TCO)       06404
                        (TRC)       06405
06441       06472       (IOU)       06446       00000
06473       07151       ERROR       06641       77466
                        YC0000      36502
                        EPMDE       07123
                        ERTRP       07132
07152       11114       *MAIN*      07167       41177

ENTRY POINTS TO SUBROUTINES REQUESTED FROM LIBRARY.
    SQRT        EXP         LOG         EXP(2
    11115       11204       EXP(2       11120       77775
    11205       11303       EXP         11210       77773
    11304       11403       LOG         11307       77774
    11404       11476       SQRT        11407       77773

    EXECUTION


 N =    11 DT =  1.0000000E-02 CO =  0.          COA =  0.8000000E+00 C =  0.1000000E+01

DAP =  0.1600000E-01 DAP2 =  0.1600000E-02 DAV2 =  0.4000000E-00 IIM2 =    100 NI =   50
K5 =      0 K6 =      0 K7 =      0 ALPHA= 0.2000000E+02 R= 0.1000000E+03 M= 21

 0.09999999E-00  0.17294537E+01  0.09999999E+01  0.62500000E-01  0.31250000E-01  0.25000000E-00

 0.50000000E+00  0.86472683E-02 -0.72945371E+00  0.43236343E-00  0.31415926E+01  0.98696040E+01
 0.09999999E-00
```

STEP COMPLETED FOR T= 1.0000E-02 17 ITERATIONS, 117 SWEEPS.

VORTICITY,E -1

J I= 1	2	3	4	5	6	7	8	9	10	11	12	13	14	15	16	17	18	19	20	21
1 0	-958	-754	-590	-479	-408	-363	-335	-319	-310	-308	-311	-320	-337	-366	-412	-486	-604	-782	-996	0
2 -253	-255	-211	-164	-132	-112	-99	-91	-86	-83	-82	-83	-85	-90	-97	-108	-125	-151	-185	-214	-282
3 1294	190	21	-22	-30	-29	-27	-25	-23	-22	-22	-22	-23	-23	-25	-27	-28	-25	7	171	1341
4 1312	291	77	14	-2	-6	-7	-7	-6	-6	-6	-6	-6	-6	-6	-6	-4	5	49	238	1416
5 430	167	46	11	1	-1	-2	-2	-2	-2	-1	-1	-1	-1	-1	-1	0	6	32	139	517
6 263	96	27	7	2	0	-0	-0	-0	-0	-0	-0	-0	-0	-0	0	1	5	21	87	316
7 177	59	17	5	2	1	1	1	1	1	1	1	1	1	1	1	2	4	15	56	205
8 116	36	11	5	3	3	4	4	4	4	4	4	4	4	4	4	4	5	11	36	130
9 64	22	10	9	10	12	14	15	16	16	17	17	16	16	15	13	11	10	10	22	70
10 25	15	19	29	38	46	52	57	60	62	63	62	60	58	53	47	39	30	20	15	26
11 0	25	64	107	144	174	197	214	225	231	233	231	225	213	197	174	144	108	66	26	0

STREAM FUNCTION,E -3

J I= 1	2	3	4	5	6	7	8	9	10	11	12	13	14	15	16	17	18	19	20	21
1 0	0	0	0	0	0	0	0	0	0	0	0	0	0	0	0	0	0	0	0	0
2 865	737	568	442	358	306	273	252	240	234	232	234	241	253	274	307	360	446	578	753	865
3 2596	2024	1515	1169	950	814	730	677	646	629	624	630	647	677	728	810	939	1148	1482	1995	2596
4 3462	2869	2257	1813	1519	1329	1208	1131	1084	1058	1051	1058	1083	1128	1202	1318	1496	1772	2195	2807	3462
5 3462	3151	2676	2278	1988	1789	1655	1567	1512	1482	1473	1482	1511	1563	1647	1775	1963	2237	2721	3100	3462
6 3462	3264	2925	2611	2366	2186	2059	1974	1919	1889	1879	1888	1917	1970	2052	2172	2344	2580	2887	3233	3462
7 3462	3327	3092	2863	2674	2529	2423	2350	2302	2275	2266	2274	2300	2346	2417	2519	2659	2843	3069	3311	3462
8 3462	3374	3220	3066	2935	2831	2753	2698	2662	2641	2634	2641	2661	2696	2750	2825	2926	3055	3207	3365	3462
9 3462	3412	3326	3238	3161	3100	3053	3020	2997	2985	2981	2985	2997	3019	3052	3097	3158	3233	3320	3409	3462
10 3462	3445	3413	3381	3353	3330	3312	3300	3292	3287	3285	3287	3292	3300	3312	3330	3352	3379	3411	3444	3462
11 3462	3462	3462	3462	3462	3462	3462	3462	3462	3462	3462	3462	3462	3462	3462	3462	3462	3462	3462	3462	3462

STEP COMPLETED FOR T= 0.2000E-01 19 ITERATIONS, 122 SWEEPS.

VORTICITY,E -1

J I=	1	2	3	4	5	6	7	8	9	10	11	12	13	14	15	16	17	18	19	20	21
1	0	-1745	-1248	-894	-653	-510	-429	-384	-360	-348	-346	-351	-364	-389	-432	-505	-630	-846	-1204	-1695	0
2	-517	-555	-536	-440	-352	-287	-244	-217	-202	-193	-190	-191	-196	-206	-223	-251	-292	-349	-415	-446	-373
3	1805	632	137	-44	-97	-104	-98	-90	-83	-79	-77	-77	-78	-80	-84	-90	-95	-90	-37	250	2620
4	1656	844	321	91	3	-25	-32	-32	-30	-29	-27	-27	-27	-27	-27	-27	-22	-2	86	470	2601
5	232	420	206	75	18	-3	-9	-10	-10	-9	-9	-8	-8	-8	-7	-6	-1	17	83	304	848
6	127	211	118	48	16	3	-1	-1	-1	-1	-1	-1	-0	-0	0	1	5	18	64	200	460
7	100	118	68	30	13	6	5	5	5	5	6	6	6	6	6	7	9	17	47	130	267
8	69	70	42	23	16	14	15	17	18	19	20	21	20	20	19	18	17	20	36	82	149
9	33	41	32	30	33	39	45	50	54	56	58	58	57	55	51	45	40	34	34	49	66
10	1	24	38	58	80	100	116	129	137	143	145	144	140	134	123	109	90	67	45	30	10
11	0	2	41	94	146	190	225	249	265	273	276	273	265	250	229	199	160	112	58	9	0

STREAM FUNCTION,E -3

J I=	1	2	3	4	5	6	7	8	9	10	11	12	13	14	15	16	17	18	19	20	21
1	0	0	0	0	0	0	0	0	0	0	0	0	0	0	0	0	0	0	0	0	0
2	1574	1369	1009	725	540	428	363	326	305	296	293	297	307	326	359	414	507	664	921	1286	1574
3	4722	4003	3013	2232	1709	1382	1186	1070	1004	971	960	968	997	1051	1143	1291	1533	1926	2563	3543	4722
4	6296	5643	4535	3570	2875	2415	2123	1944	1837	1781	1761	1773	1817	1900	2038	2255	2595	3125	3936	5099	6296
5	6296	6050	5272	4456	3800	3330	3012	2807	2681	2612	2587	2599	2651	2749	2907	3151	3514	4046	4785	5683	6296
6	6296	6149	5637	5033	4504	4097	3807	3611	3487	3417	3391	3404	3455	3552	3707	3937	4268	4724	5310	5943	6296
7	6296	6191	5856	5440	5053	4741	4508	4346	4241	4181	4158	4170	4215	4299	4430	4621	4886	5235	5659	6083	6296
8	6296	6228	6020	5756	5503	5292	5131	5015	4939	4896	4880	4889	4923	4986	5081	5218	5402	5638	5912	6174	6296
9	6296	6263	6156	6017	5881	5765	5676	5612	5569	5545	5536	5542	5563	5599	5654	5731	5833	5961	6106	6240	6296
10	6296	6290	6258	6215	6172	6135	6107	6086	6073	6066	6063	6066	6072	6084	6102	6126	6159	6199	6244	6284	6296
11	6296	6296	6296	6296	6296	6296	6296	6296	6296	6296	6296	6296	6296	6296	6296	6296	6296	6296	6296	6296	6296

STEP COMPLETED FOR T= 0.3000E-01 14 ITERATIONS, 49 SWEEPS.

VORTICITY,E -1

J	I= 1	2	3	4	5	6	7	8	9	10	11	12	13	14	15	16	17	18	19	20	21
1	0	-2372	-1733	-1206	-861	-654	-537	-472	-439	-424	-422	-430	-450	-484	-541	-636	-799	-1077	-1533	-2173	0
2	-734	-819	-808	-681	-539	-425	-348	-299	-270	-255	-248	-249	-255	-269	-292	-328	-382	-456	-542	-634	-327
3	2201	949	283	-37	-159	-188	-181	-165	-151	-141	-135	-132	-132	-135	-140	-147	-153	-147	-102	42	4072
4	1952	1200	621	242	48	-37	-66	-72	-70	-66	-62	-60	-58	-58	-57	-55	-48	-24	63	488	3936
5	108	531	423	224	86	15	-15	-25	-27	-25	-24	-22	-21	-20	-18	-15	-7	17	103	390	1346
6	34	236	238	148	69	24	4	-3	-5	-4	-3	-2	-1	-0	1	3	10	30	95	273	700
7	43	119	128	88	48	24	14	11	12	13	14	16	17	17	18	18	22	35	77	180	382
8	36	66	73	57	41	33	32	34	38	41	43	45	45	45	44	41	40	43	62	112	199
9	15	38	49	51	55	62	72	81	89	95	98	100	99	96	90	82	71	61	57	66	83
10	-1	19	39	63	91	119	144	164	178	187	191	190	186	177	163	144	118	88	59	36	16
11	0	0	27	81	147	210	261	299	323	336	339	335	324	305	278	242	193	134	68	14	0

STREAM FUNCTION,E -3

J	I= 1	2	3	4	5	6	7	8	9	10	11	12	13	14	15	16	17	18	19	20	21
1	0	0	0	0	0	0	0	0	0	0	0	0	0	0	0	0	0	0	0	0	0
2	2154	1892	1415	1012	738	568	468	411	380	366	363	369	383	410	454	527	648	852	1182	1658	2154
3	6463	5637	4370	3257	2449	1917	1588	1394	1285	1231	1214	1226	1266	1340	1463	1661	1979	2489	3303	4564	6463
4	8617	7925	6606	5272	4200	3438	2935	2622	2438	2341	2306	2319	2378	2491	2677	2969	3421	4117	5180	6751	8617
5	8617	8437	7617	6541	5547	4772	4224	3864	3643	3521	3473	3484	3553	3685	3900	4228	4716	5428	6424	7666	8617
6	8617	8528	8037	7281	6503	5847	5356	5018	4801	4678	4628	4638	4706	4836	5045	5356	5803	6419	7216	8090	8617
7	8617	8550	8244	7746	7199	6712	6329	6055	5876	5772	5729	5739	5798	5910	6087	6343	6699	7170	7742	8316	8617
8	8617	8571	8388	8086	7741	7422	7165	6977	6852	6779	6750	6758	6803	6886	7013	7194	7438	7751	8113	8454	8617
9	8617	8596	8506	8353	8174	8006	7869	7767	7699	7661	7646	7653	7679	7727	7798	7898	8030	8195	8380	8546	8617
10	8617	8614	8590	8543	8488	8436	8393	8361	8341	8329	8326	8329	8337	8353	8375	8406	8447	8497	8553	8601	8617
11	8617	8617	8617	8617	8617	8617	8617	8617	8617	8617	8617	8617	8617	8617	8617	8617	8617	8617	8617	8617	8617

STEP COMPLETED FOR T= 0.4000E-01 10 ITERATIONS, 44 SWEEPS.

VORTICITY,E -1

J	I= 1	2	3	4	5	6	7	8	9	10	11	12	13	14	15	16	17	18	19	20	21
1	0	-2902	-2134	-1484	-1047	-778	-619	-529	-481	-460	-457	-467	-493	-535	-596	-721	-933	-1254	-1744	-2444	
2	-934	-1046	-1060	-914	-731	-575	-462	-388	-343	-317	-306	-304	-311	-328	-355	-398	-459	-541	-637	-849	-1201
3	2466	1222	418	-12	-199	-257	-256	-237	-215	-197	-185	-179	-177	-179	-183	-190	-194	-186	-138	-358	5675
4	2127	1489	890	424	135	-17	-86	-109	-112	-107	-100	-95	-91	-88	-85	-80	-70	-46	26	386	5354
5	-69	607	606	408	209	74	0	-34	-46	-47	-45	-41	-38	-34	-30	-25	-15	11	97	450	1901
6	-121	246	336	278	172	84	29	2	-8	-10	-9	-6	-3	-0	3	7	15	37	109	342	950
7	-67	110	174	164	116	68	38	23	19	20	22	25	28	30	32	34	38	52	99	230	489
8	-35	55	93	97	80	62	52	51	54	59	63	67	70	70	70	67	64	66	85	144	237
9	-23	29	55	68	75	81	90	101	113	122	129	133	133	130	123	113	99	84	76	83	89
10	-13	12	33	59	92	126	160	188	209	224	231	232	228	217	200	177	146	109	73	44	13
11	0	-11	-6	35	104	182	253	308	345	365	372	368	355	333	301	260	206	140	68	11	0

STREAM FUNCTION,E -2

J	I= 1	2	3	4	5	6	7	8	9	10	11	12	13	14	15	16	17	18	19	20	21
1	0	0	0	0	0	0	0	0	0	0	0	0	0	0	0	0	0	0	0	0	0
2	263	233	176	127	92	69	56	47	43	41	40	41	43	46	51	60	74	98	135	187	263
3	789	702	557	422	318	245	198	169	152	143	140	142	147	156	171	194	231	290	382	520	789
4	1052	985	849	689	552	447	373	325	296	280	274	274	281	295	318	353	406	487	609	788	1052
5	1052	1045	969	851	727	621	541	485	449	429	420	420	427	443	469	509	566	650	769	922	1052
6	1052	1053	1015	937	843	755	683	630	596	575	566	565	573	589	614	651	704	777	873	982	1052
7	1052	1053	1032	984	920	855	809	758	730	712	704	704	711	724	746	776	819	875	943	1014	1052
8	1052	1052	1041	1013	974	933	896	868	848	836	831	831	836	846	861	883	912	949	991	1032	1052
9	1052	1052	1047	1034	1015	993	974	959	948	942	940	940	943	949	957	969	984	1003	1025	1044	1052
10	1052	1052	1051	1048	1042	1035	1029	1025	1022	1020	1019	1019	1020	1022	1025	1029	1033	1039	1045	1050	1052
11	1052	1052	1052	1052	1052	1052	1052	1052	1052	1052	1052	1052	1052	1052	1052	1052	1052	1052	1052	1052	1052

STEP COMPLETED FOR T= 0.5000E-01 10 ITERATIONS, 35 SWEEPS.

VORTICITY,E -1

J I=	1	2	3	4	5	6	7	8	9	10	11	12	13	14	15	16	17	18	19	20	21
1	0	-3344	-2472	-1721	-1211	-893	-701	-587	-523	-493	-486	-498	-527	-577	-657	-786	-996	-1339	-1864	-2520	0
2	-1101	-1237	-1276	-1128	-915	-720	-573	-473	-408	-370	-351	-346	-352	-370	-400	-446	-512	-598	-688	-1097	232
3	2664	1441	548	19	-231	-319	-328	-307	-279	-254	-236	-224	-218	-218	-221	-225	-228	-220	-132	-916	7343
4	2259	1695	1122	692	240	26	-85	-134	-148	-147	-139	-130	-122	-116	-110	-102	-89	-63	2	181	6766
5	-217	629	746	582	356	171	48	-21	-54	-66	-66	-62	-56	-49	-42	-33	-20	5	85	472	2464
6	-252	224	407	401	300	183	90	31	-0	-13	-15	-12	-7	-1	5	12	21	43	118	391	1200
7	-166	83	208	238	203	143	88	51	33	26	27	32	37	42	46	50	54	67	117	269	594
8	-99	32	106	135	130	108	86	72	69	72	78	84	89	92	93	91	87	87	105	169	275
9	-55	12	56	81	94	100	107	117	129	141	151	158	161	159	153	141	124	105	93	97	97
10	-22	1	20	44	77	116	156	192	222	244	256	261	257	246	227	201	166	125	83	49	13
11	0	-20	-38	-19	40	125	215	292	348	382	396	395	380	356	321	275	217	147	70	9	0

STREAM FUNCTION,E -2

J I=	1	2	3	4	5	6	7	8	9	10	11	12	13	14	15	16	17	18	19	20	21
1	0	0	0	0	0	0	0	0	0	0	0	0	0	0	0	0	0	0	0	0	0
2	302	269	236	150	109	82	65	54	48	45	44	45	47	50	57	66	82	107	146	195	302
3	905	817	661	509	387	298	238	198	175	162	156	157	162	173	190	216	257	320	417	553	905
4	1207	1144	1002	834	678	550	455	389	346	322	310	309	316	332	357	396	455	543	676	879	1207
5	1207	1210	1146	1028	892	764	662	582	530	498	482	478	486	504	533	577	642	734	866	1042	1207
6	1207	1218	1194	1124	1025	921	828	755	703	671	654	650	657	674	703	745	804	886	994	1121	1207
7	1207	1216	1208	1168	1104	1029	959	903	858	830	816	813	819	834	858	892	940	1002	1080	1162	1207
8	1207	1213	1211	1190	1152	1106	1059	1020	991	972	962	960	965	976	993	1017	1049	1090	1138	1185	1207
9	1207	1211	1211	1202	1184	1160	1136	1115	1099	1089	1084	1084	1087	1093	1103	1116	1133	1154	1177	1199	1207
10	1207	1209	1213	1208	1202	1195	1188	1181	1176	1173	1172	1172	1173	1175	1178	1182	1187	1193	1200	1206	1207
11	1207	1207	1207	1207	1207	1207	1207	1207	1207	1207	1207	1207	1207	1207	1207	1207	1207	1207	1207	1207	1207

STEP COMPLETED FOR T= 0.6000E-01 9 ITERATIONS, 32 SWEEPS.

VORTICITY,E -1

J I=	1	2	3	4	5	6	7	8	9	10	11	12	13	14	15	16	17	18	19	20	21
1	0	-3715	-2765	-1932	-1361	-1003	-782	-647	-567	-525	-512	-521	-552	-608	-697	-837	-1060	-1411	-1930	-2459	0
2	-1246	-1395	-1459	-1315	-1083	-860	-684	-558	-475	-423	-395	-384	-388	-405	-437	-485	-553	-642	-708	-1373	682
3	2811	1619	668	58	-252	-373	-394	-373	-339	-308	-284	-266	-256	-252	-252	-254	-254	-249	-79	-1570	9017
4	2369	1851	1311	768	349	80	-71	-146	-175	-181	-175	-165	-154	-144	-133	-121	-104	-78	1	-101	8153
5	-323	630	839	727	498	280	119	15	-45	-74	-83	-82	-75	-66	-54	-41	-24	1	72	464	3037
6	-351	196	447	500	423	298	178	87	29	-3	-17	-18	-13	-5	5	15	28	49	121	427	1455
7	-249	53	226	299	290	234	164	104	64	42	35	36	42	49	57	63	69	82	131	303	700
8	-158	8	113	167	180	164	135	108	92	87	89	96	103	109	112	112	108	105	122	192	312
9	-87	-4	52	88	110	120	125	131	141	153	165	175	181	181	176	164	145	124	108	109	106
10	-30	-11	3	24	55	95	139	183	221	251	271	280	279	269	250	221	183	138	92	54	12
11	0	-27	-69	-77	-37	44	145	245	325	379	407	413	400	375	337	287	226	152	71	8	0

STREAM FUNCTION,E -2

J I=	1	2	3	4	5	6	7	8	9	10	11	12	13	14	15	16	17	18	19	20	21
1	0	0	0	0	0	0	0	0	0	0	0	0	0	0	0	0	0	0	0	0	0
2	334	300	232	170	124	94	74	61	53	49	47	47	49	54	60	71	87	113	152	194	334
3	1001	912	750	586	451	349	277	228	198	179	171	169	174	186	204	233	276	342	442	564	1001
4	1335	1275	1136	963	793	648	535	453	397	362	344	339	344	361	388	431	494	587	726	935	1335
5	1335	1346	1294	1183	1041	900	778	681	610	564	539	530	535	553	584	632	702	801	941	1134	1335
6	1335	1353	1345	1286	1190	1078	970	878	809	761	734	723	727	744	775	820	885	973	1090	1231	1335
7	1335	1350	1355	1328	1269	1192	1110	1037	979	939	915	906	909	924	949	987	1038	1106	1191	1282	1335
8	1335	1345	1353	1342	1310	1262	1209	1160	1120	1091	1075	1068	1071	1082	1101	1127	1162	1206	1258	1310	1335
9	1335	1341	1347	1344	1329	1306	1278	1251	1230	1214	1206	1203	1205	1211	1222	1236	1254	1277	1302	1325	1335
10	1335	1337	1340	1340	1336	1329	1320	1312	1305	1301	1298	1298	1298	1301	1304	1308	1313	1320	1327	1333	1335
11	1335	1335	1335	1335	1335	1335	1335	1335	1335	1335	1335	1335	1335	1335	1335	1335	1335	1335	1335	1335	1335

STEP COMPLETED FOR T= 0.7000E-01 8 ITERATIONS, 38 SWEEPS.

VORTICITY,E 0

J I= 1	2	3	4	5	6	7	8	9	10	11	12	13	14	15	16	17	18	19	20	21
1 0	-402	-302	-212	-150	-110	-86	-70	-61	-56	-53	-54	-57	-63	-72	-87	-110	-145	-195	-230	0
2 -137	-152	-161	-148	-123	-99	-79	-64	-54	-47	-44	-42	-42	-43	-47	-51	-58	-67	-71	-166	118
3 292	176	78	10	-26	-42	-45	-43	-40	-36	-33	-31	-29	-28	-28	-28	-28	-28	1	-227	1065
4 246	197	146	92	46	14	-5	-15	-19	-21	-21	-20	-18	-17	-16	-14	-12	-9	2	-44	951
5 -40	62	90	84	63	39	20	6	-2	-7	-9	-10	-9	-8	-7	-5	-3	-0	6	43	362
6 -43	17	46	57	53	41	27	16	8	2	-1	-2	-2	-1	0	2	3	6	12	45	171
7 -31	2	23	34	36	32	25	18	11	7	5	4	5	5	6	7	8	9	14	33	80
8 -21	-1	11	19	22	22	19	16	13	11	10	11	11	12	13	13	13	12	14	21	35
9 -11	-2	4	9	12	14	15	15	15	16	17	19	19	20	19	18	16	14	12	12	11
10 -3	-2	-1	0	3	7	11	16	21	25	27	29	29	29	27	24	20	15	10	6	1
11 0	-3	-9	-13	-11	-4	6	17	27	35	40	42	41	39	35	30	23	16	7	1	0

STREAM FUNCTION,E -2

J I= 1	2	3	4	5	6	7	8	9	10	11	12	13	14	15	16	17	18	19	20	21
1 0	0	0	0	0	0	0	0	0	0	0	0	0	0	0	0	0	0	0	0	0
2 360	325	254	188	138	104	82	67	58	52	50	49	51	56	63	74	91	117	155	186	360
3 1079	991	825	654	508	396	314	258	220	197	184	181	184	195	215	245	290	357	459	560	1079
4 1439	1382	1247	1073	896	739	612	516	448	402	376	366	368	384	412	457	523	619	763	969	1439
5 1439	1456	1416	1313	1173	1025	889	776	691	631	594	577	577	593	625	675	748	852	999	1203	1439
6 1439	1464	1468	1422	1333	1220	1103	997	912	850	809	790	788	803	833	881	949	1042	1166	1319	1439
7 1439	1459	1476	1462	1412	1337	1250	1166	1095	1041	1006	988	986	999	1024	1064	1118	1190	1280	1379	1439
8 1439	1453	1470	1469	1444	1400	1345	1288	1238	1200	1175	1162	1161	1170	1189	1216	1253	1300	1356	1411	1439
9 1439	1447	1458	1461	1452	1430	1402	1371	1344	1323	1310	1303	1303	1309	1319	1334	1354	1377	1404	1429	1439
10 1439	1442	1446	1448	1446	1440	1431	1422	1413	1407	1403	1401	1401	1403	1406	1411	1417	1423	1431	1437	1439
11 1439	1439	1439	1439	1439	1439	1439	1439	1439	1439	1439	1439	1439	1439	1439	1439	1439	1439	1439	1439	1439

STEP COMPLETED FOR T= 0.8000E-01 7 ITERATIONS, 37 SWEEPS.

VORTICITY,E 0

J I= 1	2	3	4	5	6	7	8	9	10	11	12	13	14	15	16	17	18	19	20	21
1 0	-428	-323	-228	-162	-119	-92	-75	-65	-59	-56	-56	-58	-64	-73	-88	-112	-146	-194	-208	0
2 -147	-163	-174	-161	-137	-111	-89	-72	-60	-53	-48	-45	-45	-46	-49	-54	-61	-70	-69	-195	171
3 301	188	87	15	-26	-45	-50	-49	-45	-41	-37	-35	-33	-31	-31	-31	-30	-31	12	-298	1222
4 253	206	158	104	56	20	-2	-15	-21	-23	-23	-22	-21	-20	-18	-16	-14	-11	7	-82	1082
5 -46	61	93	92	73	49	28	12	1	-5	-9	-10	-11	-10	-8	-6	-4	-1	5	38	419
6 -48	14	47	61	60	50	37	24	14	6	2	-1	-2	-1	-0	1	3	6	12	47	196
7 -36	-0	23	37	42	40	33	25	18	12	8	6	5	6	7	8	9	10	15	36	91
8 -24	-3	11	21	26	27	25	21	17	14	13	12	12	13	14	14	14	14	15	23	38
9 -13	-3	4	9	13	15	17	17	17	17	18	19	20	21	21	20	18	15	13	13	12
10 -4	-3	-3	-2	0	4	9	14	19	23	27	29	30	30	28	25	21	16	11	6	1
11 0	-3	-11	-17	-17	-13	-3	9	21	31	37	41	42	40	36	31	24	16	7	1	0

STREAM FUNCTION,E -2

J I= 1	2	3	4	5	6	7	8	9	10	11	12	13	14	15	16	17	18	19	20	21
1 0	0	0	0	0	0	0	0	0	0	0	0	0	0	0	0	0	0	0	0	0
2 381	346	272	203	151	114	90	73	63	56	53	52	53	57	65	76	93	119	156	173	381
3 1143	1056	888	712	558	438	349	285	242	214	198	191	193	203	223	253	299	367	470	544	1143
4 1524	1470	1339	1167	986	820	683	575	496	442	408	392	390	403	431	476	544	642	789	987	1524
5 1524	1546	1515	1422	1285	1134	990	866	767	695	647	621	615	628	658	709	784	891	1043	1255	1524
6 1524	1554	1568	1534	1454	1343	1222	1108	1010	935	882	852	843	853	882	930	1000	1096	1226	1389	1524
7 1524	1549	1575	1572	1532	1462	1375	1285	1204	1138	1091	1064	1055	1063	1086	1126	1182	1257	1351	1457	1524
8 1524	1541	1565	1573	1557	1518	1463	1403	1346	1299	1265	1245	1239	1245	1262	1289	1328	1376	1435	1494	1524
9 1524	1534	1549	1557	1553	1535	1508	1476	1445	1419	1400	1389	1386	1390	1399	1414	1434	1459	1488	1514	1524
10 1524	1527	1533	1537	1537	1532	1524	1514	1504	1496	1490	1487	1486	1488	1491	1495	1501	1508	1516	1523	1524
11 1524	1524	1524	1524	1524	1524	1524	1524	1524	1524	1524	1524	1524	1524	1524	1524	1524	1524	1524	1524	1524

STEP COMPLETED FOR T= 0.9000E-01 7 ITERATIONS, 37 SWEEPS.

VORTICITY,E 0

J I= 1	2	3	4	5	6	7	8	9	10	11	12	13	14	15	16	17	18	19	20	21
1 0	-449	-341	-243	-173	-127	-99	-80	-68	-61	-58	-57	-59	-65	-74	-89	-112	-146	-191	-184	0
2 -156	-172	-184	-173	-148	-121	-97	-79	-66	-57	-52	-48	-47	-48	-51	-56	-62	-72	-66	-222	222
3 309	198	95	20	-25	-47	-55	-54	-50	-46	-41	-38	-36	-34	-33	-33	-32	-35	24	-367	1368
4 260	214	168	115	65	27	1	-14	-21	-25	-25	-25	-23	-22	-20	-18	-15	-13	12	-123	1207
5 -50	60	96	98	82	58	35	17	5	-3	-8	-10	-11	-11	-9	-7	-5	-1	5	31	475
6 -51	12	46	64	66	58	45	31	20	11	5	1	-1	-1	-0	1	3	6	12	47	222
7 -39	-2	23	38	46	46	40	32	24	17	12	9	7	7	7	8	10	11	16	38	101
8 -26	-5	11	21	28	31	30	26	22	18	16	14	13	14	14	15	15	15	16	24	42
9 -14	-4	3	9	13	16	18	19	19	19	19	20	21	21	21	21	19	16	14	14	13
10 -4	-4	-4	-4	-2	1	6	11	16	21	25	28	30	30	29	26	22	17	11	7	1
11 0	-4	-12	-19	-22	-19	-11	0	13	25	33	39	41	40	37	32	25	17	8	1	0

STREAM FUNCTION,E -2

J I= 1	2	3	4	5	6	7	8	9	10	11	12	13	14	15	16	17	18	19	20	21
1 0	0	0	0	0	0	0	0	0	0	0	0	0	0	0	0	0	0	0	0	0
2 399	363	288	216	161	123	97	79	67	59	55	54	55	59	66	77	94	119	155	158	399
3 1196	1109	941	761	602	475	380	311	262	230	211	202	202	210	229	259	305	372	476	522	1196
4 1594	1541	1415	1244	1062	891	746	629	542	479	439	417	411	421	447	491	559	658	806	992	1594
5 1594	1620	1596	1510	1380	1228	1079	947	838	756	699	664	652	659	687	736	812	920	1075	1292	1594
6 1594	1627	1649	1625	1554	1448	1326	1206	1100	1014	951	912	894	898	923	970	1040	1139	1273	1443	1594
7 1594	1621	1655	1661	1639	1587	1482	1393	1302	1228	1171	1134	1117	1119	1139	1177	1234	1311	1409	1521	1594
8 1594	1613	1643	1658	1649	1616	1564	1504	1443	1389	1348	1320	1307	1309	1323	1350	1388	1438	1499	1561	1594
9 1594	1605	1623	1636	1636	1622	1597	1565	1532	1502	1479	1464	1457	1458	1466	1481	1501	1526	1555	1583	1594
10 1594	1597	1604	1609	1610	1607	1600	1590	1580	1570	1563	1559	1557	1557	1560	1564	1570	1577	1586	1593	1594
11 1594	1594	1594	1594	1594	1594	1594	1594	1594	1594	1594	1594	1594	1594	1594	1594	1594	1594	1594	1594	1594

APPENDIX III

ON THE USEFULNESS OF THE ANALOGY BETWEEN ACOUSTICAL AND ELECTRIC CIRCUITS

Prepared by
H. L. Fox and F. R. Goldschmied
Sperry Utah Company
Division of Sperry Rand Corporation
Salt Lake City, Utah

TABLE OF CONTENTS

SUMMARY:

The mathematical difficulties of fluid flow phenomena has encouraged the search for and the use of analogies from other branches of physical science. This technical memorandum examines an electrical analog with the goal of determining the degree of usefulness of the analog to the fluid logic device designer.

In certain acoustical circuits an analogy exists between acoustic mass and electrical inductance, and between acoustic compliance and electrical capacitance. It is shown in this memorandum that this analog IS VALUABLE ONLY FOR LIMITED CONDITIONS OF FLUID FLOW. The mean flow of fluid through the circuit is assumed to be negligible. Thus, with this assumption, the analog becomes immediately of very limited value to the fluid logic device designer. It is shown that the analogy is useful for the case of "acoustic" flow; where the longitudinal pressure waves are of primary concern and the mean fluid flow is relatively small.

The derivation of the analogous wave equations are presented. The mathematical and experimental applications are pointed out. Further, the assumptions and restrictions have been shown, so that the user will be aware of the limitation of the analog. Experimental results are cited to illustrate the degree of accuracy which can be expected.

Because in the use of fluid logic devices we are, at present, concerned more with fluid flow than with "acoustic" circuits, the analogy discussed is of limited value. Until better analogies are developed, the fluid logic device designer will find his best tools lie not in the analogies but rather in the body of knowledge of mathematical and experimental fluid mechanics.

DEFINITION OF SYMBOLS USED:

A area, square inch

C, C_e electrical capacitance, farads (in transmission theory often capacitance per unit length)

C_a acoustic compliance or the inverse of stiffness. Compliance for the small length Δx is defined as:

$$C_a = \frac{A \Delta x}{P_o}$$, or as,

$$C_a = \frac{\Delta V}{P_o}$$ for a small volume
Units are in inch^5/pound.

See Reference 3.

c_a speed of sound, feet/sec.

c_e speed of electromagnetic wave propagation ft./sec.

c_p specific heat of the gas at constant pressure.

c_v specific heat of the gas at constant volume.

e instantaneous value of voltage, volts.

f frequency in cycles per sec.

f_{10} lowest frequency of a particular transverse mode of vibration, cps.

G electrical conductance in mhos

i instantaneous value of current, amperes.

L, L_e electrical inductance, henries (in transmission theory, often inductance per unit length.)

M_a acoustic mass (Inertance) for a small length Δx is defined as:

$$M_a = \frac{\rho \Delta x}{A}$$ the units are pound sec.^{2}/inch^5

The value $\frac{\rho}{A}$ is also called the specific inertance. The total inertance for a pipe would be $\frac{\rho}{A} L$

Reference 3 gives the definition of acoustic mass (inertance) as the quantity which when multiplied by 2π times the frequency, gives the

acoustic reactance associated with the kinetic energy of the medium (units gm/cm^4 or kg/m^4).

p	instantaneous pressure, lb. force/in.^{2}
P_o	average of mean pressure, lb. force/in.^{2}
q	volumetric flow = $\int_A u \ell A$, in.^{3}/sec.
R	electrical resistance, ohms
u	instantaneous particle velocity in the x - direction, in./sec.
V	volume, in.^{3}
v	instantaneous particle velocity in the y - direction, in./sec.
w	instantaneous particle velocity in the z - direction, in/sec.
X	body forces acting in the x-direction on a particle of fluid.
Z_a	acoustic impedance defined as p/q
Z_e	electric impedance, e/i, ohms
Z_{oe}	characteristic electrical impedance, $\sqrt{L_e/C_e}$, ohms.
γ	adiabatic exponent, = c_p/c_v, (approx. 1.4 for air at normal temp. and pressure).
μ	absolute viscosity, centipoises.
ρ	gas mass density, lb. sec.^{2}/in.^{4}
τ	volume change, in.^{3}
ω, ω_e	electrical circular frequency, rad./sec.
ω_a	acoustic circular frequency, rad./sec.

DISCUSSION OF THE ANALOGY:

Under certain conditions of fluid flow which we shall point out, an analog of electrical capacitance and electrical inductance can be usefully employed. These conditions involve "acoustic circuits" which are defined as fluid flow circuits which are primarily concerned with only the fluctuating flow. In analogous electrical terminology, only the a.c. (alternating current) is considered. The mean or average flow (the direct current) is ignored in its contribution to any effect on the fluctuating (or a.c.) flow.

References 1 and 2 employ such an analogy to aid in the design of mufflers. The analogous terms used are:

Electrical Terms

L_e	Inductance
C_e	Capacitance
e	instantaneous voltage
i	instantaneous current

Analogous Fluid Dynamics Terms

M_a	Acoustic Mass
C_a	Acoustic Compliance
p	instantaneous pressure
q	volume velocity or volumetric flow

Within the limitations of the accuracy of the analogy, the electrical terms can be replaced with the corresponding fluid terms and any of the solutions for the analogous electrical equations are also solutions for the acoustic case.

DEVELOPMENT OF ELECTRICAL EQUATIONS:

The mathematics which are useful in both systems (and indeed permit the analogy) are a special form of the one dimensional wave equations. In electrical transmission lines, the parameters of inductance and capacitance cannot be adequately treated as lumped parameters. Rather the inductance and capacitance must be considered as distributed parameters. This consideration gives rise to the partial differential equations known as the "telephone equations". These equations are:

$$(1) \quad \frac{\partial^2 e}{\partial x^2} = LC \frac{\partial^2 e}{\partial t^2} + (RC + GL) \frac{\partial e}{\partial t} + RGe$$

$$(2) \quad \frac{\partial^2 i}{\partial x^2} = LC \frac{\partial^2 i}{\partial t^2} + (RC + GL) \frac{\partial i}{\partial t} + RGi$$

where L and C are given in terms of unit length and not as lumped parameters.

For the special case in which the series R and the shunt G = 0, or where the terms involving e and $\frac{\partial e}{\partial t}$ or i and $\frac{\partial i}{\partial t}$ are small compared to the terms containing $\frac{\partial^2 e}{\partial t^2}$ and $\frac{\partial^2 i}{\partial t^2}$; the "telephone equations" (1) and (2) reduce to:

$$(3) \quad \frac{\partial^2 e}{\partial x^2} = LC \frac{\partial^2 e}{\partial t^2} \text{ and}$$

$$(4) \quad \frac{\partial^2 i}{\partial x^2} = LC \frac{\partial^2 i}{\partial t^2} .$$

In these one dimensional wave equations the quantity $\sqrt{\frac{1}{LC}}$ has the dimensions of velocity and is related to the velocity of electromagnetic propagation of a wave along the transmission line.

In reference 2, the one dimensional wave equations (3) and (4) are given in the form:

(5) $$\frac{\partial^2 e}{\partial t^2} = \frac{(\Delta x)^2}{L_e C_e} \frac{\partial^2 e}{\partial x^2}$$, and

(6) $$\frac{\partial^2 i}{\partial t^2} = \frac{(\Delta x)^2}{L_e C_e} \frac{\partial^2 i}{\partial x^2}$$.

The $(\Delta x)^2$ terms are used to indicate that the values for L_e and C_e are given per Δx lengths and not per unit lengths as is the case in equations (3) and (4). When Δx is a unit length then equations (3) and (5), and equations (4) and (6) are, of course, identical.

See references 4 & 5 for more detailed discussion of the wave equations.

The velocity of propagation then becomes:

(7) $$c_e^2 = \frac{(\Delta x)^2}{L_e C_e}$$ where the subscript e is used to refer to "electrical".

DEVELOPMENT OF FLUID EQUATIONS:

The analogous fluid equations can proceed from the equations of Navier-Stokes. The first step to simplify (or linearize) these equations will be to neglect any effects that occur in any but the x-direction. Thus, we may use but one of the three equations of Navier-Stokes:

(8)

$$\frac{\partial u}{\partial t} + \frac{u\,\partial u}{\partial x} + v\frac{\partial u}{\partial y} + w\frac{\partial u}{\partial z} = X - \frac{1}{\rho}\frac{\partial p}{\partial x} + \frac{\mu}{\rho}\left(\frac{\partial^2 u}{\partial x^2} + \frac{\partial^2 u}{\partial y^2} + \frac{\partial^2 u}{\partial z^2}\right)$$

By assuming nonviscous flow ($\mu = 0$), equation (8) becomes the Eulerian equation of motion for the x-direction:

(9) $$\frac{\partial u}{\partial t} \quad u\frac{\partial u}{\partial x} + v\frac{\partial u}{\partial y} + w\frac{\partial u}{\partial z} = X - \frac{1}{\rho}\frac{\partial p}{\partial x}$$

where X in both equations above represents the body force per unit volume.

If we assume that the effects of change in the velocity as a function of the y and z distances are negligible and that the quantity $u\frac{\partial u}{\partial x}$ is small compared to $\frac{\partial u}{\partial t}$, the (9) reduces to:

(10) $$\frac{\partial u}{\partial t} = X - \frac{1}{\rho}\frac{\partial p}{\partial x}$$

If we further assume that the body forces, X, (gravity or electromagnetic forces) are 0, then equation (10) simplifies to:

(11) $$\frac{\partial u}{\partial t} = -\frac{1}{\rho}\frac{\partial p}{\partial x}$$

We now take the adiabatic gas law:

(12) $$(P_0 + p)\ (V + \tau)^{\gamma} = P_0 V^{\gamma}$$

where γ is the adiabatic exponent and is $= c_p/c_v$, and where τ is the change in volume.

Equation (12) can be expressed as:

$$(13)\quad P_0 \left(1 + \frac{p}{P_0}\right) V^{\gamma} \left(1 + \frac{\tau}{V}\right)^{\gamma} = P_0 V^{\gamma}$$

by expanding and ignoring second order terms,

$$(14)\quad \left(1 + \frac{p}{P_0}\right) \left(1 + \gamma \frac{\tau}{V} \ldots\right) = 1$$

If we assume that p is very small compared to P_0 and that τ is very small compared to V (and, therefore, the products are negligible) then we can write:

$$(15)\quad \frac{p}{P_0} = -\frac{\gamma \tau}{V}$$

Taking the time differential equation (15) becomes,

$$(16)\quad \frac{1}{P_0} \frac{\partial p}{\partial t} = -\frac{\gamma}{V} \frac{\partial \tau}{\partial t}$$

Since the mass of the gas per unit volume is constant, we can express

$$\tau = \frac{\partial \xi}{\partial x} V \qquad (\xi = \text{particle displacement},$$

but, $u = \frac{\partial \xi}{\partial t}$ so,

$$(17)\quad \frac{\partial \tau}{\partial t} = V \frac{\partial u}{\partial x}$$

Substituting equation (16) into equation (17),

$$(18)\quad \frac{\partial u}{\partial x} = -\frac{1}{\gamma P_0} \frac{\partial p}{\partial t}$$

and, therefore,

$$(19)\quad \frac{\partial^2 u}{\partial x \partial t} = -\frac{1}{\gamma P_0} \frac{\partial^2 p}{\partial t^2}$$

Similarly, we can write from (11)

$$(20)\quad \frac{\partial^2 u}{\partial x \partial t} = -\frac{1}{\rho} \frac{\partial^2 p}{\partial x^2}$$

Combining equations (19) and (20) we have

$$(21)\quad \frac{\partial^2 p}{\partial t^2} = \frac{\gamma P_0}{\rho} \frac{\partial^2 p}{\partial x^2}$$ (compare with equation (5)).

This equation is directly analogous to the form of equation (5) or (6), and analogously, c_a, the speed of sound is

$$(22) \quad c_a = \sqrt{\frac{\gamma P_o}{\rho}}$$

Similarly, we can obtain

$$(23) \quad \frac{\partial^2 u}{\partial t^2} = c_a \frac{\partial^2 u}{\partial x^2} \quad \text{(compare with equation (6)),}$$

where (21) is the wave equation for the pressure wave and (23) is the wave equation for the particle velocity. In acoustics the symbol $q = uA$; where A is the area and q is thus defined as the volume velocity or the volumetric flow. Equation (23) holds for q as well as for u.

The similarity between equations (5) and (21), and between equations (6) and (23) permits us to proceed with the analogy in the solutions of the equations provided we realize that the accuracy of the results are limited by the assumptions made in each case.

THE USE OF SOLUTION OF THE WAVE EQUATIONS:

Reference 2. using unspecified boundary conditions, gives the solution of the electrical wave equations (5) and (6) in the form:[1]

(24) $E_i = E_r \cos k_e l + j I_r Z_{oe} \sin k_e l$

and

(25) $I_i = I_r \cos k_e l + j (E_r/Z_{oe}) \sin k_e l.$

where the subscript i refers to input or transmitter end and the subscript r refers to receiving or output end; and where I & E represent average (r.m.s.) values; and where

(26) $k_e = \omega_e/c_e$ or the "wave number"; and where

(27) $Z_{oe} = \sqrt{L_c/C_c}$ or the "characteristic electrical impedance".

Reference 2 describes the similarity between Z_e and Z_a (the electrical and acoustic impedance) by the formulas

(28) $Z_e = e/i$ electrical impedance.

(29) $Z_a = p/q$ acoustical impedance.

Inasmuch as the analogous forms of impedance are in agreement, the complete analogy between the two systems is useful. All that is necessary is to select suitable scale relations between the electrical and fluid parameters, then either system can be expressed or fabricated in terms of its analog.

[1] See Reference 4 for further details involving this same solution.

EXPERIMENTAL RESULTS:

Reference 2 reports on the comparison of actual tests performed by constructing a modified "electrical transmission line" analog of a combination of pipes and chambers. Rather than using a transmission line, several sets of capacitors and inductors were used for the analog of each pipe and chamber (See Fig. 2). This method is considerably better than the method of making an electrical analog of an acoustic system by using single lumped parameters of capacitance and inductance to represent a chamber or pipe.

Reference 1 discusses the effects of using the single lumped parameters method. (See pages 26ff). Here the analogous parameters are used in a single parameter sense in an analogous circuit. For example, all of the distributed acoustic mass in a pipe is treated as a single inductor and all the acoustic compliance in a chamber is treated as a single capacitor. (See Fig. 1) If proper correction of the lumped parameters are made for the "end effects" of the pipes and chambers, AND IF the wave length of the acoustic disturbance is very long with respect to the pipe length (say, 20) then the lumped parameter approximation can be used. The results of calculations made using lumped parameters in this manner, will give results which are generally accurate to within about 10% of the actual acoustic case.

The severe limitation of low frequency for which the lumped parameters circuit can be used as an accurate analog, can be partially overcome by using the distributed parameters method of the transmission line. The mathematics of solving the wave equations for the transmission line and of obtaining a complete description of the varying losses in

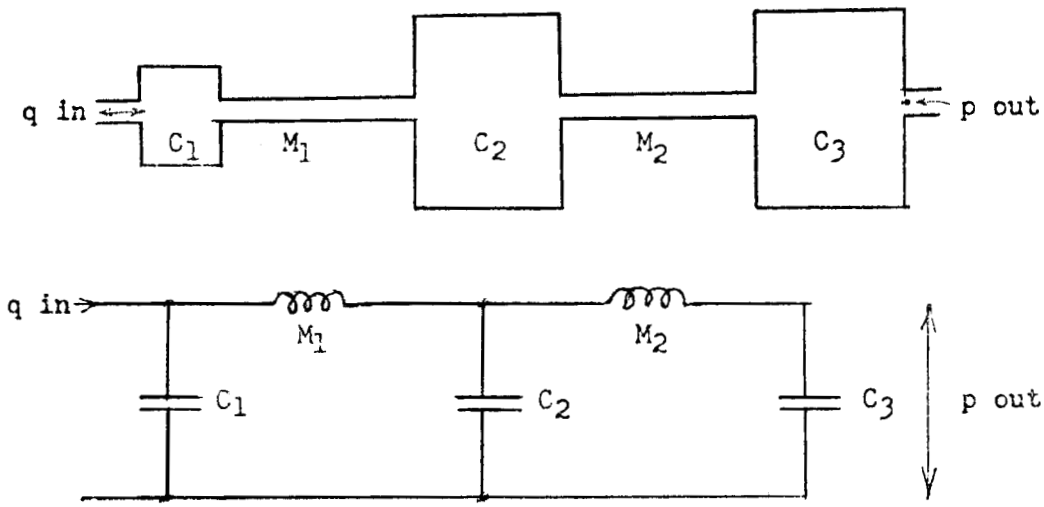

A LUMPED PARAMETERS ANALOG OF AN ACOUSTIC CIRCUIT

FIGURE 1.

such a circuit for a wide range of frequencies may be difficult. The alternative is to make a modified transmission line analog (See Fig. 2) using several inductors and capacitors for each pipe and chamber and then to make frequency vs loss measurements. This is essentially the method used in Reference 2.

In reference 2, it is described how each pipe and chamber is replaced by several inductors and capacitors so as to approach the distributed parameters analog. For example a 23 inch pipe is replaced by 6 inductors and a 6.04 inch diameter by 32.3 inch long volume is replaced by a network of 5 inductors and 6 capacitors. See Figure 2 which has been taken from Reference 2.

Such a circuit of inductors and capacitors can actually be constructed and used as a laboratory analog of the equivalent acoustic circuit.

The experimental results of tests comparing an acoustical circuit with the above electrical analog gave results which are shown in Figure 3. Figure 3 is taken from Reference 2.

Except for the differences in frequency and amplitudes of the "peaks", the analog values are generally within 10% of the measured acoustic values. The differences that do occur must be discussed. First, however, let us review the assumptions which were made to permit the analogy to be made.

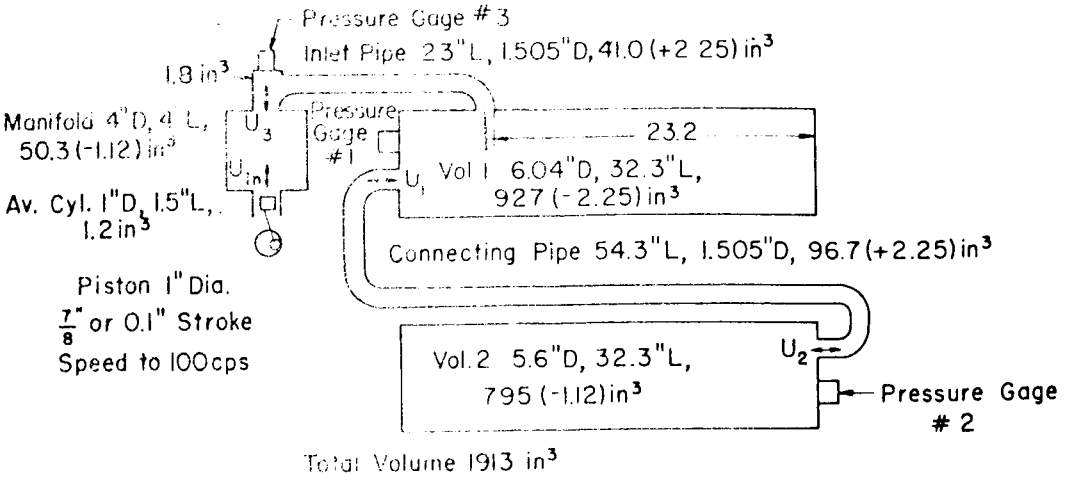

THE ACOUSTIC CIRCUIT

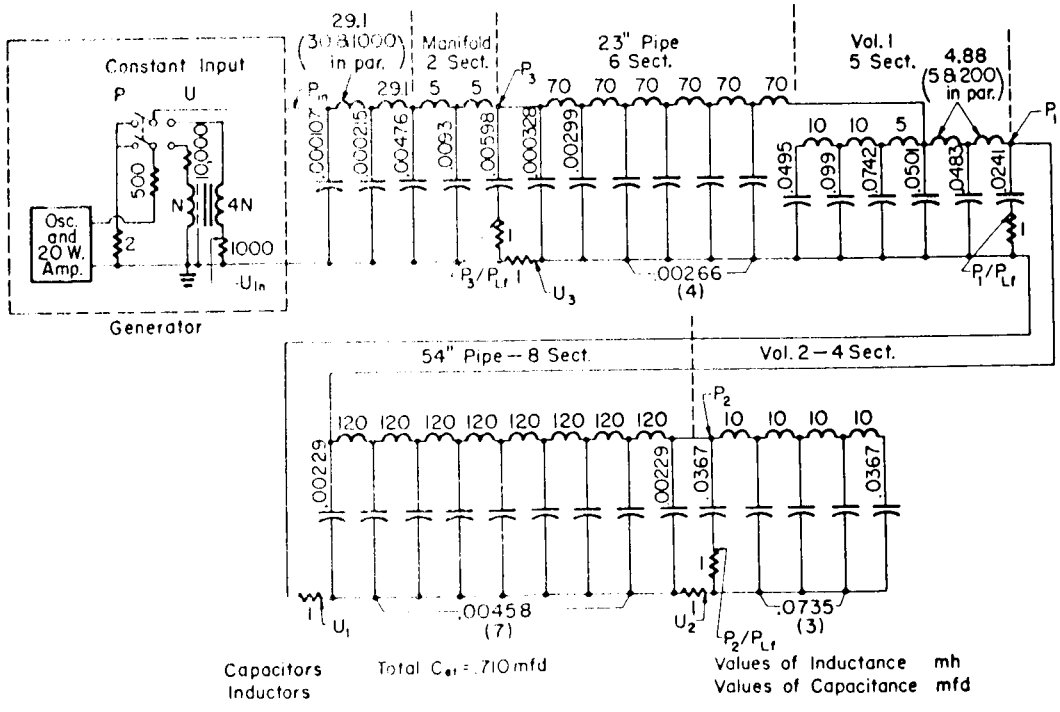

THE ELECTRICAL ANALOG

THE MODIFIED DISTRIBUTED PARAMETER ANALOG OF AN ACOUSTIC CIRCUIT

FIGURE 2

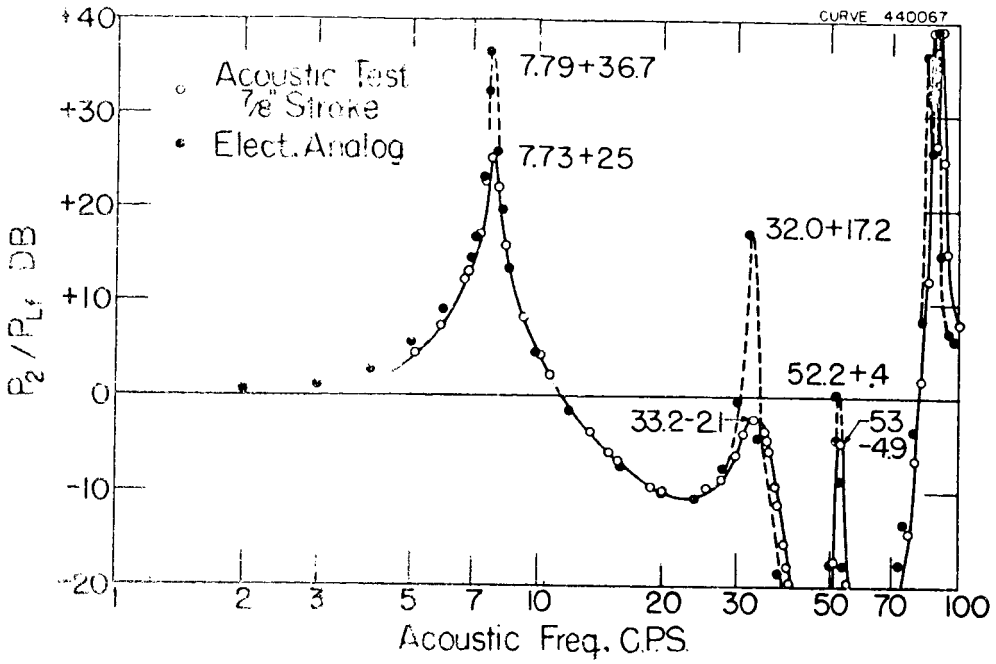

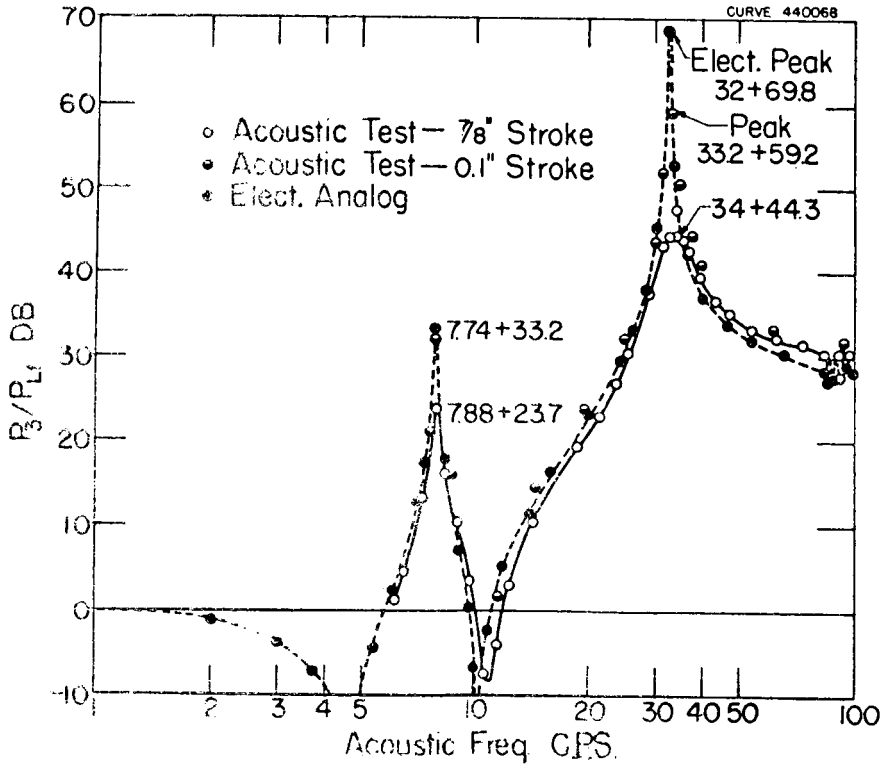

COMPARISON OF ELECTRICAL AND ACOUSTIC MEASUREMENTS

FIGURE 3

THE ASSUMPTIONS:

As mentioned in the first paragraph of page 4, the analog is based on certain conditions of fluid flow. Let us explicity list these conditions or assumptions which have been made:

1. All acoustic damping losses are zero. This also implies that walls of the pipes or chambers are non-elastic.
2. The pressure of the acoustic disturbance is small compared to the pressure of the fluid. Δ p should be less than 1/20 of P_0.
3. The change in volume of the fluid is small compared to the total volume. ΔV should be less than 1/20 V_0.
4. The fluid is deformable only in one direction (along the pipe.
5. The mean or average flow of the fluid is assumed to be zero.

Further assumptions are made with respect to the electrical equations:

1. The series resistance of the transmission line and the conductance to ground are equal to zero. Or,
2. The terms involving e and its first partial time derivative, and i and its first partial time derivative are small compared to the terms involving their second partials with respect to time.
3. The inductance and capacitance is distributed along the transmission line.

Keeping these assumptions at hand, let us again look at the accuracy.

EXPERIMENTAL ACCURACY:

Reference 2 gives us some idea as to the adequacy of the analogy for frequencies where only longitudinal vibrations are present. In particular, the curves reproduced in Figure 3 show that an error of 800% is made in value of peak power. Frequency wise maximum errors of less than 10% occur. Overall, the agreement of the two curves are good (within about 10%).

Part of the difficulty in obtaining more nearly perfect experimental results is the problem of the "Q" of the circuits in both cases. This problem is related to the resistance losses in both cases and the inability of the analog in its simpliest form of handling the "losses". The problem of fluid resistance versus electrical resistance is complex and beyond the scope of this memorandum. Suffice to say, that only in very specialized cases is the resistance in a fluid circuit a linear function of the flow. (There is not a dependable Ohm's law expression for fluids similar to E = IR.

Further inaccuracies are soon apparent with higher frequencies. The frequency limitation of this modified distributed parameter technique (and also of a pure distributed parament case) occurs at those frequencies for which the acoustic wave length is of the same order of magnitude as the pipe diameter. This defines the frequency of the first transverse vibration, f_{10} as expressed by:

(30) $f_{10} = 0.586\ c/D$ where f_{10} is the frequency of the lowest transverse wave, c is the speed of sound, and D is the diameter of the pipe. For a one inch pipe at standard atmospheric pressure $f_{10} \cong 8{,}500$ cps and for a 1/8 inch pipe $f_{10} \cong 68{,}000$ cps.

At frequencies near f_{10} and for larger values of f, various modes of vibration occur with a corresponding large change in the transmission characteristics of the pipe. Therefore, the electrical analog ceases to be useful above f_{10}.

Three transverse modes of vibration are shown in Figure 4. The modes and their harmonics begin to become numerous as f becomes larger than f_{10}.

There is some similarity between modes of vibration of acoustic waves in a pipe and the modes of transmission of electromagnetic fields in wave guides. However, a discussion of the adequacy of such a possible extended analog has not been made a part of this technical memorandum.

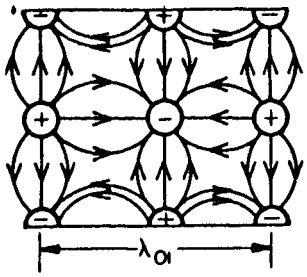

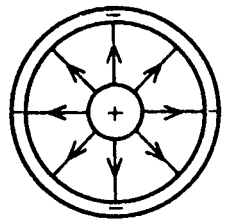

01 Mode

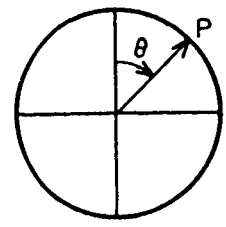

Polar Distribution
$\cos m\theta$
$f_{01} = 1.22\ c/D$

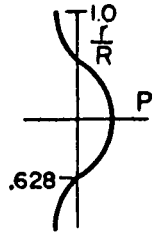

Radial Distribution
$J_m\left(\frac{\pi y_{mm} r}{R}\right)$

- Lowest Symmetric Mode

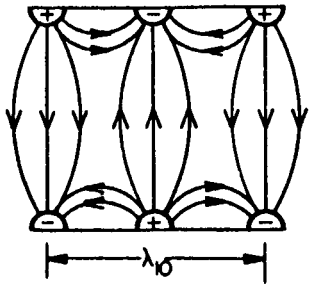

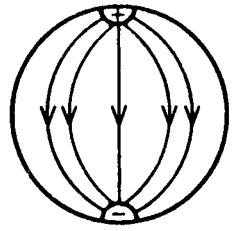

10 Mode

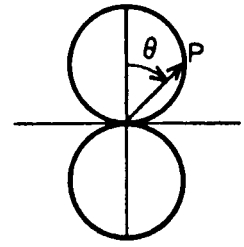

$f_{10} = .586\ c/D$

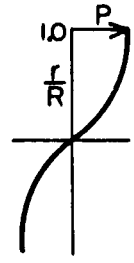

- Lowest Unsymmetric Mode

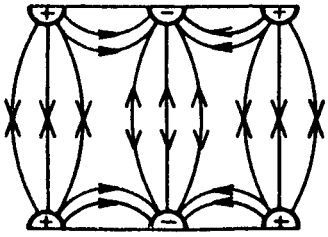

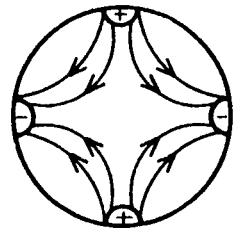

20 Mode

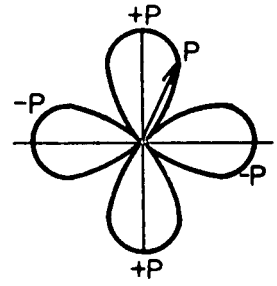

$f_{20} = .97\ c/D$

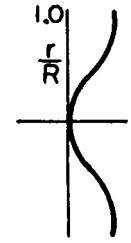

SECOND UNSYMMETRIC MODE

SOME TRANSVERSE MODES OF VIBRATION

FIGURE 4

CONCLUSIONS & RECOMMENDATIONS:

The purpose of this technical memorandum has been to evaluate the usefulness of the electrical analog of fluid circuitry to the design engineer working in the new field of fluid logic devices. If the analog is good, the design engineer can usefully employ the electrical equations with which he may be familiar to the problems of improving the design of fluid logic devices.

There are two phenomena in the transmission of information along a pipe: the acoustical disturbance or sonic wave, and the mean flow of the fluid. The fluid logic designer will, of course, be concerned with both phenomena. It is important to note that the analog explored in this paper deals by definition with a sonic wave and neglects the effect of the mean flow.

This technical memorandum will serve to illustrate that the mathematical treatment of the transient characteristics of fluid flow, either by analog, or directly, involves rather complex differential equations. The analog approach is fairly accurate for certain acoustic circuits, but useless for dealing with the nature of the mean fluid flow.

The electrical analog to fluid flow will be of value for the design engineer when faced with acoustic circuits and with impedance problems, provided the range of frequencies does not exceed the frequency of the first transverse mode of acoustic transmission.

Due to the considerable differences in the basic equations relating to fluid flow and to electrical circuitry, useful analogies between the two fields will probably be difficult to contrive. Currently used analogies have little or limited usefulness to the fluid logic circuit designer.

Due to the complex nature of the equations of motion for fluid flow and the newness of the fluid logic field, there is a great lack of either mathematical or experimental bodies of knowledge to which the design engineer can appeal for answers. However, there does exist, in the fluid dynamics literature, many reports and papers which bear on portions of the problems which face the fluid logic design engineer. It is to this existing body of knowledge, rather than to the contrived analogs, that the design engineer should perhaps address his studies.

In conslusion, it may be pointed out that the transmission of information by fluid flow means and the transient phenomena which must be understood if we are to do real engineering design work, is perhaps best approached from the mathematical point of view. The study of the motion of ideal pistons and the resultant acoustic and flow pattern which result is a possible fruitful approach. It is recommended that the literature be searched for information of studies which have been performed in this regard, and that further studies be conducted which will add to the existing body of knowledge in this field of transient analysis of fluid flow.

(References 6 & 7 discuss problems of fluid transient propagation in pipes.)

REFERENCES:

1. D. V. Wright & D. F. Miller

   Dynamics of Refrigeration Systems - I, Introduction to Gas Vibrations

   Research Report 8-0527-R2; published by Westinghouse Research Laboratories, September 3, 1957.

2. D. V. Wright & D. F. Miller

   Dynamics of Refrigeration Systems - II, Electrical Analog Analysis of Gas Vibrations

   Research Report 8-0527-R4; published by Westinghouse Research Laboratories, March 3, 1958.

3. American Institute of Physics Handbook

   Published by McGraw Hill, c1957

4. Everard M. Williams & James B. Woodford

   Transmission Circuits

   Published by MacMillan Co. c1957

5. C. R. Wiley, Jr.

   Advanced Engineering Mathematics, 2nd edition

   Published by McGraw Hill, c1960

6. Forbes T. Brown

   The Transient Response of Fluid Lines, June 1961

   To be published in Transactions, ASME

7. U. L. Streeter (Editor)

   Handbook of Fluid Dynamics. (Section 20, Fluid Transients in Engineering Systems)

   Published by McGraw Hill c1961